REACTIONS OF (PCP)Ir COMPLEXES WITH SMALL MOLECULES

by

SABUJ KUMAR KUNDU

A Dissertation submitted to the

Graduate School-New Brunswick

Rutgers, The State University of New Jersey

in partial fulfillment of the requirements

for the degree of

Doctor of Philosophy

Graduate Program in Chemistry

written under the direction of

Professor Alan S. Goldman

and approved by

_____

_____

_____

_____

New Brunswick, New Jersey

January, 2010

ABSTRACT OF THE DISSERTATION

REACTIONS OF (PCP)Ir COMPLEXES WITH SMALL MOLECULES

By SABUJ KUMAR KUNDU

Dissertation Director:

Professor Alan S. Goldman

Iridium pincer complexes (^{R4}PCP)IrH$_n$ (PCP=[κ^3-2,6-C$_6$H$_3$(CH$_2$PR$_2$)]) are effective catalysts for the dehydrogenation of alkanes. We wished to design pincer ligands in which the set of phosphinoalkyl groups would offer (a) maximal steric "protection" against cluster-formation (b) minimal hindrance to C-H addition, and (c) resistance to decomposition and self-dehydrogenation (unlike ^{i}Pr groups). Thus, we have synthesized iridium complexes of ligands ^{tBu3Me}PCP ([C$_6$H$_3$(CH$_2$P^{t}BuMe)(CH$_2$P^{t}Bu$_2$]). (^{tBu3Me}PCP)IrH$_4$ (1) shows more efficiency in dehydrogenation of alkanes than either (^{tBu4}PCP)IrH$_n$ or (^{iPr4}MePCP)IrH$_n$. (^{tBu3Me}PCP)IrH$_4$ was also found to be a very effective catalyst in alkane metathesis.

Although isocyanides are important building blocks in organic synthesis, their commercial availability is limited compared to other chemicals. (PCP)Ir complexes react with different secondary methyl amines and at ambient temperature to form corresponding iridium isocyanide complexes (PCP)Ir(H)(H)(CNR), **3-1 (a-e)** which react with CO forming (PCP)Ir(CO) to liberate the corresponding isocyanide.

The addition of PhCCH to highly stable complexes, (PCP)IrL (L = CO, CNR), is challenging. (PCP)IrL (L = CO, CNR) complexes react with PhCCH in presence of acid to form complex (PCP)Ir(CO)(H)(CCPh) (**5-3)** and (PCP)Ir(CNBz)(H)(CCPh) (**5-1**), respectively, in which hydride and acetylide group are *trans* to each other. The reaction proceeds via the cationic intermediate $[(PCP)Ir(CO)(H)]^+$.

Solid-supported catalysts have significant advantages over homogeneous systems, particularly with respect to product-catalyst separation. We have investigated several routes to the development of supported pincer-ligated iridium catalysts. The *p*-dimethylamino-substituted PCP complex is found to bind strongly to alumina while maintaining the same high activity (or even slightly greater) for alkane-dehydrogenation as found in the solution phase.

A broad range of (PCP)Ir complexes with widely varying steric and electronic effects have been synthesized and studied including (PCP)IrL, (PCP)Ir(H)(H)L and PCP)Ir(H)(Cl)L, (L = various P- and N-donors, N_2, various olefins). The relative thermodynamics of these adducts have been detected by equilibrium measurements and calculated using DFT.

Precursors of "(PCP)Ir" cleaves sp^3 C–O bonds of various esters (RCO_2R_1, R_1= alkyl) to give (PCP)Ir(R_1)(O_2CR) or, in cases where R_1 has a β-hydrogen, (PCP)Ir(H)(O_2CR) plus the corresponding alkene derived from R_1.

Dedication

To my family and village

Acknowledgement

I would like to thank my advisor, Prof. Alan S. Goldman for being the best possible boss whom I could have asked for. His perpetual energy and enthusiasm in research, continuous support, staying cool even knowing I am taking stupid, helpful advice all the time, not only greatly motivate me but also taught me the importance of fundamentally understanding the chemistry. I will never forget the freedom he provided me for exploring different projects.

I would like to specially thank my committee members, Prof. Karsten Krogh-Jespersen, Prof. Ralf Warmuth and Prof. Benjamin J. Glasser, who served on my proposal committee, for their valuable time and helpful suggestions.

I would like to thank Prof. Krogh-Jespersen and Yuriy Choliy for theoretical calculations, Dr. Tom Emge for the crystallographic analysis, and Dr. Seho Kim and Dr. Nagarajan Murali for their assistance with the NMR technique. I also thank Prof. Gene S. Hall for X-ray fluorescence measurements. I thank Prof. Maurice Brookhart and Zheng Huang at University of North Carolina at Chapel Hill for collaboration.

I thank Dr. Elizabeth Pelczar and Dr. Amlan Ray, Dr. Yury Kissin for helping and teaching many techniques in the lab. I am thankful to my former and current lab members Dr. Long van Dinh, Zhuo Gao, Dr. Ritu Ahuja, Dr. Benudhar Punji, Dr. Sahar Elkhalafy, Dr. Agnieszka Nawara-Hultzsch, David Wang, Soumik Biswas, Kathleen Field, David Laviska, Jason Hackenberg, Dr. Rob Stibrany, Dr. Carolyn Supplee, and Dr. Burke Scott Williams; it was a great pleasure to work with them.

I am thankful to all of my friends here at Rutgers and in India who helped me to keep up my smile in the last five years.

I feel a special gratitude toward my parents and sister Tanaya. Without their support and encouragement, it would be impossible for me from a rural village of India to reach what I am today. I thank Niloy, Antara and Kheya and Tutai, the new generations in our big family, my uncles and relatives in India. I also thank Bidisa, for her unconditional love and support.

Table of Contents

Lists of tables

List of illustrations

Chapter 1

Introduction

In nature alkanes are the most abundant and least expensive organic molecules, but selective transformation of alkanes is challenging. Due to lack of suitable methods to convert alkanes to useful other organic substrates, they are mostly used as fuel.

The C-H bond activation is one of the most powerful methods for the selective transformation of this inert bond to valuable organic molecules. Oxidative addition of C-H bond to metal complexes has been extensively studied.[1, 2, 3, 4]

In 1965, Chatt reported C-H activation by $Ru(0)(dmpe)_2$ (eq. 1), in which C-H activation takes place in naphthalene or ligand phosphinomethyl group.[5] After this there were many reports of intermolecular C-H activation of aryl and alkyl groups by Green (eq. 2),[6] Bergman (eq. 3),[7] Graham (eq. 4),[8] and others. Bergman first reported that in case of $Cp^*Ir(PMe_3)$ ($Cp^* = \eta^5\text{-}C_5Me_5$) C-H activation is selective for the stronger C-H bonds.[9] This result shows that breaking C-H bonds leads to quite different selectivity than other well known other regular reagents.

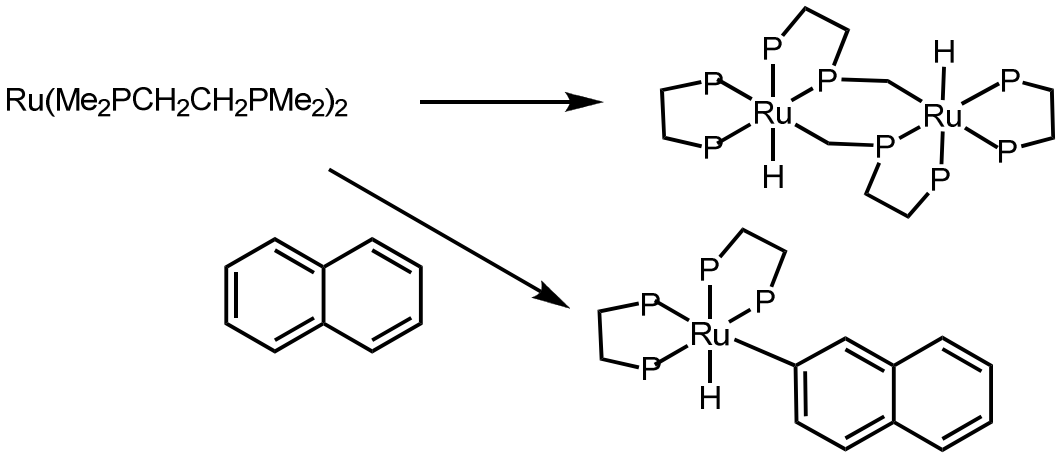
Ru(Me2PCH2CH2PMe2)2
P
Ru
H

(1)

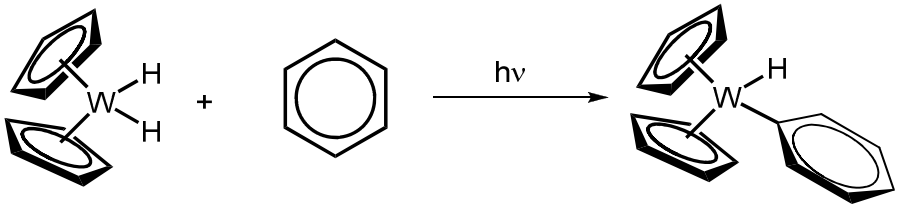
W
H
hν
+
H2

(2)

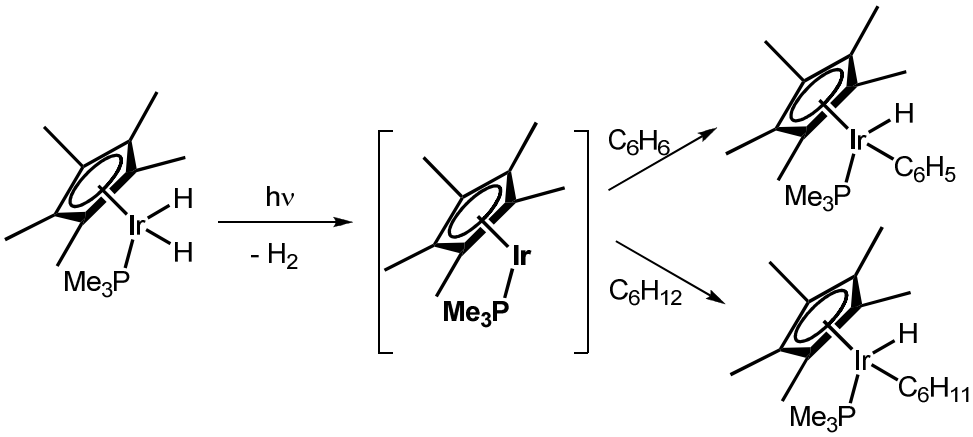
Ir
H
Me3P
hν
- H2
C6H6
C6H12
C6H5
C6H11

(3)

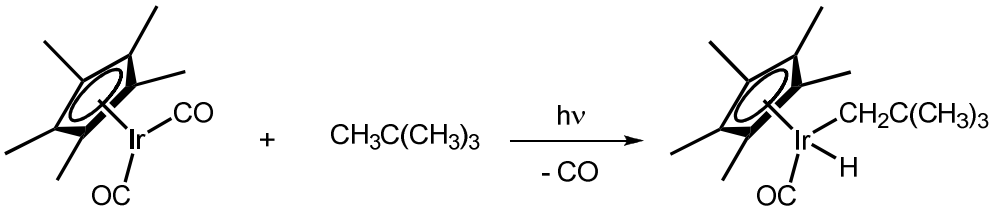
Ir
CO
OC
CH3C(CH3)3
hν
- CO
CH2C(CH3)3
H

(4)

In 1967, just a few years after Chatt's report on C-H activation, Milner reported that C-H activation of a ligand aryl group generated cyclometalated complex (eq. 5).[10] Whitesides published aliphatic γ–C-H bond activation (eq. 6).[11]

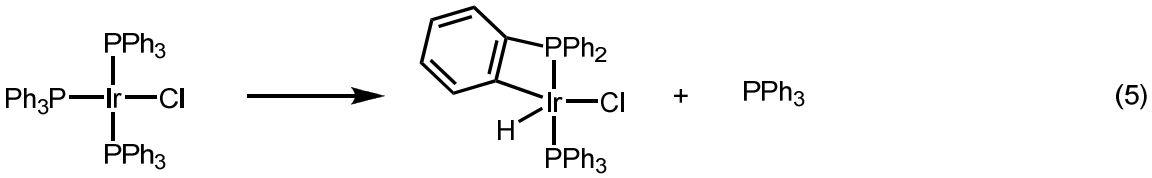

(5)

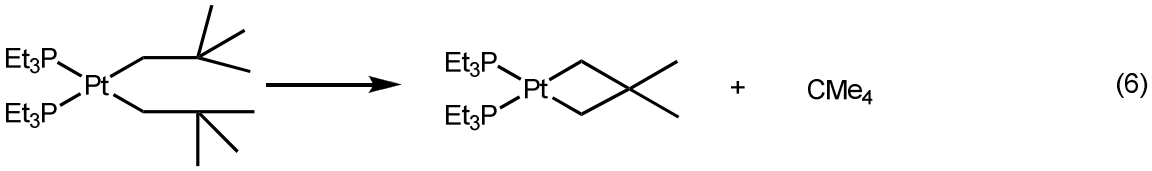

(6)

In 1976 Moulton and Shaw reported a wide range of complexes of 1, 2-bis [(di-t-butylphosphino) methyl] benzene (eq. 7) with Rh, Ir, Ni, Pd, and Pt.[12] This ligand binds strongly to the metal with two phosphorous centers and the aryl carbon. These complexes are called "pincer" complexes, and the ligand is called "PCP" ligand. These "pincer" complexes not only show high catalytic activity in Heck olefin arylation, Suzuki biaryl coupling reactions, alkane dehydrogenation, enantioselective adol condensation, hydroamination, C-C, C-O and C-N bond activation etc. but also have high thermal stability.[13, 14]

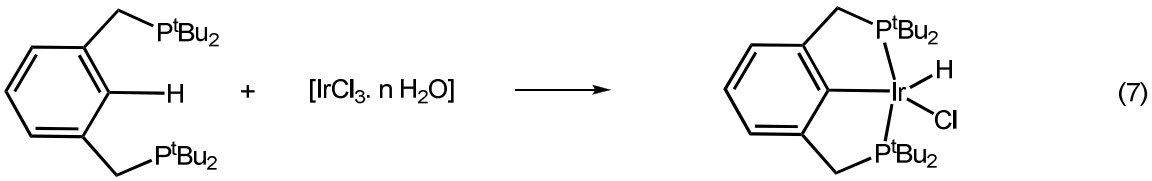

(7)

Olefins are the most important feedstock in the chemical world due to their wide range of applicability in manufacturing other useful compounds; therefore generating olefins from alkane by dehydrogenation has high potential value.

First alkane dehydrogenation was reported by Crabtree in 1979 in which cyclopentane and cyclooctane dehydrogenated by $[IrH_2(Me_2CO)_2(PPh_3)_2]^+$ were used to generate corresponding cycloalkadine iridium complexes (eq. 8).[15] After this work Baudry, Ephritikhine and Felkin also published dehydrogenation of cycloalkane and *n*-pentane using L_2ReH_7 (L= PPh_3, PEt_2Ph) and TBE.[16] Disadvantage of these reactions were stoichiometric with metal complexes as the product bound strongly to the metals centers. Three years later, the same group reported catalytic dehydrogenation of cycloalkane with up to 70 turnover numbers.[17]

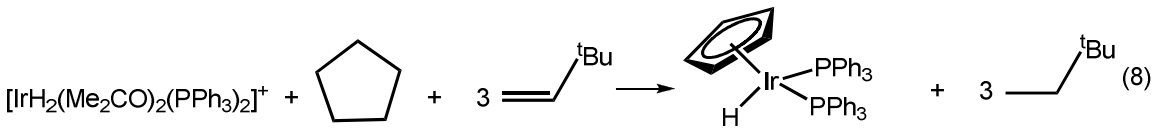

(8)

In 1984 Crabtree first reported well defined catalytic alkane dehydrogenation using $L_2IrH_2(\eta^2\text{-}O_2CCF_3)$.[18] Dehydrogenation of both cycloalkanes and *n*-alkanes was catalyzed by this complex in presence of hydrogen acceptor (like TBE) or photochemically.

In 1988 Tanaka reported alkane carbonylation catalyzed by $Rh(PMe_3)_2(CO)Cl$ complex photochemically.[19] Soon after, it was found that this catalyst can dehydrogenate alkanes to alkenes in absence of CO much more efficiently than previously reported catalytic systems (eq. 9).[20, 21]

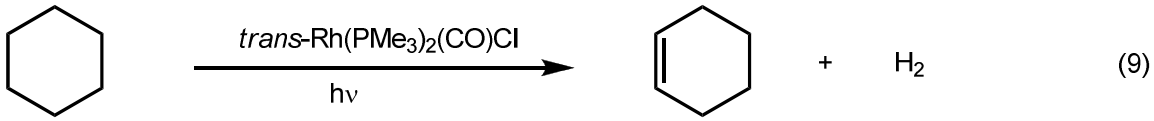

Goldman[22] and Ford and Spillet[23] reported mechanistic work on this catalyst (eq 9). They found that photochemically, $Rh(PMe_3)_2Cl$ was generated from the starting complex $[Rh(PMe_3)_2(CO)Cl]$ which reacted thermochemically with alkane C-H bond and formed $H_2Rh(PMe_3)_2Cl$. Catalytic cycle was then completed after CO replaced the H_2 from the metal center.[24] In absence of strong ligand like CO, thermally $Rh(PMe_3)_2Cl$ was generated and formed inactive dimer $[Rh(PMe_3)_2Cl]_2$. But under H_2 atmosphere, active $H_2Rh(PMe_3)_2Cl$ was generated from the dimer $[Rh(PMe_3)_2Cl]_2$. When the dehydrogenation was done under H_2 atmosphere using an acceptor, unfortunately hydrogenation of more than one equivalent of acceptor was observed per mole of dehydrogenation of alkanes. To solve this problem, other Rh complexes was studied including "(PCP)Rh", but this catalyst showed very poor activity towards dehydrogenation.[25]

In 1996 Jensen and Kaska first reported that "(PCP)Ir" pincer complex produced excellent results in dehydrogenation of cycloalkanes with high catalyst stability even at 200 °C(eq. 10).[26, 27] (^{R}PCP)IrH_n catalyst also showed great results in acceptorless dehydrogenation due to high thermal stability (eq. 11).[28, 29] Interestingly, both (^{tBu}PCP)IrH_2 and (^{iPr}PCP)IrH_4 catalysts selectively dehydrogenate in terminal position of *n*-alkanes and produce 1-alkenes.[30] Less crowded (^{iPr}PCP)IrH_4 catalyst work much faster than the (^{tBu}PCP)IrH_2 catalyst.

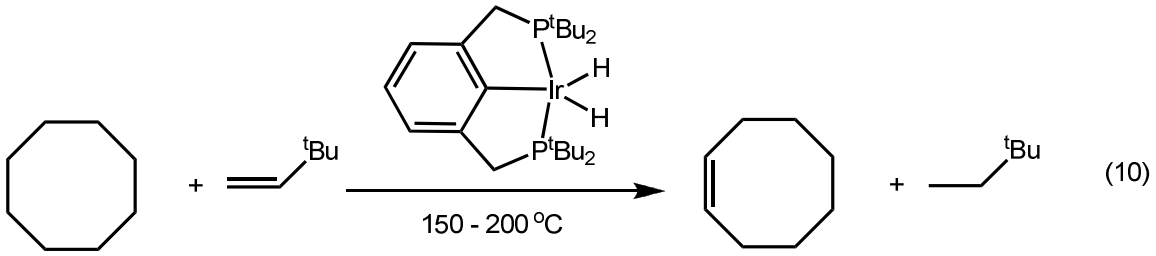

(10)

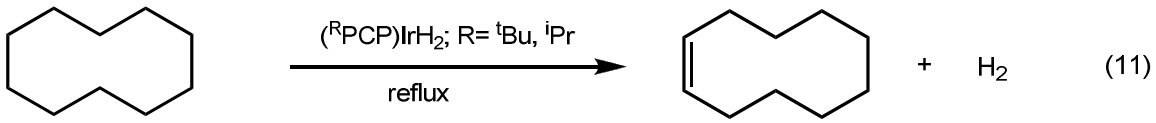

(11)

The mechanism of transfer dehydrogenation of alkanes using (PCP)Ir catalyst, has been studied both computationally and experimentally by Goldman and Krogh-Jespersen.[31, 32] Scheme 1-1 describes the proposed catalytic cycle for transfer dehydrogenation of alkanes using norbornene as acceptor. The 14-electorn active complex "(^{R}PCP)Ir" is generated after acceptor removed two hydrides from (^{R}PCP)IrH$_2$. Oxidative addition of alkane C-H bond to the active species followed by β-hydrogenation elimination generated alkenes and regenerated the catalyst. (^{R}PCP)IrH$_2$ catalyst also shows high activity in transfer dehydrogenation of ethylbenzene, tetrahydrofuran,[33] alcohols,[34] and amines.[35]

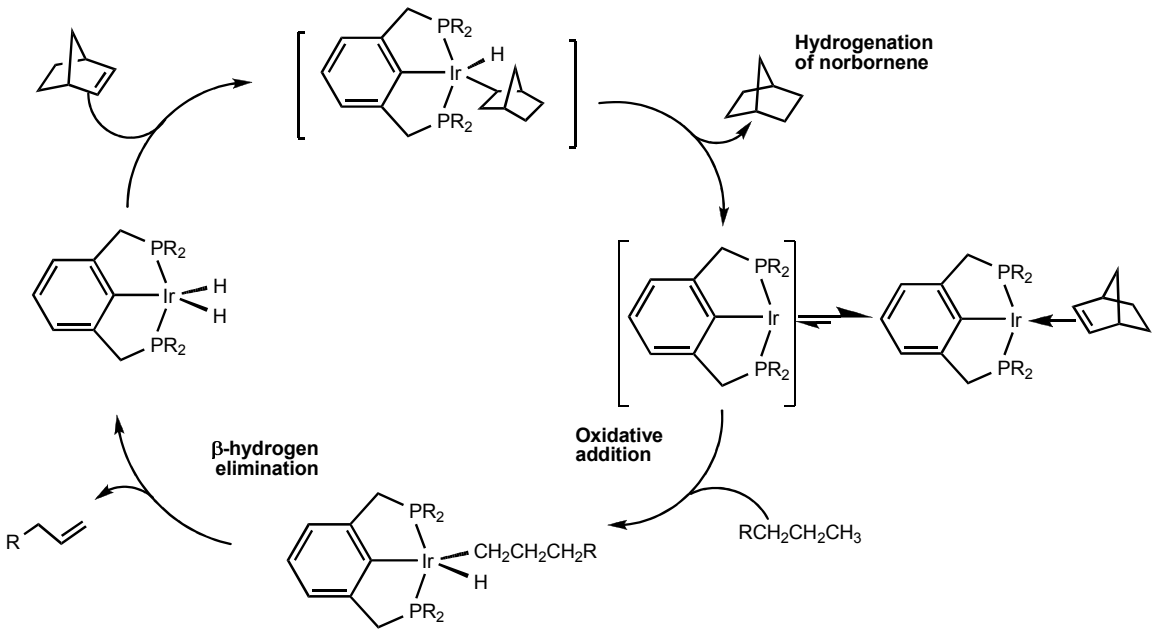

Scheme 1-1 Proposed mechanism for transfer dehydrogenation of alkane catalyzed by (^{R}PCP)IrH_2

In this thesis, in Chapter 2, the synthesis and catalytic activity of (^{tBu3Me}PCP)IrH_4 is discussed. Replacing one of the four ^{t}Bu groups on the catalyst (^{tBu4}PCP)IrH_4 results in significantly increased catalytic activity. The (^{tBu3Me}PCP)IrH_4 catalyst showed very high activity for both transfer- and acceptorless dehydrogenation. The (^{tBu3Me}PCP)IrH_4 catalyst also showed very high activity in *n*-hexane and cyclooctane metathesis reactions. Chapter 3 describes the synthesis of isocyanides from secondary methyl amines by pincer iridium complex. Chapter 4 explores the oxidative addition of methyl iodide to (PCP)Ir(L) (L = CO or CNBz) complexes. Chapter 5 describes acid catalyzed electrophilic addition of phenylacetylene to (PCP)Ir(L) (L = CO or CNBz) complexes. In Chapter 6, several routes to the development of supported pincer-ligated iridium catalysts were investigated. To measure metal-ligand binding energies, using the pincer-ligated iridium fragment

"(PCP)Ir", a broad range of complexes with widely varying steric and electronic effects, have been synthesized and studied in Chapter 7. In Chapter 8 we discuss alkyl C–O bond cleavage in esters by a (PCP)Ir complex. Mechanistic investigations suggest that the reaction proceeds via a multi-step pathway. In Chapter 9, some preliminary results of reactivity of (PCP)Ir with other substrates are summarized.

References

(1) Shilov, A. E.; Shul'pin, G. B. *Chem. Rev.* **1997**, *97*, 2879.
(2) Jones, W. D. *Science* **2000**, *287*, 1942.
(3) Crabtree, R. H. *J. Chem. Soc., Dalton Trans.* **2001**, 2437.
(4) Labinger, J. A.; Bercaw, J. E. *Nature* **2002**, *417*, 507.
(5) Chatt, J.; Davidson, J. M. *J. Chem. Soc.* **1965**, 843.
(6) Green, M. L. H.; Knowles, P. J. *J. Chem. Soc., Chem. Comm.* **1970**, 1677.
(7) Janowicz, A. H.; Bergman, R. G. *J. Am. Chem. Soc.* **1982**, *104*, 352.
(8) Hoyano, J. K.; Graham, W. A. G. *J. Am. Chem. Soc.* **1982**, *104*, 3723.
(9) Bergman, R. G. *Science* **1984**, *223*, 902.
(10) Bennett, M. A.; Milner, D. L. *Chem. Commun.* **1967**, 581.
(11) Foley, P.; Whitesides, G. M. *J. Am. Chem. Soc.* **1979**, *101*, 2732.
(12) Moulton, C. J.; Shaw, B. L. *J. Chem. Soc., Dalton Trans.* **1976**, 1020.
(13) van der Boom, M. E.; Milstein, D. *Chem. Rev.* **2003**, *103*, 1759.
(14) Albrecht, M.; van Koten, G. *Angew. Chem. Int. Ed. Engl.* **2001**, *40*, 3750.
(15) Crabtree, R. H.; Mihelcic, J. M.; Quirk, J. M. *J. Am. Chem. Soc.* **1979**, *101*, 7738.
(16) Baudry, D.; Ephritikhine, M.; Felkin, H. *J. Chem. Soc., Chem. Comm.* **1980**, 1243.
(17) Baudry, D.; Ephritikhine, M.; Felkin, H.; Holmes-Smith, R. *J. Chem. Soc., Chem. Comm.* **1983**, 788.
(18) Burk, M. J.; Crabtree, R. H.; Parnell, C. P.; Uriarte, R. J. *Organometallics* **1984**, *3*, 816.
(19) Sakakura, T.; Tanaka, M. *Chem. Lett.* **1987**, 249.
(20) Nomura, K.; Saito, Y. *Chem. Commun.* **1988**, 161.
(21) Sakakura, T.; Sodeyama, T.; Tokunaga, M.; Tanaka, M. T.; Tokunaga, M.; Tanaka, M. *Chem. Lett.* **1988**, 263.
(22) Maguire, J. A.; Boese, W. T.; Goldman, A. S. *J. Am. Chem. Soc.* **1989**, *111*, 7088.
(23) Spillett, C. T.; Ford, P. C. *J. Am. Chem. Soc.* **1989**, *111*, 1932.
(24) Maguire, J. A.; Goldman, A. S. *J. Am. Chem. Soc.* **1991**, *113*, 6706.
(25) Wang, K.; Goldman, M. E.; Emge, T. J.; Goldman, A. S. *J. Organomet. Chem.* **1996**, *518*, 55.
(26) Gupta, M.; Hagen, C.; Flesher, R. J.; Kaska, W. C.; Jensen, C. M. *Chem. Commun.* **1996**, 2083.
(27) Gupta, M.; Hagen, C.; Kaska, W. C.; Cramer, R. E.; Jensen, C. M. *J. Am. Chem. Soc.* **1997**, *119*, 840.
(28) Xu, W.; Rosini, G. P.; Gupta, M.; Jensen, C. M.; Kaska, W. C.; Krogh-Jespersen, K.; Goldman, A. S. *Chem. Commun.* **1997**, 2273.
(29) Liu, F.; Goldman, A. S. *Chem. Commun.* **1999**, 655.
(30) Liu, F.; Pak, E. B.; Singh, B.; Jensen, C. M.; Goldman, A. S. *J. Am. Chem. Soc.* **1999**, *121*, 4086.
(31) Renkema, K. B.; Kissin, Y. V.; Goldman, A. S. *J. Am. Chem. Soc.* **2003**, *125*, 7770.
(32) Krogh-Jespersen, K.; Czerw, M.; Summa, N.; Renkema, K. B.; Achord, P. D.; Goldman, A. S. *J. Am. Chem. Soc.* **2002**, *124*, 11404.

(33) Gupta, M.; Hagen, C.; Kaska, W. C.; Jensen, C. M. *J. Chem. Soc., Chem. Comm.* **1997**, 461.
(34) Morales-Morales, D.; Redon, R.; Wang, Z. H.; Lee, D. W.; Yung, C.; Magnuson, K.; Jensen, C. M. *Can. J. Chem.* **2001**, *79*, 823.
(35) Zhang, X.; Fried, A.; Knapp, S.; Goldman, A. S. *Chem. Commun.* **2003**, 2060.

Chapter 2

Rational Design and Synthesis of Highly Active Pincer-Iridium Catalysts

Abstract

Iridium pincer complexes (^{R4}PCP)IrH$_n$, (PCP=[κ^3-2,6-C$_6$H$_3$(CH$_2$PR$_2$)]) are effective catalysts for the dehydrogenation of alkanes. Bulky alkyl groups on the ligating phosphorus atoms (typically R = t-butyl) are needed to prevent formation of catalytically inactive clusters; however, DFT calculations indicate that bulky groups substantially increase the energy barriers of both alkane C-H addition and β-hydrogen elimination. We therefore wished to design pincer ligands in which the set of phosphinoalkyl groups would offer (a) maximal steric "protection" against cluster-formation (b) minimal hindrance to C-H addition, and (c) resistance to decomposition and self-dehydrogenation (unlike ^{i}Pr groups). Assuming that the reaction with alkane exerts significant steric demands at only one or two "quadrants" of the reactive site, we investigated the partial replacement of ^{t}Bu groups with Me group. Thus, we have synthesized iridium complexes of ligands ^{tBu3Me}PCP ([C$_6$H$_3$(CH$_2$P^{t}BuMe)(CH$_2$P^{t}Bu$_2$]). (^{tBu3Me}PCP)IrH$_4$ (1), shows more efficiency in dehydrogenation of alkanes than either (^{tBu4}PCP)IrH$_n$ or (^{iPr4}MePCP)IrH$_n$. (^{tBu3Me}PCP)IrH$_4$ was also found to be a very effective catalyst in alkane metathesis.

2.1 Introduction

In nature, alkanes are the most abundant and least expensive organic molecules, but selective transformation of alkanes is challenging. Due to lack of suitable methods to convert alkanes to useful other organic substrates, it is mostly used as fuel.

Olefins are ubiquitous as reagents and intermediates in organic chemistry in the synthesis of petrochemicals, commodity chemicals, and fine chemicals. For this reason, the catalytic dehydrogenation of alkanes and, more broadly, alkyl groups has a tremendous potential value.

The development of soluble transition metal complexes as catalysts for alkane dehydrogenation was pioneered in the early 1980's by the groups of Crabtree and Felkin. In their work, they reported cyclopentane and cyclooctane was dehydrogenated by $[IrH_2(Me_2CO)_2(PPh_3)_2]^+$ to generate corresponding cycloalkadienyl iridium complexes (eq. 1).[1] Later, Baudry, Ephritikhine and Felkin also published on dehydrogenation of cycloalkane and *n*-pentane using L_2ReH_7 (L= PPh_3, PEt_2Ph) and TBE as the sacrificial acceptor.[2] Disadvantage of these reactions was stoichiometric with metal complexes as the product bound strongly to the metals centers. After three years, the same group reported catalytic dehydrogenation of cycloalkane with up to 70 turnover numbers.[3]

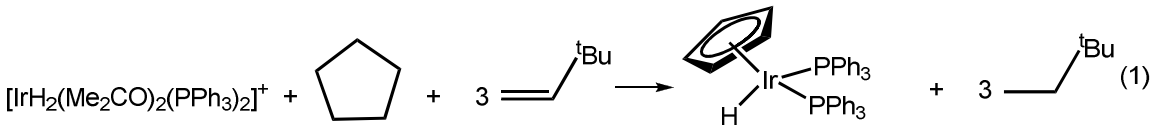

(1)

In 1984 Crabtree *et al*. first reported well defined catalytic alkane dehydrogenation.[4] Dehydrogenation of both cycloalkanes and *n*-alkanes was catalyzed by

Ir-complexes in the presence of hydrogen acceptors (e.g. TBE) or photochemically (eq. 2).

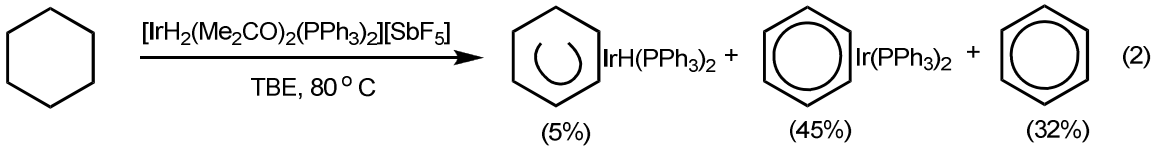

(2)

In 1988, Tanaka reported that a $Rh(PMe_3)_2(CO)Cl$ complex catalyzed alkane carbonylation photochemically.[5] Soon after, it was found that this catalyst can dehydrogenate alkanes to alkenes in the absence of CO much more efficiently than previously reported catalytic systems (eq. 3).[6,7]

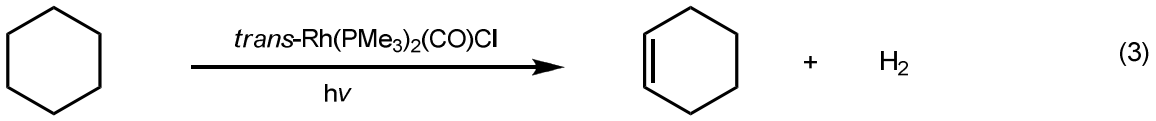

(3)

Goldman[8] and Ford and Spillet[9] reported mechanistic work on this catalytic system. They found that photochemically $Rh(PMe_3)_2Cl$ was generated from the starting complex, which reacts thermochemically with alkane C-H bond and formed $H_2Rh(PMe_3)_2Cl$. The catalytic cycle was completed after the CO replaced H_2 (Scheme 2-1).[10] In the absence of strongly bound ligand like CO, $Rh(PMe_3)_2Cl$ generated thermally formed inactive dimer $[Rh(PMe_3)_2Cl]_2$. Under H_2 atmosphere, active $H_2Rh(PMe_3)_2Cl$ was generated from the dimer $[Rh(PMe_3)_2Cl]_2$. When the dehydrogenation was carried out under H_2 atmosphere using an acceptor, unfortunately hydrogenation of more than one equivalent of acceptor was observed per mole of dehydrogenation of alkanes. To prevent the dimerization of the catalyst, the bulky ligand "(^{tBu4}PCP)" was introduced.

Unfortunately, pincer rhodium complex, (PCP)RhH_2 showed very poor activity towards dehydrogenation.[11]

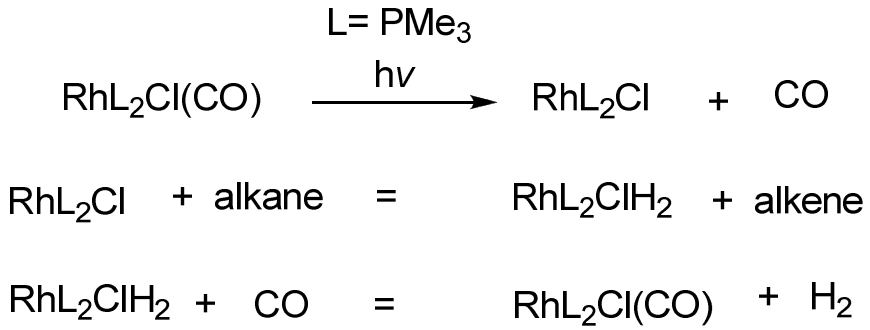

Scheme 2-1 Mechanistic pathway of dehydrogenation of alkane by $Rh(PMe_3)_2Cl(CO)$

In 1996, Jensen and Kaska first reported that the "(^{tBu4}PCP)Ir" pincer complex showed excellent catalytic activity in dehydrogenation of cycloalkanes with high catalyst stability even at 200 °C(eq. 4).[12,13]

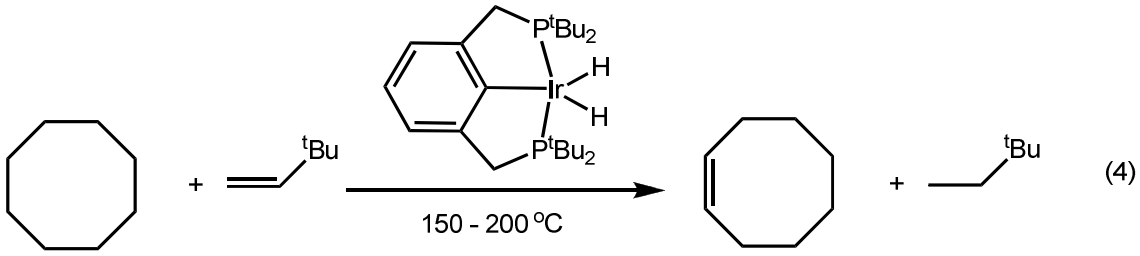

(^{R4}PCP)IrH_2 catalyst not only shows high catalytic activity in transfer dehydrogenation but also shows high turnover numbers in acceptorless dehydrogenation due to its high thermal stability (eq. 5).[14,15]

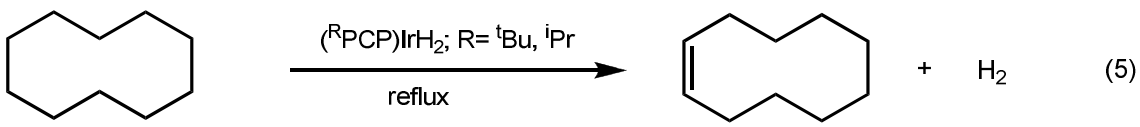

These complexes ware subsequently found to show high kinetic selectivity for the terminal position of *n*-alkanes[16] and also shows high activity in transfer dehydrogenation of ethylbenzene, tetrahydrofuran,[17] alcohols,[18]and amines.[19]

Steric and electronic properties of pincer catalysts can be modified or tuned by varying R, X or Ygroups (Figure 2-1).

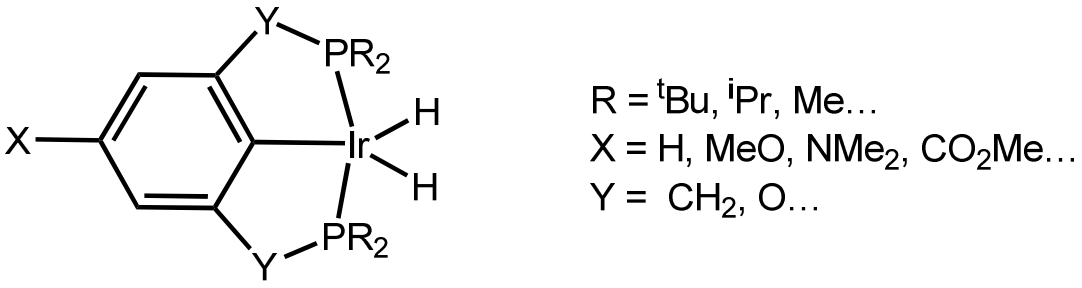

Figure 2-1 Possible variation of pincer ligand with Ir

Our group reported electron donating '-OMe' group makes (MeO-^{tBu4}PCP)IrH_2 faster catalyst than (H-^{tBu4}PCP)IrH_2 in dehydrogenation of alkanes.[20] In the process to put more π–electron donating group in the *para* position of the PCP ring, (Me_2N-^{tBu4}PCP)IrH_2 was synthesized and it improved catalytic activity.[21] Our group also reported less bulky (MeO-^{iPr4}PCP)IrH_2 give much higher turnovers than bulky (MeO-^{tBu4}PCP)IrH_2 catalyst.

The presence of sterically bulky, robust, phosphinoalkyl groups (e.g. ^{t}Bu) presumably offers protection against cluster formation and bimolecular catalyst deactivation. However, it appears that such groups also strongly contribute to the activation barriers to both C-H bond addition and the requisite β-H elimination of the resulting iridium alkyl intermediate. Thus, these bulky groups afford advantages and

disadvantages. We considered, however, that not all four R groups in a fragment (^{R4}PCP)Ir contribute equally to this equation. Both C-H addition and β-H elimination are distinctly unsymmetrical with respect to a (^{R4}PCP)Ir unit, and different ^{t}Bu groups of the (^{tBu4}PCP)Ir fragment are expected to exert substantially different steric effects on the respective transition states. A simple schematic (Figure 2-2) would suggest that, in the case of (^{tBu4}PCP)Ir, replacement of even just one ^{t}Bu group with a sterically much less demanding unit, viz. Me, could substantially favor these reaction steps and, importantly, it seems unlikely that such a substitution would strongly promote the undesirable formation of dinuclear clusters. Conversely, however, potential resting states could also be stabilized by the decreased crowding resulting from even a single Me-for-^{t}Bu substitution. To explore these issues in detail, we have conducted a combined computational/experimental study on the effect of substituting ^{t}Bu groups on the ^{tBu4}PCP ligand by Me groups.

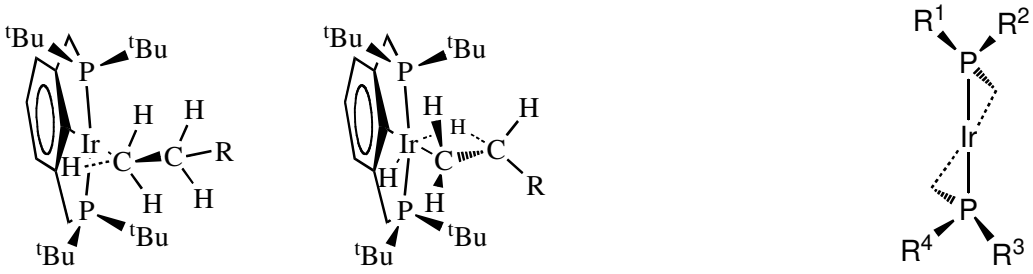

Figure 2-2 Schematic illustration indicating that different ^{t}Bu groups of the (^{tBu4}PCP)Ir fragment are expected to exert substantially different steric effects on the transition states for C-H addition (left) and β-H elimination (center). The canting of the PCP aryl ring plane relative to the P-Ir-P axis and a general labeling scheme for the phosphine substituents are also illustrated (right).

In this chapter we report synthesis and catalytic activity of new highly active pincer catalyst (^{tBu3Me}PCP)IrH_4 as well as computational studies of this catalyst.

2.2 Results and Discussion

2.2.1 Computational Studies[22]

Reactions (6 to 9) in Scheme 2-2 comprise the established pathway for dehydrogenation of an alkane (specifically of an ethyl group) by (^{tBu4}PCP)Ir to produce (^{tBu4}PCP)IrH_2 and alkene;[23] the same reactions, but in the reverse order, describe the hydrogenation of a terminal alkene. The two reaction sequences 7 to 9 and 9 to 7 therefore constitute a catalytic cycle for transfer-dehydrogenation of an alkane using an olefinic sacrificial hydrogen acceptor. Reaction 6 describes the entry into the catalytic cycle from an out-of-cycle alkene-bound resting state.

Scheme 2-2 Reaction pathway for dehydrogenation of an alkane CH_3CH_2R by (PCP)Ir

(PCP)Ir(CH_2=CHR) = (PCP)Ir + CH_2=CHR (alkene loss from out-of-cycle resting state) (6)

(PCP)Ir + CH_3CH_2R = (PCP)Ir(H)(CH_2CH_2R) (C-H addition) (7)

(PCP)Ir(H)(CH_2CH_2R) = (PCP)Ir$(H)_2$(CH_2=CHR)(β-H elimination) (8)

(PCP)Ir$(H)_2$(CH_2=CHR) = (PCP)IrH_2 + CH_2=CHR (loss of product alkene) (9)

Table 2.1 Computed relative Gibbs free energies (kcal/mol) for the catalytic cycle defined in Scheme 2-2.[a]

Species[a]	R_{1-4} = ^{t}Bu	R_{1-4} = ^{i}Pr	R_{1-3} = ^{t}Bu; R_4 = Me	$R_{1,2}$ = ^{t}Bu; $R_{3,4}$ = Me *gem*	$R_{1,3}$ = ^{t}Bu; $R_{2,4}$ = Me *trans*	$R_{1,4}$ = ^{t}Bu; $R_{2,3}$ = Me *meso*	R_1 = ^{t}Bu; R_{2-4} =Me	R_{1-4} = Me
Ir(butene) + butane	-2.2	-8.9	-7.9	-10.0	-10.4	-11.6	-13.8	-15.8
Ir + butene + butane	0.0	0.0	0.0	0.0	0.0	0.0	0.0	0.0
TS: C-H-addition + butene	20.8	16.7	15.8	15.4	12.9	15.2	12.0	10.1
Ir(H)(butyl) + butene	14.4	10.9	9.9	8.5	8.5	8.4	7.9	5.4
TS: β-H-elimination + butene	30.6	23.3	20.4	18.7	16.8	12.6	12.3	9.1
$Ir(H)_2$(butene) + butene	16.9	10.5	6.4	6.2	4.7	5.3	1.6	-1.9
Ir(H)(H) + butene + butene	3.2	5.1	2.4	3.0	2.8	3.0	2.5	3.3
ΔG = G[highest TS + butene] - G[Ir(butene) + butane]	32.7	32.2	28.3	28.7	27.3	26.8	26.1	25.9
Ir + H_2 –> $Ir(H)_2$	-14.3	-12.3	-15.0	-14.4	-14.6	-14.4	-14.9	-14.1

[a]For each catalyst species, the sum of the free energies of ($^{R1-4}$PCP)Ir, *n*-butane, and 1-butene defines the reference energy of 0.0 kcal/mol. Assumed reaction conditions are T = 423 K (150 °C), [*n*-butane] = 10 M, and [1-butene] = 1 M. The numbering scheme used for the phosphine alkyl groups is shown in Fig. 2.2

The columns in Table 2.1 are ordered left to right according to decreasing Gibbs energy for β-H elimination (eq 8). This step is computed to be rate-determining in the dehydrogenation cycle (Scheme 2.2) for all investigated (PCP)Ir catalysts, except (*meso*-^{tBu2Me2}PCP)Ir. With the same single exception of (*meso*-^{tBu2Me2}PCP)Ir, Table 2.1 also shows (from left to right) decreasing Gibbs energy for the C-H activation step. Substitution of a ^{t}Bu group for smaller alkyl groups (^{i}Pr or Me) only slightly diminishes substituent electron donation to P (electron donating ability ^{t}Bu > ^{i}Pr > Me) and renders the phosphine slightly more electron withdrawing from the central Ir atom (relative to

$P(CH_2R)^tBu_2$). Such electronic effects would be expected to induce very modest changes in the activation barriers for C-H activation and β-H elimination; moreover, they might be expectedly small *increases* as the degree of alkyl substitution is reduced ("less electron-rich" Ir metal center). The general *decrease* in activation energies observed with decreasing extent of phosphine alkylation may thus be safely attributed to diminishing steric interactions (from left to right, approximately, in Table 2.1).

From the data presented in the first three columns of Table 2.1 ($R_{1-4} = {}^tBu$; $R_{1-4} = {}^iPr$; and $R_{1-3} = {}^tBu$, $R_4 = Me$), we note that not only are the calculated energetic effects on reactions (1)-(4) arising from a single Me-for-^{t}Bu substitution substantial (5 - 10 kcal/mol), but also that just a single Me-for-^{t}Bu substitution engenders energetic effects generally larger than those resulting from four ^{i}Pr-for-^{t}Bu substitutions. In particular, the TS for β-H elimination is lower by 10 kcal/mol in the (^{tBu3Me}PCP)Ir reaction manifold than in the (^{tBu4}PCP)Ir manifold; the computed relative stabilization is about 7 kcal/mol when (^{iPr4}PCP)Ir is the catalyst. The differential energy lowering for the C-H activation step is about half these values: 5 kcal/mol in the case of (^{tBu3Me}PCP)Ir and 4 kcal/mol for (^{iPr4}PCP)Ir. Considering the overall potential efficiency improvement to the catalytic dehydrogenation process, we find that the significant stabilization of the rate determining β-H transition state is unfortunately (but not unexpectedly) partially offset by the stronger affinity of 1-butene for (^{tBu3Me}PCP)Ir and (^{iPr4}PCP)Ir; the calculations predict differential binding energy increases of 6-7 kcal/mol. Thus, whereas the predicted overall catalytic free energy of activation in the case of the (^{tBu3Me}PCP)Ir catalyst is 4.3 kcal/mol less than that of (^{tBu4}PCP)Ir, it is only 0.5 kcal/mol less in the case of (^{iPr4}PCP)Ir. It is reassuring,

however, that experimental data already reported support an increased efficiency of (^{iPr4}PCP)Ir relative to (^{tBu4}PCP)Ir in alkane dehydrogenation.[15]

2.2.2 Synthesis of various (^{R4}PCP)IrH$_n$ complex

2.2.2.1 Synthesis of (^{tBu4}PCP)IrH$_4$

Synthesis of (^{tBu4}PCP) ligand and its corresponding iridium hydro chloride complex was first reported by Moultan and Shaw.[24] This iridium hydro chloride was then reduced under H_2 atmosphere to obtain (^{tBu4}PCP)IrH$_4$.[12] This catalyst can loose H_2 in heating under vacuum and form (^{tBu4}PCP)IrH$_2$.

2.2.2.2 Synthesis of (^{iPr4}PCP)IrH$_4$

(^{iPr4}PCP) ligand and its corresponding iridium hydro chloride and (^{iPr4}PCP)IrH$_4$ was prepared as described in the literature.[16]

2.2.2.3 Synthesis of (^{tBu3Me}PCP)IrH$_4$ (1)

2.2.2.3.1 Synthesis of ^{t}BuMePH

Racemic ^{t}BuMePH was synthesized by the reaction, in diethyl ether, of $LiAlH_4$ with P(^{t}Bu)MeCl, prepared as reported by the reaction of $PMeCl_2$ with ^{t}BuMgCl according to the method of Wolfsberger[25] (Scheme 2-3).

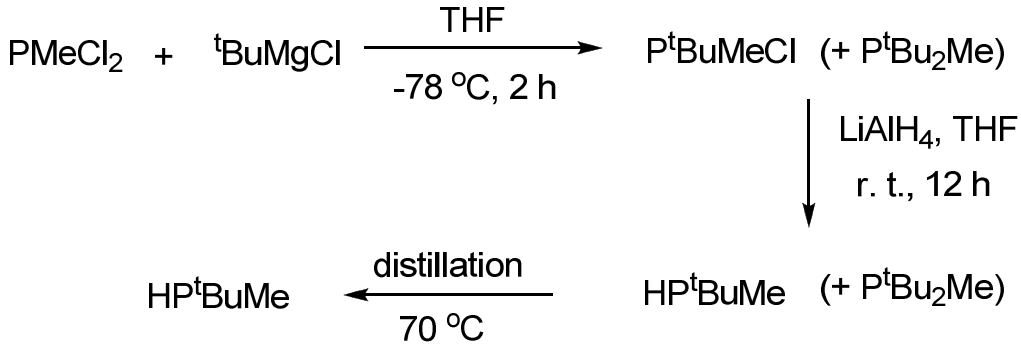

Scheme 2-3 Synthesis of HP^{t}BuMe

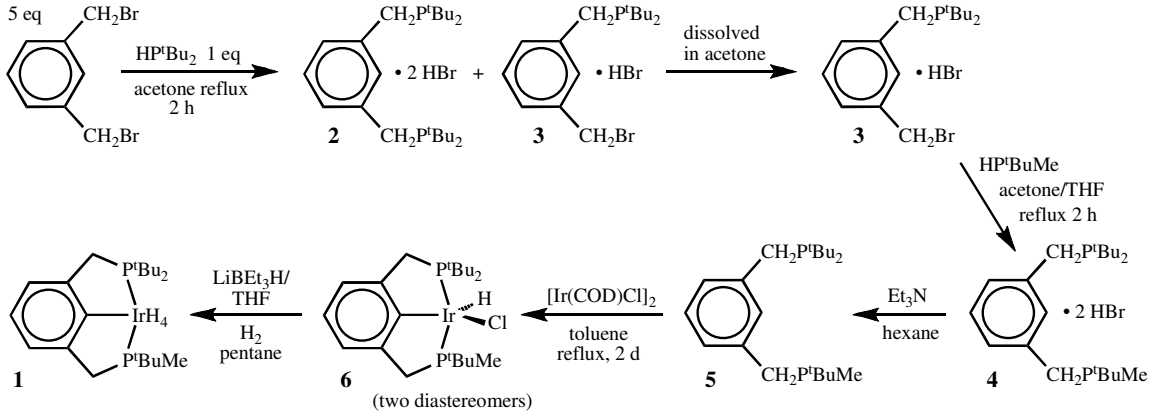

Scheme 2-4 Synthesis of (^{tBu3Me}PCP)IrH_4 (1)

2.2.2.3.2 Synthesis of monophosphine ligand salt (3)

Excess of 1,3-bis(bromomethyl)benzene (5 eq) reacted with HP^{t}Bu_2 in acetone formed compound **2** and **3.** Compound **2** was insoluble in acetone so it was removed by filtratation. The acetone solution containing compound **3** and excess 1,3-bis(bromomethyl)benzene was concentrated under vacuum and was added slowly to fast stirring Et_2O (300 mL). Sticky solid was formed at the bottom and the supernatant was removed by filtration. The solid was redissolved in acetone and reprecipitated with excess Et_2O and was filtered again. After repeating this procedure five times, all 1,3-bis(bromomethyl)benzene was removed in Et_2O solution and compound **3** remained as a white solid.

2.2.2.3.3 Synthesis of ligand salt (4) and ligand (5)

Compound **3** was dissolved in acetone and 1.1eq. HP^{t}BuMe/THF (concentration of this phosphine was determined by ^{31}P NMR, using PPh_3 as standard) was added. Then

this mixture was refluxed for two hours and insoluble compound **4** was formed asa white solid. Treating ligand salt (4) with excess of triethylamine in hexane gave ^{tBu3Me}PCP-H.

2.2.2.3.4 Synthesis of (^{tBu3Me}PCP)IrHCl (6) and (^{tBu3Me}PCP)IrH$_4$ (1)

In analogy with the synthesis of the parent (^{tBu4}PCP)IrH$_4$, this pincer ligand precursor was then reacted with [Ir(cyclooctadiene)Cl]$_2$ to give pure (^{tBu3Me}PCP)IrHCl (two isomers) as characterized by ^{1}H, ^{31}P and ^{13}C NMR. We were unable to obtain X-ray quality crystals of (^{tBu3Me}PCP)IrHCl, perhaps because of the formation of two isomers (presumably diastereomers with the hydride cis and trans to the phosphinomethyl group respectively). A reaction batch in which a slight excess of [Ir(cyclooctadiene)Cl]$_2$ was (inadvertently) present, however, yielded crystals of (^{tBu3Me}PCP)Ir(H)(μ-Cl$_2$)Ir(COD); a single-crystal X-ray diffraction structure of this compound was obtained (Figure 2-3), revealing the presence of a chloride-bridged (^{tBu3Me}PCP)IrHCl unit. An X-ray quality crystal of complex 1 was not obtained. However, in analogy with the known reaction of (^{tBu4}PCP)IrH$_4$, addition of 1 atm of CO gave (^{tBu3Me}PCP)Ir(CO), the single crystal X-ray diffraction structure of this complex affords supporting evidence of the structure of the (^{tBu3Me}PCP)Ir unit (Figure 2-4).

2.2.3 Transfer dehydrogenation study of alkane using different PCP-pincer catalysts

The transfer dehydrogenation mechanism of alkanes using (PCP)Ir catalysts, has been studied both computationally and experimentally by Goldman and Krogh-Jespersen.[26] Scheme 2-5 describes the proposed catalytic cycle of transfer dehydrogenation of alkanes using norbornene as acceptor. A 14-electron active complex "(^{R4}PCP)Ir" is generated after acceptor removes two hydrides from (^{R4}PCP)IrH$_2$.

Oxidation addition of the alkane C-H bond to the active species followed by β-hydrogenation elimination generates alkenes and regenerates the catalyst.

In this chapter we report transfer dehydrogenation of *n*-octane catalyzed by (^{tBu3Me}PCP)IrH$_4$ and compare with other known pincer catalysts.

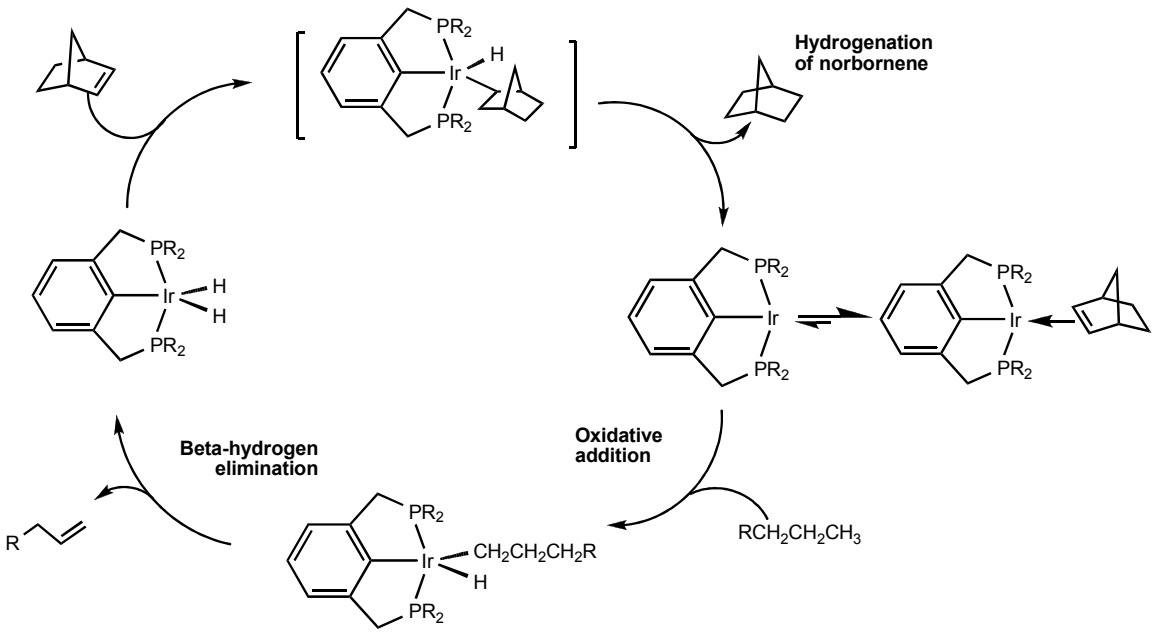

Scheme 2-5 Proposed mechanism of transfer dehydrogenation of alkane catalyzed by (^{R4}PCP)IrH$_2$

2.2.3.1 Transfer dehydrogenation of *n*-octane using different pincer catalysts

(^{R4}PCP)IrH$_2$ (R = ^{t}Bu, ^{i}Pr) selectively dehydrogenate *n*-octane in terminal position. However, these catalysts also catalyze isomerization of 1-octene to internal octane.

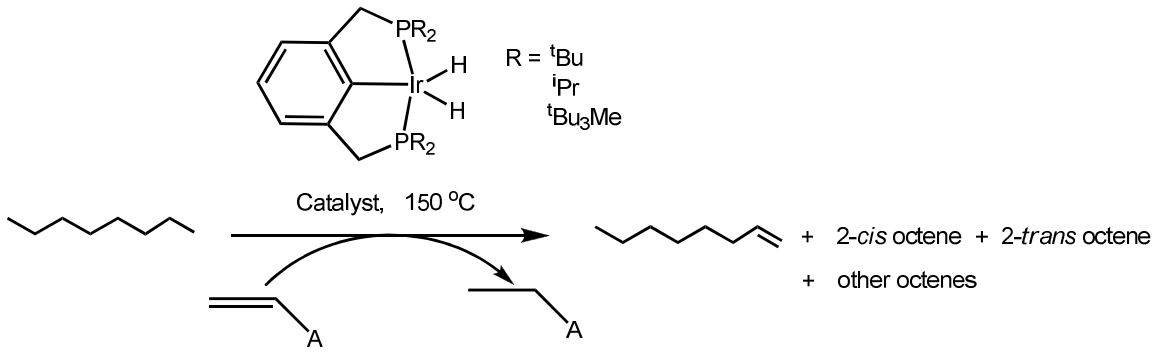

Scheme 2-6 Transfer dehydrogenation of *n*-octane catalyzed by (^{R4}PCP)IrH_4

In this study of transfer dehydrogenation of *n*-octane, three different pincer catalysts (1mM) have been investigated with varying concentration of both TBE and NBE as acceptor (Scheme 2-6). In accord with the calculated results, complex **1** was found to be a significantly more effective catalyst for alkane transfer-dehydrogenation than (^{tBu4}PCP)IrH_4, or even the presumably much less crowded (^{iPr4}PCP)IrH_4 (Table 2.2, 2.3, 2.4 and 2.5).

The results in Table 2.2 and 2.3 (NBE and TBE (~ 0.2 M) as the acceptor) show that after 5 minute at 150 °C catalyst **1** dehydrogenates not only with much faster rate but also it is selective at the terminal position than other two catalysts. When 0.47 M of TBE was used, catalyst **1** took only 1 hour at 150 °C to consume 95 % of TBE and produce ~ 0.45 M of octenes, while (^{iPr4}PCP)IrH_4 produced 0.26 M of octenes and (^{tBu4}PCP)IrH_4 only 0.07 M of octenes (Table 2.4). (^{tBu3Me}PCP)IrH_4 (1) catalyst remain active even at high concentration of acceptor (~ 1.1 M of NBE), while (^{t}Bu4PCP)IrH_4 loses its catalytic activity. In case of the (^{iPr4}PCP)IrH_4 catalyst, NBE polymerizes at this high concentration (Table 2.5). Dehydrogenation rate in high concentration of acceptor was slower than low concentration of acceptor, because high concentration of alkene (acceptor and octenes) shifts the equilibrium to (PCP)Ir(alkene).

Not only does (^{tBu3Me}PCP)IrH_4 (**1**) dehydrogenate *n*-octane in much faster rate or can survive high concentration of acceptor; it can also be recycled and can be used up to 4th cycles. 1 mM catalyst **1** produces 1.5 M octenes in just 4.5 h (Table 2.6). All three catalysts gave kinetic selectivity for dehydrogenation of *n*-octane at the terminal position.

However, 1-octene undergoes isomerization and internal alkenes soon became the major products.

Table 2.2 Transfer dehydrogenation of n-octane using NBE (~ 0.2 M) as the acceptor (150 °C).[a]

Catalyst (1mM) 150 °C	Time (min)	[NBE]	1-octene	2-trans-octene	2-cis octene	Other	Loss of NBE	Total
($^{t\text{Bu4}}$PCP)IrH_4	0	197						
	5	180	12	5	0	0	17	17
	10	174	11	10	2	0	23	23
	20	168	7	15	5	0	29	27
	30	159	6	22	7	4	38	39
($^{i\text{Pr4}}$PCP)IrH_4	0	188						
	5	143	21	16	8	0	45	45
	10	120	19	33	13	3	68	68
	20	77	24	54	25	7	111	110
	30	30	17	87	39	13	158	156
($^{t\text{Bu3Me}}$PCP)IrH_4(**1**)	0	191						
	5	121	31	28	11	4	70	74
	10	84	20	55	22	10	107	107
	20	0	13	92	37	48	191	190
	30	0						

[a][catalyst] = 1.0 mM, Product concentrations (mM) measured by GC.

Table 2.3 Transfer dehydrogenation of n-octane using TBE (~ 0.2 M) as the acceptor (150 °C).[a]

Catalyst (1mM) 150 °C	Time (min)	[TBE]	1-octene	2-trans-octene	2-cis octene	Other	Loss of TBE	Total
(^{tBu4}PCP)IrH_4	0	186						
	5	164	8	8	3	0	22	19
	10	153	11	15	5	0	33	31
	20	129	18	22	9	4	57	53
	30	121	15	28	13	4	65	60
(^{iPr4}PCP)IrH_4	0	200						
	5	140	30	17	11	0	60	58
	10	107	28	36	22	0	93	86
	20	75	25	57	33	8	125	123
	30	43	19	76	42	15	157	152
(^{tBu3Me}PCP)IrH_4(**1**)	0	208						
	5	126	23	35	14	10	82	82
	10	74	14	62	26	24	134	126
	20	10	6	79	33	77	198	195

[a][catalyst] = 1.0 mM. Product concentrations (mM) measured by GC.

Table 2.4 Transfer dehydrogenation of n-octane using TBE (~ 0.5 M) as the acceptor (150 °C).[a]

Catalyst (1mM) 150 °C	Time (min)	[TBE]	1-octene	2-trans-octene	2-cis octene	Other	Loss of TBE	Total
($^{t\text{Bu4}}$PCP)IrH$_4$	0	455						
	5	433	10	4	2	0	22	116
	15	408	21	14	7	0	47	42
	30	391	22	23	11	0	64	56
	60	378	18	32	15	3	77	68
($^{i\text{Pr4}}$PCP)IrH$_4$	0	476						
	5	426	28	11	7	0	50	46
	15	371	42	38	26	0	105	106
	30	316	38	66	45	6	160	156
	60	206	31	126	74	34	270	265
($^{t\text{Bu3Me}}$PCP)IrH$_4$	0	475						
	5	398	31	31	12	0	77	74
	15	300	26	87	35	23	175	171
	30	214	21	121	51	59	261	252
	60	22	10	137	59	240	453	446

[a][catalyst] = 1.0 mM. Product concentrations (mM) measured by GC.

Table 2.5 Transfer dehydrogenation of n-octane using NBE (~ 1.1 M) as the acceptor (150 °C).[a]

Catalyst (1mM) 150 °C	Time (**h**)	[NBE]	1-octene	2-trans-octene	2-cis octene	Other	Loss of NBE	Total
($^{t\text{Bu4}}$PCP)IrH$_4$	0	1146						
	1	1099	29	12	6	0	47	47
	3	1064	46	27	9	3	82	85
	5	1047	45	35	11	5	99	96
	7	1027	44	47	14	9	119	114
($^{i\text{Pr4}}$PCP)IrH$_4$	0	1128						
	1	1037	45	22	16	0	91	83
	3	936	53	73	45	6	192	184
	5	913	52	89	53	14	215	208
	7[b]							
($^{t\text{Bu3Me}}$PCP)IrH$_4$	0	1142						
	1	735	66	192	73	77	407	408
	3	316	56	318	140	316	826	830
	5	153	46	338	154	441	989	979
	7	101	41	319	147	530	1041	1037

[a][catalyst] = 1.0 mM. Product concentrations (mM) measured by GC. [b]At high concentration NBE was polymerized in presence of ($^{i\text{Pr4}}$PCP)IrH$_4$

Table 2.6 Recycling the catalyst: Transfer dehydrogenation of *n*-octane using NBE (~ 0.5 M) as the acceptor (multiple times) (150 °C).[a]

catalyst (1 mM) ($^{t\text{Bu3Me}}$PCP)IrH$_4$	time (h)	[NBE]	loss NBE	total octenes	1-octene	2-*trans*-octene	2-*cis* octene	other
1st cycle	0	542						
	1.25	8	534	530	12	141	65	304
2nd cycle	0	582						
	1.25	76	506	503	37	216	93	157
3rd cycle	0	514						
	1	220	304	301	53	150	58	40
4th cycle	0	408						
	1	239	169	167	49	67	25	41
5th cycle	0	162						
	1	160						2

[a][catalyst] = 1.0 mM. Product concentrations (mM) measured by GC.

When 1-hexene was used as the hydrogen acceptor, rates were somewhat slower but the same order of activity among the catalysts was obtained (Table 2.7). This combination of experimental substrates (*n*-octane/1-hexene) probably resembles the computational choice (*n*-butane/1-butene) most closely. (However, NBE and TBE are generally preferred as acceptors for studies of this type, since isomerization of □-olefin acceptors introduces an additional complicating factor.)

Table 2.7 Transfer dehydrogenation of *n*-octane using 1-hexene acceptor (150 °C).[a]

catalyst (1 mM) (approx initial [1-hex].)	time (min)	[1-hex]	2-*trans* hex	2-*cis*-hexene	hexane	total octenes	1-octene	2-*trans*-octene	2-*cis* octene
($^{t\text{Bu4}}$PCP)IrH$_4$	0	464							
[1-hex] = 0.45 M	10	437	10	4	9	7	6	1	0
	15	424	20	7	12	11	10	1	0
	30	342	70	23	28	20	16	3	1
($^{t\text{Bu3Me}}$PCP)IrH$_4$	0	470							
[1-hex] = 0.45 M	10	300	81	23	52	48	40	6	2
	15	264	109	32	73	64	49	11	4
	30	141	146	44	120	111	71	29	11

[a][catalyst] = 1.0 mM. Product concentrations (mM) measured by GC.

2.2.3.2 Transfer Dehydrogenation of 4-propylheptane

To test the dehydrogenation capability and selectivity of these pincer catalysts other than *n*-octane, 4-propylheptane was used. Transfer dehydrogenation of 4-propylheptane using NBE acceptor was followed by ^{1}H NMR. In 0.5 mL *p*-xylene-d$_{10}$, 4-propylheptane (2 M), ~ 0.4 M NBE, 1 mM catalyst was taken in a J-young tube. The NMR tube was heated at 150 °C and the reaction was monitored by ^{1}H NMR using

hexamethyldisiloxane as standard. Results are summarized in Table 2.8. From the data it's clear that catalyst **1a** is the most effective and selective dehydrogenation catalyst.

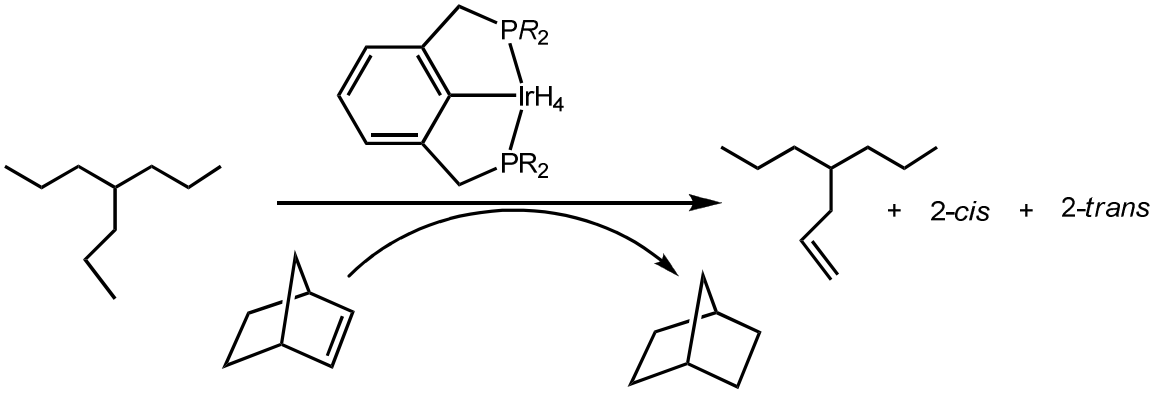

Scheme 2-7 Transfer dehydrogenation of 4-propylheptane catalyzed by (^{R4}PCP)IrH$_4$

Table 2.8 Transfer dehydrogenation of 4-propylheptane using NBE as the acceptor (150 °C).[a]

Catalyst (1mM) 150 °C	[NBE]	Time (min)	1-alkene	2-*trans*	2- *cis*	Total
($^{t\text{Bu4}}$PCP)IrH$_4$	470	10	20	0	0	20
		40	30	4	3	37
		90	65	20	15	100
		140	71	38	31	140
		280	75	70	65	210
($^{i\text{Pr4}}$PCP)IrH$_4$	420	10	51	**7**	**6**	64
		40	90	41	33	164
		90	93	92	78	263
		140	93	142	114	349
		160	80	146	145	371
($^{t\text{Bu3Me}}$PCP)IrH$_4$	475	10	58	17	11	86
		40	66	49	43	155
		90	55	144	143	342
		140	35	208	187	430
		160	28	240	205	473

[a][catalyst] = 1.0 mM. Product concentrations (mM) measured by GC

2.2.3.3 Resting state of the catalyst during transfer dehydrogenation

The catalytic transfer-dehydrogenation of *n*-octane by **1**, using 1-hexene, NBE, or TBE as the hydrogen acceptor, was studied by ^{31}P and ^{1}H NMR under conditions comparable to those employed in the catalytic studies described above but with a higher concentration, 20 mM, of catalyst **1**. The NMR spectrum reveals a single major resting state, which is apparently independent of the nature of the hydrogen acceptor. Although we have been unable to isolate the observed complex species, the observations described below strongly indicate that it is the π-bound 1-alkene complex, (^{tBu3Me}PCP)Ir(1-alkene), complex **1a** (either 1-hexene or 1-octene), in accord with the results of the electronic structure calculations (Table 1.1) which predict that such complexes would form the resting state in the catalytic cycle.

Complex **1a** is observed when 1-alkene is added to solutions of **1**, or when other hydrogen acceptors react in the presence of *n*-alkane resulting in formation of 1-alkene, in accord with the proposed formulation as (^{tBu3Me}PCP)Ir(1-alkene). Thus, the reaction of **1** with 1-octene in *p*-xylene-d_{10} or COA solvent gives the same species (by ^{31}P and ^{1}H NMR) as observed in *n*-alkane solvent, which is consistent with lack of direct participation of solvent and the proposed formulation as (^{tBu3Me}PCP)Ir(1-alkene). Conversely, the reaction of **1** with hydrogen acceptors that are not 1-alkenes, NBE or TBE, in the absence of *n*-alkane (in either COA or *p*-xylene-d_{10} solvent) gives species that are distinct from **1a** (presumably these are the NBE and TBE adducts, respectively).

A solution of **1a** was formed under the catalytic conditions described above. Volatiles were removed and the residue was dissolved in *p*-xylene-d_{10}. ^{31}P and ^{1}H NMR showed that species **1a** was still present. When CO (1 atm) was added to the solution, the

formation of (^{tBu3Me}PCP)Ir(CO) (^{31}P and ^{1}H NMR) and free 1-alkene (^{1}H NMR) were observed.

2.2.3.4 Transfer Dehydrogenation of cyclooctane using NBE and 1-hexene acceptor

To find out the resting state of these pincer catalysts in transfer dehydrogenation of cyclooctane using NBE as acceptor, the following experiment was done. Transfer dehydrogenation of *n*-undecane was done with 28 mM of pincer catalysts using 0.5 M NBE at 55 °C (Scheme 2-8). Reaction was monitored by NMR and product concentrations (mM) were measured by NMR, and the results are shown in Table 2.9. For both (^{t}Bu4PCP)IrH_4 and (^{t}Bu3MePCP)IrH_4 after 6 h, ^{31}P NMR spectrum indicates only (^{R4}PCP)Ir(NBE) bound species. The dehydrogenation rate is slower for (^{t}Bu3MePCP)IrH_4 compare to (^{t}Bu4PCP)IrH_4 at 55 °C due to NBE binds more strongly to (^{t}Bu3MePCP)IrH_4.

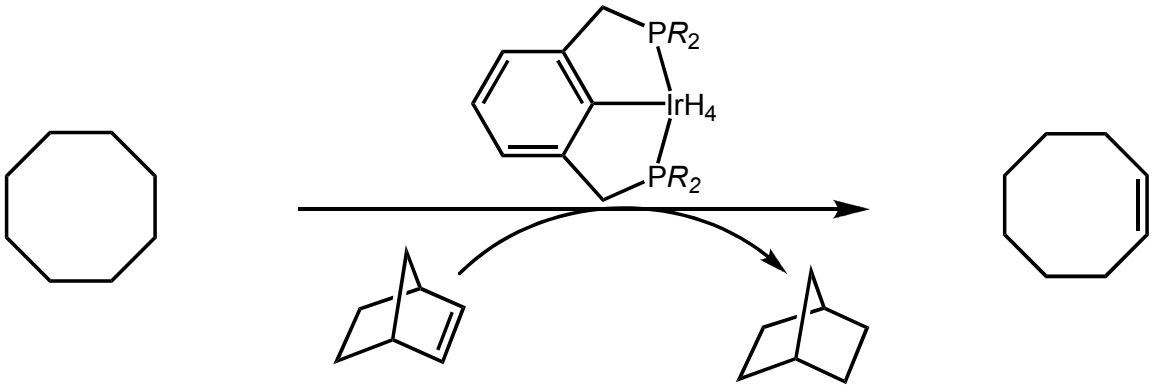

Scheme 2-8 Transfer dehydrogenation of cyclooctane using NBE

Table 2.9 Transfer dehydrogenation of cyclooctane using NBE (0.5 M) as acceptor[a]

Catalyst (28 mM)	Time (h)	Temp (55 °C)	COE (mM)
(^{t}Bu4PCP)IrH$_4$	0.5		4
	1		10
	2		23
	4		37
	6		51
(^{t}Bu3MePCP)IrH$_4$	0.5		6
	1		9
	4		17
	9		34

[a]Product concentrations (mM) measured by NMR

Transfer dehydrogenation of COA was performed with 28 mM of pincer catalysts using 0.5 M 1-hexene at 55 °C (Scheme 2-9), which is the same condition as using NBE acceptor (Scheme 2-8). Reaction was monitored by ^{1}H and ^{31}P NMR and product concentrations (mM) were measured by NMR and the results are shown in Table 2.10. In the ^{31}P NMR spectrum in both catalytic systems only 1-hexene bound complex was observed throughout the reaction time.

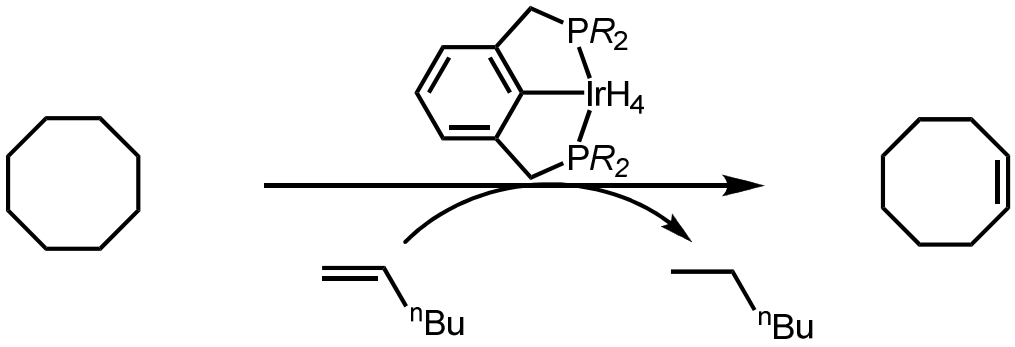

Scheme 2-9 Transfer dehydrogenation of cyclooctane using 1-hexene

Table 2.10 Transfer dehydrogenation of cyclooctane using 1-hexene as the acceptor[a]

Catalyst (28 mM)	Time (h)	Temp (55 °C)	COE (mM)
(^{t}Bu4PCP)IrH$_4$	2		<0.5
	3		8
	4		11
	5		15
	7		20
	10		34
(^{t}Bu3MePCP)IrH$_4$	0.5		38
	1		48
	2		66
	4		142
	4.5		163
	5		197

[a][catalyst] = 1.0 mM. Product concentrations (mM) measured by GC

2.2.4 Acceptorless dehydrogenation using different pincer catalyst

Economically acceptorless dehydrogenation of alkanes has potential as it does not require any sacrificial acceptor (eq. 10). But direct dehydrogenation of alkanes is endothermic and has high activation barrier. In presence of acceptor, hydrogenation of acceptor (which is exothermic), lower the overall endothermicity of the dehydrogenation process.[27]

In 1997, our group reported that (^{t}Bu4PCP)IrH$_4$ was highly active catalyst in acceptorless dehydrogenation of alkane.[14] In acceptorless dehydrogenation of COA, using 1 mM (^{t}Bu4PCP)IrH$_4$, 144 mM of cyclooctene (COE) was observed after refluxing

44 hours. When an alkane with higher boiling point, such as cyclodecane (CDA, b.p. 201 °C), was used, 170 mM cyclodecenes was observed after 4 hours reflux.[14]

2.2.4.1 Acceptorless dehydrogenation of cyclodecane using different pincer catalyst

Acceptorless dehydrogenation of cyclodecane was carried out with 1 mM of pincer catalysts (Scheme 2-10) at two different temperatures under constant argon flow, so that byproduct H_2 can be removed from the reaction mixture and equilibrium can favor the products. Product concentrations (mM) measured by GC and the results are shown in Table 2.11 and 2.12.

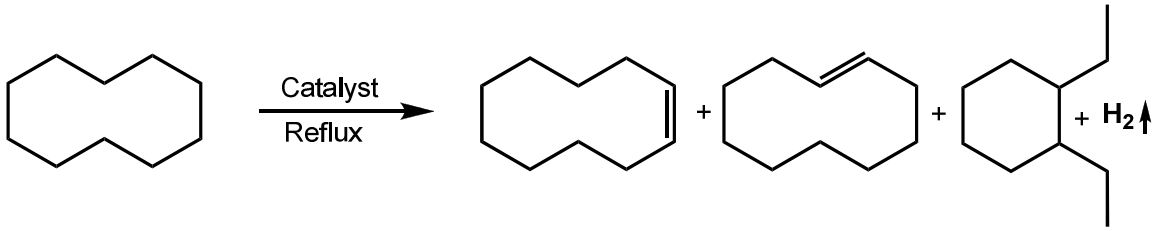

Scheme 2-10 Acceptorless dehydrogenation of cyclodecane catalyzed by (^{R4}PCP)IrH_4

Table 2.11 Acceptorless-dehydrogenation of cyclodecane (CDA, b.p. = 201 °C)[a] [b]

Catalyst (1 mM)	Time (h)	*cis*-CDE	*trans*-CDE	DEC	Total
($^{i\text{Pr4}}$PCP)IrH$_4$	1	115	27	4	146
	2	175	34	7	216
	4	212	399	10	261
	7	218	45	11	274
	18	279	53	12	344
($^{t\text{Bu3Me}}$PCP)IrH$_4$	1	152	24	7	183
	2	199	40	5	244
	4	245	55	15	315
	7	261	59	16	336
	23	288	53	17	358

[a] Oil bath temp. = 210 °C, DEC = diethylcyclohexane, Total = concentration of *cis*-CDE + *trans*-CDE + DEC. [b][catalyst] = 1.0 mM. Product concentrations (mM) measured by GC.

Table 2.12 Acceptorless-dehydrogenation of cyclodecane (CDA, b.p. = 201 °C)[a] [b]

Catalyst(1mM)	Time(h)	*cis*-CDE	*trans*-CDE	DEC	Total
($^{t\text{Bu4}}$PCP)IrH$_4$	1	49	49	3	101
	2	104	61	4	169
	4	209	82	7	298
	9	325	72	11	408
	15	341	72	13	426
($^{i\text{Pr4}}$PCP)IrH$_4$	1	153	31	12	196
	2	226	44	26	296
	4	301	62	37	400
	9	410	86	96	592
	23	577	126	194	897
($^{t\text{Bu3Me}}$PCP)IrH$_4$ (**1**)	1	388	65	36	489
	2	550	111	75	736
	4	679	149	101	929
	9	807	163	119	1089

[a] Oil bath temp. = 230 °C, DEC = diethylcyclohexane, Total = concentration of *cis*-CDE + *trans*-CDE + DEC. [b][catalyst] = 1.0 mM. Product concentrations (mM) measured by GC.

For the acceptorless dehydrogenation of cyclodecane, the same order of activity among the catalysts was found as for transfer-dehydrogenation, although the differences between the three catalysts were much less pronounced. Given the reversibility of this dehydrogenation reaction, we suspect that loss of H_2 from solution plays an important role in the kinetics of the observed reaction; in that case the nature of the catalyst is accordingly less important as one approaches equilibrium conditions in solution. In addition, under conditions where the resting state is the dihydride and loss of H_2 is rate-determining,[26,28] catalyst **1** would offer no steric advantage. As a result, when the oil bath temperature was kept at 210 °C, the rate of the acceptorless reaction (Table 2.11) was not fast compared to when the oil bath temperature was at 230 °C (Table 2.12). As shown in Table 2.12, after 1 hour, (^{iPr4}PCP)IrH_4 produced 196 mM of product where as (^{tBu3Me}PCP)IrH_4 and (^{tBu4}PCP)IrH_4 produced 489 mM and 101 mM respectively. After 9 hours, (^{iPr4}PCP)IrH_4 and (^{tBu3Me}PCP)IrH_4 produced a total of 592 mM and 1089 mM products respectively, while (^{tBu4}PCP)IrH_4 after 15 hour produced 426 mM of product. These results indicate that (^{tBu3Me}PCP)IrH_4 is the most active catalyst among the three catalysts for the acceptorless dehydrogenation of cyclodecane.

2.2.4.2 Acceptorless dehydrogenation of *n*-undecane

Acceptorless dehydrogenation of *n*-undecane was done with 1 mM of pincer catalysts (Scheme 2-11), under the same conditions used for cyclodecane. Product concentrations (mM) was measured by GC and the results are shown in Table 2.13.

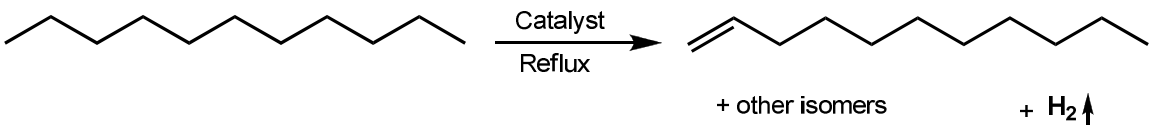

Scheme 2-11 Acceptorless dehydrogenation of *n*-undecane catalyzed by (^{R4}PCP)IrH$_4$

Table 2.13 Acceptorless dehydrogenation of *n*-undecane (b.p.= 196 °C)[a]

catalyst (1 mM)	time (h)	1-undecene	2-*trans*-undecene	2-*cis*-undecene	Total
(^{tBu4}PCP)IrH$_4$	1	12	6	2	20
	2	17	9	3	29
	4	33	12	4	49
	8	30	18	6	54
(^{iPr4}PCP)IrH$_4$	1	10	6	2	18
	2	11	7	2	20
	4	11	7	3	21
	8	12	8	3	23
(^{tBu3Me}PCP)IrH$_4$	1	18	12	3	33
	2	22	17	5	44
	4	30	21	6	57
	8	28	35	10	63

[a]Oil bath temp. = 230 °C, [catalyst] = 1.0 mM. Product concentrations (mM) measured by GC.

All three catalysts show the low turnover number in acceptorless dehydrogenation of *n*-undecane probably because at high temperature in the presence of linear olefin decomposition rates of the catalysts also increased. After 8 hour almost all the catalysts decomposed and black precipitate was formed at the bottom and surface of the reaction flask. To understand the low activity of these pincer catalysts in acceptorless dehydrogenation of *n*-undecane, decomposition of these catalysts in presence of 1-undecene was studied by NMR spectroscopy. Catalysts (20 mM) was dissolved in *p*-xylene-d_{10} containing 0.1 M of 1-undecene in sealed NMR tubes and the tube was heated at 230 °C and monitored by NMR spectroscopy. All the catalyst were almost

decomposed after 10 hour heating and for (^{tBu4}PCP)IrH_4, ^{31}P NMR spectrum indicates inequivalent phosphorous atoms, and in case of other two catalyst ^{31}P NMR shows complex spectra.

2.2.5 Competition transfer dehydrogenation experiments: *n*-octane vs. COA

A competitive experiment was done with mixture of 1:1 ratio of *n*-octane and cyclooctane using 20 mM pincer catalyst at 55 °C using NBE acceptor. The reaction was monitored by ^{1}H and ^{31}P NMR spectroscopy. After 20 minute heating at 55 °C, CO was added to the solution to remove the bound 1-octene from catalyst and concentration of COE and octenes ware measured by ^{1}H NMR spectroscopy. Competition experiments revealed that the kinetic preference for dehydrogenation of *n*-octane versus cyclooctane was 5.7:1 for (^{tBu4}PCP)Ir versus 2.3:1 for complex **1**; this preference exists in spite of the very large thermodynamic effect favoring the dehydrogenation of cyclooctane.[29,30]

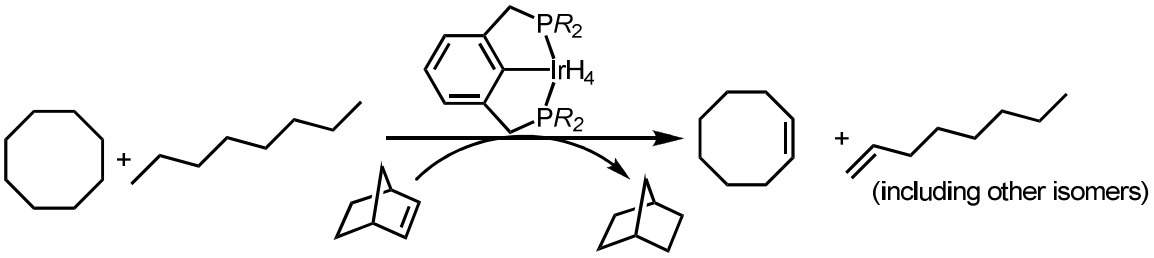

Scheme 2.12 Competition experiments: *n*-octane is more reactive than COA

Table 2.14 Competition experiments: *n*-octane vs. COA[a]

Catalyst	[Octene]/[COE]
(^{tBu4}PCP)IrH$_4$	5.7
(^{tBu3Me}PCP)IrH$_4$	2.3

[a]Product concentrations (mM) measured by ^{1}H NMR spectroscopy.

2.2.6 Alkane metathesis

2.2.6.1 Alkane metathesis of *n*-hexane using pincer iridium and Schrock's catalyst[31]

Brookhart and Goldman have recently reported that alkane dehydrogenation catalysts, acting in tandem with olefin metathesis catalysts, can catalyze the metathesis of n-alkanes.[32] Catalysts **1** acting in tandem with the Schrock olefin metathesis catalyst Mo(NAr)(CHCMe$_2$Ph)(OR$_{F6}$)$_2$ (Ar = 2,6-i-Pr$_2$C$_6$H$_3$; OR$_{F6}$ = OCMe(CF$_3$)$_2$) (**3**), give significantly greater rates than obtained with (^{tBu4}PCP)IrH$_4$ (Table 2.15).

Table 2.15 Alkane metathesis of *n*-hexane[a]

Ir catalyst (10 mM)	time (h)	C2	C3	C4	C5	C7	C8	C9	C10	C11	C12	C13	C14	Total
(^{tBu4}PCP)IrH$_4$	2	20	19	13	39	17	3	3	29	1	0	0	0	144
	8	40	39	31	93	49	8	10	114	4	1	1	2	391
(^{iPr4}PCP)IrH$_4$	21	12	140	83	229	137	41	51	75	11	3	2	1	786
(^{tBu3Me}PCP)IrH$_4$	1	5	29	23	63	46	18	27	13	1	0	0	0	208
	3	11	78	62	154	120	50	70	38	3	2	1	1	574
	8	19	160	114	252	167	70	92	62	7	4	3	1	936

[a](10 mM Ir, 6.4 mM Mo, 20 mM TBE in *n*-hexane (7.6 M) at 125 °C) ; Product concentrations (mM) measured by GC.

2.2.6.2 Alkane metathesis of cyclooctane using pincer iridium and Schrock's catalyst[31]

The success of with *n*-alkanes metathesis by Brookhart and Goldman group suggested the possibility of catalyzing reactions of cycloalkanes analogous to those known for cycloolefins. Metathesis of cycloalkanes offers the prospect of facile synthesis of large saturated rings which, upon partial oxidation, are important building blocks for pharmaceutical intermediates, fragrances, corrosion inhibitors and polymers. Cyclooctane (COA) is a commonly used substrate in studies of alkane dehydrogenation,[33,34] while cyclooctene is a commonly used monomer for ROMP. Thus COA seemed an ideal starting point for the investigation of catalytic cycloalkane metathesis based on tandem dehydrogenation-olefin-metathesis.

Pincer-iridium catalysts,[30] as well as **3**, readily catalyze olefin isomerization (double-bond migration) under the conditions of these experiments. If the ring-opened intermediate (Scheme 2-13) isomerizes to an internal olefin, subsequent ring-closing would give smaller, less strained rings.

As seen in Table 2.16, the combination of catalysts ($^{t\text{Bu3Me}}$PCP)IrH_4 (**1**) and **3** gives significantly greater yields of ring-expanded products, in shorter reaction times, than does catalyst combination ($^{t\text{Bu4}}$PCP)IrH_4 **(2)/3**. [35] Furthermore, catalyst combinations **1/3** offer significantly higher selectivity for $C_{8n}H_{16n}$ products, with very little cycloheptane formed and relatively smaller quantities of cycloalkanes with carbon numbers that are not multiples of 8. These results may suggest that the rate of double by **1** is lower than that by **2**.

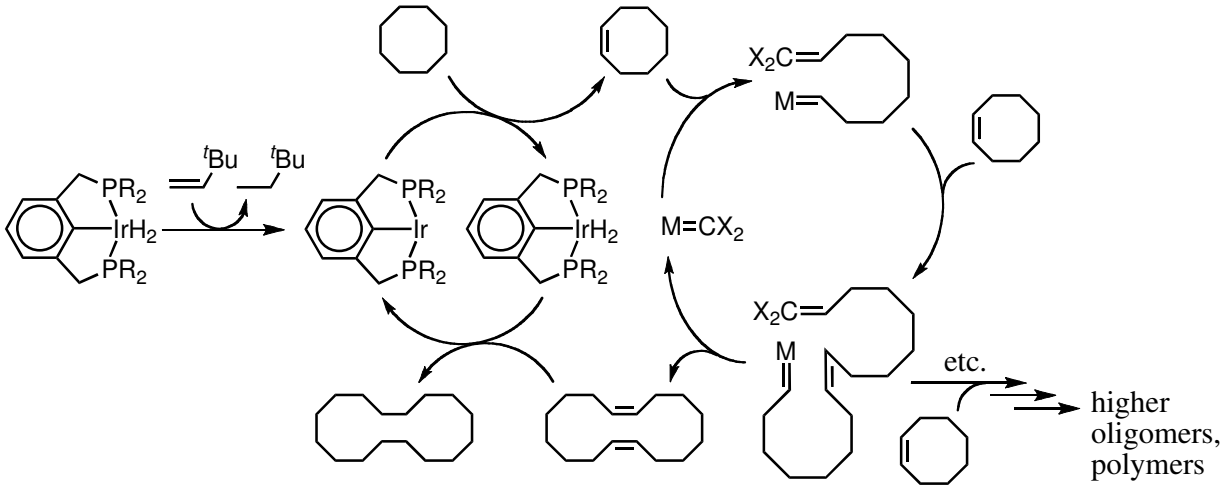

Scheme 2-13 Proposed mechanism of cycloalkane oligomerization

Table 2.16 Results of metathesis of COA by Schrock's catalyst (**3**) and of catalysts 1 or 2, at 125 °C. Distribution of products (weight %).[a,b]

			cycloalkanes (% by weight)												
cat.	TBE (mM)	time (h)	C_6	C_7	C_8	C_{15}	C_{16}	C_{17}	C_{24}	C_{32}	C_{33}	C_{40}	sum C_{6-40} prod.	insol. %	% conv. C_8
2[c]	10	24	0.0	1.3	79	0.0	0.7	0.3	0.3	0.2	0.1	0.1	3.8	7.8	21
2[c]	10	72	0.2	2.7	61	0.1	1.9	0.6	0.7	0.4	0.2	0.2	7.8	16	39
2[c]	20	24	0.1	2.7	73	0.1	0.7	0.4	0.3	0.1	0.1	0.1	5.3	11	27
2[c]	20	72	0.3	4.0	47	0.1	3.2	0.7	1.2	0.5	0.2	0.3	11.5	29	53
2[c]	100	24	0.3	5.3	45	0.1	0.7	0.4	0.3	0.1	0.1	0.1	8.2	32	55
2[c]	100	72	0.5	5.6	43	0.1	1.3	0.4	0.6	0.2	0.1	0.1	9.9	33	57
1[d]	20	6	0.1	0.2	41	0.0	14	0.3	9.4	4.6	0.1	2.2	32	4.0	59
1[d]	20	12	0.1	0.3	20	0.0	14	0.3	10	5.6	0.2	2.7	34	10	80

[a] Heating beyond times given did not afford significant additional product. Other ring sizes, formed in lesser amounts, are described in the Supporting Information. [b] insol. = material insoluble in toluene at ambient temperature. [c] C_8H_{16} (0.75 mL, 625 mg); **2** (4.4 mg; 10 mM); **3** (3.7 mg; 6.5 mM). [d] C_8H_{16} (0.75 mL, 625 mg); **1** (4.2 mg; 10 mM); **3** (3.7 mg; 6.5 mM).

2.3 Conclusions

Substitution of one of the four ^{t}Bu groups by a methyl group on (^{tBu4}PCP)Ir catalyst has been studied, both computationally and experimentally, for its effect on catalytic alkane dehydrogenation activity. DFT calculations predict the rate-determining step in the *n*-alkane/1-alkene transfer dehydrogenation cycle to be β-H elimination by ($^{R3R'}$PCP)Ir(*n*-alkyl)(H) (R_3R' = ^{t}Bu$_4$ or ^{t}Bu$_3$Me; modeled with *n*-butane/1-butene substrates). The electronic structure calculations predict that a single Me-for-^{t}Bu substitution has a large favorable energetic effect on this step; the transition state is calculated to be ca. 10 kcal/mol lower for (^{tBu3Me}PCP)Ir(*n*-butyl)(H) than for (^{tBu4}PCP)Ir(*n*-butyl)(H) (relative to the corresponding free (PCP)Ir fragments). However, this stabilizing effect on the overall barrier is predicted to be offset and reduced to ca. 4 kcal/mol by the stronger binding of 1-butene to (^{tBu3Me}PCP)Ir.

(^{tBu3Me}PCP)IrH_4 has been synthesized and isolated and its catalytic activity has been investigated. In accord with the DFT calculations, (^{tBu3Me}PCP)Ir is indeed found to be more active than (^{tBu4}PCP)Ir for catalytic transfer-dehydrogenation. Also in agreement with the calculations, the resting state in *n*-alkane/1-alkene transfer-dehydrogenation by ($^{R3R'}$PCP)Ir is found to be ($^{R3R'}$PCP)Ir(1-alkene) for both (^{tBu3Me}PCP)Ir and (^{tBu4}PCP)Ir.

Thus, computationally it is predicted that the initial Me-for-^{t}Bu substitution on (^{tBu4}PCP)Ir should have a substantial favorable effect on catalytic dehydrogenation activity; this conclusion is supported by experiment. The DFT calculations predict subsequent substitutions to have a smaller effect. This seems to be supported by experiment and reinforced by an increased tendency to form clusters which are presumably inactive.

2.4 Experimental

General Considerations. All reactions were carried out under argon atmosphere using standard Schlenk techniques or in an argon-filled dry box. Anhydrous acetone, hexane and pentane were purchased from Aldrich and were deoxygenated by purging with argon gas. *p*-xylene, *p*-xylene-d_{10} and C_6D_6 were dried using Na/K and collected by vacuum transfer. All solvents (COA, *n*-octane, *n*-hexane) were distilled under vacuum from Na/K alloy. NBE was purified by vacuum sublimation. TBE and 1-hexene were dried under Na/K alloy and vacuum transferred under argon. 300 MHz, 400 MHz or 500 MHz Varian instruments were used for the ^1H, ^{13}C and ^{31}P NMR experiments. The residual peak of the deuterated solvent was used as a reference for ^1H chemical shifts. ^{31}P NMR chemical shifts were referenced to a PMe_3 standard, which appears at –62.1 ppm. PMe_3 internal standard in ^{31}P NMR was employed in determining the yield. (^{tBu4}PCP)IrH_2,[34] (^{iPr4}PCP)IrH_2[15] (PCP= κ^3-2,6-(^{t}Bu$_2$PCH$_2$)$_2$C$_6$H$_3$) was prepared as described in the literature. GC analyses were carried out with a Thermal Focus GC with a flame ionization detector (FID) on the Agilent HP-1 column (100% dimethylpolysiloxane, 30 m length × 0.32 mm ID × 0.25 μm film thickness) or Supelco Petrocol DH column (100m length × 0.25 mm ID × 0.5 μm film thickness). Calibration curves were prepared using standard samples.

Synthesis of P^{t}BuMeCl: t-Butylmethylchlorophosphine was synthesized as reported by Wolfsberger[25] as follows. To 5.0 g (42.8 mmol) of dichloromethylphosphine ($PMeCl_2$, Aldrich) in 100 mL anhydrous THF cooled to −78 °C, 31.44 mL of *tert*-butylmagnesium chloride solution (1.36 M in THF; Aldrich) was added slowly for 30 min and stirred for 1 h. The cooling bath was then removed and stirring was continued at room temperature for an additional 1 h. $^{31}P\{^1H\}$ NMR (THF): δ 118.2 (P^{t}BuMeCl) (60 % yield) and δ 12.2 (P^{t}Bu$_2$Me).

Synthesis of P^{t}BuMeH: To 1.63 g (42.8 mmol) of $LiAlH_4$ in 300 mL anhydrous THF the mixture of P^{t}BuMeCl and P^{t}Bu$_2$Me (described above) was added dropwise under argon atmosphere. 12 h room temperature stirring gave a mixture of HP^{t}BuMe and P^{t}Bu$_2$Me. Pure HP^{t}BuMe was separated out of the mixture by distillation. $^{31}P\{^1H\}$ NMR (THF, 122 MHz): δ –39.5.

Synthesis of 1,3-$C_6H_5(CH_2Br)(CH_2P^tBu_2)$•HBr (3): To 25 g (85 mmol) of 1,3-bis(bromomethyl)benzene (Aldrich) dissolved in 250 mL degassed acetone, 3.2 mL (17 mmol) HP^{t}Bu$_2$ (Aldrich) was added. The mixture was refluxed for 2 h. After the reaction was over, **2** forms a white precipitate and **3** stays in acetone solution along with excess 1,3-bis(bromomethyl)benzene. This solution was concentrated by removing acetone in vacuum and was added slowly to rapidly stirring Et_2O (300 mL). An oily solid formed at the bottom. The solution was stirred well and the supernatant was removed by filtration. The solid was redissolved in acetone and reprecipitated with excess Et_2O and was filtered out again. After repeating this procedure five times all 1,3-

bis(bromomethyl)benzene was removed in Et_2O solution and compound **3** remained as a pure white solid in 85% yield (5.9 g). $^{31}P\{^1H\}$ NMR (acetone-d_6, 122 MHz): δ 34.96 (t, J_{PD} = 72.4 Hz, P^{t}Bu$_2$.HBr). ^1H NMR (acetone-d_6, 300 MHz): δ 8.03 (s, 1H, Ar-*H*), 7.75 (d, J_{HH} = 7.5 Hz, 2H, Ar-*H*), 7.39 (m, 1H, Ar-*H*), 4.71 (s, 2H, CH_2Br), 4.23 (d, J_{PH} = 13.8 Hz, 2H, CH_2P), 1.56 (d, J_{PH} = 16.5 Hz, 18H, P^{t}Bu$_2$).

Synthesis of ^{tBu3Me}PCP-H•2HBr (4): 100 mL HP^{t}BuMe (12.5 mmol) in THF was added to 5 g (12.2 mmol) of **3**, followed by addition of 100 mL acetone (to ensure **3** dissolves entirely in the solution). This mixture was refluxed for 2 h under argon atmosphere and the HBr salt of the ligand (**4**) precipitated as a white solid (5.5 g). $^{31}P\{^1H\}$ NMR (D_2O, 122 MHz): δ 48.09 (t, J_{PD} = 66.7 Hz, P^{t}Bu$_2$, HBr), 27.59 (t, J_{PD} = 73.9 Hz, P^{t}BuMe, HBr).

Synthesis of ^{tBu3Me}PCP-H (5): To 4.0 g of **4** (7.79 mmol) 4.5 mL Et_3N (15.6 mmol) and 100 mL anhydrous hexane was added. This mixture was stirred for 4 days at room temperature. Afterwards the solution was filtered and hexane was removed under vacuum to give 1.22 g (yield: 44.6%) of the ligand precursor **5**. $^{31}P\{^1H\}$ NMR (C_6D_6, 162 MHz): δ 33.37 (s, P^{t}Bu$_2$), -7.27 (s, P^{t}BuMe), ^1H NMR (C_6D_6, 300 MHz): δ 7.46 (s, 1H, Ar-*H*), 7.3 (d, J_{HH} = 7.5 Hz, 1H, Ar-*H*), 7.16 (t, J_{HH} = 7.5 Hz, 1H, Ar-*H*), 7.06 (d, J_{HH} = 7.8 Hz, 1H, Ar-*H*), 2.82 (dd, J_{HH} = 12.9 Hz, J_{PH} = 4.5 Hz, 1H, C*H*HP^{t}BuMe) 2.40 (dd, J_{HH} = 12.9 Hz, J_{PH} = 4.5 Hz, 1H, CH*H*P^{t}BuMe), 2.77 (d, J_{PH} = 2.4 Hz, 2H, CH_2P^{t}Bu$_2$), 1.08 (d, J_{HH} = 9.6 Hz, 18H, P^{t}Bu$_2$), 0.962 (d, J_{PH} = 11.4 Hz, 9H, P^t*Bu*Me), 0.785 (d, J_{PH} = 3.9 Hz, 3H, P^{t}Bu*Me*).

Synthesis of ($^{t\mathrm{Bu3Me}}$PCP)IrHCl (6): To 1.0 g (2.84 mmol) of **5**, 70 mL of toluene and 0.953 g (2.84 mmol) of [Ir(1,5-cyclooctadiene)Cl]$_2$ (Strem) was added. This mixture was refluxed for 1 day under hydrogen atmosphere and the solvent was then removed in vacuum. Compound **6** was extracted from the mixture with pentane, to give 1.57 g purple-red solid after removal of pentane (95% yield). NMR indicates a mixture of two isomers in a ratio of ca. 1.1:1 (the species in higher concentration appeared to give slightly broader peaks in both the ^{1}H and ^{31}P NMR spectra). ^{31}P{^{1}H} NMR (*p*-xylene-d$_{10}$, 202 MHz): δ 69.98 (d, J_{PP} = 345 Hz, P^{t}Bu$_2$), 69.27 (d, J_{PP} = 345 Hz, P^{t}Bu$_2$), 48.94 (d, J_{PP} = 342 Hz, P^{t}BuMe), 43.27 (d, J_{PP} = 346 Hz, P^{t}BuMe), ^{1}H NMR (*p*-xylene-d$_{10}$, 500 MHz): δ 7.16 (m, 1H, Ar-*H*), 7.08 (m, 1H, Ar-*H*), 7.04 (m, 2H, Ar-*H*), 6.91(m, 2H, Ar-*H*), 3.12 (m, 6H, from two isomers, C*H*$_2$P^{t}Bu$_2$ and C*H*HP^{t}BuMe), 2.69 (m, 2H, from two isomers, CH*H*P^{t}BuMe), 1.41 (d, J_{PH} = 8 Hz, 6H, from two isomers, PMe), 1.32 (m, 36H, from two isomer, P^{t}Bu$_2$), 1.22 (d, ^{t}Bu, J_{PH} = 14 Hz, 9H, minor isomer, P^t*Bu*Me), 1.09 (d, ^{t}Bu, J_{PH} = 14 Hz, 9H, major isomer, P^t*Bu*Me), -36.88 (broad, 1H, major isomer, Ir-H), -41.54 (t, J_{PH} = 14.25 Hz, minor isomer, Ir-H). ^{13}C NMR (C_6D_6, 126 MHz) (isomer with sharper peaks): δ 152.1 (dd, $^2J_{CP}$ = 12.0 Hz, $^3J_{CP}$ = 4.7 Hz, Ar), 149.8 (dd, $^2J_{CP}$ = 12.4 Hz, $^3J_{CP}$ = 4.2 Hz, Ar), 148.8 (dd, $^2J_{CP}$ = 13.3 Hz, $^3J_{CP}$ = 4.8 Hz, Ar), 123.5 (s, Ar), 122.3 (d, J_{CP} = 16.4 Hz, Ar), 121.1 (d, J_{CP} = 15.6 Hz, Ar), 39.4 (d, J_{CP} = 32.6 Hz, PCH$_2$), 38.5 (dd, J_{CP} = 16.4 Hz, $^3J_{CP}$ = 3.5 Hz, P*C*(CH$_3$)$_3$), 35.9 (d, J_{CP} = 29.6 Hz, PCH$_2$), 35.1 (dd, J_{CP} = 18.2 Hz, $^3J_{CP}$ = 4.0 Hz, P*C*(CH$_3$)$_3$), 32.9 (dd, J_{CP} = 25.6 Hz, $^3J_{CP}$ = 4.2 Hz, P*C*(CH$_3$)$_3$), 30.2 (dd, $^2J_{CP}$ = 3.6 Hz, $^4J_{CP}$ = 1.3 Hz, PC(*C*H$_3$)$_3$), 29.6 (dd, $^2J_{PC}$ = 3.6 Hz, $^4J_{CP}$ = 1.1 Hz, PC(*C*H$_3$)$_3$), 27.2 (dd, $^2J_{CP}$ = 3.7 Hz, $^4J_{CP}$ = 1.0 Hz, PC(*C*H$_3$)$_3$), 10.2 (dd, J_{CP} = 26.5 Hz,

$^3J_{CP}$ = 2.5 Hz, PCH_3). For the other isomer, with slightly broader peaks, the ^{13}C NMR shows peaks close to those of the isomer with sharper peaks.

Synthesis of (^{tBu3Me}PCP)IrH$_4$ (1). 0.7 g (1.2 mmol) of **6** was dissolved in 200 mL pentane. 1.2 mL $LiBEt_3H$ (1 M in THF 1.2 mmol) was added slowly at room temperature under H_2 atmosphere. The solution changed color from red to light brown and some precipitate formed. The solution was stirred for 1 day at room temperature under H_2 atmosphere and the precipitate was removed by filtration. After removing the solvent in vacuum, 0.49 g (yield: 74%) of compound **1** was isolated as a brown solid. $^{31}P\{^1H\}$ NMR (*p*-xylene-d_{10}, 202 MHz): δ 72.84 (d, J_{PP} = 327 Hz, P^{t}Bu$_2$) 33.58 (d, J_{PP} = 327 Hz, P^{t}BuMe), ^1H NMR (*p*-xylene-d_{10}, 400 MHz): δ 7.11 (m, 1H, Ar-*H*), 7.09 (m, 2H, Ar-*H*), 3.38 (m, 2H, $CH_2P^tBu_2$), 3.31 (m, 1H, CHP^{t}BuMe), 3.10 (m, 1H, CHP^{t}BuMe), 1.52 (dd, J_{PH} = 9.5 Hz, J_{PH} = 3 Hz, 3H, PMe), 1.19 (d, J_{PH} = 12.8 Hz, 9H, $PC(CH_3)_3$), 1.17 (d, J_{PH} = 12.8 Hz, 9H, $PC(CH_3)_3$), 1.05 (d, CH_3, J_{PH} = 14 Hz, 9H, P^t*Bu*Me), -9.02 (t, J_{PH} = 9.9 Hz, $Ir(H)_4$). ^{13}C NMR (C_6D_6, 126 MHz): δ 151.9 (m, Ar), 149.52 (dd, $^2J_{CP}$ = 10.8 Hz, $^3J_{CP}$ = 4.7 Hz, Ar), 147.3 (dd, $^2J_{CP}$ = 11.0 Hz, $^3J_{CP}$ = 4.7 Hz, Ar), 123.7 (s, Ar), 121.5 (d, J_{CP} = 15.6 Hz, Ar), 121.2 (d, J_{CP} = 15.5 Hz, Ar), 45.6 (d, J_{CP} = 35.7 Hz, PCH_2), 41.7 (d, J_{CP} = 30.5 Hz, PCH_2), 33.4 (dd, J_{CP} = 18.7 Hz, $^3J_{CP}$ = 4.0 Hz, P*C*$(CH_3)_3$), 32.8 (dd, J_{CP} = 19.6 Hz, $^3J_{CP}$ = 4.4 Hz, P*C*$(CH_3)_3$), 30.1 (d, J_{CP} = 3.5 Hz, PC(*C*$H_3)_3$), 29.6 (d, J_{PC} = 3.6 Hz, PC(*C*$H_3)_3$), 27.6 (dd, J_{CP} = 28.9 Hz, $^3J_{CP}$ = 4.5 Hz, P*C*$(CH_3)_3$), 26.1 (d, J_{CP} = 4.7 Hz, PC(*C*$H_3)_3$), 18.4 (dd, J_{CP} = 28.1 Hz, $^3J_{CP}$ = 4.3 Hz, PCH_3). Elemental analysis experimental (theoretical) in %: C: 46.22 (46.11), P: 11.30 (11.34), H: 7.61 (7.5).

(^{t}Bu3MePCP)Ir(CO): To a *p*-xylene-d_{10} solution of 5 mg (^{tBu3Me}PCP)IrH_4 (**1**; 9 μmol) in a J-Young tube, 1 atmosphere CO was added. An immediate color change from red to yellow was observed. The solvent was removed and crystals were obtained from hexane solution. $^{31}P\{^{1}H\}$ NMR (*p*-xylene-d_{10}, 202 MHz): δ 84.2 (d, J_{PP} = 288 Hz, P^{t}Bu$_2$), 51.3 (d, J_{PP} = 288 Hz, P^{t}BuMe), ^{1}H NMR (*p*-xylene-d_{10}, 500 MHz): δ 7.07 (m, 2H, Ar-*H*), 7.03 (m, 1H, Ar-*H*), 3.28 (m, 2H, CH$_2$P^{t}Bu$_2$), 3.01 (m, 1H, CHP^{t}BuMe), 2.80 (m, 1H, CHP^{t}BuMe), 1.31 (d, J_{PH} = 9.5 Hz, 3H, PMe), 1.23 (d, J_{PH} = 14 Hz, 9H, P^{t}*Bu*Me), 1.08 (t, CH_3, J_{PH} = 16.7 Hz, 18H, P^{t}Bu$_2$). IR: ν_{CO}(C_6H_6 solution) 1920 cm^{-1} (cf. 1917 cm^{-1} measured for (^{tBu4}PCP)Ir(CO) in C_6H_6 solution).

(^{t}Bu3MePCP)Ir(1-hexene) (1a). To a *p*-xylene-d_{10} solution of 5 mg (^{tBu3Me}PCP)IrH_4 (9.1 μmol) in a J-Young tube, 1-hexene 4.5μL (36 μmol) was added at room temperature. After 30 min, solvent was removed in vacuum and the resulting complex was characterized by NMR. $^{31}P\{^{1}H\}$ NMR (*p*-xylene-d_{10}, 202 MHz): δ 64.1 (d, J_{PP} = 353 Hz, P^{t}Bu$_2$), 40.8 (d, J_{PP} = 353 Hz, P^{t}BuMe), ^{1}H NMR (*p*-xylene-d_{10}, 500 MHz): δ 7.29 (d, J_{HH} = 7 Hz, 1H, Ar-*H*), 7.20 (d, J_{HH} = 7 Hz, 1H, Ar-*H*), 7.15 (d, J_{HH} = 7 Hz, 1H, Ar-*H*), 4.65 (m, 1H, H_A, Ir-hexene), 3.54 (m, 1H, H_C, Ir-hexene), 3.24 (m, 4H, CH$_2$P^{t}Bu$_2$ and CH$_2$P^{t}BuMe), 2.96 (m, 2H, CH_2, Ir-hexene), 2.77 (dd, J_{HH} = 7.5 Hz, J_{HH} = 1.5 Hz (geminal), 1H, H_B, Ir-hexene), 1.71 (m, 2H, CH_2, Ir-hexene), 1.61 (m, 2H, CH_2, Ir-hexene), 1.50 (dd, J_{PH} = 7.5 Hz, J_{PH} = 2.5 Hz, 3H, PMe), 1.28 (d, J_{PH} = 11 Hz, 9H, P^{t}Bu), 1.24 (d, J_{PH} = 11 Hz, 9H, P^{t}Bu), 1.09 (t, J_{PH} = 7.2 Hz, 3H, CH_3, Ir-hexene), 1.05 (d, J_{PH} = 12.5 Hz, 9H, P^{t}*Bu*Me).

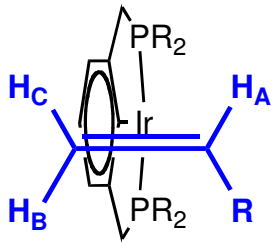

(^{t}Bu4PCP)Ir(1-hexene). To 0.5 mL of a *p*-xylene-d_{10} solution of (^{t}Bu4PCP)IrH_4 (5 mg, 8.3 μmol) in a J-Young tube, 1-hexene (4.1 μL, 33.2 μmol) was added at room temperature. After 30 min solvent was removed in vacuum and the compound was characterized by NMR. $^{31}P\{^{1}H\}$ NMR (*p*-xylene-d_{10}, 202 MHz): δ 59.7 (s, broad, P^{t}Bu$_2$), 57.1 (s, broad, P^{t}Bu$_2$). ^{1}H NMR (*p*-xylene-d_{10}, 500 MHz): δ 7.28 (d, J_{HH} = 8 Hz, 2H, Ar-*H*), 7.16 (t, J_{HH} = 5.5 Hz, 1H, Ar-*H*), 4.52 (m, 1H, H_A, Ir-hexene), 3.78 (dt, J_{HH} = 12 Hz (cis), J_{HH} = 4.5 Hz, 1H, H_C, Ir-hexene), 3.33 (broad, 4H, CH_2P^{t}Bu$_2$), 2.86 (d, J_{HH} = 7.5 Hz, 1H, H_B, Ir-hexene), 2.32 (m, 2H, CH_2, Ir-hexene), 1.68 (m, 2H, CH_2, Ir-hexene), 1.58 (m, 2H, CH_2, Ir-hexene), 1.35 (broad, 18H, P^{t}Bu$_2$), 1.23 (broad, 18H, P^{t}Bu$_2$), 1.09 (t, J_{PH} = 7.2 Hz, 3H, CH_3, Ir-hexene).

Transfer Dehydrogenation. In an argon-filled glove-box, the iridium complexes (1 μmol, taken from a stock solution (1 M) were dissolved in *n*-octane or COA (1 mL) in a flask with a Kontes high-vacuum stopcock and an Ace Glass "Adjustable Electrode Ace-Thred Adapter", which allows removal of small samples (0.5 μL) with a micro-liter syringe. 1-alkene, TBE or NBE was added to the solution as acceptor. The flask was sealed tightly with a teflon plug under an argon atmosphere, and the solution was removed from the glovebox and stirred in an oil bath at the specified temperature. Periodically, the flask was removed from the bath and cooled in an ice bath. An aliquot

was removed from the flask with a 1-μL GC syringe and analyzed by GC. Turnover numbers were calculated for each aliquot using mesitylene which was added as a GC standard.

Acceptorless Dehydrogenation of Alkanes. 1.5 mL of catalyst solution (1 mM) was added in an argon-atmosphere glovebox to a reactor consisting of a 5-mL round-bottom cylindrical flask fused to a water-jacketed condenser (ca. 15 cm). The top of the condenser was fused to two Kontes high-vacuum valves and an Ace Glass "Adjustable Electrode Ace-Thred Adapter". The solution was refluxed in an oil bath held 230 °C (CDA b.p. = 201°C or *n*-undecane b.p = 196 °C). Escape of H_2 is facilitated by a continuous argon stream above the condenser. Turnover numbers were calculated for each aliquot using mestylene as GC standard.

Alkane metathesis. In the glovebox, Ir catalyst (0.021 mmol), Mo catalyst (10 mg, 0.013 mmol) and TBE (5.4 μl, 0.042 mmol) were added to *n*-hexane (2 mL, 15.3 mmol) containing mesitylene (0.034 M as an internal standard). Two aliquots of this solution (0.5 mL each) were transferred to NMR tubes containing capillaries of PMe_3 in mesitylene-d_{12} for reference and locking. The contents were cooled under liquid nitrogen and sealed under vacuum. The tubes were heated (in parallel) in a preheated oven at 125 °C and NMR spectra were recorded at regular intervals. $^{13}C\{^1H\}$NMR spectroscopy permits the resolution of all *n*-alkanes in the range C1-C12 although quantification is significantly less precise than is obtained by GC analysis (but improved by the use of inverse gating). No significant differences between spectra of the two aliquots were

observed. When NMR did not show any further change in the composition of *n*-alkanes (23h), the reaction mixture was analyzed by GC. The seal of one of the tubes was broken, and the solution and headspace were analyzed by GC (using the above-noted methods A and B respectively).

Alkane metathesis: analysis of headspace (methane, ethane and propane). After heating, the contents of the tube were brought to RT and the tube was then cooled under liquid nitrogen and shaken repeatedly to equilibrate and dissolve the gaseous products. The seal was then broken and replaced with a septum and the solution was brought to RT. 200 μl of the headspace was sampled using a gas tight syringe and analyzed by GC. Authentic samples of methane, ethane, and propane were used for calibration.

2.5 References

(1) Crabtree, R. H.; Mihelcic, J. M.; Quirk, J. M. *J. Am. Chem. Soc.* **1979**, *101*, 7738.
(2) Baudry, D.; Ephritikhine, M.; Felkin, H. *J. Chem. Soc., Chem. Comm.* **1980**, 1243.
(3) Baudry, D. E., M.; Felkin, H.; Holmes-Smith, R. *J. Chem. Soc., Chem. Comm.* **1983**, 788.
(4) Burk, M. J.; Crabtree, R. H.; Parnell, C. P.; Uriarte, R. J. *Organometallics* **1984**, *3*, 816.
(5) Sakakura, T.; Tanaka, M. *Chem. Lett.* **1987**, 249.
(6) Nomura, K.; Saito, Y. *Chem. Commun.* **1988**, 161.
(7) Sakakura, T.; Sodeyama, T.; Tokunaga, M.; Tanaka, M. *Chem. Lett.* **1988**, 263.
(8) Maguire, J. A.; Boese, W. T.; Goldman, A. S. *J. Am. Chem. Soc.* **1989**, *111*, 7088.
(9) Spillett, C. T.; Ford, P. C. *J. Am. Chem. Soc.* **1989**, *111*, 1932.
(10) Maguire, J. A.; Goldman, A. S. *J. Am. Chem. Soc.* **1991**, *113*, 6706.
(11) Wang, K.; Goldman, M. E.; Emge, T. J.; Goldman, A. S. *J. Organomet. Chem.* **1996**, *518*, 55.
(12) Gupta, M.; Hagen, C.; Flesher, R. J.; Kaska, W. C.; Jensen, C. M. *Chem. Commun.* **1996**, 2083.
(13) Gupta, M.; Hagen, C.; Kaska, W. C.; Cramer, R. E.; Jensen, C. M. *J. Am. Chem. Soc.* **1997**, *119*, 840.
(14) Xu, W.; Rosini, G. P.; Gupta, M.; Jensen, C. M.; Kaska, W. C.; Krogh-Jespersen, K.; Goldman, A. S. *Chem. Commun.* **1997**, 2273.
(15) Liu, F.; Goldman, A. S. *Chem. Commun.* **1999**, 655.
(16) Liu, F.; Pak, E. B.; Singh, B.; Jensen, C. M.; Goldman, A. S. *J. Am. Chem. Soc.* **1999**, *121*, 4086.
(17) Gupta, M.; Hagen, C.; Kaska, W. C.; Jensen, C. M. *J. Chem. Soc., Chem.Commun* **1997**, 461.
(18) Morales-Morales, D.; Redon, R.; Wang, Z. H.; Lee, D. W.; Yung, C.; Magnuson, K.; Jensen, C. M. *Can. J. Chem.* **2001**, *79*, 823.
(19) Zhang, X.; Fried, A.; Knapp, S.; Goldman, A. S. *Chem. Commun.* **2003**, 2060.
(20) Zhu, K.; Achord, P. D.; Zhang, X.; Krogh-Jespersen, K.; Goldman, A. S. *J. Am. Chem. Soc.* **2004**, *126*, 13044.
(21) A. Ray *PhD thesis, Rutgers University, 2007.*
(22) *Computational studies are done by Yuriy Choliy and Karsten Krogh-Jespersen.*
(23) Renkema, K. B.; Kissin, Y. V.; Goldman, A. S. *J. Am. Chem. Soc.* **2003**, *125*, 7770.
(24) Moulton, C. J.; Shaw, B. L. *J. Chem. Soc., Dalton Trans.* **1976**, 1020.
(25) Wolfsberger, W. *Chemiker-Zeitung* **1986**, *110*, 449.
(26) Krogh-Jespersen, K.; Czerw, M.; Summa, N.; Renkema, K. B.; Achord, P. D.; Goldman, A. S. *J. Am. Chem. Soc.* **2002**, *124*, 11404.
(27) Krogh-Jespersen, K.; Czerw, M.; Goldman, A. S. *In Activation and Functionalization of C-H Bonds* Goldberg, K. I.; Goldman, A. S., Eds.; ACS Symposium Series 885; American Chemical Society: Washington, DC, 2004; pp 216-233.
(28) Krogh-Jespersen, K.; Czerw, M.; Goldman, A. S. *J. Mol. Catal.,A* **2002**, *189*, 95.

(29) Roth, W. R.; Lennartz, H. W. *Chem. Ber.* **1980**, *113*, 1806.
(30) Doering, W. E. R., W. R.; Bauer, F.; Breuckmann, R.; Ebbrecht,; T.; Herbold, M. S., R.; Lennartz, H.-W.; Lenoir, D.; Boese, R. *Chem. Ber.* **1989**, *122*, 1263.
(31) *This reaction was done by Ritu Ahuja*.
(32) Goldman, A. S.; Roy, A. H.; Huang, Z.; Ahuja, R.; Schinski, W.; Brookhart, M. *Science* **2006**, *312*, 257-261.
(33) Burk, M. J.; Crabtree, R. H.; Parnell, C. P.; Uriarte, R. J. *Organometallics* **1984**, *3*, 816-817.
(34) Gupta, M.; Hagen, C.; Flesher, R. J.; Kaska, W. C.; Jensen, C. M. *Chem. Commun.* **1996**, 2083-2084.
(35) Ahuja, R.; Kundu, S.; Goldman, A. S.; Brookhart, M.; Vicente, B. C.; Scott, S. L. *Chem. Commun.* **2008**, 253.

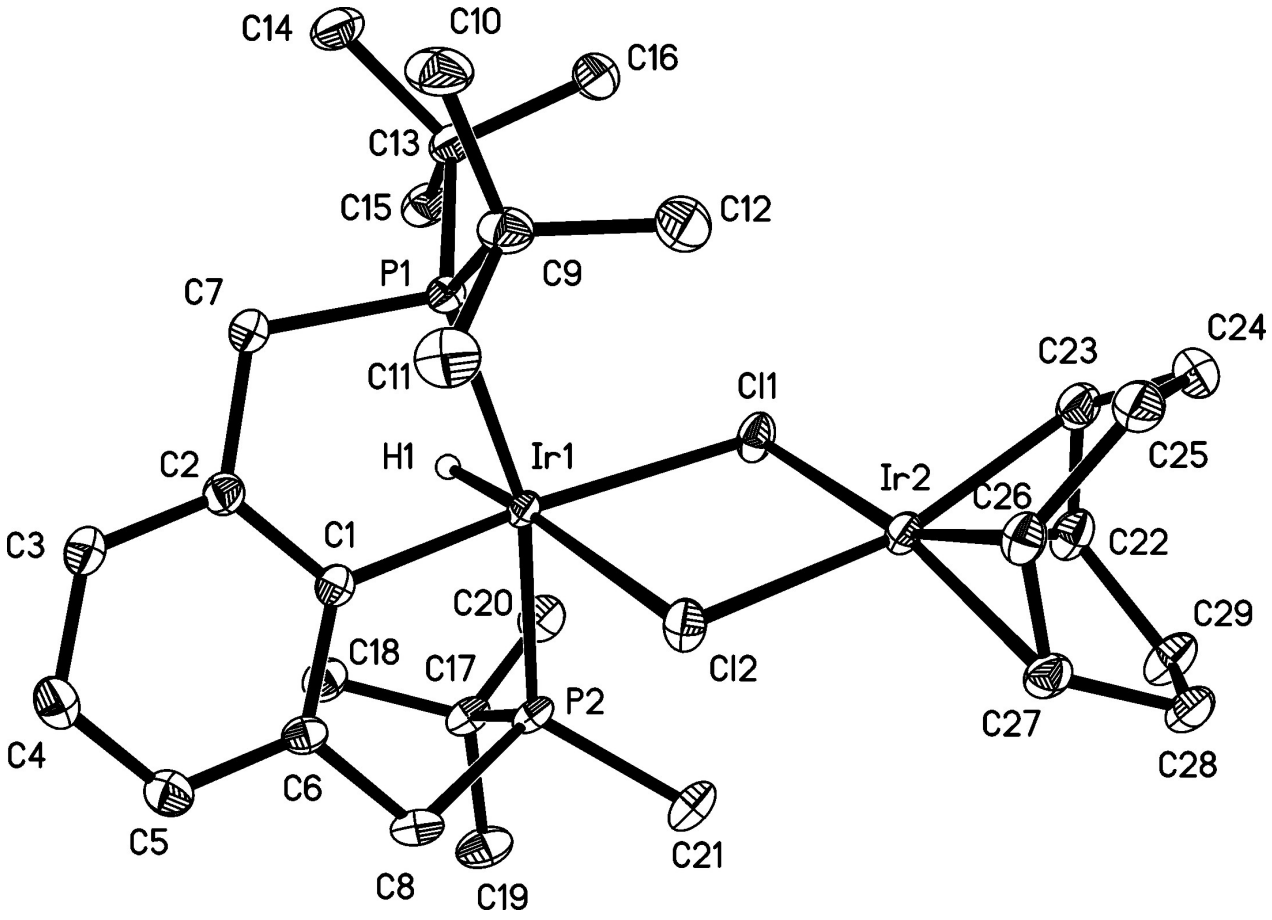

Figure 2-3 Crystal structure of (^{tBu3Me}PCP)Ir(H)(μ-Cl_2)Ir(COD)

Table 2.17 Crystal data and structure refinement for (^{tBu3Me}PCP)Ir(H)(μ-Cl_2)Ir(COD)

Empirical formula	C29 H50 Cl2 Ir2 P2	
Formula weight	915.93	
Temperature	100(2) K	
Wavelength	0.71073 Å	
Crystal system	Monoclinic	
Space group	P2(1)/n	
Unit cell dimensions	a = 11.8686(10) Å	α= 90°.
	b = 14.9454(13) Å	β= 91.739(2)°.
	c = 17.6158(15) Å	γ = 90°.
Volume	3123.3(5) $Å^3$	
Z	4	
Density (calculated)	1.948 Mg/m^3	
Absorption coefficient	8.804 mm^{-1}	
F(000)	1768	
Crystal size	0.19 x 0.11 x 0.05 mm^3	
Theta range for data collection	1.79 to 30.52°.	
Index ranges	-16<=h<=16, -21<=k<=21, -25<=l<=25	
Reflections collected	37387	
Independent reflections	9521 [R(int) = 0.0332]	
Completeness to theta = 30.52°	99.8 %	
Absorption correction	Semi-empirical from equivalents	
Max. and min. transmission	0.9999 and 0.5729	
Refinement method	Full-matrix least-squares on F^2	
Data / restraints / parameters	9521 / 1 / 341	
Goodness-of-fit on F^2	1.019	
Final R indices [I>2sigma(I)]	R1 = 0.0253, wR2 = 0.0654	
R indices (all data)	R1 = 0.0320, wR2 = 0.0684	
Largest diff. peak and hole	2.827 and -1.856 e.$Å^{-3}$	

Table 2.18 Selective bond lengths [Å] and angles [°] for (^{tBu3Me}PCP)Ir(H)(μ-Cl_2)Ir(COD)

Ir(1)-C(1)	2.019(3)	C(2)-C(3)	1.394(4)
Ir(1)-P(2)	2.2823(8)	C(2)-C(7)	1.513(5)
Ir(1)-P(1)	2.3223(8)	C(3)-C(4)	1.385(5)
Ir(1)-Cl(1)	2.5125(8)	C(4)-C(5)	1.391(5)
Ir(1)-Cl(2)	2.5698(8)	C(5)-C(6)	1.393(5)
Ir(1)-H(1)	1.564(18)	C(5)-H(5)	0.9500
Cl(1)-Ir(2)	2.3830(8)	C(6)-C(8)	1.504(4)
Cl(2)-Ir(2)	2.3772(8)	C(9)-C(10)	1.533(5)
P(1)-C(7)	1.842(3)	C(9)-C(11)	1.539(5)
P(1)-C(9)	1.884(4)	C(9)-C(12)	1.544(5)
P(1)-C(13)	1.889(3)	C(13)-C(16)	1.535(5)
P(2)-C(21)	1.821(3)	C(13)-C(15)	1.536(5)
P(2)-C(8)	1.842(3)	C(13)-C(14)	1.548(5)
P(2)-C(17)	1.853(3)	C(17)-C(19)	1.532(5)
C(1)-C(2)	1.410(4)	C(17)-C(18)	1.533(5)
C(1)-C(6)	1.423(5)	C(17)-C(20)	1.535(5)
C(1)-Ir(1)-P(2)	82.78(9)	C(7)-P(1)-C(13)	103.46(16)
C(1)-Ir(1)-P(1)	83.80(9)	C(9)-P(1)-C(13)	110.65(16)
P(2)-Ir(1)-P(1)	164.04(3)	C(7)-P(1)-Ir(1)	100.38(11)
C(1)-Ir(1)-Cl(1)	175.06(9)	C(9)-P(1)-Ir(1)	118.94(12)
P(2)-Ir(1)-Cl(1)	94.27(3)	C(13)-P(1)-Ir(1)	116.65(11)
P(1)-Ir(1)-Cl(1)	99.69(3)	C(21)-P(2)-C(8)	105.59(16)
C(1)-Ir(1)-Cl(2)	95.64(9)	C(21)-P(2)-C(17)	104.34(16)
P(2)-Ir(1)-Cl(2)	86.62(3)	C(8)-P(2)-C(17)	107.27(16)
P(1)-Ir(1)-Cl(2)	103.29(3)	C(21)-P(2)-Ir(1)	119.69(13)
Cl(1)-Ir(1)-Cl(2)	80.19(3)	C(8)-P(2)-Ir(1)	101.08(11)
C(1)-Ir(1)-H(1)	87.7(15)	C(17)-P(2)-Ir(1)	117.64(11)
P(2)-Ir(1)-H(1)	83.4(15)	C(2)-C(1)-C(6)	117.8(3)
P(1)-Ir(1)-H(1)	87.5(15)	C(2)-C(1)-Ir(1)	121.6(2)
Cl(1)-Ir(1)-H(1)	95.9(15)	C(6)-C(1)-Ir(1)	120.6(2)
Cl(2)-Ir(1)-H(1)	168.9(15)	C(3)-C(2)-C(1)	120.6(3)
Ir(2)-Cl(1)-Ir(1)	97.11(3)	C(3)-C(2)-C(7)	120.9(3)
Ir(2)-Cl(2)-Ir(1)	95.72(3)	C(1)-C(2)-C(7)	118.3(3)
C(7)-P(1)-C(9)	103.92(16)	C(4)-C(3)-C(2)	120.8(3)

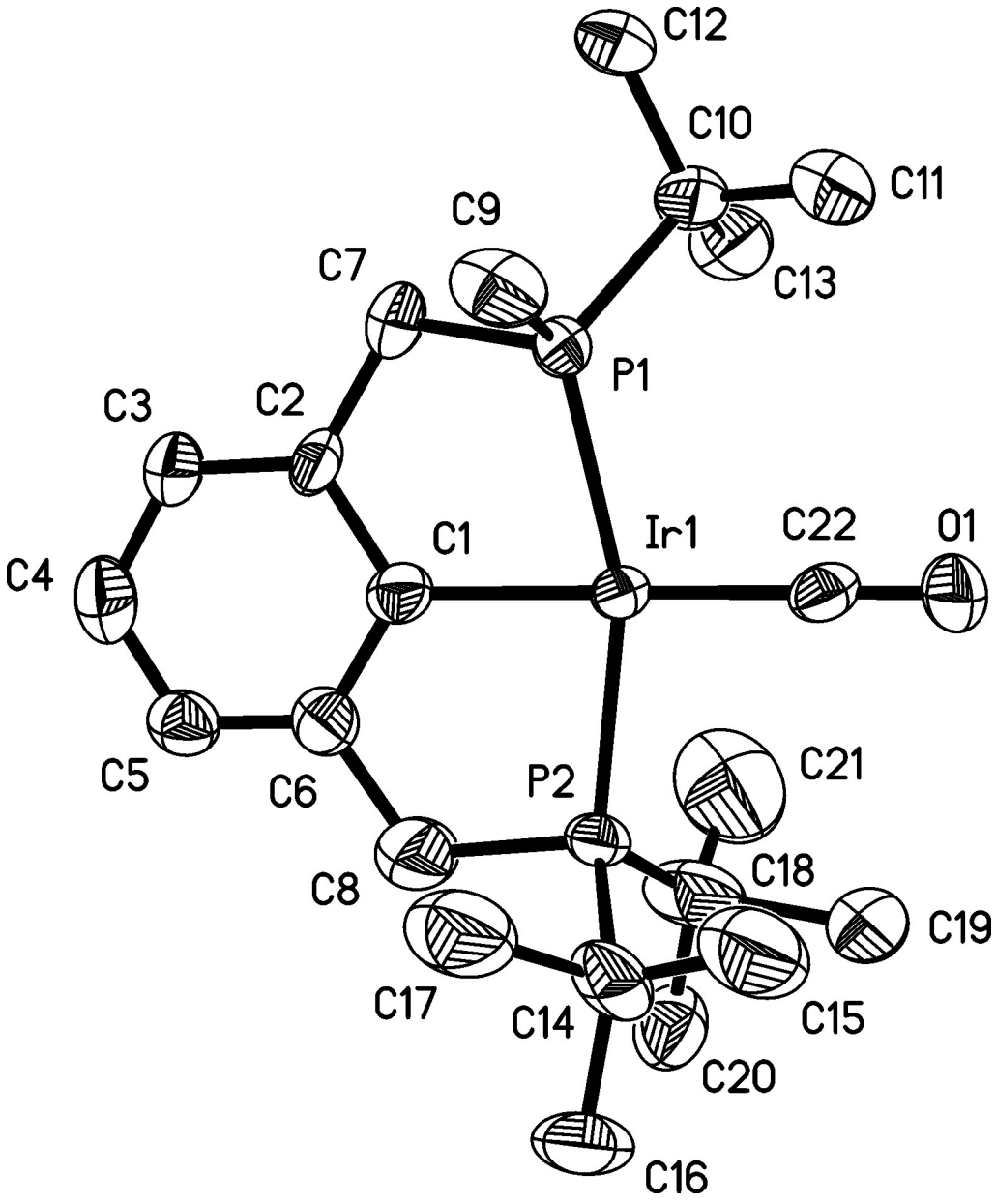

Figure 2-4 Crystal structure of (^{tBu3Me}PCP)Ir(CO)

Table 2.19 Crystal data and structure refinement for(^{tBu3Me}PCP)Ir(CO)

Empirical formula	C44 H74 Ir2 O2 P4	
Formula weight	1143.31	
Temperature	100(2) K	
Wavelength	0.71073 Å	
Crystal system	Orthorhombic	
Space group	Pca2(1)	
Unit cell dimensions	a = 11.4336(10) Å	α= 90°.
	b = 15.3744(13) Å	β= 90°.
	c = 26.225(2) Å	γ = 90°.
Volume	4610.0(7) Å^3	
Z	4	
Density (calculated)	1.647 Mg/m^3	
Absorption coefficient	5.940 mm^{-1}	
F(000)	2272	
Crystal size	0.35 x 0.30 x 0.04 mm^3	
Theta range for data collection	2.04 to 28.28°.	
Index ranges	-15<=h<=15, -20<=k<=20, -34<=l<=34	
Reflections collected	46411	
Independent reflections	11428 [R(int) = 0.0416]	
Completeness to theta = 28.28°	100.0 %	
Absorption correction	Semi-empirical from equivalents	
Max. and min. transmission	0.9999 and 0.4947	
Refinement method	Full-matrix least-squares on F^2	
Data / restraints / parameters	11428 / 271 / 470	
Goodness-of-fit on F^2	1.001	
Final R indices [I>2sigma(I)]	R1 = 0.0586, wR2 = 0.1769	
R indices (all data)	R1 = 0.0793, wR2 = 0.1922	
Absolute structure parameter	0.049(16)	
Largest diff. peak and hole	5.412 and -2.170 e.Å^{-3}	

Table 2.20 Selective bond lengths [Å] and angles [°] for (^{tBu3Me}PCP)Ir(CO)

Ir(1)-C(22)	1.839(11)	C(14)-C(16)	1.499(16)
Ir(1)-C(1)	2.106(11)	C(14)-C(17)	1.585(19)
Ir(1)-P(1)	2.275(2)	C(18)-C(21)	1.31(3)
Ir(1)-P(2)	2.303(2)	C(18)-C(20)	1.45(2)
P(1)-C(7)	1.774(16)	C(18)-C(19)	1.71(3)
P(1)-C(9)	1.802(12)	C(22)-O(1)	1.153(12)
P(1)-C(10)	1.855(10)	Ir(2)-C(44)	1.889(11)
P(2)-C(8)	1.777(14)	Ir(2)-C(23)	2.067(11)
P(2)-C(18)	1.842(17)	Ir(2)-P(3)	2.275(3)
P(2)-C(14)	1.864(12)	Ir(2)-P(4)	2.293(2)
C(1)-C(6)	1.404(14)	P(3)-C(31)	1.834(19)
C(1)-C(2)	1.426(14)	P(3)-C(32)	1.834(12)
C(2)-C(3)	1.399(15)	P(3)-C(29)	1.896(17)
C(2)-C(7)	1.499(17)	P(4)-C(30)	1.802(12)
C(3)-C(4)	1.377(16)	P(4)-C(36)	1.819(12)
C(4)-C(5)	1.355(17)	P(4)-C(40)	1.931(13)
C(5)-C(6)	1.372(15)	C(23)-C(24)	1.347(14)
C(6)-C(8)	1.496(17)	C(23)-C(28)	1.428(13)
C(10)-C(13)	1.515(19)	C(24)-C(25)	1.373(16)
C(10)-C(12)	1.542(15)	C(24)-C(29)	1.578(17)
C(10)-C(11)	1.567(19)	C(25)-C(26)	1.402(16)
C(22)-Ir(1)-C(1)	175.8(4)	C(10)-P(1)-Ir(1)	120.9(4)
C(22)-Ir(1)-P(1)	100.4(3)	C(8)-P(2)-C(18)	100.2(9)
C(1)-Ir(1)-P(1)	80.7(3)	C(8)-P(2)-C(14)	105.3(7)
C(22)-Ir(1)-P(2)	97.6(3)	C(18)-P(2)-C(14)	114.0(7)
C(1)-Ir(1)-P(2)	81.6(3)	C(8)-P(2)-Ir(1)	104.0(5)
P(1)-Ir(1)-P(2)	161.68(10)	C(18)-P(2)-Ir(1)	116.2(5)
C(7)-P(1)-C(9)	100.0(9)	C(14)-P(2)-Ir(1)	114.7(4)
C(7)-P(1)-C(10)	106.5(6)	C(6)-C(1)-C(2)	115.5(10)
C(9)-P(1)-C(10)	105.4(6)	C(6)-C(1)-Ir(1)	122.7(8)
C(7)-P(1)-Ir(1)	105.6(6)	C(2)-C(1)-Ir(1)	121.6(8)
C(9)-P(1)-Ir(1)	116.1(5)	C(3)-C(2)-C(1)	120.0(11)

Chapter 3

Synthesis of isocyanides from secondary methyl amine using (PCP)Ir

Abstract

The pincer complex (PCP)Ir complex (PCP = κ^3-2,6-(^{t}Bu$_2$PCH$_2$)$_2$C$_6$H$_3$) reacts with different secondary methyl amines and at ambient temperature it forms corresponding iridium isocyanide complexes (PCP)Ir(H)(H)(CNR), **3-1 (a-e)**. Formation of **3-1 (a-e)** from the corresponding secondary methyl amines is believed to be multistep process, in which dehydrogenation of the amines followed by the migration of a proton to generate (PCP)Ir(H)(H)(CNR).

Further heating of complexes **3-1 (a-e)** in the presence of a hydrogen acceptor generates corresponding 4-coordinate (PCP)Ir(CNR) species, **3-2 (a-e)**. Complexes **3-2 (a-e)** react to CO and form (PCP)Ir(CO) to liberate the corresponding isocyanide.

3.1 Introduction

Isocyanides are important building blocks in organic synthesis. The unique reactivity of this class of compounds, particularly nucleophilic and electrophilic attack at the unsaturated terminal carbon, creates a lot of attention.[1, 2, 3] Isocyanides are one of the most useful members in multicomponent reactions[4, 5, 6] and used in the synthesis of a wide range of peptides, depsipeptides,[7] heterocycles[8, 9, 10, 11] and drugs.[12, 13, 14, 15] Isocyanide can be adsorbed on metal surfaces which has many applications, particularly in catalysis, nanochemistry, and molecular electronics.[16]

Metal complexes of isocyanides are also used as building blocks for coordination polymers and supramolecular assemblies.[17,18] Gold (I) complexes of crown-ether-isocyanide also show interesting luminescence properties.[19] Fluorous isocyanide complexes of many metals such as Ag, Au, Cu, Fe, Pd, and Pt have been synthesized and their effect in metallomesogens have been studied.[20]

Table 3.1 Survey of Some Functional Groups and Their Commercial Availability According to the ACD[a]

Compound	Functional group	Availability
isothiocyanate	R−NCS	854
isocyanate	R−NCO	508
isocyanide	R−NC	380
sulfonyl chloride	RSO_2Cl	793
α-amino acid	H2NCHRCOOH	2480
β-amino acid	H2NCHRCHRCOOH	1004
boronic acid	$R-B(OH)_2$	1000
α-ketoaldehyde	R−COCHO	43

[a] The molecular weight of the corresponding compounds was limited to below 500 Dalton

Although isocyanides are highly useful chemicals, their commercial availability is limited compared to other chemicals (Table 3.1).[7] Normally isocyanides are synthesized by the reaction of a dichloro or dibromo carbene with a corresponding primary amine[21, 22, 23] or by the reaction of formamide with phosphorus oxychloride (eq. 1).[11, 18]

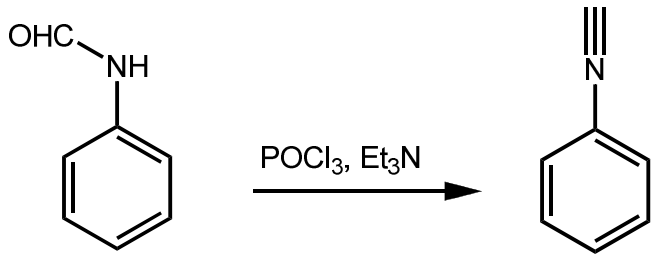

(1)

Previously, our group reported the formation of an isocyanide complex from a secondary amine having an ethyl group by a pincer iridium catalyst via a multistep pathway.[24]

In this chapter we report the synthesis of isocyanides from secondary methyl amines by a pincer iridium complex.

3.2 Results and discussion

3.2.1 Reaction of (PCP)Ir with *N*-methylphenylamine

In an effort to have a polar RNH-group at the *para* position of the PCP ligand (with the goal of binding the (PCP)Ir complex strongly to the solid support like γ–Al_2O_3, or silica), reaction of *N*-methylphenylamine with (PCP)Ir was performed to test whether the N-H bond will react with the Ir metal center. After 12 h at room temperature complex **3-1d** was formed in 98% yield. Complex **3-1d** was characterized by NMR spectroscopy and X-ray crystallography. The ^{31}P NMR spectra shows a single peak at 72.9 ppm, and

the ^{1}H NMR spectrum shows a triplet at -9.49 ppm (J_{PH} = 13.7 Hz), which corresponds to the two hydrides. Complex **3-1d** was crystallized from a hexane solution and its structure was solved by X-ray crystallography. The ORTEP diagram of complex **3-1d** is shown in Figure 3-1. Crystal parameters, bond angles and bond distances are listed in Table 3.2 and Table 3.3. The geometry of complex **3-1d** is octahedral, in which the two hydrides are *trans* to each other while the isocyanide group is *trans* to the PCP *ipso*-carbon.

Heating complex **3-1d** (6 h at 125 °C) in the presence of a hydrogen acceptor (TBE or 1-hexene) formed a new complex **3-2d** in 95% yield. Complex **3-2d** was characterized by NMR spectroscopy. The ^{31}P NMR spectrum shows a single peak at 79.2 ppm, and the ^{1}H NMR spectrum has no hydrides.

Previously, our group reported the formation of an isocyanide by a pincer iridium catalyst from a secondary amine having an ethyl group.[24] In contrast, a secondary amine bearing a methyl group in this case was used. To explore the possibilities of this reaction towards the synthesis of valuable isocyanides, many secondary anime substrates having a methyl group were tested.

3.2.2 Reaction of (PCP)Ir with *N*-methylcyclohexylamine, *N*-methylbutylamine and *N*-methylethylamine

(PCP)Ir reacts with *N*-methylcyclohexylamine, *N*-methylbutylamine and *N*-methylethylamine. After 12 h at room temperature complexes **3-1(a-c)** were formed (Scheme 3-1). Heating of complexes **3-1(a-c)** (6 h 125 °C) in the presence of an acceptor (TBE or 1-hexene) formed new complexes **3-2(a-c)**. Complexes **3-1(a-c)** and **3-2(a-c)** were characterized by NMR.

3.2.3 Reaction of (PCP)Ir with *N*-methylbenzylamine

When aromatic amine *N*-methylbenzylamine was reacted with (PCP)Ir under the same reaction conditions (12 h at room temperature), the product of C-H activation of the aromatic ring (**3e**) as major and isocyanide product **3-1e** as minor was observed.

Formation of **3-1e** from the reaction of *N*-methylbenzylamine and (PCP)Ir precursor requires a longer reaction time with heating (6 h at 70 °C), while the formation of other isocyanides requires only a one hour reaction time at ambient temperature. In contrast to formation of **3-1(a-d)**, formation of stable six-coordinate intermediate **3e** generated by the C-H activation of the aromatic ring and the coordination of amine nitrogen is thought to slow down the process.

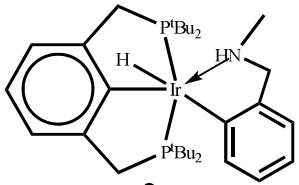

3e

Further heating of complex **3-1e** (6 h at 125 °C) in the presence of hydrogen acceptor (TBE or 1-hexene) formed new complex **3-2e** in 95% yield (Scheme 3-1). Complexes **3e** and **3-1e** were characterized by NMR spectroscopy. In the ^{31}P NMR spectrum, complex **3-1e** shows a single peak at 72.4 ppm, and in the ^{1}H NMR spectrum, there is a triplet at -9.93 ppm (J_{PH} = 14.2 Hz) which corresponds to the two hydrides. Complex **3-2e** was characterized by NMR spectroscopy. In the ^{31}P NMR spectrum, complex **3-2e** shows a single peak at 78.9 ppm, and in the ^{1}H NMR spectrum there is no hydride.

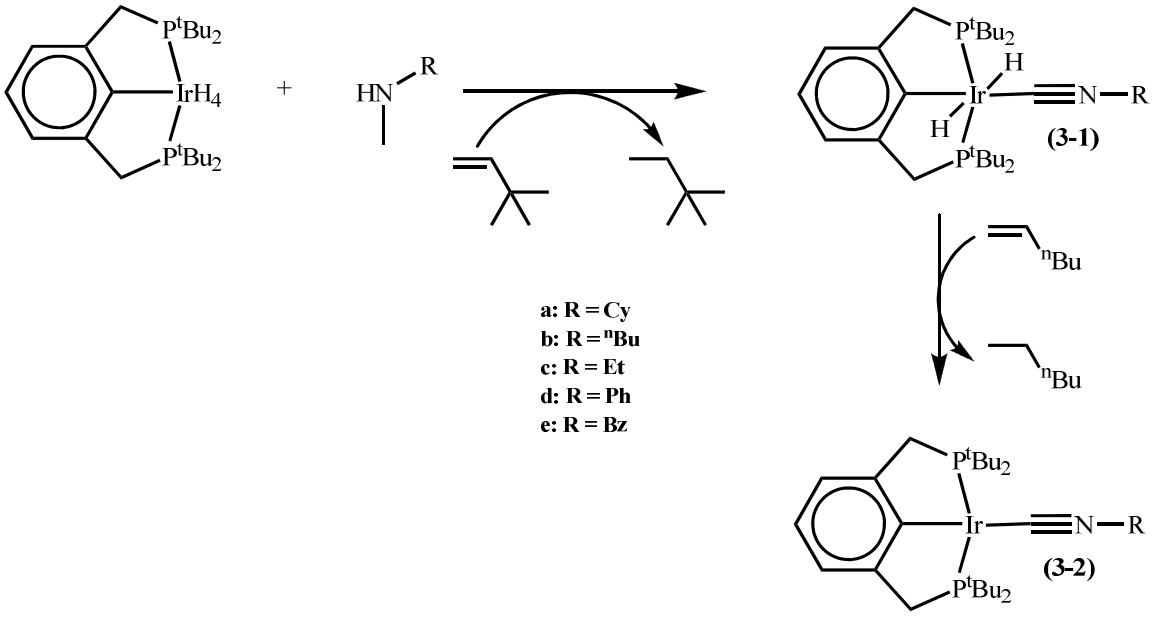

Scheme 3-1 Synthesis of (PCP)Ir(CNR)

3.2.4 Mechanistic investigation

When an aliphatic amine (2 equiv) (*N*-methylcyclohexylamine, *N*-methylbutylamine or *N*-methylethylamine) was added to a *p*-xylene-d_{10} solution of (PCP)Ir(H)(TBV) [formed by addition of TBE to (PCP)IrH_4)], no N-H addition product was observed by NMR spectroscopy after 10 min at ambient temperature; only product **3-1(a-c)** was formed. When aromatic amines (*N*-methylphenylamine, *N*-methylbenzylamine) were subjected to the same reactions conditions, the product of C-H activation of the aromatic ring along with complexes 3-**1d** and **3-1e** was observed.

Formation of isocyanide from secondary methyl amine is believed to be a multistep process as proposed previously by our group (Scheme 3.2).[24] Dehydrogenation of secondary amines to imines has been reported by Jensen and co-workers,[25] is proposed to be the initial step in the mechanism of isocyanide formation. The imine's sp^2 C-H bond then oxidatively adds to (PCP)Ir, followed by rapid hydrogen migration to form the products **3-1(a-e)** (Scheme 3-2).

Dehydrogenation of *N*-methylethanamine could in theory generate *N*-methyleneethanamine or *N*-ethylidenemethanamine, but the reaction of *N*-methylethanamine with (PCP)Ir(H)(TBV) [formed by addition of TBE to (PCP)IrH_4)] yield only one product **3-1c**. This is because migration of a hydrogen atom is much more favorable than migration of a methyl group. Formation of only isocyanide complex **3-1c** indicates under these reaction conditions, dehydrogenation of *N*-methylethanamine only generate *N*-methyleneethanamine.

The 4-coordinate isocyanides **3-2(a-e)** (PCP)Ir(CNR) react with CO (1 atmosphere pressure, 10 min, ambient temperature) and form (PCP)Ir(CO) and liberate

the corresponding isocyanides (Scheme 3-3). Refluxing **3-1(a-e)** in C_6D_6 for 6 h under 1 atmosphere CO also liberate isocyanides and form (PCP)Ir(CO) (Scheme 3-3).

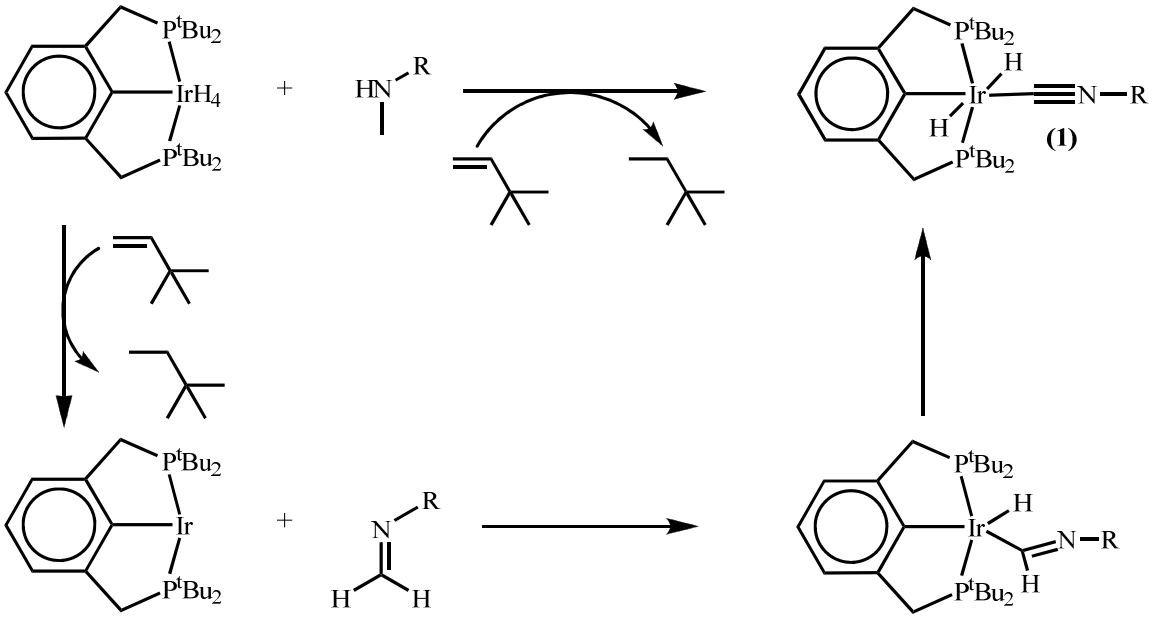

Scheme 3-2 Proposed mechanism of synthesis of (PCP)Ir(H_2)(CNR)

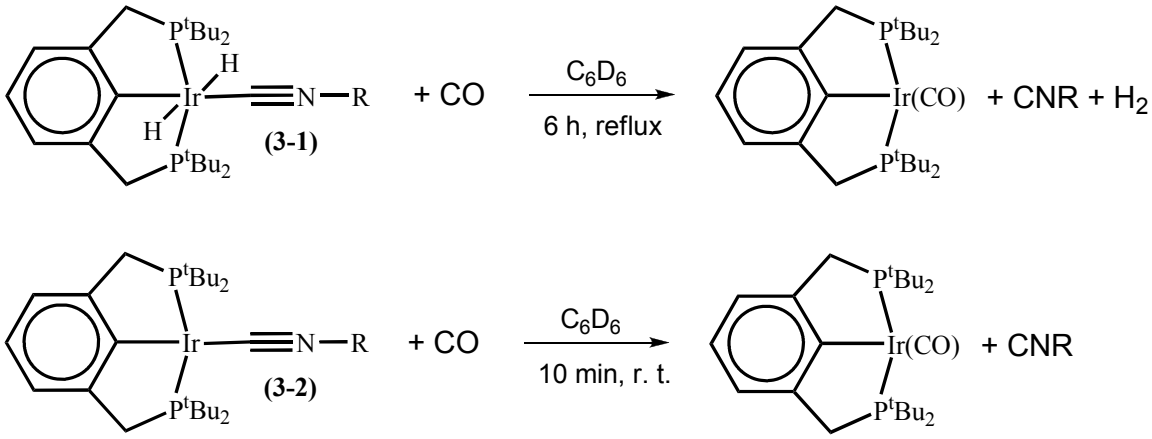

Scheme 3.3 Reaction of isocyanides with CO

3.2.5 To test if formation of isocyanide is catalytic

3.2.5.1 *N*-methylbenzylamine and (PCP)Ir

N-methylbenzylamine was reacted with (^{tBu4}PCP)IrH_4 under the same reaction conditions (0.26 mmol amine, 0.26 mmol TBE, and 0.037 mmol catalyst in 1 mL toluene was heated for 72 h at 200 °C) as reported by Jensen.[25] After the reaction sample was analyzed by GC, GC-MS and NMR spectroscopy. GC and GC-MS traces indicated the formation of imines in 49 % yield and no isocyanide, and this result is consistent with the yield reported by Jensen (53% yield).

3.2.5.2 *N*-methylphenylamine and (PCP)Ir

A 0.5 mL *p*-xylene solution of 10 mM (^{tBu4}PCP)IrH_4, 40 mM amine, and 200 mM TBE was sealed under vacuum in NMR tubes. Four of these NMR sealed tubes were heated (at room temperature, 100 °C, 150 °C, and 200 °C) for 24 h. No imines or isocyanides were observed after the reaction in GC and GC-MS traces. NMR spectroscopy indicated formation of only (PCP)Ir(H_2)CNPh when kept at room temperature, and (PCP)IrCNPh when heated at 100 °C, 150 °C, and 200 °C in quantitative yields.

3.3 Experimental

General Methods. All reactions were carried out under an argon atmosphere using standard Schlenk techniques or in an argon-filled dry box. All the amines were purchased from Aldrich and were degassed by passing argon. *p*-Xylene, *p*-xylene-d_{10}, C_6D_6, TBE, and 1-hexene were dried using Na/K and collected by vacuum transfer. 400 MHz or 500 MHz Varian instruments were used for the ^1H, ^{13}C and ^{31}P NMR experiments. The residual peak of the deuterated solvent was used as a reference for ^1H chemical shifts. ^{31}P NMR chemical shifts were referenced to PMe_3 standard, which appears at –62.2 ppm. PMe_3 internal standard in ^{31}P NMR was employed in determining the yield. (^{tBu4}PCP)IrH_4 was prepared as described in the literature.[26]

(PCP)Ir(H_2)(CNCy) (3-1a): To a 0.5 mL *p*-xylene solution of 5 mg (PCP)IrH_4 (0.0083 mmol) in a J-Young tube, 5.4 μL TBE (0.0415 mmol) and 1.6 μL $CyNHCH_3$ (0.0124 mmol) were added. After 12 h room temperature, all the solvent was removed in vacuum and NMR spectrum indicates formation of this compound in 100% yield. ^{31}P NMR (C_6D_6, 202 MHz): δ 72.07 (s). ^1H NMR (C_6D_6, 400 MHz): δ 7.12 (d, J_{HH} = 6.0 Hz, 2H, Ar, PCP), 7.09 (t, J_{HH} = 4.4 Hz, 1H, Ar, PCP), 3.38 (vt, J_{PH} = 4.0 Hz, 4H, ***CH₂***P^{t}Bu$_2$), 1.40 (vt, J_{PH} = 6.2 Hz, 36H, PC(C***H***$_3$)$_3$), 1.23 (m, 8H, CN***Cy***), 0.92 (m, 3H, CN***Cy***), -10.1 (t, J_{PH} = 14.2 Hz, 2H, Ir(***H₂***)). ^{13}C NMR (C_6D_6, 100 MHz): δ 157.7 (t, J_{CP} = 2.3 Hz, Ar, PCP), 148.5 (t, J_{CP} = 8.6 Hz, Ar, PCP), 137.5 (t, J_{CP} = 7.5 Hz, Ir-***C***NCy), 122.1 (s, Ar, PCP), 120.2 (t, J_{CP} = 7.8 Hz, Ar, PCP), 53.9 (s, Cy), 42.2 (vt, J_{CP} = 15.0 Hz, ***CH₂***P^{t}Bu$_2$), 34.5 (vt, J_{CP} = 11.3 Hz, P***C***(CH$_3$)$_3$), 34.2 (s, Cy), 30.4 (vt, J_{CP} = 2.3 Hz, PC(***C***H$_3$)$_3$), 25.6 (s, Cy), 24.1 (s, Cy).

(PCP)Ir(CNCy) (3-2a): To a 0.5 mL *p*-xylene solution of 5 mg (PCP)IrH_4 (0.0083 mmol) in a J-Young tube, 5.2 μL 1-hexene (0.0415 mmol) and 1.6 μL $CyNHCH_3$ (0.0124 mmol) were added. After 6 h at 125 °C, all the solvent was removed in vacuum and NMR spectrum indicates formation of this compound in 100% yield.

Alternate method to synthesize this compound: To a *p*-xylene solution of **(PCP)Ir(H_2)(CNCy)** (synthesized previously), 2.6 μL 1-hexene was added and after 6 h 125 °C, all the solvent was removed in vacuum and NMR spectrum indicates the formation of this compound in 100% yield.

^{31}P NMR (C_6D_6, 202 MHz): δ 78.85 (s). ^{1}H NMR (C_6D_6, 400 MHz): δ 7.36 (d, J_{HH} = 7.6 Hz, 2H, Ar, PCP), 7.18 (t, J_{HH} = 7.6 Hz, 1H, Ar, PCP), 3.44 (vt, J_{PH} = 3.6 Hz, 4H, ***CH*$_2$**P^{t}Bu$_2$), 1.38 (vt, J_{PH} = 6.2 Hz, 36H, PC(C***H***$_3$)$_3$), 1.25 (m, 7H, CN***Cy***), 1.02 (m, 4H, CN***Cy***). ^{13}C NMR (C_6D_6, 125 MHz): δ 182.5 (t, J_{CP} = 4.3 Hz, ***C***NCy), 164.7 (t, J_{CP} = 8.9 Hz, Ar, PCP), 155.5 (t, J_{CP} = 11.3 Hz, Ar, PCP), 124.2 (s, Ar, PCP), 120.1 (t, J_{CP} = 8.3 Hz, Ar, PCP), 53.9 (s, Cy), 40.4 (vt, J_{CP} = 13.7 Hz, ***CH*$_2$**P^{t}Bu$_2$), 36.3 (vt, J_{CP} = 10 Hz, P***C***$(CH_3)_3$), 34.3 (s, Cy), 30.4 (vt, J_{CP} = 2.8 Hz, PC(***C***$H_3)_3$), 25.9 (s, Cy), 24.5 (s, Cy).

(PCP)Ir(H_2)(CN^{n}Bu) (3-1b): To a 0.5 mL *p*-xylene solution of 5 mg (PCP)IrH_4 (0.0083 mmol) in a J-Young tube, 5.4 μL TBE (0.0415 mmol) and 1.5 μL ^{n}BuNHCH$_3$ (0.0124 mmol) were added. After 12 h room temperature, all the solvent was removed in vacuum and NMR spectrum indicates the formation of this compound in 100% yield. ^{31}P NMR (C_6D_6, 202 MHz): δ 72.4 (s). ^{1}H NMR (C_6D_6, 400 MHz): δ 7.11 (d, J_{HH} = 5.6 Hz, 2H, Ar, PCP), 7.08 (t, J_{HH} = 4.4 Hz, 1H, Ar, PCP), 3.37 (vt, J_{PH} = 3.8 Hz, 4H, ***CH*$_2$**P^{t}Bu$_2$), 2.95

(t, J_{HH} = 5.6Hz, 2H, N***CH₂***CH_2), 1.38 (vt, J_{PH} = 6.2 Hz, 36H, PC(C***H***$_3)_3$), 1.21 (m, 4H, NCH_2***CH_2CH_2***CH_3), 0.71 (t, J_{HH} = 7.0 Hz, 3H, $NCH_2CH_2CH_2$***CH_3***), -10.08 (t, Jp_H = 14.0 Hz, 2H, Ir(***H₂***)). ^{13}C NMR (C_6D_6, 125 MHz): δ 157.7 (t, J_{CP} = 2.9 Hz, Ar, PCP), 148.5 (t, J_{CP} = 8.6 Hz, Ar, PCP), 139.4 (t, J_{CP} = 4.5 Hz, CNBu), 122.1 (s, Ar, PCP), 120.2 (t, J_{CP} = 7.9 Hz, Ar, PCP), 43.3 (s, NCH_2), 42.1 (vt, J_{CP} = 15 Hz, ***CH₂***P^tBu_2), 34.5 (vt, J_{CP} = 11.3 Hz, P***C***$(CH_3)_3$), 32.4 (s, NCH_2***CH_2***), 30.3 (vt, J_{CP} = 2.2 Hz, PC(***C***$H_3)_3$), 20.2 (s, NCH_2CH_2***CH_2***CH_3), 13.6 (s, $NCH_2CH_2CH_2$***CH_3***).

(PCP)Ir(CN*n*Bu) (3-2b): To a 0.5 *p*-xylene solution of 5 mg (PCP)IrH_4 (0.0083 mmol) in a J-Young tube, 5.2 µL 1-hexene (0.0415 mmol) and 1.5 µL ^{n}BuNHCH$_3$ (0.0124 mmol) were added. After 6 h 125 °C, all the solvent was removed in vacuum and NMR spectrum indicates the formation of this compound in 100% yield.

Alternate method to synthesize this compound: To a 0.5 mL *p*-xylene solution of **PCP)Ir(H₂)(CN*n*Bu)** (synthesized previously), 2.6 µL 1-hexene was added and after 6 h 125 °C, all the solvent was removed in vacuum and NMR spectrum indicates the formation of this compound in 100% yield.

^{31}P NMR (C_6D_6, 202 MHz): δ 78.9 (s). ^{1}H NMR (C_6D_6, 400 MHz): δ 7.35 (d, J_{HH} = 5.6 Hz, 2H, Ar, PCP), 7.17 (t, J_{HH} = 7.5 Hz, 1H, Ar, PCP), 3.44 (vt, J_{PH} = 3.5 Hz, 4H, ***CH₂***P^tBu_2), 3.01 (t, J_{HH} = 6.7 Hz, 2H, N***CH₂***CH_2), 1.37 (vt, J_{PH} = 6.5 Hz, 36H, PC(C***H***$_3)_3$), 1.28 (m, 4H, NCH_2***CH_2CH_2***CH_3), 0.78 (t, J_{HH} = 7.2 Hz, 3H, $NCH_2CH_2CH_2$***CH_3***). ^{13}C NMR (C_6D_6, 125 MHz): δ 182.5 (t, J_{CP} = 4.3 Hz, Ir-***C***N^{n}Bu), 167.8 (t, J_{CP} = 6.8 Hz, Ar, PCP), 155.5 (t, J_{CP} = 11.3 Hz, Ar, PCP), 124.2 (s, Ar, PCP), 120.1 (t, J_{CP} = 8.4 Hz, Ar, PCP), 43.3 (s, N***CH₂***$CH_2CH_2CH_3$), 40.3 (vt, J_{CP} = 13.8 Hz,

CH₂P^{t}Bu$_2$), 36.2 (vt, J_{CP} = 10.1 Hz, P***C***(CH$_3$)$_3$), 32.5 (s, NCH$_2$***CH***$_2$CH$_2$CH$_3$), 30.3 (vt, J_{CP} = 3.0 Hz, PC(***C***H$_3$)$_3$), 20.5 (s, NCH$_2$CH$_2$***CH₂***CH$_3$), 13.8 (s, NCH$_2$CH$_2$CH$_2$***CH₃***).

(PCP)Ir(H$_2$)(CNEt) (3-1c): To a 0.5 mL *p*-xylene solution of 5 mg (PCP)IrH$_4$ (0.0083 mmol) in a J-Young tube, 5.4 µL TBE (0.0415 mmol) and 1.1 µL EtNHCH$_3$ (0.0124 mmol) were added. After 12 h room temperature, all the solvent was removed in vacuum and NMR spectrum indicates the formation of this compound in 100% yield. ^{31}P NMR (C$_6$D$_6$, 202 MHz): δ 72.45 (s). ^{1}H NMR (C$_6$D$_6$, 400 MHz): δ 7.11 (d, J_{HH} = 5.2 Hz, 2H, Ar, PCP), 7.08 (t, J_{HH} = 4.0 Hz, 1H, Ar, PCP), 3.37 (vt, J_{PH} = 3.8 Hz, 4H, ***CH₂***P^{t}Bu$_2$), 2.85 (q, J_{HH} = 7.2 Hz, 2H, N***CH₂***CH$_3$), 1.38 (vt, J_{PH}= 6.2 Hz, 36H, PC(C***H***$_3$)$_3$), 0.81 (t, J_{HH} = 7.2 Hz, 3H, NCH$_2$***CH₃***), -10.06 (t, J_{PH} = 14.2 Hz, 2H, Ir(***H₂***)). ^{13}C NMR (C$_6$D$_6$, 100 MHz): δ 157.7 (t, J_{CP} = 2.8 Hz, Ar, PCP), 148.5 (t, J_{CP} = 8.5 Hz, Ar, PCP), 140.1 (t, J_{CP} = 7.2 Hz, Ir-***C***NEt), 122.1 (s, Ar, PCP), 120.2 (t, J_{CP} = 7.8 Hz, Ar, PCP), 42.1 (vt, J_{CP} = 15 Hz, ***CH₂***P^{t}Bu$_2$), 38.5 (s, N***CH₂***CH$_3$), 34.5 (vt, J_{CP} = 11.4 Hz, P***C***(CH$_3$)$_3$), 30.3 (vt, J_{CP} = 2.3 Hz, PC(***C***H$_3$)$_3$), 16.1 (s, NCH$_2$***CH₃***).

(PCP)Ir(CNEt) (3-2c): To a 0.5 mL *p*-xylene solution of 5 mg (PCP)IrH$_4$ (0.0083 mmol) in a J-Young tube, 5.2 µL 1-hexene (0.0415 mmol) and 1.1 µL EtNHCH$_3$ (0.0124 mmol) were added. After 6 h 125 °C, all the solvent was removed in vacuum and NMR spectrum indicates the formation of this compound in 100% yield.

Alternate method to synthesize this compound: To a 0.5 mL *p*-xylene solution of **PCP)Ir(H$_2$)(CNEt)** (synthesized previously), 2.6 µL 1-hexene was added and after 6h

125 °C, all the solvent was removed in vacuum and NMR spectrum indicates the formation of this compound in 100% yield.

^{31}P NMR (C_6D_6, 202 MHz): δ 78.7 (s). ^{1}H NMR (C_6D_6, 400 MHz): δ 7.35 (d, J_{HH} = 7.2 Hz, 2H, Ar, PCP), 7.17 (t, J_{HH} = 7.6 Hz, 1H, Ar, PCP), 3.44 (vt, J_{PH} = 3.6 Hz, 4H, ***CH₂***P^{t}Bu$_2$), 3.01 (q, J_{HH} = 7.2 Hz, 2H, N***CH₂***CH$_3$), 1.36 (vt, J_{PH} = 6.2 Hz, 36H, PC(C***H***$_3$)$_3$), 0.99 (t, J_{HH} = 7.2 Hz, 3H, NCH$_2$***CH₃***). ^{13}C NMR (C_6D_6, 100 MHz): δ 182.6 (t, J_{CP} = 4.2 Hz, Ir-***C***NEt), 168.7 (t, J_{CP} = 8.9 Hz, Ar, PCP), 155.6 (t, J_{CP} = 11.3 Hz, Ar, PCP), 124.3 (s, Ar, PCP), 120.1 (t, J_{CP} = 8.4 Hz, Ar, PCP), 40.3 (vt, J_{CP} = 13.7 Hz, ***CH₂***P^{t}Bu$_2$), 38.1 (s, N***CH₂***CH$_3$), 36.2 (vt, J_{CP} = 10.1 Hz, P***C***(CH$_3$)$_3$), 30.3 (vt, J_{CP} = 2.9 Hz, PC(***C***H$_3$)$_3$), 15.9 (s, NCH$_2$***CH₃***).

(PCP)Ir(H$_2$)(CNPh) (3-1d): .To a 0.5 mL *p*-xylene solution of 5 mg (PCP)IrH$_4$ (0.0083 mmol) in a J-Young tube, 5.4 μL TBE (0.0415 mmol) and 1.3 μL PhNHCH$_3$ (0.0124 mmol) were added. After 12 h room temperature, all the solvent was removed in vacuum and NMR spectrum indicates the formation of this compound in 98 % yield. ^{31}P NMR (C_6D_6, 202 MHz): δ 72.9 (s). ^{1}H NMR (C_6D_6, 500 MHz): δ 7.11 (m, 6H, 4H from Ph and 2H from PCP), 6.88 (t, J_{HH} = 7.7 Hz, 2H, Ar), 3.39 (vt, J_{PH} = 4.0 Hz, 4H, ***CH₂***P^{t}Bu$_2$), 1.37 (vt, J_{PH} = 6.2 Hz, 36H, PC(C***H***$_3$)$_3$), -9.49 (t, J_{PH} = 13.7 Hz, 2H, Ir(***H₂***)). ^{13}C NMR (C_6D_6, 125 MHz): δ 157.1 (t, J_{CP} = 2.5 Hz, Ar, PCP), 153.8 (t, J_{CP} = 8.1 Hz, Ir-***C***NPh), 148.6 (t, J_{CP} = 8.4 Hz, Ar, PCP), 129.9 (s, Ph), 129.7 (s, Ph), 126.7 (s, Ph), 125.7 (s, Ph), 122.6 (s, Ar, PCP), 120.4 (t, J_{CP} = 7.8 Hz, Ar, PCP), 42.0 (vt, J_{CP} = 15.1 Hz, ***CH₂***P^{t}Bu$_2$), 34.5 (vt, J_{CP} = 11.5 Hz, P***C***(CH$_3$)$_3$), 30.3 (vt, J_{CP} = 2.3 Hz, PC(***C***H$_3$)$_3$). IR: ν(NC) (*n*-octane) 2072.7 cm^{-1}.

(PCP)Ir(CNPh) (3-2d): To a 0.5 mL *p*-xylene solution of 5 mg (PCP)IrH_4 (0.0083 mmol) in a J-Young tube, 5.2 µL 1-hexene (0.0415 mmol) and 1.3 µL $PhNHCH_3$ (0.0124 mmol) were added. After 6 h 125 °C, all the solvent was removed in vacuum and NMR spectrum indicates the formation of this compound in 100% yield.

Alternate method to synthesize this compound: To a 0.5 mL *p*-xylene solution of **(PCP)Ir(H_2)(CNPh)** (synthesized previously), 2.6 µL 1-hexene was added and after 6 h 125 °C, all the solvent was removed in vacuum and NMR spectrum indicates the formation of this compound in 100% yield.

^{31}P NMR (C_6D_6, 202 MHz): δ 79.2 (s). ^{1}H NMR (C_6D_6, 400 MHz): ^{1}H NMR (C_6D_6, 400 MHz): δ 7.34 (d, J_{HH} = 7.2 Hz, 2H, PCP), 7.26 (m, 3H, 2H from Ph and 1H from PCP), 6.99 (m, 2H, Ph), 6.93 (m, 1H, Ph), 3.49 (vt, J_{PH} = 3.6 Hz, 4H, ***CH*$_2$**P^{t}Bu$_2$), 1.35 (vt, J_{PH} = 6.4 Hz, 36H, PC(C***H***$_3$)$_3$). ^{13}C NMR (C_6D_6, 125 MHz): δ 182.9 (t, J_{CP} = 4.2 Hz, Ir-***C***NPh), 177.8 (t, J_{CP} = 7.6 Hz, Ar, PCP), 156.1 (t, J_{CP} = 11.1 Hz, Ar, PCP), 133.8 (s, Ph), 130.1 (s, Ph), 125.3 (s, Ph), 124.8 (s, Ph), 124.4 (s, Ar, PCP), 120.2 (t, J_{CP} = 8.3 Hz, Ar, PCP), 40.1 (vt, J_{CP} = 13.9 Hz, ***CH*$_2$**P^{t}Bu$_2$), 36.3 (vt, J_{CP} = 10.5 Hz, P***C***$(CH_3)_3$), 30.3 (vt, J_{CP} = 2.7 Hz, PC(***C***$H_3)_3$). IR: ν(NC) (*n*-octane) 1983.2 cm^{-1}.

(PCP)Ir(H_2)(CNBz) (3-1e): .To a 0.5 mL *p*-xylene solution of 5 mg (PCP)IrH_4 (0.0083 mmol) in a J-Young tube, 5.4 µL TBE (0.0415 mmol)and 1.6 µL $BzNHCH_3$ (0.0124 mmol) was added. After 6 h 70 °C, all the solvent was removed in vacuum and NMR spectrum indicates the formation of this compound in 100% yield. ^{31}P NMR (C_6D_6, 202 MHz): δ 72.4 (s). ^{1}H NMR (C_6D_6, 400 MHz): δ 7.10 (m, 3H, Ar), 7.07 (m, 5H, Ar), 4.13

(s, N***CH₂***Ph), 3.37 (vt, J_{PH} = 3.8 Hz, 4H, ***CH₂***P^{t}Bu$_2$), 1.34 (vt, J_{PH} = 6.4 Hz, 36H, PC(C***H***$_3$)$_3$), -9.93 (t, J_{PH} = 14.2 Hz, 2H, Ir(***H₂***)). ^{13}C NMR (C_6D_6, 125 MHz): δ 157.5 (t, J_{CP} = 2.8 Hz, Ar, PCP), 148.5 (t, J_{CP} = 8.5 Hz, Ar, PCP), 143.6 (t, J_{CP} = 8.5 Hz, Ir-***C***NBz), 135.5 (s, Ar), 129.2 (s, Ar), 128.6 (s, Ar), 127.6 (s, Ar), 122.3 (s, Ar, PCP), 120.3 (t, J_{CP} = 7.8 Hz, Ar, PCP), 47.7 (s, N***CH₂***Ph), 42.1 (vt, J_{CP} = 15.0 Hz, ***CH₂***P^{t}Bu$_2$), 34.4 (vt, J_{CP} = 11.4 Hz, P***C***(CH$_3$)$_3$), 30.3 (vt, J_{CP} = 2.3 Hz, PC(***C***H$_3$)$_3$).

(PCP)Ir(CNBz) (3-2e): To a 0.5 *p*-xylene solution of 5 mg (PCP)IrH$_4$ (0.0083 mmol) in a J-Young tube, 5.2 μL 1-hexene (0.0415 mmol) and 1.6 μL BzNHCH$_3$ (0.0124 mmol) were added. After 6 h 125 °C, all the solvent was removed in vacuum and NMR spectrum indicates the formation of this compound in 100% yield.

Alternate method to synthesize this compound: To a 0.5 mL *p*-xylene solution of **PCP)Ir(H₂)(CNBz)** (synthesized previously), 2.6 μL 1-hexene was added and after 6 h 125 °C, all the solvent was removed in vacuum and NMR indicates the formation of this compound in 100 % yield.

^{31}P NMR (C_6D_6, 202 MHz): δ 78.9 (s). ^{1}H NMR (C_6D_6, 400 MHz): δ 7.34 (d, J_{HH} = 7.6 Hz, 2H, Ar, PCP), 7.27 (m, 3H, Ar), 7.12 (m, 2H, Ar), 7.04 (t, J_{HH} = 7.0 Hz, 1H, Ar, PCP), 4.31 (s, N***CH₂***Ph), 3.44 (vt, J_{PH} = 3.8 Hz, 4H, ***CH₂***P^{t}Bu$_2$), 1.33 (vt, J_{PH} = 6.2 Hz, 36H, PC(C***H***$_3$)$_3$). ^{13}C NMR (C_6D_6, 125 MHz): δ 182.7 (t, J_{CP} = 4.2 Hz, CNBz), 173.4 (t, J_{CP} = 8.7 Hz, Ar, PCP), 155.7 (t, J_{CP} = 11.2 Hz, Ar, PCP), 136.8 (s, Ar), 129.1 (s, Ar), 127.9 (s, Ar), 127.7 (s, Ar), 124.6 (s, Ar, PCP), 120.2 (t, J_{CP} = 8.4 Hz, Ar, PCP), 47.2 (s, N***CH₂***Ph), 40.2 (vt, J_{CP} = 13.7 Hz, ***CH₂***P^{t}Bu$_2$), 36.1 (vt, J_{CP} = 10.2 Hz, P***C***(CH$_3$)$_3$), 30.3 (vt, J_{CP} = 2.9 Hz, PC(***C***H$_3$)$_3$).

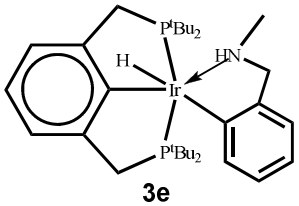

3e

Complex 3e: .To a 0.5mL *p*-xylene solution of 5 mg (PCP)IrH_4 (0.0083 mmol) in a J-Young tube, 5.4 µL TBE (0.0415 mmol) was added. After 1 day room temperature form (PCP)Ir(H)(TBV) formed, and 2.2 µL BzNHCH_3 (0.0166 mmol) was added to the solution. The NMR spectrum was recorded 15 min after the addition of amine. NMR spectrum indicates the formation of (PCP)Ir(H_2)(CNBz) in 10% yield, while the major compound (90 % yield) was the 6-coordinate amine complex **3e**. ^{31}P NMR (*p*-xylene-d_{10}, 202 MHz): δ 46.4 (s). ^{1}H NMR (*p*-xylene-d_{10}, 500 MHz): δ 7.38 (m, 1H, Ar), 7.24 (m, 1H, Ar), 7.16 (m, 1H, Ar), 6.99 (m, 2H, Ar), 6.96 (m, 2H, Ar), 4.12 (m, 1H, PhC***H***H-N(H)(CH_3)), 4.04 (dd, J_{HH} = 12.5 Hz, $^3J_{HH}$ = 4.0 Hz, 1H, PhC***H***H-N(H)(CH_3)), 3.78 (d of vt, J_{PH} = 1.7 Hz, J_{HH} = 14.5, 1H, ***CH***HP^{t}Bu$_2$), 3.44 (d of vt, J_{PH} = 2 Hz, J_{HH} = 15.0, 1H, ***CH***HP^{t}Bu$_2$), 3.27 (d of vt, J_{PH} = 3 Hz, J_{HH} = 15.5, 1H, ***CH***HP^{t}Bu$_2$), 3.07 (m, 1H, N(***H***)(CH_3)), 2.87 (d of vt, J_{PH} = 4.3 Hz, J_{HH} = 15.0, 1H, ***CH***HP^{t}Bu$_2$), 2.93 (d, $^3J_{HH}$ = 6.5 Hz, 3H, NH(***CH$_3$***)), 1.46 (t, J_{PH} = 5.8 Hz, 9H, PC(C***H***$_3$)$_3$), 1.17 (t, J_{PH} = 6.0 Hz, 9H, PC(C***H***$_3$)$_3$), 0.86 (dd, J_{PH} = 4.5 Hz, J_{PH} = 5.5 Hz, 18H, PC(C***H***$_3$)$_3$), -10.64 (t, J_{PH} = 18.2 Hz, 1H, , Ir-***H***).

3.4 References

(1) Michelin, R. A.; Pombeiro, A. J. L.; Guedes da Silva, M. F. C. *Coord. Chem. Rev.* **2001**, *218*, 75.
(2) Pombeiro, A. J. L.; Guedes da Silva, M. F. C.; Michelin, R. A. *Coord. Chem. Rev.* **2001**, *218*, 43.
(3) Tobisu, M.; Chatani, N. *Chem. Soc. Rev.* **2008**, *37*, 300.
(4) Alexander Dömling; Ivar Ugi *Angew. Chemie* **2000**, *39*, 3168.
(5) Diego J. Ramón; Miguel Yus *Angew. Chem., Int. Ed.* **2005**, *44*, 1602.
(6) Ivar Ugi; Winfried Betz; Uwe Fetzer; Klaus Offermann *Chem. Ber.* **1961**, *94*, 2814.
(7) Domling, A. *Chem. Rev.* **2006**, *106*, 17.
(8) Tsukada, N.; Wada, M.; Takahashi, N.; Inoue, Y. *J. Organomet. Chem.* **2009**, *694*, 1333.
(9) Janza, B.; Studer, A. *Org. Lett.* **2006**, *8*, 1875.
(10) Nicolas Isambert; Rodolfo Lavilla *Chem.A-Eur. J.* **2008**, *14*, 8444.
(11) Rainier, J. D.; Kennedy, A. R. *J. Org. Chem.* **2000**, *65*, 6213.
(12) Gilley, C. B.; Buller, M. J.; Kobayashi, Y. *Org. Lett.* **2007**, *9*, 3631.
(13) Fan, L.; Lobkovsky, E.; Ganem, B. *Org. Lett.* **2007**, *9*, 2015.
(14) Lacerda, R. B.; de Lima, C. K. F.; da Silva, L. L.; Romeiro, N. C.; Miranda, A. L. P.; Barreiro, E. J.; Fraga, C. A. M. *Bioorg. Med. Chem.* **2009**, *17*, 74.
(15) Sunderhaus, J. D.; Dockendorff, C.; Martin, S. F. *Org. Lett.* **2007**, *9*, 4223.
(16) Angelici, R. J.; Lazar, M. *Inorg. Chem.* **2008**, *47*, 9155.
(17) Mao, L.-F.; Mayr, A. *Inorg. Chem.* **1996**, *35*, 3183.
(18) Mayr, A.; Guo, J. *Inorg. Chem.* **1999**, *38*, 921.
(19) Arias, J.; BardajÃ, M.; Espinet, P. *Inorg. Chem.* **2008**, *47*, 3559.
(20) Roman Dembinski; Pablo Espinet; Sergio Lentijo; Marcin W. Markowicz; Jose M. Martín-Alvarez; Arnold L. Rheingold; Daniel J. Schmidt; Adam Sniady *Eur. J. Inorg. Chem.* **2008**, *2008*, 1565.
(21) Weber, W. P.; Gokel, G. W. *Tetrahedron Lett.* **1972**, *13*, 1637.
(22) Callan, B.; Manning, A. R.; Stephens, F. S. *J. Organomet. Chem.* **1987**, *331*, 357.
(23) Smith, P. A. S.; Kalenda, N. W. *J. Org. Chem.* **1958**, *23*, 1599.
(24) Zhang, X.; Emge, T. J.; Ghosh, R.; Goldman, A. S. *J. Am. Chem. Soc.* **2005**, *127*, 8250.
(25) Gu, X.-Q.; Chen, W.; Morales-Morales, D.; Jensen, C. M. *J. Mol. Catal. A* **2002**, *189*, 119.
(26) Gupta, M.; Hagen, C.; Flesher, R. J.; Kaska, W. C.; Jensen, C. M. *Chem. Commun.* **1996**, 2083.

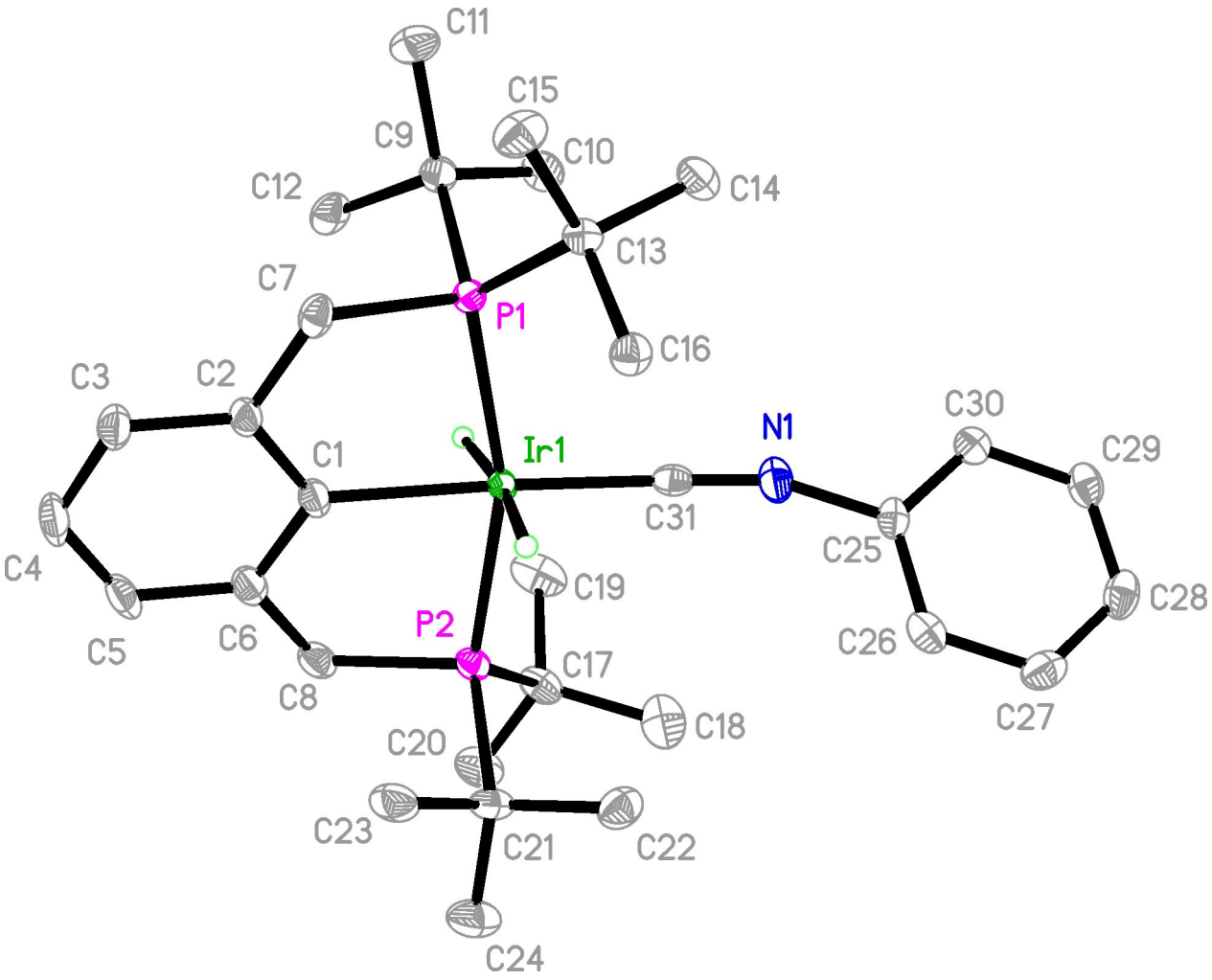

Figure 3-1 Crystal structure of complex **3-1d**

Table 3.2 Crystal data and structure refinement for **3-1d**

Empirical formula	C31 H50 Ir N P2	
Formula weight	690.86	
Temperature	100(2) K	
Wavelength	0.71073 Å	
Crystal system	Tetragonal	
Space group	P4(2)/mbc	
Unit cell dimensions	a = 20.6757(7) Å	α= 90°.
	b = 20.6757(7) Å	β= 90°.
	c = 14.2508(7) Å	γ = 90°.
Volume	6092.0(4) $Å^3$	
Z	8	
Density (calculated)	1.507 Mg/m^3	
Absorption coefficient	4.508 mm^{-1}	
F(000)	2800	
Crystal size	0.40 x 0.12 x 0.09 mm^3	
Theta range for data collection	1.97 to 30.64°.	
Index ranges	-29<=h<=20, -29<=k<=16, -19<=l<=20	
Reflections collected	29947	
Independent reflections	9262 [R(int) = 0.0267]	
Completeness to theta = 30.64°	99.7 %	
Absorption correction	None	
Max. and min. transmission	0.6871 and 0.2657	
Refinement method	Full-matrix least-squares on F^2	
Data / restraints / parameters	9262 / 3 / 334	
Goodness-of-fit on F^2	0.906	
Final R indices [I>2sigma(I)]	R1 = 0.0209, wR2 = 0.0417	
R indices (all data)	R1 = 0.0237, wR2 = 0.0424	
Absolute structure parameter	-0.004(3)	
Largest diff. peak and hole	1.488 and -0.392 $e.Å^{-3}$	

Table 3.3 Selective bond lengths [Å] and angles [°] for complex **3-1d**

Ir(1)-C(31)	1.930(3)	N(1)-C(25)	1.407(3)
Ir(1)-C(1)	2.094(2)	C(25)-C(30)	1.390(3)
Ir(1)-P(2)	2.2989(6)	C(25)-C(26)	1.392(3)
Ir(1)-P(1)	2.3073(6)	C(26)-C(27)	1.391(4)
Ir(1)-H(1)	1.597(10)	C(27)-C(28)	1.387(4)
Ir(1)-H(2)	1.609(10)	C(28)-C(29)	1.373(4)
P(1)-C(7)	1.840(2)	C(29)-C(30)	1.391(3)
P(1)-C(13)	1.882(2)	(31)-Ir(1)-C(1)	177.06(10)
P(1)-C(9)	1.894(2)	C(31)-Ir(1)-P(2)	97.05(7)
P(2)-C(8)	1.841(2)	C(1)-Ir(1)-P(2)	81.65(7)
P(2)-C(17)	1.891(3)	C(31)-Ir(1)-P(1)	100.26(7)
P(2)-C(21)	1.891(2)	C(1)-Ir(1)-P(1)	81.10(7)
C(1)-C(2)	1.408(3)	P(2)-Ir(1)-P(1)	162.67(2)
C(1)-C(6)	1.413(3)	C(31)-Ir(1)-H(1)	100.0(10)
C(2)-C(3)	1.395(3)	C(1)-Ir(1)-H(1)	82.5(10)
C(2)-C(7)	1.505(4)	P(2)-Ir(1)-H(1)	83.6(9)
C(3)-C(4)	1.395(4)	P(1)-Ir(1)-H(1)	92.6(9)
C(4)-C(5)	1.379(4)	C(31)-Ir(1)-H(2)	87.4(10)
C(5)-C(6)	1.404(3)	C(1)-Ir(1)-H(2)	90.0(10)
C(6)-C(8)	1.506(4)	P(2)-Ir(1)-H(2)	92.5(9)
C(9)-C(12)	1.532(4)	P(1)-Ir(1)-H(2)	89.1(9)
C(9)-C(11)	1.534(4)	H(1)-Ir(1)-H(2)	172.0(14)
C(9)-C(10)	1.543(3)	C(7)-P(1)-C(13)	104.17(11)
C(13)-C(14)	1.531(4)	C(7)-P(1)-C(9)	104.19(11)
C(13)-C(15)	1.539(3)	C(13)-P(1)-C(9)	110.52(11)
C(13)-C(16)	1.540(3)	C(7)-P(1)-Ir(1)	102.61(8)
C(14)-H(14A)	0.9800	C(13)-P(1)-Ir(1)	118.23(8)
C(17)-C(20)	1.535(4)	C(9)-P(1)-Ir(1)	115.07(8)
C(17)-C(18)	1.536(4)	C(8)-P(2)-C(17)	103.68(14)
C(17)-C(19)	1.543(4)	C(8)-P(2)-C(21)	104.40(14)
C(21)-C(24)	1.533(4)	C(17)-P(2)-C(21)	110.06(13)
C(21)-C(23)	1.534(4)	C(8)-P(2)-Ir(1)	102.48(7)
C(21)-C(22)	1.540(4)	C(17)-P(2)-Ir(1)	118.83(9)
N(1)-C(31)	1.177(3)	C(21)-P(2)-Ir(1)	115.25(8)

Chapter 4

Oxidation addition of MeI to (PCP)Ir carbonyl and isocyanide complexes

Abstract

(PCP)IrL (L = CO and CNR) reacts with methyl iodide to form corresponding 6-cordinated (PCP)Ir(Me)(I)(L) efficiently. The mechanism of this oxidative addition and the properties of these 6-cordinated (PCP)Ir(Me)(I)(L) complexes is studied.

To understand the structure of these complexes, CO and CNBz was added to (PCP)Ir(Me)(I) and immediately 6-cordinated (PCP)Ir(Me)(I)(L) was formed.

4.1 Introduction

Oxidative addition to metal centers is a fundamental step in organometallic chemistry and a critical step in many orgamometallic processes.[1]

The oxidative addition of methyl iodide to iridium (I) and rhodium (I) carbonyl complexes is one of the key steps in the Monsanto process.[2, 3] Extensive research has been done to understand the oxidative addition of methyl iodide as well as migration of methyl group.[4, 5]

In this chapter we discuss the oxidative addition of methyl iodide to (PCP)Ir(CO or CNR) complexes.

4.2 Results and Discussion

4.2.1 Reaction of (PCP)Ir(CO) with MeI

Milstein and coworkers have reported that MeI reacts quantitatively to (^{iPr4}PCP)Ir(CO) to form (^{iPr4}PCP)Ir(CO)(Me)(I) (Me and I are *trans* to each other).[6]

In contrast, Mira Kanzelberger reported (^{tBu4}PCP)Ir(CO) reacts with MeI to form only PCP iridium acyl iodide complex **4-2** (eq.1).[7] This is a different observation than what Milstein reported with (^{iPr4}PCP)Ir(CO). Complex **4-2** is believed to be formed through the six-coordinated intermediate **4-1**.

In intermediate **4-1**, steric crowding is much more pronounced than corresponding (^{iPr4}PCP)Ir(CO)(Me)(I) because of the bulky ^{t}Bu group on the phosphorous atoms. The migration of the methyl group to the carbonyl carbon is facilitated by the steric crowding in **4-1**.

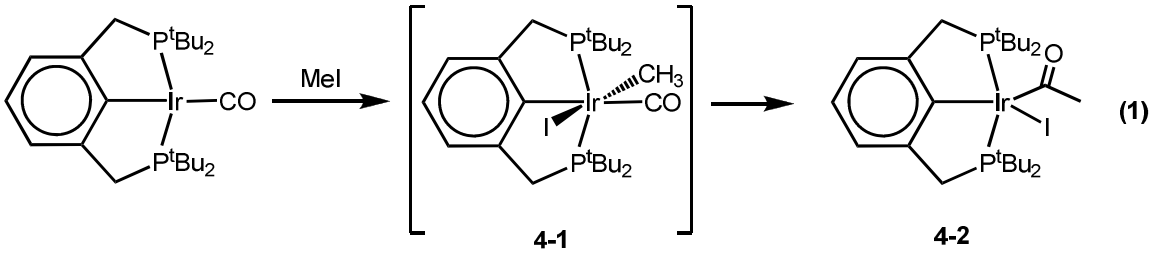

4.2.2 Reaction of (PCP)Ir(CNBz) with MeI

(^{tBu4}PCP)Ir(CNBz) reacts with MeI quite readily in comparison to (^{tBu4}PCP)Ir(CO) to form complex **4-3** (eq. 2). Complex **4-3** was characterized by NMR spectroscopy and X-ray crystallography. In the ^{1}H NMR spectrum Ir-**CH$_3$** appears as a triplet at 1.34 ppm (J_{PH} = 5.0 Hz) and in the ^{13}C NMR spectrum a triplet at -19.2 ppm (J_{PC} = 7.4 Hz). In ^{31}P NMR spectroscopy complex **4-3** appears at 30.84 ppm as a singlet.

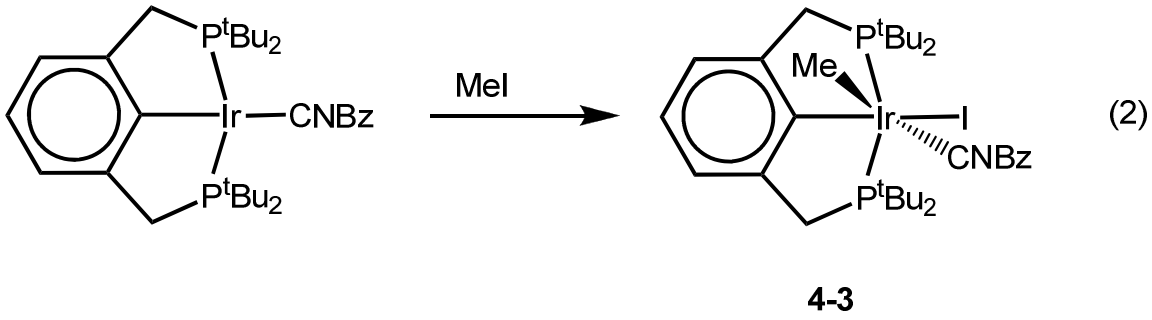

Complex **4-3** was crystallized from *n*-hexane and the structure is confirmed by X-ray crystallography. Figure 4.1 shows an ORTEP of this complex, refinement parameters are given in Table 4.1 and bond angles and bond distances are listed in Table 4.2. Interestingly in this structure methyl and isocyanide groups are mutually *trans* to each other while the iodide is *trans* to PCP ipsocarbon. Milstein reported that methyl and iodide groups are *trans* to each other in his work with (^{iPr4}PCP)Ir(CO)(Me)(I)) and Mira Kanzelberger also reported formation of (PCP)Ir(C(O)Me)(I) was expected through

intermediate **4-1**, in which Me and I are *trans* to each other. In complex **4-3** methyl and iodide are *cis* to each other, possibly due to isomerization of the *trans* product, when kept for crystallization. To rule out the possibility of isomerization, isocyanide was added to complex **4-4**, synthesized as shown in Scheme 4-1, and immediately complex **4-3** was formed as confirmed by NMR spectroscopy (Scheme 4-1).

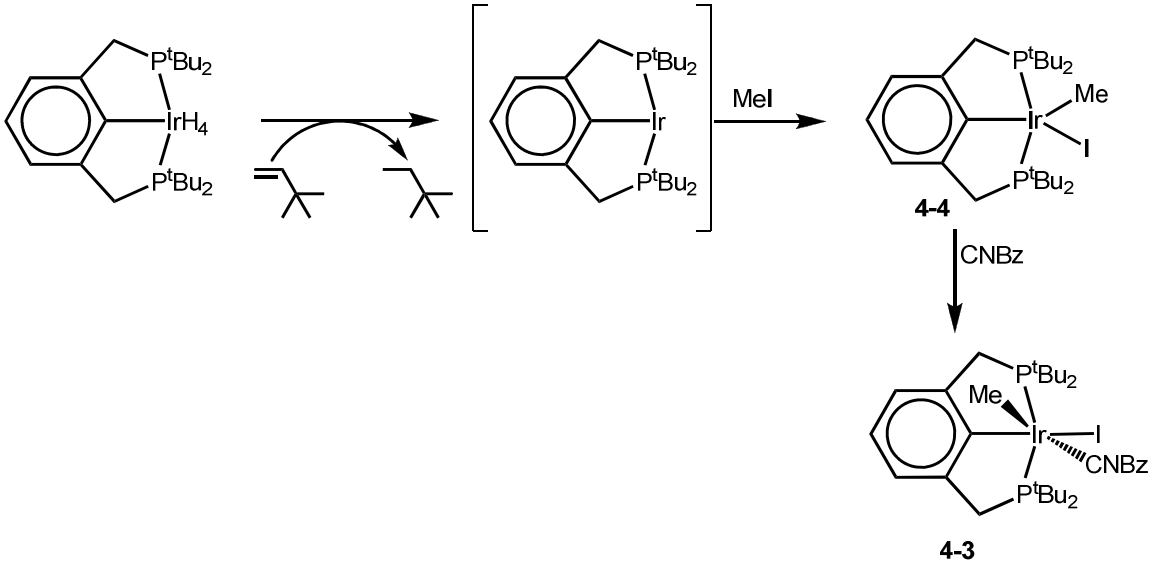

Scheme 4-1 Synthesis of complexes **4-4** and **4-3**

Complex **4-3** is kinetically stable at room temperature but it is not stable thermally. The elimination of MeI from complex **4-3** gave complex **4-4** and (PCP)Ir(CNBz) along with some minor uncharacterized product when heated at 100 °C for 2 hours. When complex **4-3** was heated with 2 equivalent of free MeI at 100 °C for 2 hours, uncharacterized products were formed but no (PCP)Ir(CNBz) was observed by NMR spectroscopy. After adding CO to these uncharacterized products, complex **4-5** was crystallized from hexane/benzene.

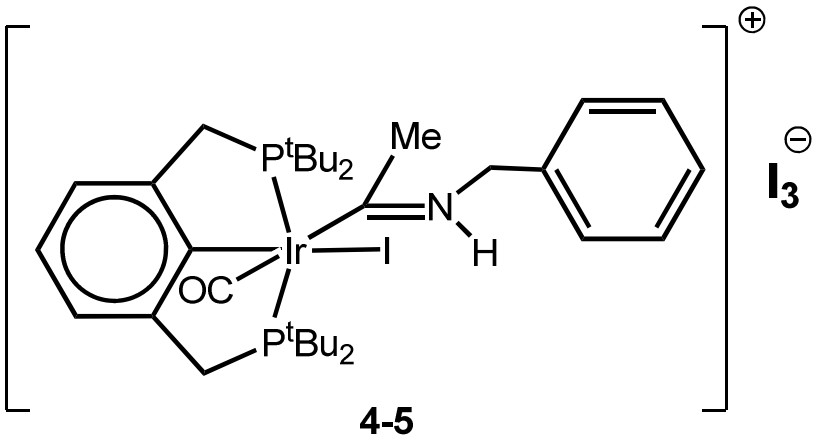

4-5

4.3 Experimental

General Methods. All reactions were carried out under an argon atmosphere using standard Schlenk techniques or in an argon-filled dry box. *p*-Xylene, *p*-xylene-d_{10}, C_6D_6, 1-hexene and TBE were dried using Na/K alloy and collected by vacuum transfer. Benzyl isocyanide was purchased from Aldrich. NBE was sublimed before use. 400 MHz or 500 MHz Varian instruments were used for the ^{1}H, ^{13}C and ^{31}P NMR spectroscopic experiments. The residual peak of the deuterated solvent was used as a reference for ^{1}H chemical shifts. ^{31}P NMR chemical shifts were referenced to PMe_3 standard, which appears at –62.2 ppm. PMe_3 internal standard in ^{31}P NMR was employed in determining the yield. (^{tBu4}PCP)IrH_4 (PCP= κ^3-2,6-($^{t}Bu_2PCH_2)_2C_6H_3$) was prepared as described in the literature.[8]

(PCP)Ir(Me)(I)(CNBz) (4-3): To a 0.5 mL C_6D_6 solution of 5 mg (PCP)IrH_4 (0.0083 mmol), 5.2 μL 1-hexene (0.0415 mmol) was added after 20 minute at room temperature, NMR indicates formation of (PCP)Ir(1-hexene). (PCP)Ir(CNBz) was formed immediately after addition of 1.1 μL CNBz (0.0083 mmol) to this solution. 1.1 μL MeI (0.0166 mmol) was added to the solution, after 10 h at room temperature, NMR spectrum showed the formation of complex **4-3** in 100 % yield. ^{31}P NMR (C_6D_6, 162 MHz): δ 30.84 (s). ^{1}H NMR (C_6D_6, 400 MHz): δ 7.02 (m, 6H, Ar), 7.14 (m, 5H, Ar), 6.95 (m, 2H, Ar), 3.93 (s, 2H, ***CH₂***Ph), 3.42 (d of vt, J_{PH} = 3.8 Hz, J_{HH} = 16.0 Hz, 2H, ***CH₂***P^{t}Bu$_2$), 2.87 (d of vt, J_{PH} = 3.6 Hz, J_{HH} = 16.0 Hz, 2H, ***CH₂***P^{t}Bu$_2$), 1.39 (t, J_{PH} = 6.0 Hz, 18H, PC(C***H***$_3$)$_3$), 1.34 (t, J_{PH} = 5.0 Hz, 3H, Ir-***C***H$_3$), 1.27 (t, J_{PH} = 6.0 Hz, 18H, PC(C***H***$_3$)$_3$). ^{13}C NMR (C_6D_6, 125 MHz): δ 148.1 (s, Ar), 146.7 (t, J_{PC} = 5.8 Hz, Ar, PCP), 136.2 (t, J_{PC} = 7.2 Hz, Ir-***C***NBz), 132.8 (s, Ar), 129.4 (s, Ar), 128.7 (s, Ar), 127.7 (s, Ar), 123.6 (s, Ar, PCP), 122.0 (t, J_{PC} = 6.8 Hz, PCP), 48.4 (s, ***C***H$_2$Ph), 39.2 (vt, J_{PC} = 9.5 Hz, P***C***(CH$_3$)$_3$)), 37.9 (vt, J_{PC} = 9.7 Hz, P***C***(CH$_3$)$_3$), 37.4 (vt, J_{PC} = 12.6 Hz, ***CH₂***P^{t}Bu$_2$), 32.1 (vt, J_{PC} = 1.1 Hz, PC(***C***H$_3$)$_3$)), 31.3 (vt, J_{PC} = 1.1 Hz, PC(***C***H$_3$)$_3$)), -19.2 (t, J_{PC} = 7.4 Hz, Ir-***C***H$_3$).

(PCP)Ir(Me)(I) (4-4): To a 0.5 mL *p*-xylene-d_{10} solution of 5 mg (PCP)IrH_4 (0.0083 mmol) in a J-Young tube, 2.4 mg NBE (0.025 mmol) and 0.82 μL MeI (0.0083 mmol) ware added. After 30 minutes at room temperature, complex **4-4** was quantitatively formed. ^{31}P NMR (C_6D_6, 162 MHz): δ 42.2 (s). ^{1}H NMR (C_6D_6, 400 MHz): δ 6.78 (d, J_{HH} = 7.3 Hz, 2H, Ar), 6.70 (d, J_{HH} = 7.3 Hz, 1H, Ar), 2.72 (d of vt, J_{PH} = 4.3 Hz, J_{HH} = 17.4 Hz, 2H, ***CH₂***P^{t}Bu$_2$), 2.67 (d of vt, J_{PH} = 3.8 Hz, J_{HH} = 17.4 Hz, 2H, ***CH₂***P^{t}Bu$_2$), 1.36 (t, J_{PH} = 4.8 Hz, 3H, Ir-**C*H*₃**), 1.11 (t, J_{PH} = 6.4 Hz, 18H, PC(C***H***$_3$)$_3$), 0.84 (t, J_{PH} = 6.0 Hz,

18 H, PC(C***H***$_3$)$_3$). ^{13}C NMR (C_6D_6,100 MHz) 158.4 (s, Ar), 149.8 (t, J_{CP} = 7.4 Hz., Ar), 122.9, 121.5 (vt, J_{CP} = 7.9 Hz. Ar), 36.9 (vt, J_{CP} = 11.4 Hz., P***C***(CH$_3$)$_3$), 34.2 (vt, J_{CP} = 12.1 Hz., ***C***H$_2$P), 31.7 (vt, J_{CP} = 1.7 Hz., PC(***C***H$_3$)$_3$), 29.7 (vt, J_{CP} = 1.5 Hz., PC(***C***H$_3$)$_3$), -25.6 (vt, J_{CP} = 4.3 Hz., Ir-***C***H$_3$).

When CNBz was added to (PCP)Ir(Me)(I) complex **4-3** was formed. In which Me and iodide groups were *cis* to each other.

4.4 References

(1) Crabtree, R. H., The Organometallic Chemistry of Transition Metals; 3rd ed.; Jon Wiley & Sons, Inc: New York, **2001**.
(2) Zoeller, J. R.; Agreda, V. H.; Cook, S. L.; Lafferty, N. L.; Polichnowski, S. W.; Pond, D. M. *Catal. Today* **1992**, *13*, 73.
(3) Bassetti, M.; Capone, A.; Mastrofrancesco, L.; Salamone, M. *Organometallics* **2003**, *22*, 2535.
(4) Bennett, M. A.; Crisp, G. T. *Organometallics* **1986**, *5*, 1800.
(5) Bassetti, M.; Capone, A.; Salamone, M. *Organometallics* **2003**, *23*, 247.
(6) Rybtchinski, B. Ben-David, Y.; Milstein, D. *Organometallics* **1997**, *16*, 3786.
(7) *Mira Kanzelberger PhD thesis Rutgers* **2004**.
(8) Gupta, M.; Hagen, C.; Flesher, R. J.;Kaska, W. C.; Jensen, C. M. *Chem. Commun.* **1996**, 2083.

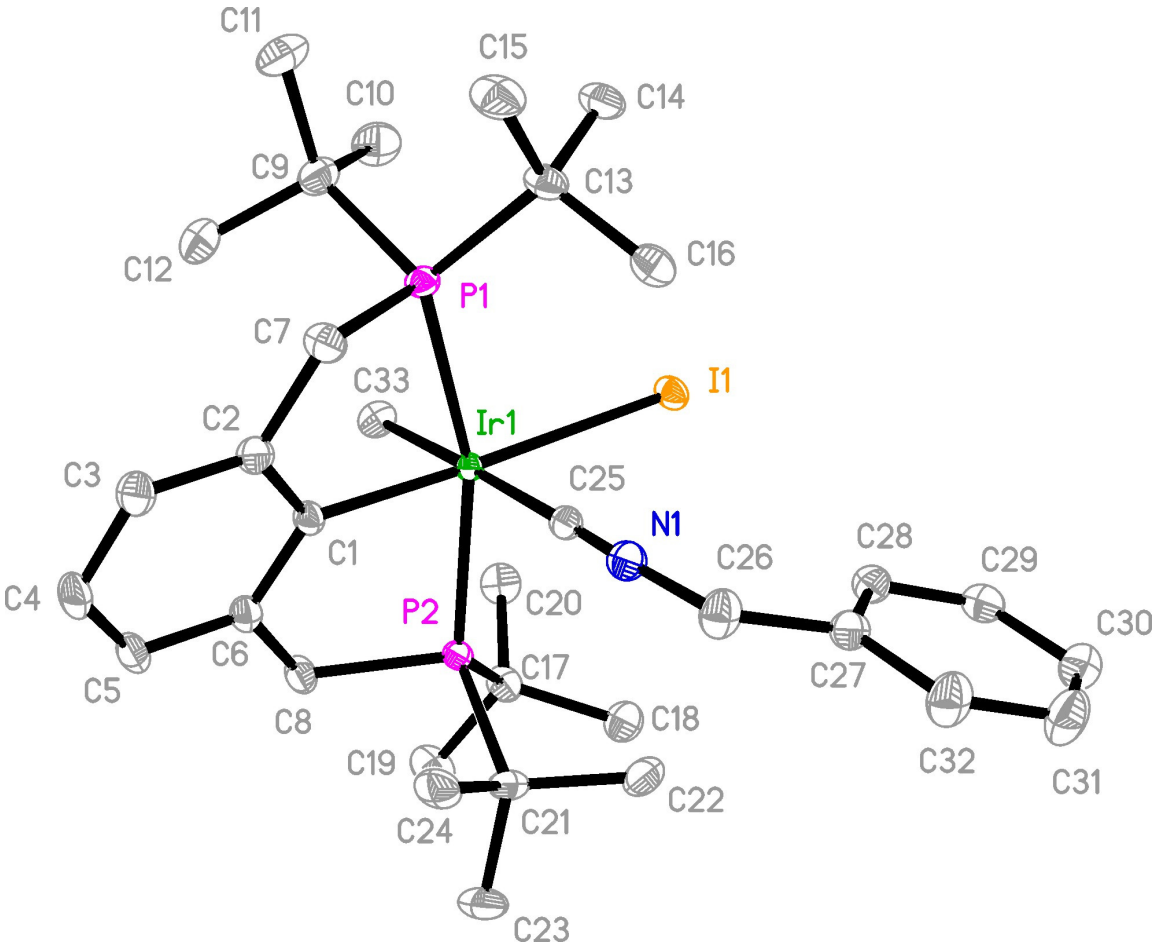

Figure 4.1 Crystal structure of complex **4-3**

Table 4.1 Crystal data and structure refinement for complex **4-3**

Empirical formula	C33 H53 I Ir N P2	
Formula weight	844.80	
Temperature	100(2) K	
Wavelength	0.71073 Å	
Crystal system	Triclinic	
Space group	P-1	
Unit cell dimensions	a = 8.7459(4) Å	α= 81.260(1)°.
	b = 13.1837(6) Å	β= 85.779(1)°.
	c = 14.6622(7) Å	γ = 82.248(1)°.
Volume	1653.26(13) $Å^3$	
Z	2	
Density (calculated)	1.697 Mg/m^3	
Absorption coefficient	5.091 mm^{-1}	
F(000)	836	
Crystal size	0.39 x 0.23 x 0.08 mm^3	
Theta range for data collection	2.26 to 31.00°.	
Index ranges	-12<=h<=12, -19<=k<=19, -20<=l<=21	
Reflections collected	20922	
Independent reflections	10368 [R(int) = 0.0167]	
Completeness to theta = 31.00°	98.2 %	
Absorption correction	Semi-empirical from equivalents	
Max. and min. transmission	0.686 and 0.241	
Refinement method	Full-matrix least-squares on F^2	
Data / restraints / parameters	10368 / 0 / 356	
Goodness-of-fit on F^2	1.001	
Final R indices [I>2sigma(I)]	R1 = 0.0201, wR2 = 0.0486	
R indices (all data)	R1 = 0.0214, wR2 = 0.0492	
Largest diff. peak and hole	1.429 and -1.534 e.$Å^{-3}$	

Table 4.2 Selected bond lengths [Å] and angles [°] for complex **4-3**

Ir(1)-C(25)	1.973(2)	C(3)-C(4)	1.392(3)
Ir(1)-C(1)	2.0398(19)	C(4)-C(5)	1.388(3)
Ir(1)-C(33)	2.145(2)	C(5)-C(6)	1.397(3)
Ir(1)-P(1)	2.3799(5)	C(6)-C(8)	1.514(3)
Ir(1)-P(2)	2.3829(5)	C(9)-C(11)	1.542(3)
Ir(1)-I(1)	2.81439(17)	C(9)-C(12)	1.546(3)
P(1)-C(7)	1.843(2)	C(9)-C(10)	1.551(3)
P(1)-C(13)	1.899(2)	C(13)-C(16)	1.534(3)
P(1)-C(9)	1.899(2)	C(13)-C(14)	1.538(3)
P(2)-C(8)	1.845(2)	C(13)-C(15)	1.542(3)
P(2)-C(21)	1.896(2)	C(17)-C(20)	1.532(3)
P(2)-C(17)	1.899(2)	C(17)-C(19)	1.538(3)
C(1)-C(6)	1.412(3)	C(17)-C(18)	1.543(3)
C(1)-C(2)	1.413(3)	C(21)-C(23)	1.541(3)
C(2)-C(3)	1.396(3)	C(21)-C(24)	1.543(3)
C(2)-C(7)	1.510(3)	C(21)-C(22)	1.545(3)
C(25)-Ir(1)-C(1)	93.30(8)	C(7)-P(1)-Ir(1)	97.41(7)
C(25)-Ir(1)-C(33)	177.13(8)	C(13)-P(1)-Ir(1)	121.67(7)
C(1)-Ir(1)-C(33)	87.49(8)	C(9)-P(1)-Ir(1)	119.03(7)
C(25)-Ir(1)-P(1)	90.17(6)	C(8)-P(2)-C(21)	101.93(10)
C(1)-Ir(1)-P(1)	81.75(6)	C(8)-P(2)-C(17)	106.29(9)
C(33)-Ir(1)-P(1)	92.68(6)	C(21)-P(2)-C(17)	106.66(10)
C(25)-Ir(1)-P(2)	92.72(6)	C(8)-P(2)-Ir(1)	99.20(7)
C(1)-Ir(1)-P(2)	81.27(6)	C(21)-P(2)-Ir(1)	115.68(7)
C(33)-Ir(1)-P(2)	84.67(6)	C(17)-P(2)-Ir(1)	123.99(7)
P(1)-Ir(1)-P(2)	162.915(17)	C(6)-C(1)-C(2)	118.54(18)
C(25)-Ir(1)-I(1)	88.93(5)	C(6)-C(1)-Ir(1)	121.31(14)
C(1)-Ir(1)-I(1)	177.38(5)	C(2)-C(1)-Ir(1)	120.15(14)
C(33)-Ir(1)-I(1)	90.35(6)	C(3)-C(2)-C(1)	120.32(19)
P(1)-Ir(1)-I(1)	96.885(13)	C(3)-C(2)-C(7)	121.03(18)
P(2)-Ir(1)-I(1)	100.002(12)	C(1)-C(2)-C(7)	118.65(17)
C(7)-P(1)-C(13)	104.28(9)	C(4)-C(3)-C(2)	120.41(19)
C(7)-P(1)-C(9)	104.08(10)	C(5)-C(4)-C(3)	119.88(19)
C(13)-P(1)-C(9)	107.08(10)	C(4)-C(5)-C(6)	120.6(2)

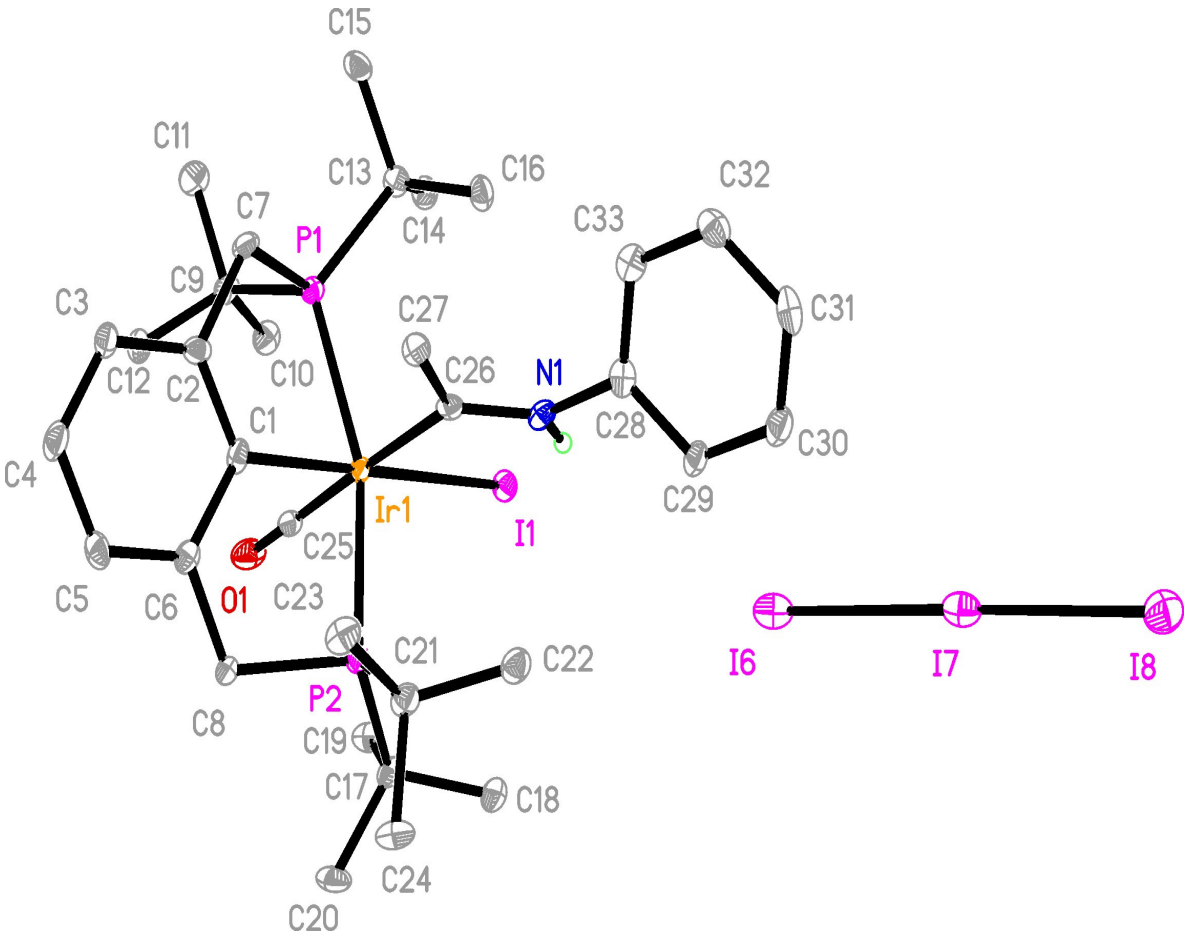

Figure 4.2 Crystal structure of complex **4-5**

Table 4.3 Crystal data and structure refinement for complex **4-5**

Empirical formula	C45 H67 I4 Ir N O P2	
Formula weight	1399.74	
Temperature	100(2) K	
Wavelength	0.71073 Å	
Crystal system	Monoclinic	
Space group	P2(1)/c	
Unit cell dimensions	a = 19.2899(14) Å	α= 90°.
	b = 15.9012(11) Å	β= 97.498(1)°.
	c = 31.875(2) Å	γ = 90°.
Volume	9693.5(12) $Å^3$	
Z	8	
Density (calculated)	1.918 Mg/m^3	
Absorption coefficient	5.402 mm^{-1}	
F(000)	5368	
Crystal size	0.17 x 0.08 x 0.06 mm^3	
Theta range for data collection	1.73 to 28.28°.	
Index ranges	-25<=h<=24, -21<=k<=15, -35<=l<=42	
Reflections collected	49632	
Independent reflections	23556 [R(int) = 0.0368]	
Completeness to theta = 28.28°	97.8 %	
Absorption correction	Semi-empirical from equivalents	
Max. and min. transmission	0.737 and 0.460	
Refinement method	Full-matrix least-squares on F^2	
Data / restraints / parameters	23556 / 0 / 1011	
Goodness-of-fit on F^2	1.001	
Final R indices [I>2sigma(I)]	R1 = 0.0416, wR2 = 0.0819	
R indices (all data)	R1 = 0.0579, wR2 = 0.0874	
Largest diff. peak and hole	3.733 and -2.321 $e.Å^{-3}$	

Table 4.4 Selected bond lengths [Å] and angles [°] for complex **4-5**

Ir(1)-C(25)	1.896(6)	C(3)-C(4)	1.385(8)
Ir(1)-C(1)	2.070(5)	C(4)-C(5)	1.385(8)
Ir(1)-C(26)	2.121(6)	C(5)-C(6)	1.393(7)
Ir(1)-P(1)	2.4189(14)	C(6)-C(8)	1.528(8)
Ir(1)-P(2)	2.4456(15)	C(9)-C(12)	1.552(8)
Ir(1)-I(1)	2.8029(4)	C(9)-C(11)	1.554(8)
P(1)-C(7)	1.843(6)	C(9)-C(10)	1.561(8)
P(1)-C(13)	1.884(6)	C(13)-C(16)	1.525(8)
P(1)-C(9)	1.884(5)	C(13)-C(14)	1.532(8)
P(2)-C(8)	1.839(5)	C(13)-C(15)	1.545(8)
P(2)-C(21)	1.899(6)	C(17)-C(19)	1.540(8)
P(2)-C(17)	1.901(6)	C(17)-C(18)	1.542(7)
C(1)-C(2)	1.390(8)	C(17)-C(20)	1.543(8)
C(1)-C(6)	1.417(8)	C(21)-C(23)	1.536(8)
C(2)-C(3)	1.396(8)	C(21)-C(22)	1.540(8)
C(2)-C(7)	1.521(8)	C(21)-C(24)	1.546(8)
C(25)-Ir(1)-C(1)	89.4(2)	C(7)-P(1)-Ir(1)	98.76(18)
C(25)-Ir(1)-C(26)	178.1(2)	C(13)-P(1)-Ir(1)	122.24(17)
C(1)-Ir(1)-C(26)	92.5(2)	C(9)-P(1)-Ir(1)	114.79(19)
C(25)-Ir(1)-P(1)	89.27(17)	C(8)-P(2)-C(21)	102.7(3)
C(1)-Ir(1)-P(1)	80.13(16)	C(8)-P(2)-C(17)	105.1(3)
C(26)-Ir(1)-P(1)	91.66(15)	C(21)-P(2)-C(17)	108.5(3)
C(25)-Ir(1)-P(2)	86.42(17)	C(8)-P(2)-Ir(1)	96.32(18)
C(1)-Ir(1)-P(2)	81.36(16)	C(21)-P(2)-Ir(1)	120.93(19)
C(26)-Ir(1)-P(2)	93.24(15)	C(17)-P(2)-Ir(1)	119.50(19)
P(1)-Ir(1)-P(2)	161.03(5)	C(2)-C(1)-C(6)	119.1(5)
C(25)-Ir(1)-I(1)	86.92(17)	C(2)-C(1)-Ir(1)	121.3(4)
C(1)-Ir(1)-I(1)	176.01(15)	C(6)-C(1)-Ir(1)	119.5(4)
C(26)-Ir(1)-I(1)	91.24(14)	C(1)-C(2)-C(3)	120.2(5)
P(1)-Ir(1)-I(1)	98.27(4)	C(1)-C(2)-C(7)	119.9(5)
P(2)-Ir(1)-I(1)	99.93(3)	C(3)-C(2)-C(7)	119.8(5)
C(7)-P(1)-C(13)	106.4(3)	C(4)-C(3)-C(2)	120.6(5)
C(7)-P(1)-C(9)	104.0(3)	C(3)-C(4)-C(5)	119.8(5)
C(13)-P(1)-C(9)	108.2(3)	C(3)-C(4)-H(4)	120.1(5)

Chapter 5

Acid catalyzed addition of phenyl acetylene to (PCP)Ir(CO) and (PCP)Ir(CNBz)

Abstract

The addition of PhCCH or CH_3NO_2 to highly stable complexes, (PCP)IrL (L = CO, CNR), (PCP = κ^3-2,6-(^{t}Bu$_2$PCH$_2$)$_2$C$_6$H$_3$) is challenging. (PCP)IrL (L = CO, CNR) complexes reacts with PhCCH in presence of acid to form complex (PCP)Ir(CO)(H)(CCPh) (**5-3)** and (PCP)Ir(CNBz)(H)(CCPh) (**5-1)**, respectively, in which the hydride and acetylide group are *trans* to each other. The reaction proceeds via a cationic intermediate $[(PCP)Ir(CO)(H)]^+$. Addition of PhCCH to (PCP)Ir(CO) is also catalyzed by an independently synthesized complex $[(PCP)Ir(CO)(H)]^+B(C_6F_5)_4^-$.

5.1 Introduction

Activation of alkynes by transition metal catalysts has been extensively studied for decades.[1-4] Alkynes bearing electron withdrawing groups react to a metal center quite easily, but alkynes without any activating group, such as PhCCH or PhCCPh, fail to react.[5]

Phenyl acetylene was dimerized by the (PCP)Ir complex, and its mechanistic details were studied.[6] But alkyne addition to 4-coordinated (PCP)Ir(CO) or (PCP)Ir(CNR) is challenging due to the high stability of these 16-electron complexes. In the previous chapter we discussed oxidative addition of MeI to these complexes. In this chapter we will discuss acid catalyzed electrophilic addition of PhCCH and CH_3NO_2 to (PCP)Ir(CO) and (PCP)Ir(CNR).

Addition of phenyl acetylene to (PCP)Ir(CO) and (PCP)Ir(CNR) was catalyzed by an acid, and not by a base.[7] Addition of other substrates such as PhOH, EtOH, $PhNH_2$, CH_3NO_2, and CH_3CN was studied; of these only CH_3NO_2 reacted with both (PCP)Ir(CO) and (PCP)Ir(CNR).

5.2 Results and Discussion

5.2.1 Synthesis and characterization of (PCP)Ir(CNBz)(H)(CCPh) (H and CCPh *trans*) (5-1)

(PCP)Ir(CNBz) did not react with PhCCH even at a high concentration (3 M) at room temperature; however, upon heating at 100 °C for 2 days, addition product (PCP)Ir(CNBz)(H)(CCPh) (**5-1**) was formed, where H and CCPh are *trans* to each other. Interestingly, (PCP)Ir(CNBz) reacted with phenyl acetylene at room temperature, in presence of 2 mM acid (4-(trifluoromethyl)benzoic acid) to give the same product (**5-1**)

without the formation any acid adduct (eq. 1). Complex **5-1** was characterized by NMR spectroscopy and X-ray crystallography.

Complex **5-1** was crystallized from a benzene and hexane (1:1 ratio) solution mixture. The ORTEP diagram of complex **5-1** is shown in Figure 5-1. Crystal parameters, bond angles and bond distances are listed in Table 5.1 and Table 5.2. In complex **5-1** the isocyanide carbon is *trans* to the PCP *ipso*-carbon, while the hydride is *trans* to the acetylide group.

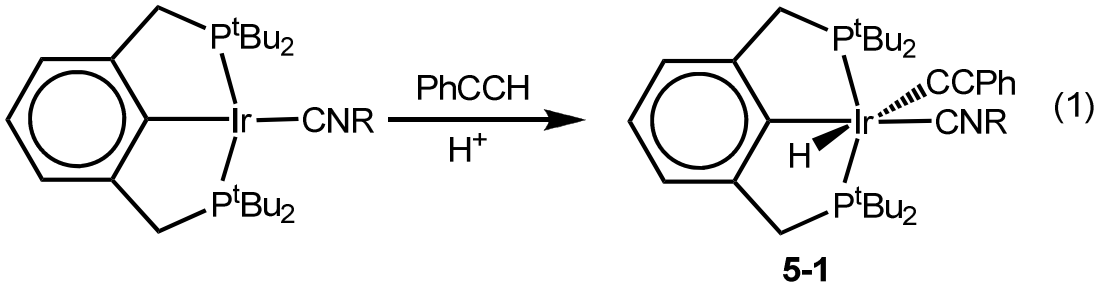

(1)

5-1

5.2.2 Synthesis and characterization of (PCP)Ir(CNBz)(H)(CCPh) (H and CCPh *cis*) (5-2)

(PCP)Ir(H)(CCPh) was generated by the addition of 1 equivalent PhCCH to (PCP)Ir(NBE). Complex (PCP)Ir(CNBz)(H)(CCPh) (**5-2**), in which where H and CCPh are *cis* to each other, was formed immediately after addition of CNBz to the solution (eq. 2). Complex **5-2** was characterized by NMR spectroscopy. It resonates at 55.98 ppm in ^{31}P NMR spectrum as a singlet and in the ^{1}H NMR spectrum t hehydride showed as a triplet at -11.51 ppm (J_{PH} = 16.2 Hz).

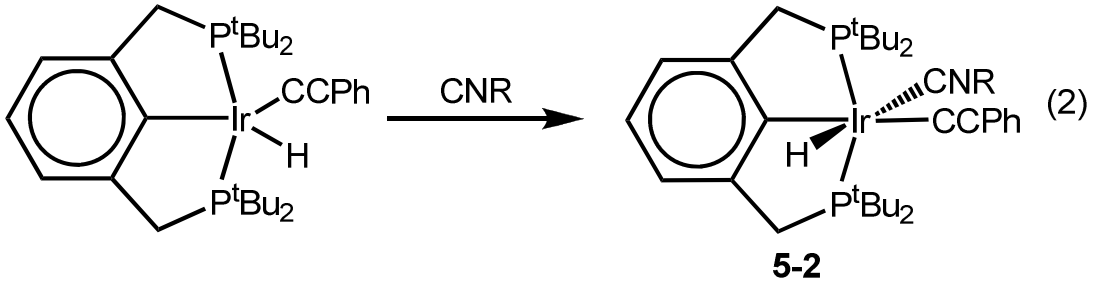

(2)

5-2

5.2.3 Synthesis and characterization of (PCP)Ir(CO)(H)(CCPh) (H and CCPh *trans*) (5-3)

(PCP)Ir(CO) did not react with PhCCH even with a high concentration (3 M) with heating at 120 °C for 3 days. But in the presence of 2 mM 4-(trifluoromethyl)benzoic acid, complex **5-3** was formed in 11% yield after heating for 2 h at 80 °C. Complex **5-3** was formed in 82% yield after heating at 80 °C for 7 days; along with 2% acid adduct (**5-8**) (eq. 3). This acid catalyzed reaction was tested with varying concentrations of acid. After heating for 2 h at 80 °C with 5 mM or 10 mM of acid, complex **5-3** was observed in 30% and 60% yield, respectively. Complex **5-3** was characterized by NMR spectroscopy. It resonates as a singlet at 64.3 ppm in ^{31}P NMR spectrum and the ^{1}H NMR spectrum showed the hydride signal as a triplet at -11.78 ppm (J_{PH} = 14.4 Hz).

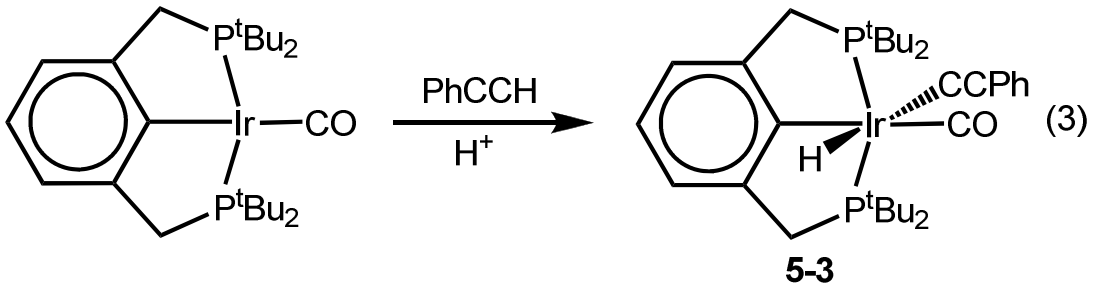

(3)

5-3

5.2.4 Synthesis and characterization of (PCP)Ir(CO)(H)(CCPh) (H and CCPh *cis*) (5-4)

(PCP)Ir(H)(CCPh) was generated by the addition of 1 equivalent of PhCCH to (PCP)Ir(NBE). When 1 atmosphere CO was added, an immediate color change from purple to yellow was observed, and complex (PCP)Ir(CO)(H)(CCPh) (**5-4**) was formed (eq. 4). Complex **5-4** was characterized by NMR spectroscopy and X-ray crystallography. It resonates at 58.05 ppm in ^{31}P NMR spectrum as a singlet, while in ^{1}H NMR spectrum hydride showed as a triplet at -9.64 ppm (J_{PH} = 15.6 Hz).

Complex **5-4** was crystallized from a benzene and hexane (1:1 ratio) solution mixture. The ORTEP diagram of complex **5-4** is shown in Figure 5-2. Crystal parameters, bond angles and bond distances are listed in Table 5.3 and Table 5.4. In complex **5-4**, the CO group is *trans* to the hydride, while the PCP *ipso*-carbon is *trans* to the acetylide group.

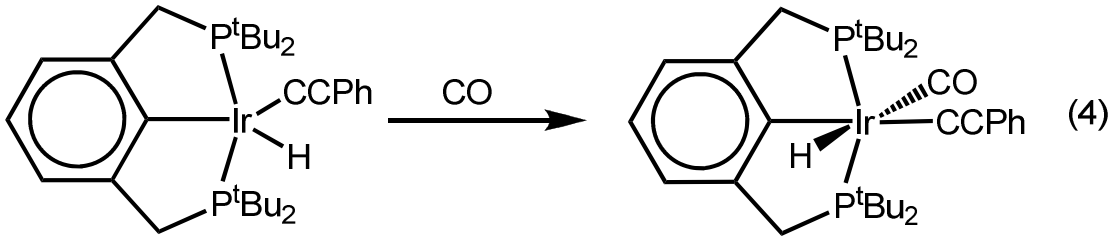

(4)

5-4

5.2.5 Reaction of (PCP)Ir(CO) with CH_3NO_2

(PCP)Ir(CO) reacts with nitromethane (0.3 M) at room temperature and formed complex (PCP)Ir(H)(CO)(ON(=CH_2)O) **5-5** in low yield (4%) (eq. 5). When this solution was heated at 80 °C for 3 days, yield of complex **5-5** was increased to 27%, while other remained as (PCP)Ir(CO). Addition of acid (4 mM, 4-

(trifluoromethyl)benzoic acid) had no effect on the formation of complex **5-5**. However, when (PCP)Ir(CO) in neat nitromethane was heated at 120 °C for 2 h, complex **5-5** was formed in 98% yield. Complex **5-5** was characterized by NMR spectroscopy.

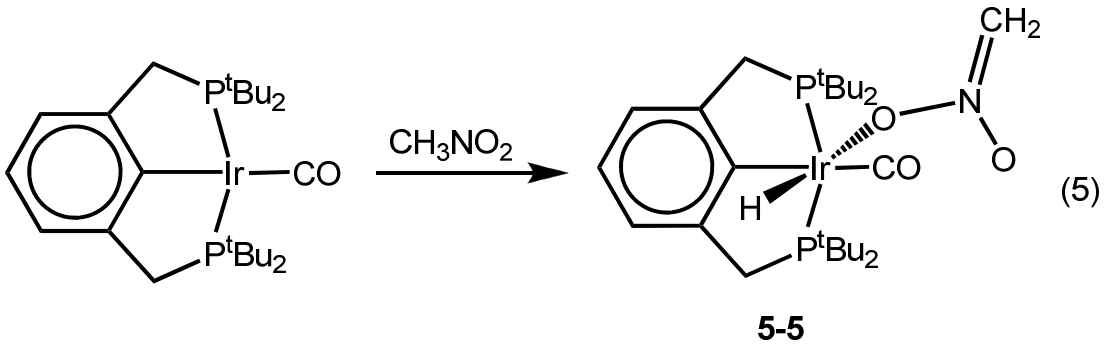

(5)

5-5

5.2.6 Reaction of (PCP)Ir(CNBz) with CH_3NO_2

(PCP)Ir(CNBz) reacted immediately with neat nitromethane at room temperature. The ^{31}P NMR spectrum indicated formation of three new complexes at 62.1, 60.7 and 58.3 ppm in 4:2:1 ratio. The ^{1}H NMR spectrum showed three hydride signals at -12.03 ppm (t, J_{PH} = 16.0 Hz), -12.48 ppm (t, J_{PH} = 14.3 Hz), -13.33 ppm (t, J_{PH} = 14.8 Hz) in 1:2:4 ratio. After 5 days at room temperature, the ratio of these complexes did not change. These complexes decomposed after heating for 1 hour at 80 °C.

5.2.7 Reaction of (PCP)Ir(CO) with PhOH

Regardless of the presence or absence of an acid catalyst, (PCP)Ir(CO) did not react with PhOH, even at a high concentration of PhOH (3 M) either at room temperature or heating at 80 °C for 3 days in *p*-xylene solvent. In the presence of 4-(trifluoromethyl)benzoic acid, only the acid adduct (complex **5-8)** was observed (eq. 6). Complex **5-8** was characterized by NMR spectroscopy.

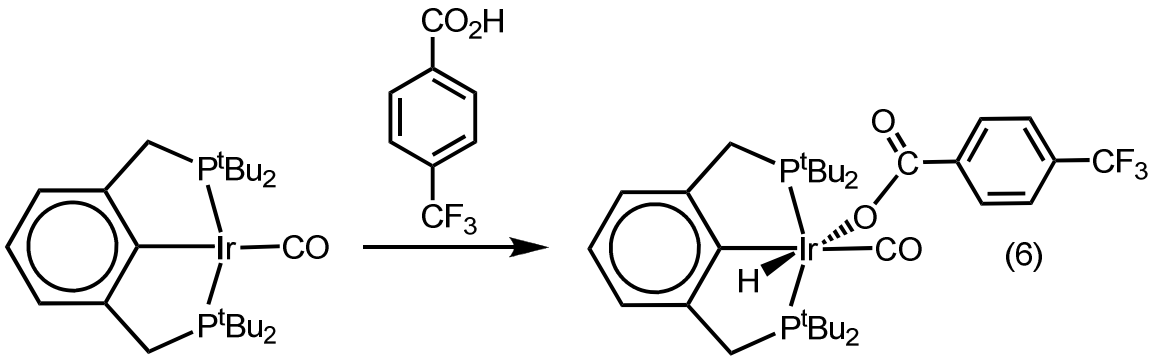

5-8

5.2.8 Reaction of (PCP)Ir(CO) with a (1:1) mixture of PhCCH and PhOH

(PCP)Ir(CO) (10 mM) reacted with a mixture of PhCCH (3 M) and PhOH (3 M) at room temperature, and the color of the solution immediately changed from yellow to colorless. In ^{31}P NMR spectrum two singlet peaks at 84.6 ppm (**UN1**) and 82.1 (**UN2**) ppm (1.2:1 ratio) and in ^{1}H NMR spectrum two hydride signal at -11.5 ppm (t, J_{PH} = 5.7 Hz, **UN2**) and -13.5 ppm (t, J_{PH} = 6.3 Hz, **UN1**) were observed. Upon heating at 100 °C for 1 day, **UN1**, **UN2** and new unknown complex (**UN3**) were formed in 50%, 28% and 22% yield, respectively. In ^{31}P NMR spectrum, this new unknown complex (**UN3**) appeared as a singlet at 15.1 ppm and had no hydride signal in ^{1}H NMR spectrum.

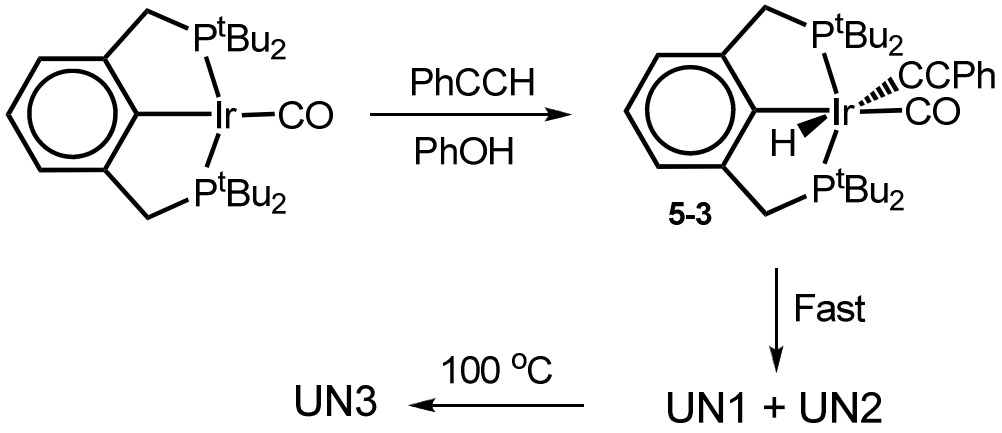

Scheme 5-1 Reaction of (PCP)Ir(CO) with a mixture of PhCCH and PhOH

When the same reaction was carried out with 0.3 M PhCCH and 0.3 M PhOH at room temperature, complex **5-3** was formed in 90% yield. When this solution was heated at 100 °C for 45 minutes, **UN1**, **UN2** and complex **5-3** were formed in 21%, 55% and 24% yield, respectively.

In the presence of 4-(trifluoromethyl)benzoic acid (4 mM), (PCP)Ir(CO) (10 mM) reacted immediately with a mixture of 1.5 M PhCCH and 1.5 M PhOH at room temperature. The ^{31}P NMR spectrum showed formation of 68% **UN1**, 30% **UN2**, and 2% **UN4** [^{31}P: 79.2 ppm, ^{1}H: -23.6 ppm (J_{PH} = 8 Hz, 1H)]. After heating for 2 h at 80 °C, 50% **UN1**, 44% **UN2** and 6% **UN3** were observed. Upon further heating of this mixture (7 h at 125 °C), 60% **UN1**, 40% **UN3** and no **UN2** were formed.

In the presence of 4-(trifluoromethyl)benzoic acid (4 mM), (PCP)Ir(CO) (10 mM) reacted immediately, even with lesser concentrations of PhCCH (0.3 M) and PhOH (0.3 M) mixture, at room temperature. In this case, the ^{31}P NMR spectrum showed the formation of 36% **UN1**, 14% **UN2** and 50% **UN4** [^{31}P: 79.2 ppm, ^{1}H: -23.6 ppm (J_{PH} = 8

Hz, 1H)]. From this mixture of compounds we were able to obtain a crystal and the corresponding X-ray crystal structure (complex **5-9**). The ORTEP diagram of complex **5-9** is shown in Figure 5-3. Crystal parameters, bond angles, and bond distances are listed in Table 5.5 and Table 5.6.

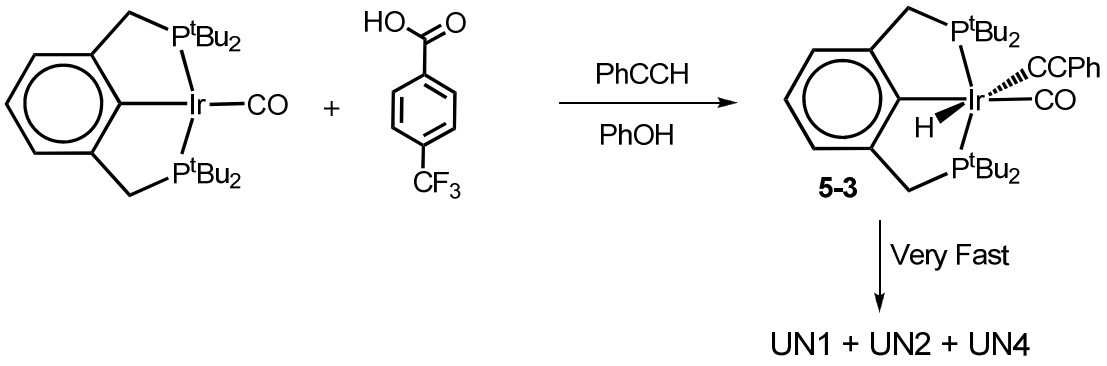

Scheme 5-2 Reaction of (PCP)Ir(CO) with mixture of PhCCH and PhOH in presence of acid

5.2.9 Mechanistic investigation

Higgins and Shaw reported that addition of PhCCH to [ClPd(μ-dppm)$_2$PdCl] was catalyzed by acid ($HBF_4{\cdot}Et_2O$, CF_3CO_2H). In the case of $HBF_4{\cdot}Et_2O$ they were able to identify the proposed intermediate $[ClPd(\mu\text{-dppm})_2(\mu\text{-H})PdCl]^+$ by I.R. spectroscopy and ^{31}P NMR spectroscopy. They did not observe any hydride signal in ^1H and $^1H\{^{31}P\}$NMR spectrum probably due to rapid exchange of the proton with acid. When PhCCH (excess) was added to this intermediate, the final product [CIPd(μ-dppm)$_2$(μ-PhC=CH)PdCl] was formed immediately.[8]

We proposed that the intermediate in the acid catalyzed addition of phenyl acetylene to (PCP)Ir(CO) was $[(PCP)Ir(CO)(H)]^+$. To prove this hypothesis, complex **5-12** was synthesized by adding CO to complex **5-11** (eq. 8).[9] Complex **5-11** and **5-12** were characterized by NMR spectroscopy.

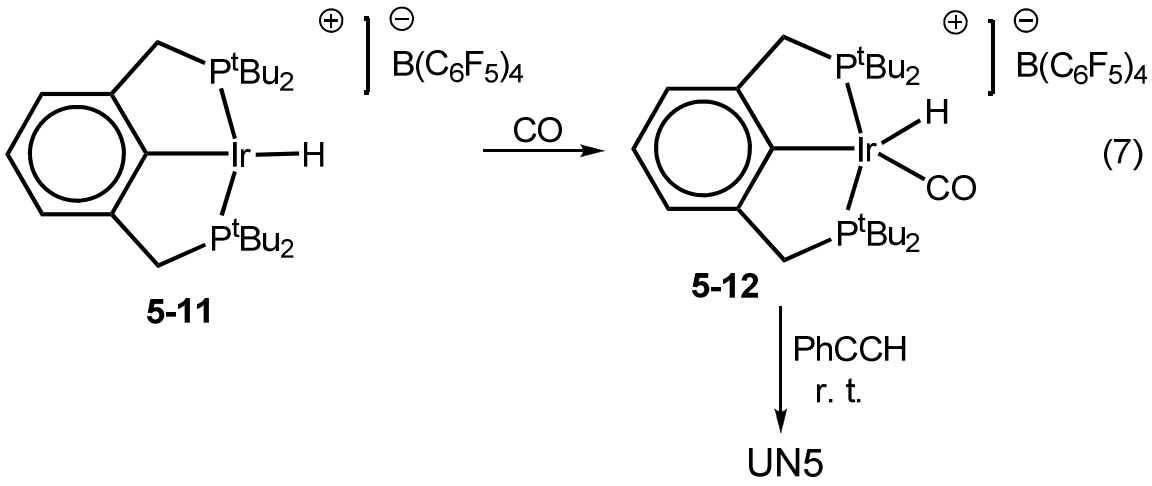

(7)

Complex **5-12**, after heating for 30 min at 80 °C, reacted with PhCCH (3 eq) and formed new complex **UN5** in 60% yield. After heating for 1 h at 80 °C, complex **5-12** completely converted to complex **UN5** (eq. 7). In ^{31}P NMR spectrum **UN5** showed a singlet peak at 97.7 ppm and in ^{1}H NMR spectrum showed a hydride signal at -11.55 ppm (t, J_{PH} = 2 Hz).

In the presence of complex **5-12** (1mM), (PCP)Ir(CO) (10 mM) reacted with PhCCH (3 M) at room temperature. After 2 h at room temperature formation of complex **5-3** (20%), **UN1** (20%) and **UN2** (10%) were observed, while remaining compound was (PCP)Ir(CO). After keeping this solution for 10 h at room temperature, all of the (PCP)Ir(CO) was converted to **UN1** (67%), **UN2** (33%) and complex **5-12** remained at

same concentration as started (Scheme 5-3). From this mixture of compounds we were able to obtain a crystal and the corresponding X-ray crystal structure (complex **5-10**).

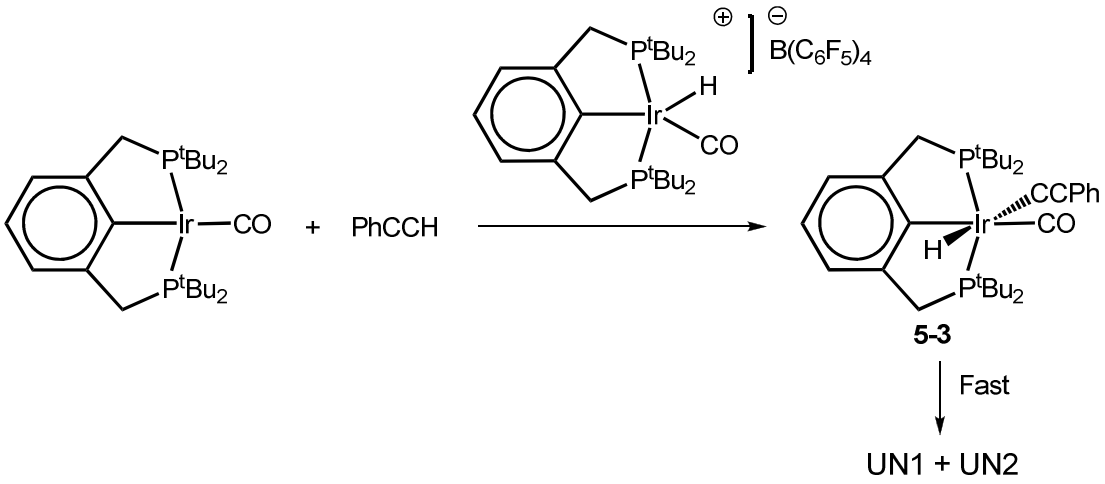

Scheme 5-3 Reaction of (PCP)Ir(CO) with PhCCH in the presence of complex **5-12**

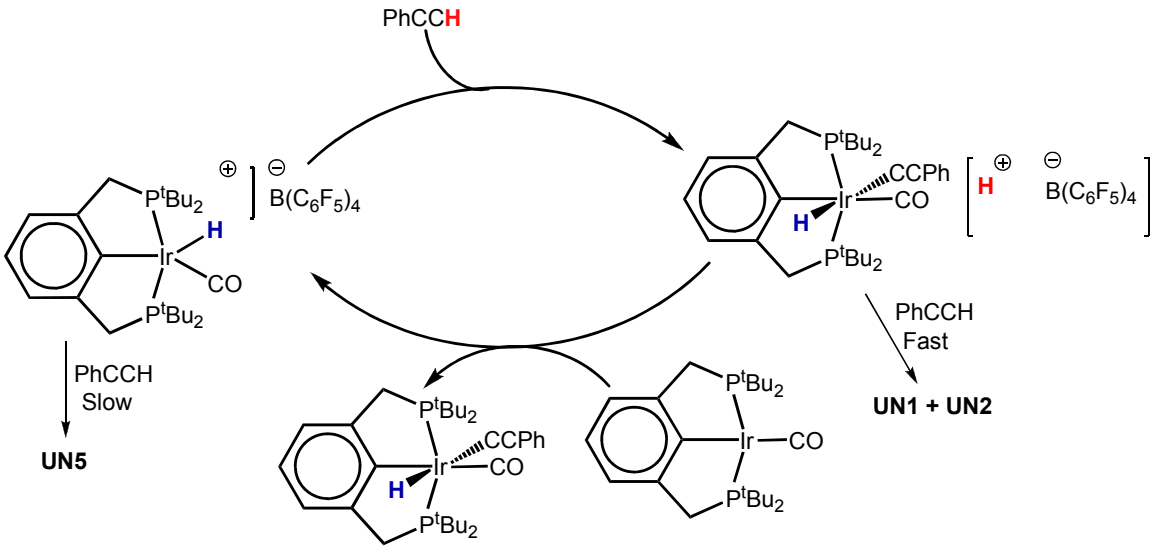

Scheme 5-4 Proposed catalytic cycle of PhCCH addition to (PCP)Ir(CO)

5.2.10 Proposed structure of UN1, UN2 and UN4

In the reaction of (PCP)Ir(CO) with a mixture of PhCCH and PhOH in the absence of 4-(trifluoromethyl)benzoic acid, we observed two complexes **UN1** and **UN2** (Scheme 5-1). But in the same reaction, in presence of 4-(trifluoromethyl)benzoic acid we observed three complexes **UN1**, **UN2** and **UN4** (Scheme 5-2). In the absence of both PhOH and 4-(trifluoromethyl)benzoic acid we also observed formation of complexes **UN1** and **UN2** (Scheme 5-3). Interestingly, in these complexes in hydride signal, J_{PH} is low.

From these results and because crystal **5-9** has a 4-(trifluoromethyl)benzoate ligand, we confirmed that complex **UN4** is complex **5-9**. From the mixture of **UN1**, **UN2** and **5-12**, we were able to obtain the crystal structure of complex **5-10**. We propose complex **UN1** and **UN2** to be complex **5-10** and its isomer; further study is necessary for confirmation.

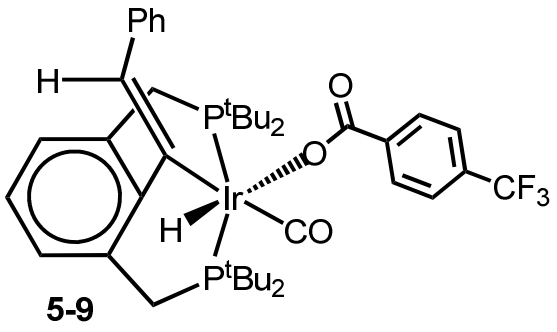

5-9

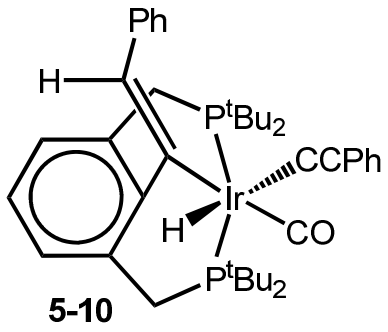

5-10

5.3 Experimental

General Methods. All reactions were carried out under an argon atmosphere using standard Schlenk techniques or in an argon-filled dry box. Benzyl isocyanide, nitromethane and phenylacetylene were purchased from Aldrich. *p*-Xylene, *p*-xylene-d_{10}, TBE and C_6D_6 were dried using Na/K alloy and collected by vacuum transfer. PhCCH was distilled after stirring for 1 day with K_2CO_3. 400 MHz and 500 MHz Varian instruments were used for the ^1H, ^{13}C and ^{31}P NMR experiments. The residual peak of the deuterated solvent was used as a reference for ^1H NMR chemical shifts. ^{31}P NMR chemical shifts were referenced to PMe_3 standard, which appears at –62.2 ppm. PMe_3 internal standard in ^{31}P NMR was employed in determining the yield. (^{tBu4}PCP)IrH_4 (PCP= κ^3-2,6-(^{t}Bu$_2$PCH$_2$)$_2$C$_6$H$_3$) was prepared as described in the literature. [10]

(PCP)Ir(H)(CCPh)(CNBz) (5-1): To a 0.4 mL *p*-xylene-d_{10} solution, 5 mg (PCP)IrH_4 (0.0083 mmol), 5.2 μL 1-hexene (0.0415 mmol) were added. After 10 minutes at room temperature, NMR spectroscopy indicated the formation of (PCP)Ir(1-hexene), then 1.1 μL CNBz (0.0083 mmol) was added to the solution and (PCP)Ir(CNBz) was formed immediately. Subsequently, all of the solvent was removed. This complex was dissolved in 0.33 mL C_6D_6 and 0.3 mg 4-(trifluoromethyl)benzoic acid (0.00158 mmol) and 0.17 mL distilled PhCCH were added. After 10 min at room temperature color of the solution changed from dark red to light red. All the solvent was removed in vacuum and NMR spectra showed the formation of **5-1** in 90% yield. $^{31}P\{^1H\}$ NMR (C_6D_6, 202 MHz): δ 60.84 (s). ^1H NMR (C_6D_6, 400 MHz): δ 7.45 (d, J_{HH} = 6 Hz, 2H, PCP), 7.14 (m, 5H, Ar),

7.07 (d, J_{HH} = 6 Hz, 2H, Ar), 6.99 (m, 2H, Ar), 6.94 (t, J_{HH} = 7.6 Hz, 2H, Ar), 4.04 (s, CH_2Bz), 3.81 (d of vt, J_{PH} = 3.2 Hz, J_{HH} = 15.2 Hz, 2H, ***CH₂***PCP), 3.20 (d of vt, J_{PH} = 4 Hz, J_{HH} = 15.2 Hz, 2H, ***CH₂***PCP), 1.50 (t, J_{PH} = 6.4 Hz, 18H, PC(C***H***$_3$)$_3$), 1.17 (t, J_{PH} = 6.2 Hz, 18H, PC(C***H***$_3$)$_3$), -12.51 (t, J_{PH} = 15.4 Hz, 1H, Ir-***H***). ^{13}C NMR (C_6D_6, 125 MHz): δ 156.7 (t, J_{CP} = 2.7 Hz, PCP), 147.9 (t, J_{CP} = 7.4 Hz, PCP), 136.6 (t, J_{CP} = 7.0 Hz, Ir-***C***NBz), 134.3 (s, Ar), 132.2 (s, Ar), 131.5 (s, Ar), 131.1 (s, Ar), 129.3 (s, Ar), 128.9 (s, Ar), 127.5 (s, Ar), 123.9 (s, Ar), 123.6 (s, PCP), 120.7 (t, J_{CP} = 7.5 Hz, PCP), 110.8 (t, J_{CP} = 1.0 Hz, Ir-***C***CPh), 89.9 (t, J_{CP} = 10.0 Hz, Ir-C***C***Ph), 47.4 (s, ***C***H$_2$Ph), 41.5 (vt, J_{CP} = 13.6 Hz, ***CH₂***PCP), 36.7 (vt, J_{CP} = 13.2 Hz, P***C***(CH$_3$)$_3$), 36.1 (vt, J_{CP} = 9.6 Hz, P***C***(CH$_3$)$_3$), 30.4 (vt, J_{CP} = 2.1 Hz, PC(***C***H$_3$)$_3$), 29.9 (vt, J_{CP} = 2.0 Hz, PC(***C***H$_3$)$_3$).

PCP)Ir(H)(CCPh)(CNBz) (5-2): To a 0.5 mL C_6D_6 solution, 5 mg (PCP)IrH_4 (0.0083 mmol), 2.7 μL TBE (0.0207mmol) and 0.92 μL PhCCH (0.0083 mmol) were added. After 5 minutes at room temperature, NMR spectra indicated the formation of (PCP)Ir(H)(CCPh) 1.1 μL CNBz (0.0083 mmol) was then added to the solution and immediate color change from purple to light red was observed. All of the solvent was removed in vacuum and NMR spectra showed the formation of **5-2** in 98% yield. ^{31}P{^{1}H} NMR (C_6D_6, 202 MHz): δ 55.98 (s). ^{1}H NMR (C_6D_6, 400 MHz): δ 8.12 (d, J_{HH} = 6 Hz, 2H, PCP), 7.09 (t, J_{HH} = 4.4 Hz, 1H, PCP), 3.81 (s, CH_2Bz), 3.27 (d of vt, J_{PH} = 4.0 Hz, J_{HH} = 16.4 Hz, 2H, ***CH₂***PCP), 3.17 (d of vt, J_{PH} = 4.0 Hz, J_{HH} = 16.4 Hz, 2H, ***CH₂***PCP), 1.38 (t, J_{PH} = 5.2 Hz, 18H, PC(C***H***$_3$)$_3$), 1.35 (t, J_{PH} = 5.2 Hz, 18H, PC(C***H***$_3$)$_3$), -11.51 (t, J_{PH} = 16.2 Hz, 1H, Ir-***H***). ^{13}C NMR (C_6D_6, 100 MHz): δ 154.6 (t, J_{CP} = 1.0 Hz, PCP), 149.4 (t, J_{CP} = 7.0 Hz, PCP), 139.5 (t, J_{CP} = 5.5 Hz, Ir-***C***NBz), 133.5(s, Ar),

132.4(s, Ar), 130.2 (s, Ar), 129.3(s, Ar), 128.9 (s, Ar), 127.1(s, Ar), 123.8 (s, Ar), 123.2 (s, PCP), 120.6 (t, J_{CP} = 7.2 Hz, PCP), 110.8 (t, J_{CP} = 1.0 Hz, Ir-***C***CPh), 89.9 (t, J_{CP} = 10.0 Hz, Ir-C***C***Ph), 47.4 (s, ***C***H_2Ph), 41.5 (vt, J_{CP} = 13.6 Hz, ***CH₂***PCP), 36.7 (vt, J_{CP} = 13.2 Hz, P***C***$(CH_3)_3$), 36.1 (vt, J_{CP} = 9.6 Hz, P***C***$(CH_3)_3$), 30.4 (vt, J_{CP} = 2.1 Hz, PC(***C***$H_3)_3$), 29.9 (vt, J_{CP} = 2.0 Hz, PC(***C***$H_3)_3$).

(PCP)Ir(H)(CCPh)(CO) (5-3): To a 0.33 mL C_6D_6 soultion, 5.1 mg (PCP)Ir(CO) (0.0083 mmol), 3.1 mg 4-(trifluoromethyl)benzoic acid (0.0158 mmol) and 0.17 mL distilled PhCCH were added and was heated for 2 h at 80 °C. All the solution was removed in vacuum and NMR spectrum showed the formation of this compound in 90 % yield. $^{31}P\{^1H\}$ NMR (C_6D_6, 202 MHz): δ 64.3 (s). ^1H NMR (C_6D_6, 400 MHz): δ (We can't assign the aromatic peak due to overlap with other organic impurities), 3.75 (d of vt, J_{PH} = 3.5 Hz, J_{HH} = 16.0 Hz, 2H, ***CH₂***PCP), 3.12 (d of vt, J_{PH} = 3.6 Hz, J_{HH} = 15.6 Hz, 2H, ***CH₂***PCP), 1.44 (t, J_{PH}= 6.8 Hz, 18H, PC(C***H***$_3)_3$), 1.08 (t, J_{PH} = 6.8 Hz, 18H, PC(C***H***$_3)_3$), -11.78 (t, J_{PH} = 14.4 Hz, 1H, Ir-***H***).

(PCP)Ir(H)(CCPh)(CO) (5-4): To a 0.5 mL C_6D_6 solution, 5 mg (PCP)IrH_4 (0.0083 mmol), 2.7 μL TBE (0.0207mmol) and 0.92 μL PhCCH (0.0083 mmol) were added. After 5 minutes at room temperature, NMR spectra indicated formation of (PCP)Ir(H)(CCPh) 1 atm CO was then added to the solution, and complex **5-4** was formed immediately. All the solvent was removed in vacuum and NMR spectrum showed the formation of this compound in 95% yield. $^{31}P\{^1H\}$ NMR (C_6D_6, 202 MHz): δ 58.05 (s). ^1H NMR (C_6D_6, 400 MHz): δ 7.59 (d, J_{HH} = 6.8 Hz, 2H, PCP), 7.25 (m, 1H, Ar), 7.02

(m, 5H, Ar), 3.18 (d of vt, J_{PH} = 4.0 Hz, J_{HH} = 16.0 Hz, 2H, ***CH₂***PCP), 3.14 (d of vt, J_{PH} = 3.5 Hz, J_{HH} = 16.5 Hz, 2H, ***CH₂***PCP), 1.34 (t, J_{PH} = 6.8 Hz, 18H, PC(C***H***$_3$)$_3$), 1.23 (t, J_{PH} = 6.8 Hz, 18H, PC(C***H***$_3$)$_3$), -9.64 (t, J_{PH} = 15.6 Hz, 1H, Ir-***H***).

(PCP)Ir(H)(CH_2NO_2)(CO) (5-5): In a J-Young tube 5.1 mg (PCP)Ir(CO) (0.0083 mmol) was dissolved in 0.5 mL neat CH_3NO_2. At room temperature (PCP)Ir(CO) was partially soluble. After heating for 2 h at 120 °C it was dissolved completely and the color was changed from yellow to colorless. All of the nitromethane was removed in vacuum, and NMR spectra showed the formation of complex **5-5** in 98% yield. $^{31}P\{^1H\}$ NMR (C_6D_6, 202 MHz): δ 65.6(s). ^1H NMR (C_6D_6, 400 MHz): δ 7.07 (t, J_{HH} = 7.5 Hz, 1H, Ar, PCP), 6.98 (d, J_{HH} = 7.5 Hz, 2H, Ar, PCP), 3.62 (d of vt, J_{PH} = 3.8 Hz, J_{HH} = 16.5 Hz, 2H, ***CH₂***PCP), 3.05 (d of vt, J_{PH} = 4.0 Hz, J_{HH} = 15.5 Hz, 2H, ***CH₂***PCP), 2.96 (s, 2H, Ir-ONO***CH₂***), 1.37 (t, J_{PH} = 7.0 Hz, 18H, PC(C***H***$_3$)$_3$), 0.98 (t, J_{PH} = 6.8 Hz, 18H, PC(C***H***$_3$)$_3$), -12.56 (t, J_{PH} = 13.8 Hz, 1H, Ir-***H***).

(PCP)Ir(H)(OC(O)Ar)(CO) (5-8): To a 0.5 mL C_6D_6 solution of 5.1 mg (PCP)Ir(CO) (0.0083 mmol) and 0.64 mg 4-(trifluoromethyl)benzoic acid (0.0033 mmol) were added. After 20 minutes at room temperature complex **5-8** was formed (yield 20%). $^{31}P\{^1H\}$ NMR (C_6D_6, 202 MHz): δ 66.62 (s). ^1H NMR (C_6D_6, 500 MHz): δ 8.19 (d, J_{HH} = 8.5 Hz, 2H, Ar), 7.35 (d, J_{HH} = 8.5 Hz, 2H, Ar), 7.15 (m, 1H, Ar), 7.12 (m, 2H, Ar), 3.59 (d of vt, J_{PH} = 3.5 Hz, J_{HH} = 15.5 Hz, 2H, ***CH₂***PCP), 3.16 (d of vt, J_{PH} = 4.3 Hz, J_{HH} = 15.5 Hz, 2H, ***CH₂***PCP), 1.17 (t, J_{PH} = 6.8 Hz, 18H, PC(C***H***$_3$)$_3$), 1.09 (t, J_{PH} = 6.8 Hz, 18H, PC(C***H***$_3$)$_3$), -21.52 (t, J_{PH} = 13.6 Hz, 1H, Ir-***H***)

Complex 5-12: In a J-Young tube, 5 mg complex **5-11** was dissolved in 0.5 mL C_6D_5Cl. At room temperature, 1 atm CO was added to the solution, and the color was changed from red to light yellow. $^{31}P\{^1H\}$ NMR (C_6D_5Cl, 162 MHz): δ 68.89 (s, PCP). ^1H NMR (C_6D_5Cl, 400 MHz): δ 7.12 (m, 2H, Ar), 7.08 (m, Ar, PCP), 3.41 (d of vt, J_{PH} = 4.4 Hz, J_{HH} = 18.0 Hz, 2H, ***CH₂***PCP), 3.23 (d of vt, J_{PH} = 3.6 Hz, J_{HH} = 17.6 Hz, 2H, ***CH₂***PCP), 1.22 (t, J_{PH} = 7.6 Hz, 18H, PC(C***H***$_3$)$_3$), 1.08 (t, J_{PH} = 7.6 Hz, 18H, PC(C***H***$_3$)$_3$), -10.33 (t, J_{PH} = 12.4 Hz, 1H, Ir-***H***).

Complex 5-9: To a 0.48 mL C_6D_6 solution of 3.1 mg (PCP)Ir(CO) (0.005 mmol), 4 mM 4-(trifluoromethyl)benzoic acid (from 1 M stock solution), 16 μL PhCCH (0.168 mmol) and 14 mg PhOH (0.168 mmol) were added. An immediate color change from yellow to light yellow was observed. After 10 minutes at room temperature, NMR spectra showed formation of **UN1** (36%), **UN2** (14%) and **5-9** (50%).

Complex 5-9: $^{31}P\{^1H\}$ NMR (C_6D_6, 202 MHz): δ 79.2 (s). ^1H NMR (C_6D_6, 500 MHz): δ 1.21 (t, J_{PH} = 6.8 Hz, 18H, PC(C***H***$_3$)$_3$), 0.87 (t, J_{PH} = 6.8 Hz, 18H, PC(C***H***$_3$)$_3$), -23.62 (t, J_{PH} = 8.0 Hz, 1H, Ir-***H***)

UN1 and UN2: To a 0.3 mL C_6D_6 solution of 3.1 mg (PCP)Ir(CO) (0.005 mmol), 160 μL PhCCH (1.68 mmol) and 140 mg PhOH (1.68 mmol) were added. An immediate color change from yellow to colorless was observed. After 10 minutes at room temperature, NMR spectra showed formation of **UN1** and **UN2** in a 1.2 to 1 ratio.

UN1: $^{31}P\{^{1}H\}$ NMR (C_6D_6, 202 MHz): δ 84.6 (s). ^{1}H NMR (C_6D_6, 500 MHz): δ 2.83 (d of vt merge, 4H, ***CH₂***PCP), 1.53 (t, J_{PH} = 5.4 Hz, 18H, PC(C***H***$_3$)$_3$), 0.93 (t, J_{PH} = 6.8 Hz, 18H, PC(C***H***$_3$)$_3$), -13.44 (t, J_{PH} = 6.3 Hz, 1H, Ir-***H***).

UN2: $^{31}P\{^{1}H\}$ NMR (C_6D_6, 202 MHz): δ 82.1 (s). ^{1}H NMR (C_6D_6, 500 MHz): δ 2.93 (d of vt, J_{PH} = 2.5 Hz, J_{HH} = 13.5 Hz, 2H, ***CH₂***PCP), 2.72 (d of vt, J_{PH} = 4 Hz, J_{HH} = 13.0 Hz, 2H, ***CH₂***PCP), 1.37 (t, J_{PH} = 6.5 Hz, 18H, PC(C***H***$_3$)$_3$), 0.93 (t, J_{PH} = 6.8 Hz, 18H, PC(C***H***$_3$)$_3$), -11.49 (t, J_{PH} = 5.8 Hz, 1H, Ir-***H***).

5.4 Conclusions

Phenylacetylene addition to (PCP)Ir(L) (L = CO and CNR) is catalyzed by acid. Since isocyanide is a significantly better electron donor than CO, in this electrophilic addition reaction, we observed that (PCP)Ir(CNR) reacted much faster than (PCP)Ir(CO). We also studied the mechanism of this acid catalyzed addition and found that the $[(PCP)Ir(CO)(H)]^{+}$ complex formed in presence of acid, which catalyzed the phenylacetylene addition. In presence of acid, phenylacetylene was inserted into the PCP *ipso*-carbon and iridium bond.

5.5 References

(1) Bianchini, C.; Meli, A.; Peruzzini, M.; Zanobini, F.; Bruneau, C.; Dixneuf, P. H. *Organometallics* **1990**, *9*, 1155.
(2) Marcuzzi, F.; Melloni, G. *Tetrahedron Lett.***1975**, *16*, 2771.
(3) Marcuzzi, F.; Melloni, G. *J. Am. Chem. Soc* **1976**, *98*, 3295.
(4) Li, X.; Vogel, T.; Incarvito, C. D.; Crabtree, R. H. *Organometallics* **2004**, *24*, 62.
(5) Higgins, S.; Shaw, B. *J. Chem. Soc., Chem. Commun* 1986, 1629.
(6) Ghosh, R.; Zhang, X.; Achord, P.; Emge, T. J.; Krogh-Jespersen, K.; Goldman, A. S. *J. Am. Chem. Soc* **2007**, *129*, 853.
(7) Lee, C.-L.; Hunt, C. T.; Balch, A. L. *Inorg. Chem.* **1981**, *20*, 2498.
(8) Higgins, S.; Shaw, B. *J. Chem. Soc. Dalton Trans.* **1988**, 457.
(9) *Complex 5-9 was synthesized by Benudhar Punji,* unpublished work.
10) Gupta, M. H., C.; Flesher, R. J.; Kaska, W. C.; Jensen, C. M. *Chem. Commun* **1996**, 2083.

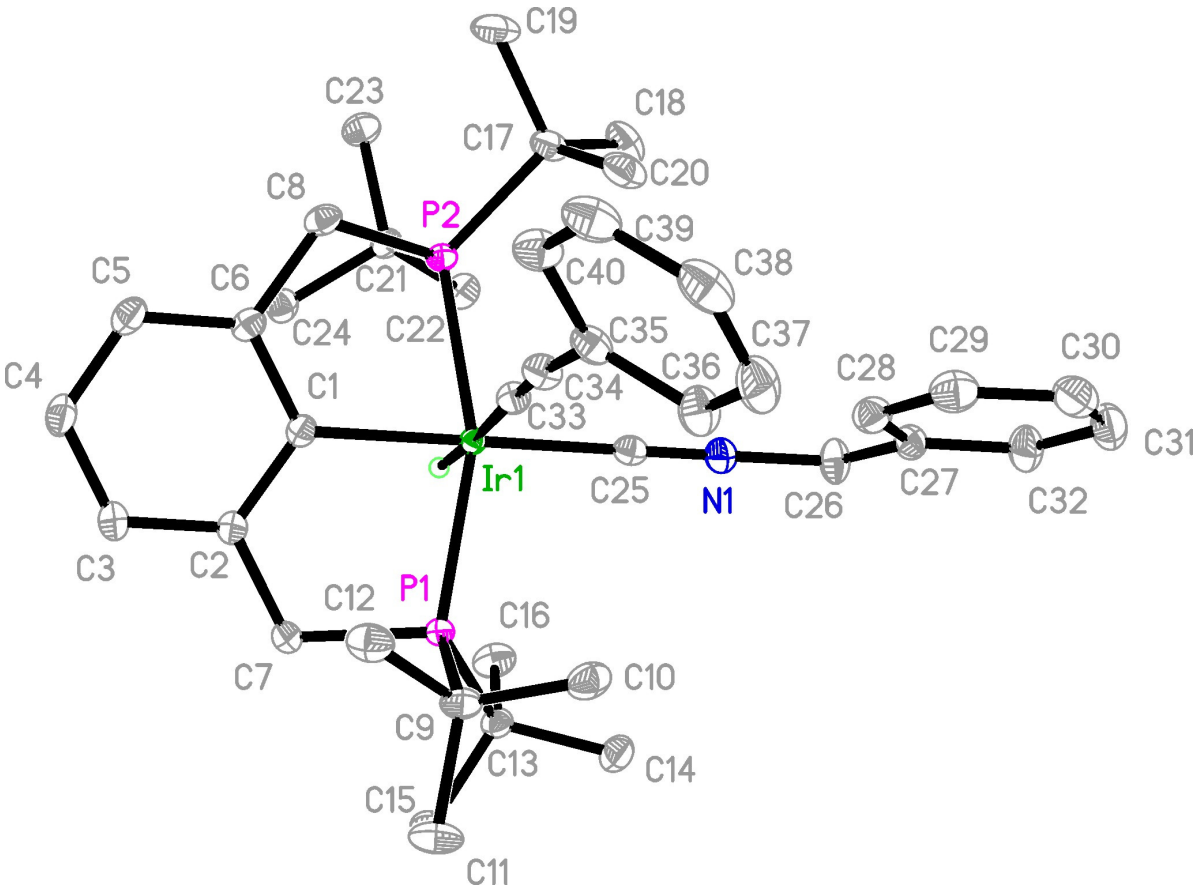

Figure 5-1 Crystal structure of complex **5-1**

Table 5.1 Crystal data and structure refinement for complex **5-1**

Empirical formula	C40 H56 Ir N P2	
Formula weight	805.00	
Temperature	100(2) K	
Wavelength	0.71073 Å	
Crystal system	Monoclinic	
Space group	P2(1)/c	
Unit cell dimensions	a = 22.087(2) Å	α= 90°.
	b = 10.7339(10) Å	β= 112.207(2)°.
	c = 17.0570(16) Å	γ = 90°.
Volume	3743.9(6) $Å^3$	
Z	4	
Density (calculated)	1.428 Mg/m^3	
Absorption coefficient	3.679 mm^{-1}	
F(000)	1640	
Crystal size	0.40 x 0.20 x 0.10 mm^3	
Theta range for data collection	1.99 to 31.51°.	
Index ranges	-32<=h<=32, -15<=k<=15, -24<=l<=25	
Reflections collected	46180	
Independent reflections	12459 [R(int) = 0.0221]	
Completeness to theta = 31.51°	99.8 %	
Absorption correction	Semi-empirical from equivalents	
Max. and min. transmission	0.71 and 0.32	
Refinement method	Full-matrix least-squares on F^2	
Data / restraints / parameters	12459 / 1 / 412	
Goodness-of-fit on F^2	1.004	
Final R indices [I>2sigma(I)]	R1 = 0.0163, wR2 = 0.0399	
R indices (all data)	R1 = 0.0183, wR2 = 0.0406	
Largest diff. peak and hole	1.397 and -0.428 e.$Å^{-3}$	

Table 3.3 Selective bond lengths [Å] and angles [°] for complex **3-1d**

Ir(1)-C(25)	1.9731(14)	C(3)-C(4)	1.392(2)
Ir(1)-C(1)	2.0795(13)	C(4)-C(5)	1.392(2)
Ir(1)-C(33)	2.0827(14)	C(5)-C(6)	1.3982(19)
Ir(1)-P(1)	2.3225(4)	C(6)-C(8)	1.5144(19)
Ir(1)-P(2)	2.3233(4)	C(9)-C(10)	1.536(2)
Ir(1)-H(1)	1.583(9)	C(9)-C(11)	1.538(2)
P(1)-C(7)	1.8455(14)	C(9)-C(12)	1.545(2)
P(1)-C(9)	1.8892(14)	C(13)-C(14)	1.533(2)
P(1)-C(13)	1.8936(14)	C(13)-C(16)	1.540(2)
P(2)-C(8)	1.8386(14)	C(13)-C(15)	1.541(2)
P(2)-C(17)	1.8909(14)	C(17)-C(20)	1.535(2)
P(2)-C(21)	1.8919(13)	C(17)-C(18)	1.538(2)
C(1)-C(2)	1.4059(18)	C(17)-C(19)	1.539(2)
C(1)-C(6)	1.4086(18)	C(21)-C(23)	1.5371(19)
C(2)-C(3)	1.3971(19)	C(21)-C(24)	1.540(2)
C(2)-C(7)	1.5133(19)	C(21)-C(22)	1.5389(19)
C(25)-Ir(1)-C(1)	178.56(5)	C(8)-P(2)-C(21)	104.73(6)
C(25)-Ir(1)-C(33)	91.75(5)	C(17)-P(2)-C(21)	109.01(6)
C(1)-Ir(1)-C(33)	89.66(5)	C(8)-P(2)-Ir(1)	99.90(4)
C(25)-Ir(1)-P(1)	98.07(4)	C(17)-P(2)-Ir(1)	121.41(5)
C(1)-Ir(1)-P(1)	82.02(4)	C(21)-P(2)-Ir(1)	114.45(4)
C(33)-Ir(1)-P(1)	98.13(4)	C(2)-C(1)-C(6)	118.06(12)
C(25)-Ir(1)-P(2)	99.02(4)	C(2)-C(1)-Ir(1)	121.25(10)
C(1)-Ir(1)-P(2)	80.63(4)	C(6)-C(1)-Ir(1)	120.65(10)
C(33)-Ir(1)-P(2)	91.79(4)	C(3)-C(2)-C(1)	120.88(13)
P(1)-Ir(1)-P(2)	159.924(12)	C(3)-C(2)-C(7)	120.91(12)
C(7)-P(1)-C(9)	104.38(7)	C(1)-C(2)-C(7)	118.12(12)
C(7)-P(1)-C(13)	103.80(6)	C(4)-C(3)-C(2)	120.19(13)
C(9)-P(1)-C(13)	109.92(6)	C(3)-C(4)-C(5)	119.87(13)
C(7)-P(1)-Ir(1)	100.97(5)	C(4)-C(5)-C(6)	120.07(13)
C(9)-P(1)-Ir(1)	117.65(5)	C(5)-C(6)-C(1)	120.87(13)
C(13)-P(1)-Ir(1)	117.65(5)	C(5)-C(6)-C(8)	121.50(12)
C(8)-P(2)-C(17)	105.05(7)	C(1)-C(6)-C(8)	117.57(12)

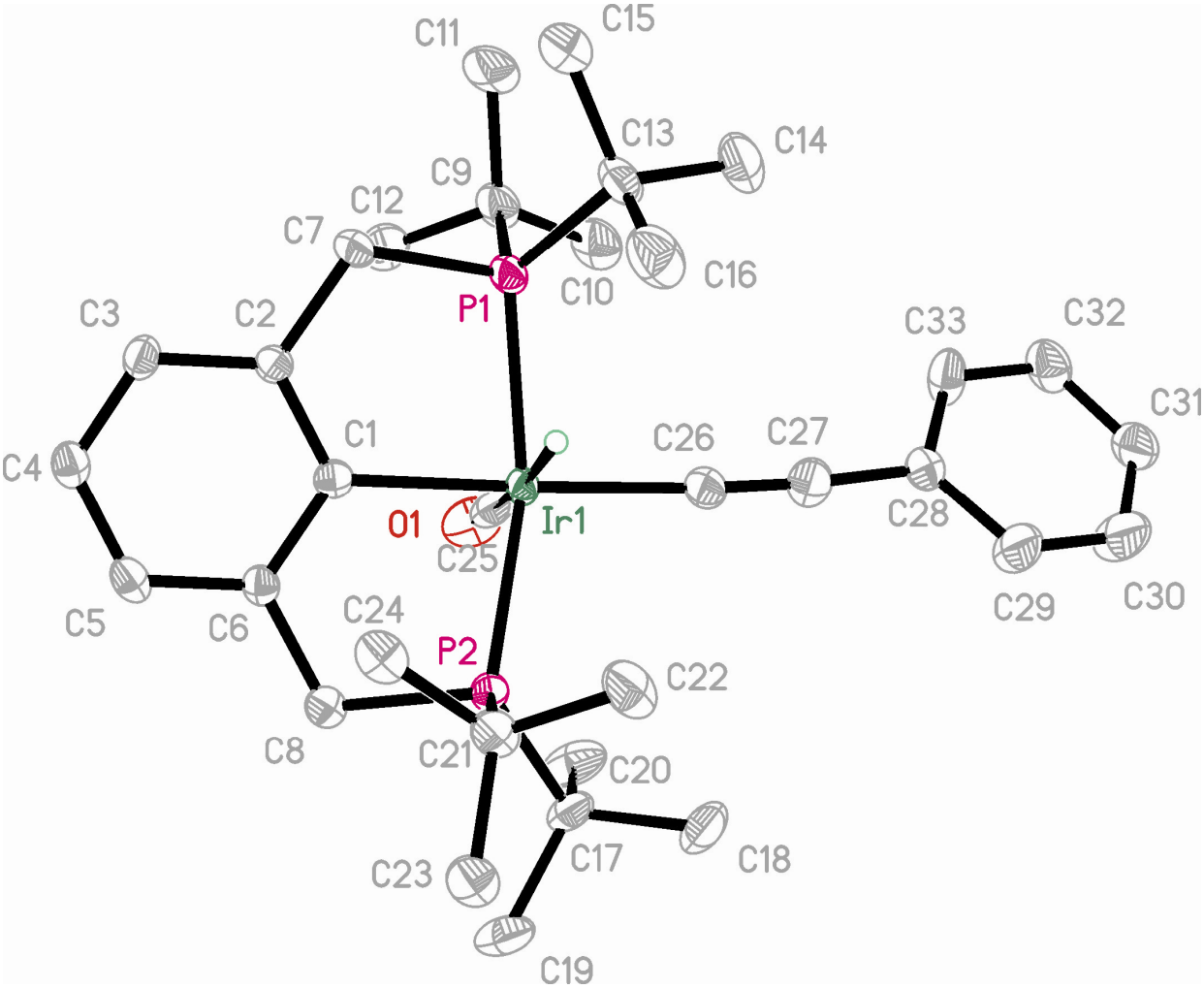

Figure 5-2 Crystal structure of complex **5-4**

Table 5.3 Crystal data and structure refinement for complex **5-4**

Empirical formula	C33 H49 Ir O P2	
Formula weight	715.86	
Temperature	100(2) K	
Wavelength	0.71073 Å	
Crystal system	Orthorhombic	
Space group	Pca2(1)	
Unit cell dimensions	a = 15.8713(9) Å	α= 90°.
	b = 11.7642(7) Å	β= 90°.
	c = 16.8804(10) Å	γ = 90°.
Volume	3151.8(3) $Å^3$	
Z	4	
Density (calculated)	1.509 Mg/m^3	
Absorption coefficient	4.361 mm^{-1}	
F(000)	1448	
Crystal size	0.35 x 0.07 x 0.02 mm^3	
Theta range for data collection	2.15 to 31.54°.	
Index ranges	-23<=h<=23, -17<=k<=17, -24<=l<=24	
Reflections collected	38050	
Independent reflections	10449 [R(int) = 0.0454]	
Completeness to theta = 31.54°	99.8 %	
Absorption correction	Semi-empirical from equivalents	
Max. and min. transmission	0.937 and 0.310	
Refinement method	Full-matrix least-squares on F^2	
Data / restraints / parameters	10449 / 2 / 349	
Goodness-of-fit on F^2	1.006	
Final R indices [I>2sigma(I)]	R1 = 0.0377, wR2 = 0.0889	
R indices (all data)	R1 = 0.0574, wR2 = 0.0989	
Absolute structure parameter	0.031(9)	
Largest diff. peak and hole	4.209 and -0.604 e.$Å^{-3}$	

Table 5.4 Selective bond lengths [Å] and angles [°] for complex **5-4**

Ir(1)-C(25)	1.923(6)	C(3)-C(4)	1.373(7)
Ir(1)-C(26)	2.047(5)	C(4)-C(5)	1.399(7)
Ir(1)-C(1)	2.089(5)	C(5)-C(6)	1.395(7)
Ir(1)-P(2)	2.3306(12)	C(6)-C(8)	1.510(7)
Ir(1)-P(1)	2.3339(14)	C(9)-C(10)	1.504(9)
Ir(1)-H(1)	1.580(10)	C(9)-C(12)	1.532(8)
P(1)-C(7)	1.845(5)	C(9)-C(11)	1.543(8)
P(1)-C(9)	1.887(6)	C(13)-C(16)	1.531(8)
P(1)-C(13)	1.888(5)	C(13)-C(15)	1.537(8)
P(2)-C(8)	1.851(5)	C(13)-C(14)	1.542(8)
P(2)-C(21)	1.872(5)	C(17)-C(20)	1.521(7)
P(2)-C(17)	1.885(5)	C(17)-C(19)	1.537(8)
C(1)-C(6)	1.395(6)	C(17)-C(18)	1.548(7)
C(1)-C(2)	1.415(7)	C(21)-C(23)	1.514(7)
C(2)-C(3)	1.401(6)	C(21)-C(24)	1.544(8)
C(2)-C(7)	1.524(7)	C(21)-C(22)	1.554(7)
C(25)-Ir(1)-C(26)	93.1(2)	C(21)-P(2)-C(17)	110.0(2)
C(25)-Ir(1)-C(1)	91.2(2)	C(8)-P(2)-Ir(1)	100.32(15)
C(26)-Ir(1)-C(1)	175.5(2)	C(21)-P(2)-Ir(1)	114.63(17)
C(25)-Ir(1)-P(2)	96.18(16)	C(17)-P(2)-Ir(1)	119.73(16)
C(26)-Ir(1)-P(2)	100.32(14)	C(6)-C(1)-C(2)	118.3(4)
C(1)-Ir(1)-P(2)	80.41(13)	C(6)-C(1)-Ir(1)	121.2(3)
C(25)-Ir(1)-P(1)	100.05(15)	C(2)-C(1)-Ir(1)	120.4(3)
C(26)-Ir(1)-P(1)	94.51(15)	C(3)-C(2)-C(1)	120.1(4)
C(1)-Ir(1)-P(1)	83.52(13)	C(3)-C(2)-C(7)	120.8(4)
P(2)-Ir(1)-P(1)	157.34(5)	C(1)-C(2)-C(7)	119.0(4)
C(7)-P(1)-C(9)	105.9(2)	C(4)-C(3)-C(2)	120.3(4)
C(7)-P(1)-C(13)	103.4(3)	C(3)-C(4)-C(5)	120.4(4)
C(9)-P(1)-C(13)	109.6(2)	C(6)-C(5)-C(4)	119.6(4)
C(7)-P(1)-Ir(1)	101.47(16)	C(1)-C(6)-C(5)	121.0(4)
C(9)-P(1)-Ir(1)	116.15(19)	C(1)-C(6)-C(8)	118.2(4)
C(13)-P(1)-Ir(1)	118.26(18)	C(5)-C(6)-C(8)	120.8(4)
C(8)-P(2)-C(21)	104.8(2)	C(2)-C(7)-P(1)	110.7(3)
C(8)-P(2)-C(17)	105.3(2)	C(6)-C(8)-P(2)	108.3(3)

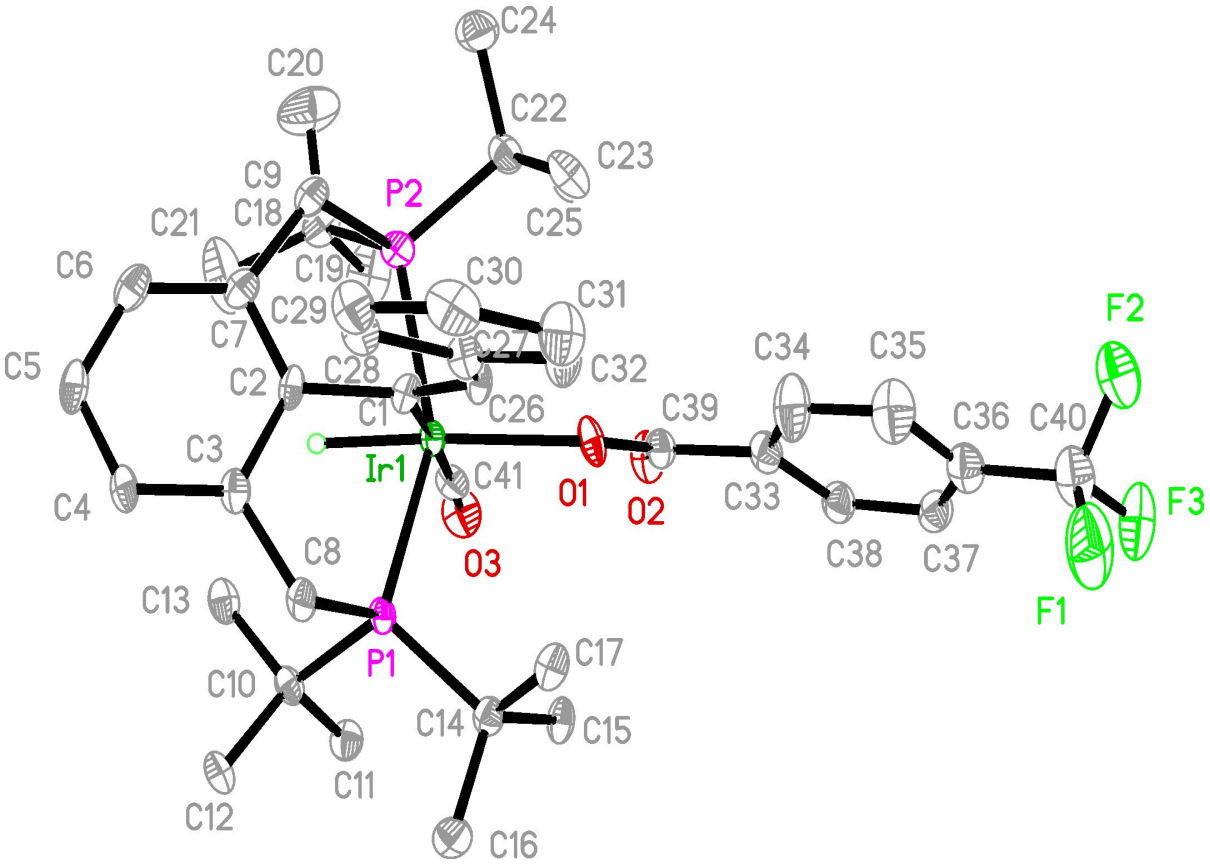

Figure 5-3 Crystal structure of complex **5-9**

Table 5.5 Crystal data and structure refinement for complex **5-9**

Empirical formula	C50 H67 F3 Ir O4 P2	
Formula weight	1043.18	
Temperature	100(2) K	
Wavelength	0.71073 Å	
Crystal system	Triclinic	
Space group	P-1	
Unit cell dimensions	a = 9.926(2) Å	α= 103.91(3)°.
	b = 15.260(3) Å	β= 102.42(3)°.
	c = 17.146(3) Å	γ = 99.98(3)°.
Volume	2391.6(8) $Å^3$	
Z	2	
Density (calculated)	1.449 Mg/m^3	
Absorption coefficient	2.912 mm^{-1}	
F(000)	1066	
Crystal size	0.07 x 0.05 x 0.03 mm^3	
Theta range for data collection	2.16 to 28.36°.	
Index ranges	-13<=h<=12, -19<=k<=20, -22<=l<=18	
Reflections collected	17013	
Independent reflections	11239 [R(int) = 0.0380]	
Completeness to theta = 28.36°	93.9 %	
Absorption correction	Semi-empirical from equivalents	
Max. and min. transmission	0.917 and 0.822	
Refinement method	Full-matrix least-squares on F^2	
Data / restraints / parameters	11239 / 1 / 561	
Goodness-of-fit on F^2	1.007	
Final R indices [I>2sigma(I)]	R1 = 0.0541, wR2 = 0.1322	
R indices (all data)	R1 = 0.0665, wR2 = 0.1377	
Largest diff. peak and hole	5.157 and -3.320 e.$Å^{-3}$	

Table 5.6 Selective bond lengths [Å] and angles [°] for complex **5-9**

Ir(1)-C(41)	1.906(6)	C(3)-C(4)	1.405(8)
Ir(1)-C(1)	2.113(6)	C(3)-C(8)	1.511(8)
Ir(1)-O(1)	2.193(4)	C(4)-C(5)	1.388(9)
Ir(1)-P(1)	2.3846(18)	C(5)-C(6)	1.396(9)
Ir(1)-P(2)	2.3993(19)	C(6)-C(7)	1.399(9)
P(1)-C(8)	1.887(6)	C(7)-C(9)	1.522(8)
P(1)-C(14)	1.897(6)	C(10)-C(13)	1.529(9)
P(1)-C(10)	1.922(6)	C(10)-C(12)	1.546(8)
P(2)-C(22)	1.884(6)	C(10)-C(11)	1.558(8)
P(2)-C(9)	1.899(6)	C(14)-C(17)	1.534(8)
P(2)-C(18)	1.912(7)	C(14)-C(16)	1.536(8)
C(1)-C(26)	1.354(8)	C(14)-C(15)	1.551(8)
C(1)-C(2)	1.462(8)	C(18)-C(21)	1.506(10)
C(2)-C(3)	1.404(8)	C(18)-C(19)	1.532(10)
C(2)-C(7)	1.409(8)	C(18)-C(20)	1.544(10)
C(22)-C(23)	1.539(9)	C(22)-P(2)-C(9)	103.6(3)
C(22)-C(25)	1.547(10)	C(22)-P(2)-C(18)	110.9(3)
C(22)-C(24)	1.555(9)	C(9)-P(2)-C(18)	102.7(3)
C(41)-Ir(1)-C(1)	176.9(2)	C(22)-P(2)-Ir(1)	116.9(2)
C(41)-Ir(1)-O(1)	94.8(2)	C(9)-P(2)-Ir(1)	107.96(19)
C(1)-Ir(1)-O(1)	85.7(2)	C(18)-P(2)-Ir(1)	113.2(2)
C(41)-Ir(1)-P(1)	95.71(18)	C(26)-C(1)-C(2)	127.1(5)
C(1)-Ir(1)-P(1)	81.19(16)	C(26)-C(1)-Ir(1)	128.0(4)
O(1)-Ir(1)-P(1)	99.80(13)	C(2)-C(1)-Ir(1)	104.7(4)
C(41)-Ir(1)-P(2)	102.31(19)	C(3)-C(2)-C(7)	121.0(5)
C(1)-Ir(1)-P(2)	80.50(16)	C(3)-C(2)-C(1)	117.9(5)
O(1)-Ir(1)-P(2)	103.58(13)	C(7)-C(2)-C(1)	118.7(5)
P(1)-Ir(1)-P(2)	148.97(6)	C(2)-C(3)-C(4)	118.5(6)
C(8)-P(1)-C(14)	104.3(3)	C(2)-C(3)-C(8)	116.0(5)
C(8)-P(1)-C(10)	102.1(3)	C(4)-C(3)-C(8)	125.0(5)
C(14)-P(1)-C(10)	110.4(3)	C(5)-C(4)-C(3)	120.2(6)
C(8)-P(1)-Ir(1)	107.77(19)	C(4)-C(5)-C(6)	121.0(6)
C(14)-P(1)-Ir(1)	116.38(19)	C(5)-C(6)-C(7)	119.7(6)
C(10)-P(1)-Ir(1)	114.34(19)	C(6)-C(7)-C(2)	118.8(5)

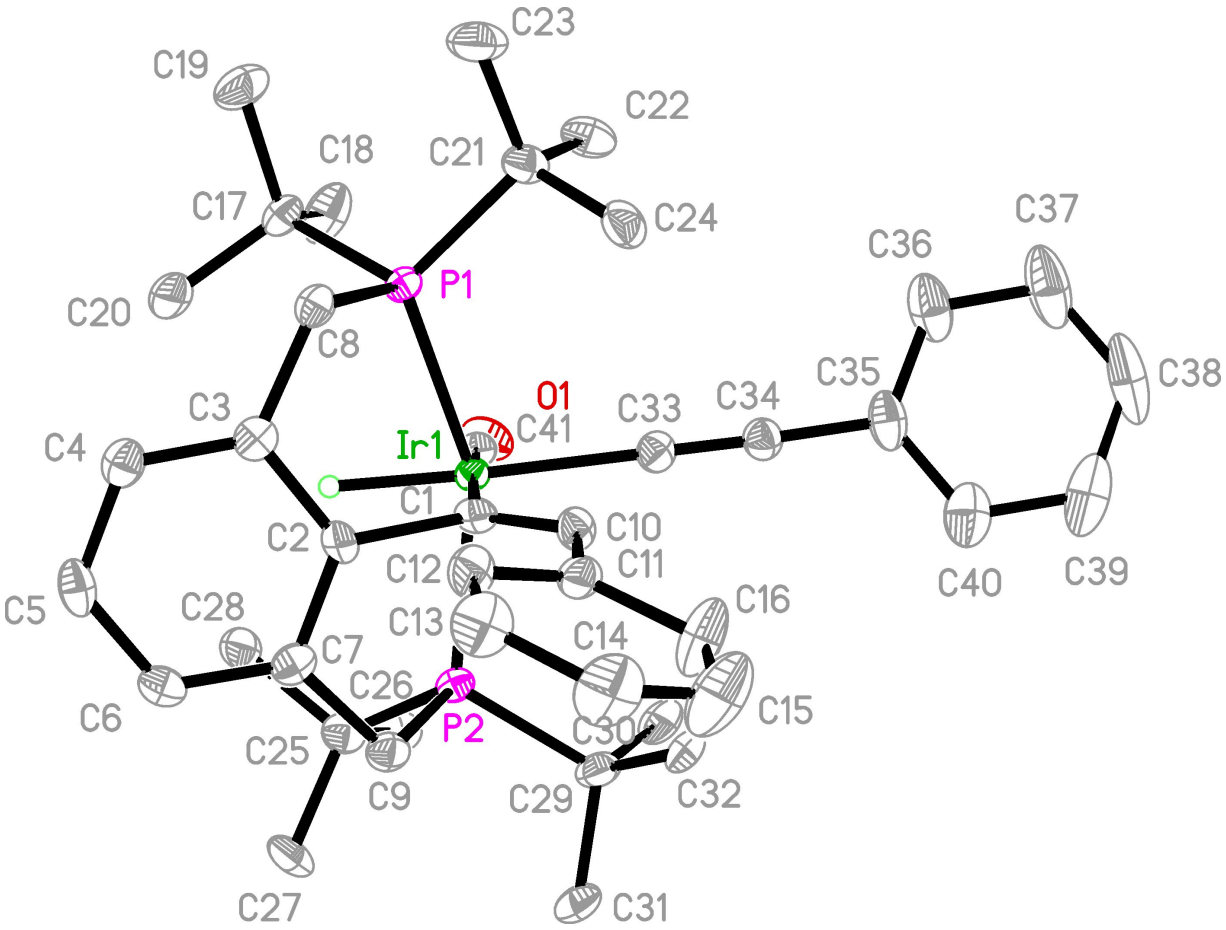

Figure 5-4 X-ray crystal structure of complex **5-10**

Table 5.7 Crystal data and structure refinement for complex **5-10**

Empirical formula	C41 H55 Ir O P2	
Formula weight	817.99	
Temperature	100(2) K	
Wavelength	1.54178 Å	
Crystal system	Monoclinic	
Space group	P2(1)/c	
Unit cell dimensions	a = 20.8477(4) Å	α= 90°.
	b = 11.8734(2) Å	β= 109.470(1)°.
	c = 16.0707(3) Å	γ = 90°.
Volume	3750.55(12) $Å^3$	
Z	4	
Density (calculated)	1.449 Mg/m^3	
Absorption coefficient	7.912 mm^{-1}	
F(000)	1664	
Crystal size	0.30 x 0.20 x 0.10 mm^3	
Theta range for data collection	4.35 to 68.24°.	
Index ranges	-24<=h<=24, -14<=k<=13, -19<=l<=19	
Reflections collected	23493	
Independent reflections	6396 [R(int) = 0.0313]	
Completeness to theta = 68.24°	93.2 %	
Absorption correction	Semi-empirical from equivalents	
Max. and min. transmission	0.50 and 0.20	
Refinement method	Full-matrix least-squares on F^2	
Data / restraints / parameters	6396 / 1 / 423	
Goodness-of-fit on F^2	1.000	
Final R indices [I>2sigma(I)]	R1 = 0.0406, wR2 = 0.0864	
R indices (all data)	R1 = 0.0438, wR2 = 0.0881	
Extinction coefficient	0.000225(17)	
Largest diff. peak and hole	2.398 and -1.177 $e.Å^{-3}$	

Table 5.8 Selective bond lengths [Å] and angles [°] for complex **5-10**

Ir(1)-C(41)	1.881(5)	C(4)-C(5)	1.389(9)
Ir(1)-C(33)	2.075(5)	C(5)-C(6)	1.391(9)
Ir(1)-C(1)	2.112(5)	C(6)-C(7)	1.389(8)
Ir(1)-P(2)	2.3721(14)	C(7)-C(9)	1.500(8)
Ir(1)-P(1)	2.3769(14)	C(8)-H(8A)	0.9900
Ir(1)-H(1)	1.598(10)	C(10)-C(11)	1.480(7)
P(1)-C(8)	1.889(5)	C(11)-C(12)	1.393(8)
P(1)-C(21)	1.902(6)	C(11)-C(16)	1.408(8)
P(1)-C(17)	1.910(6)	C(12)-C(13)	1.388(8)
P(2)-C(29)	1.888(6)	C(13)-C(14)	1.377(9)
P(2)-C(9)	1.889(5)	C(14)-C(15)	1.373(10)
P(2)-C(25)	1.916(6)	C(15)-C(16)	1.379(9)
O(1)-C(41)	1.147(6)	C(17)-C(19)	1.527(8)
C(1)-C(10)	1.332(7)	C(17)-C(18)	1.528(8)
C(1)-C(2)	1.482(7)	C(17)-C(20)	1.536(8)
C(2)-C(3)	1.404(8)	C(21)-C(22)	1.532(8)
C(2)-C(7)	1.406(8)	C(21)-C(23)	1.536(8)
C(3)-C(4)	1.385(8)	C(21)-C(24)	1.542(8)
C(3)-C(8)	1.518(8)	C(25)-C(26)	1.514(8)
C(41)-Ir(1)-C(33)	86.0(2)	C(8)-P(1)-C(21)	102.6(2)
C(41)-Ir(1)-C(1)	176.0(2)	C(8)-P(1)-C(17)	102.4(2)
C(33)-Ir(1)-C(1)	91.7(2)	C(21)-P(1)-C(17)	110.3(3)
C(41)-Ir(1)-P(2)	96.89(17)	C(8)-P(1)-Ir(1)	109.02(18)
C(33)-Ir(1)-P(2)	101.65(16)	C(21)-P(1)-Ir(1)	117.32(19)
C(1)-Ir(1)-P(2)	80.36(15)	C(17)-P(1)-Ir(1)	113.54(18)
C(41)-Ir(1)-P(1)	104.11(17)	C(29)-P(2)-C(9)	103.7(3)
C(33)-Ir(1)-P(1)	102.49(16)	C(29)-P(2)-C(25)	110.0(3)
C(1)-Ir(1)-P(1)	79.57(15)	C(9)-P(2)-C(25)	102.3(3)
P(2)-Ir(1)-P(1)	148.88(5)	C(29)-P(2)-Ir(1)	116.46(19)
C(41)-Ir(1)-H(1)	91(2)	C(9)-P(2)-Ir(1)	108.90(19)
C(33)-Ir(1)-H(1)	177(2)	C(25)-P(2)-Ir(1)	113.99(19)
C(1)-Ir(1)-H(1)	91(2)	C(10)-C(1)-C(2)	126.0(5)
P(2)-Ir(1)-H(1)	80(2)	C(10)-C(1)-Ir(1)	129.9(4)
P(1)-Ir(1)-H(1)	76(2)	C(2)-C(1)-Ir(1)	103.8(3)

Chapter 6

Synthesis and catalytic activity of heterogenized (supported) pincer-ligated iridium catalysts for alkane dehydrogenation

Abstract

Solid-supported catalysts have significant advantages over homogeneous systems, particularly with respect to product-catalyst separation. Pincer-ligated iridium-based catalysts "(^{R}PCP)Ir" ((^{R}PCP = [κ^3-C_6H_3-2,6-$(CH_2PR_2)_2$]) are effective for the dehydrogenation of alkanes to give alkenes, a reaction of great potential value. We have therefore investigated several routes to the development of supported pincer-ligated iridium catalysts. The *p*-dimethylamino-substituted PCP complex is found to bind strongly to alumina while maintaining the same high activity (or even slightly greater) for alkane-dehydrogenation as found in the solution phase. We can recycle this catalyst multiple times; the decomposition rate for the alumina-bound complex is no different than the solution phase catalyst. Like the solution phase catalyst, the supported system shows selectivity for the terminal position of *n*-alkanes, indicating that the active site is essentially the same in bound and solution states. We have attempted to quantify the strength of catalyst binding to alumina by X-ray fluorescence measurements, UV-Vis spectroscopy, and other methods, none of which reveal any complex in solution under our conditions. From UV-Vis studies the upper limit of iridium complex in solution is < 0.006% that bound to alumina under our conditions.

6.1 Introduction

Solid-supported catalysts have significant advantages over homogeneous systems, particularly with respect to product-catalyst separation. In industry, heterogeneous catalysts are used in cracking saturated hydrocarbon feedstocks to higher-value olefins and arenes through reforming processes which typically operated at high temperatures (400–600 °C), that result in low product selectivities and poor energy efficiency.[1] Pincer-ligated iridium-based catalysts are effective for the dehydrogenation of alkanes to give alkenes, a reaction of great potential value.[2] We have therefore investigated several routes to the development of supported pincer-ligated iridium catalysts.

6.2 Results and discussion

6.2.1 Different strategies toward making supported pincer catalysts

There are many strategies for preparing supported catalysts; in this chapter, we discuss two strategies for preparing supported iridium pincer complexes: 1) covalent attachment of iridium pincer complexes to silica and 2) adsorption of Ir pincer complexes (particularly those containing basic functional groups) on γ-Al_2O_3 through a Lewis acid/Lewis base interaction.

6.2.2 Covalent attachment of iridium pincer complexes to silica

One of the most common methods to covalently bind the catalyst is putting a -$Si(OMe)_3$ group in the *para* position of the catalyst and immobilizing it on silica. Iridium pincer complexes containing a -$Si(OMe)_3$ group, **6-6**, were prepared by multistep synthesis as shown in Scheme 6-1.

The synthesis of complex **6-7** is outlined in Scheme 6-1. Deprotection of the methoxy group of the previously reported (MeO-^{tBu}PCP)IrHCl (**6-1**) was done with 9-I-BBN (9-I-BBN = 9-iodo-9-borabicyclo- [3.3.1]nonane, 1M in hexanes), followed by hydrolysis with methanol, leading to the formation of (HO-^{tBu}PCP)IrHI) **6-3** in 85 % yield. One atmosphere CO was added to complex **6-3**, forming complex **6-4** immediately.

CO acts as a protecting group to the iridium center. Without CO, complex **6-4** would react with NaH and to (NaO-PCP)IrH_2, which would subsequently react with MeOH (formed during the binding of -Si(OMe)$_3$ to silica) to become inactive (X-PCP)IrCO. Treatment of **6-4** with 2 equivalents of NaH in benzene produces complex **6-5**, which upon treatment with 3-iodopropyltrimethoxysilane in THF under argon atmosphere produces complex **6-7** (Scheme 6-1).

Attachment to silica was achieved by heating 300 mg silica (Grace XPO 2402) with 16 mg complex **6-6** in toluene-d_8 at 120 °C. Periodic analysis of the solution by ^{1}H NMR showed that as the concentration of **6-6** decreased, methanol concentration increased. After 2 days, the original red solution became colorless and the silica acquired a pink color. No detectable **6-6** remained in solution and *ca.* two equivalents of methanol were produced, indicating that, on average, two methoxy groups of **6-6** reacted with the silanol groups on the silica surface to produce a siloxane linkage and methanol. Excess trimethylsilyldimethylamine was added to cap the remaining silanol groups. This supported catalyst, which contained 63 mmol Ir/g, was isolated, washed three times with pentane, toluene, and THF, respectively, and dried under high vacuum.

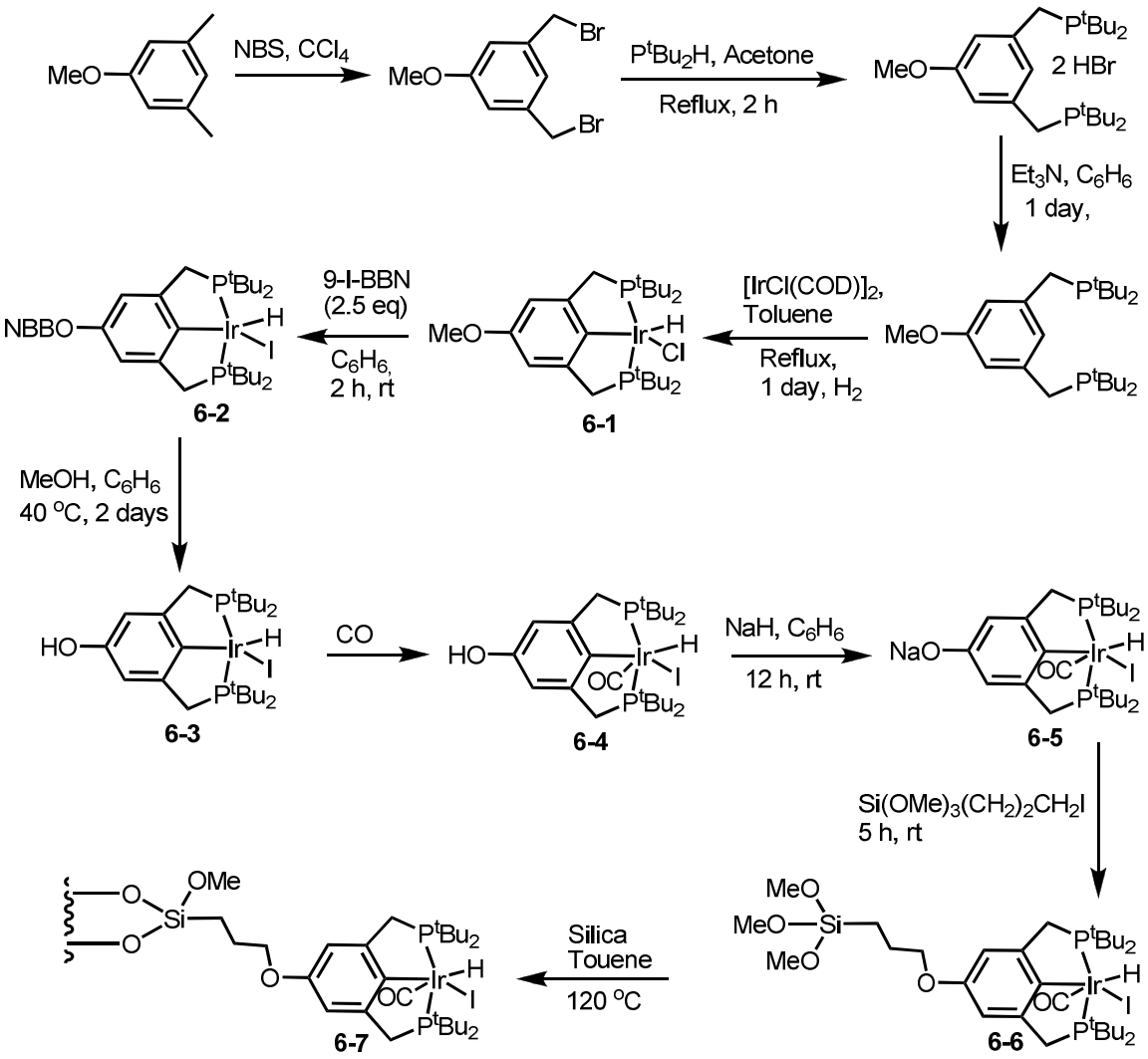

Scheme 6-1 Synthesis of covalently bound iridium pincer complexes to silica

6.2.2.1 Removing CO from (PCP)Ir(H)(I)(CO)

Removing CO from complex **6-7** followed by reduction of (X-PCP)Ir(H)(I) will generate the supported active catalyst. Removing CO from the iridium center was tested with some model reactions. We made (PCP)Ir(H)(Cl)(CO) by adding CO to (PCP)Ir(H)(Cl). When trimethylamine oxide was reacted with (PCP)Ir(H)(Cl)(CO) to remove CO, the reaction was not clean, forming many unknown complexes. The other attempted strategy to remove CO from (PCP)Ir(H)(Cl)(CO) was refluxing at high temperature under argon flow. In this case the reaction was clean, yielding a 2:1 mixture of (PCP)Ir(CO): (PCP)Ir(H)(Cl) (eq. 1).

To mimic the iridium center as it exists in complex **6-7**, complex (PCP)Ir(H)(I)(CO) was synthesized by passing CO over (PCP)Ir(H)(I). Refluxing (PCP)Ir(H)(I)(CO) for 80 minute at 210 °C under argon flow removed CO from the metal center quite successfully (eq. 2). As a result, we endeavored to employ the same reaction conditions to the silica-supported pincer complex, with the expectation that CO could be removed successfully. Now we will follow the same reaction conditions with complex **6-7** and hopefully it will remove CO successfully.

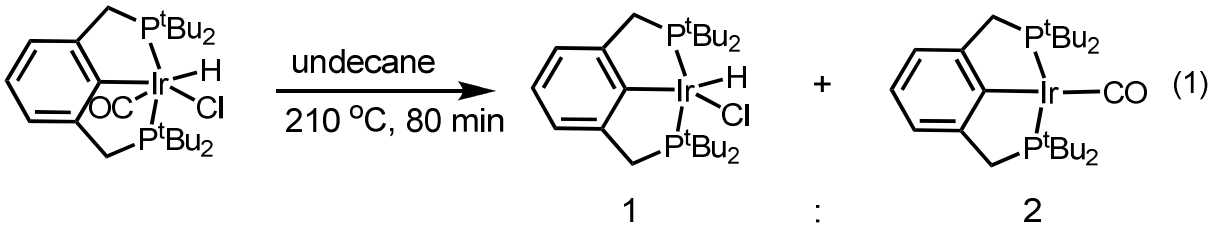

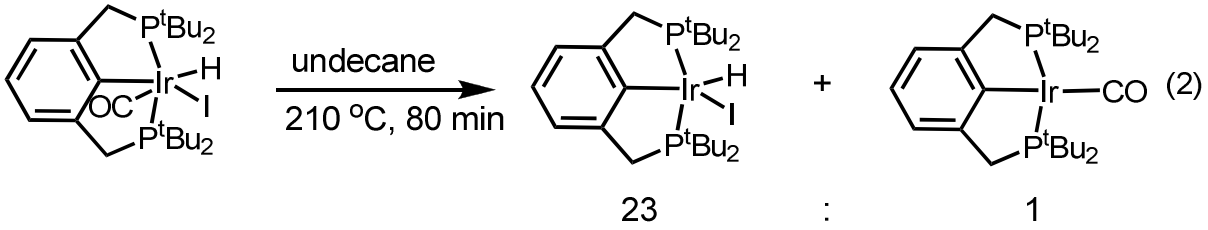

6.2.3 Alumina-supported iridium pincer catalyst systems

Complexes (H-PCP)IrH_2 (**1a**),[3] (MeO-PCP)IrH_2 (**1b**),[4] (MeOC(O)-PCP)IrH_2 (**1c**),[5] (Me_2N-PCP)IrH_2 (**1b**)[6] have been synthesized previously. The methoxy-substituted complex **1b** was previously reported to be a more robust alkane dehydrogenation catalyst than the parent complex **1a**,[7] while giving slightly higher rates of acceptorless dehydrogenation (of cyclodecane) but slightly lower rates of *n*-octane/NBE transfer-dehydrogenation. As reported in Table 6.1, turnover frequencies (TOFs) for solution phase COA/TBE transfer-dehydrogenation by **1b** are also somewhat lower than is found for **1a**. The ester-substituted complex **1c** is found to afford slightly greater initial rates for catalytic COA/TBE transfer dehydrogenation than either **1b** or **1a** (Table 6.1).

However, **1c** apparently undergoes significant decomposition under the catalytic conditions as indicated by a decrease in catalytic activity. Accordingly, ^{31}P and ^{1}H NMR spectroscopy independently reveal that in the presence of TBE, **1c** reacts to give six-coordinate iridium hydride complexes. This decomposition is attributable to intermolecular addition of a C-H bond ortho to the ester functionality, in accord with the previously reported reaction of (PCP)Ir with acetophenone.[8]

6.2.3.1 Transfer-dehydrogenation of COA by solution-phase and γ-alumina-supported catalyst systems

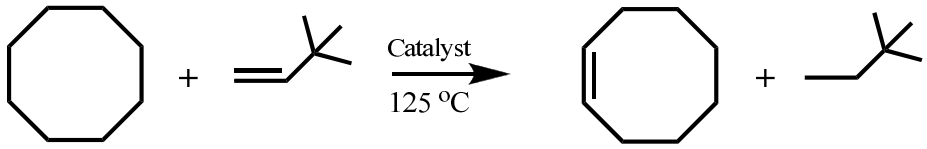

Scheme 6-2 Transfer dehydrogenation of cyclooctane using TBE

Table 6.1 COA/TBE transfer-dehydrogenation by solution-phase and γ–alumina-supported catalyst systems

Catalyst (5 mM) ([TBE] = 0.4 M)	time (min)	**homogeneous** (solution phase) [COE] (mM)	**heterogeneous** (γ-alumina) [COE] (mM)
$(PCP)IrH_2$ (**1a**)	15	61	3
	60	164	3
	240	368	4
$(MeO\text{-}PCP)IrH_2$ (**1b**)	15	36	28
	60	115	60
	240	352	84
$(MeO_2C\text{-}PCP)IrH_2$ (**1c**)	15	73	49
	60	155	119
	240	258	354
$(Me_2N\text{-}PCP)IrH_2$ (**1d**)	15	20	42
	60	68	111
	240	200	283

Upon addition of γ-alumina to a COA solution of unsubstituted PCP iridium complex **1a** (5 mM), the red solution turned clear and the solid acquired the characteristic red color of the complex. Upon heating to 125 °C, the red solid rapidly turned orange,

suggesting that decomposition had occurred. Accordingly, very little COA/TBE transfer-hydrogenation occurred in the presence of alumina at 125 °C (less than 5 mM COE formed; Table 6.1).[9]

Attempts to support iridium PCP catalysts on alumina were more promising with MeO-PCP complex **1b** than with **1a**, but still not satisfactory. As in the case of **1a**, upon addition of alumina the solution lost its red color (which was acquired by the alumina), but in contrast to alumina-supported **1a**, no color change was observed upon heating. After 15 minutes at 125 °C, **1b** (5 mM), in the presence of alumina only, afforded product yields slightly less than in the absence of alumina (28 mM vs. 36 mM). But after 240 minutes the total yield was substantially less than was obtained in the absence of alumina (84 vs. 258 mM).

In contrast to results with **1a** and **1b**, the catalyst lifetime and total turnovers effected by ester-substituted complex **1c** were increased in the presence of alumina. As with all the bound iridium PCP catalysts, adsorption of **1c** visually appeared to be complete. Although initial rates of COA/TBE transfer-dehydrogenation were slightly lowered by the presence of alumina (49 mM vs. 73 mM after 15 min), the yield of COE was appreciably greater after 240 min than was obtained with the solution-phase catalyst (354 vs. 258 mM). This effect can be rationalized by assuming that adsorption of the catalyst to alumina inhibits the inter-molecular catalyst de-activation reaction noted above (addition to Ir of the C-H bonds ortho to the ester functionality).

However, attempts to recycle the **1c**/γ-alumina catalyst system met with only partial success. The solution was removed from the solid, which was then washed twice

with COA (2 x 2 mL) and a fresh TBE/COA solution was then added. The subsequent catalytic runs each showed significantly decreased reactivity (Table 6.2).

Table 6.2 COA/TBE transfer dehydrogenation: recycling catalysts **1c** and **1d**

catalyst (5 mM equivalent)	Time (h)	1st cycle	2nd cycle	3rd cycle	4th cycle	5th cycle	6th cycle	7th cycle	8th cycle
(MeO_2C-PCP)IrH_2	1	117	101	27					
heterogeneous	4	331	188	41					
(γ-alumina-supported)	8	440	259	49					
(Me_2N-PCP)IrH_2	1	75	67	56	47	30	15	9	4
homogeneous	4	281	222	154	116	70	41	20	11
(solution-phase)	8	465	339	246	161	114	65	30	14
(Me_2N-PCP)IrH_2	1	115	91	66	61	46	16	10	6
heterogeneous	4	314	173	135	119	74	43	23	12
(γ-alumina-supported)	8	464	315	216	197	117	65	31	15

Very promising results were obtained with the new catalyst (Me_2N-PCP)IrH_2 (**1d**). Of the four X-PCP iridium catalysts used in this study, **1d** gave the lowest TOFs for COA/TBE transfer-dehydrogenation in solution (Table 6.1). Thus it was found that initial COA/TBE solution-phase transfer-dehydrogenation rates increase with decreasing electron-donating ability of the group X: $Me_2N < MeO < H < CO_2Me$. However, when **1d** was adsorbed on γ-alumina, initial rates of COA/TBE transfer-dehydrogenation were greater than obtained by solution-phase **1d**. This is consistent with the correlation with electron-withdrawing ability of X; binding of the Me_2N group to a Lewis acidic surface site would indeed be expected, based on this correlation, to increase catalytic activity. Perhaps even more significant than the increased TOFs observed upon binding **1d** to alumina, the total TONs effected by the **1d**/γ-alumina system after 4 h were significantly

greater than achieved with the homogeneous system (283 vs. 200 mM). Moreover, the system proved to be extremely robust. The solution was removed after 8 h of catalysis at 125 °C and the remaining solid was washed two times with COA; upon addition of fresh TBE/COA solution to the solid, each subsequent run showed only a relatively small decrease in catalytic activity. This process involves extensive exposure of the catalyst (which is sensitive to O_2, H_2O and even N_2) to an imperfect glove-box atmosphere; thus the observed decrease in TOF for each cycle represents only an upper limit of the degree of decomposition that occurred during the actual catalytic run.

Recycling of the solution-phase catalyst necessarily involves a different protocol, namely, removal of solvent *in vacuo* before adding fresh solution. While this presumably involves less exposure to impurities, the loss of activity with each cycle is approximately the same as that observed in the case of the alumina-supported system (Table 6.2).

6.2.3.2 *n*-octane transfer-dehydrogenation by (Me_2N-PCP)IrH_2

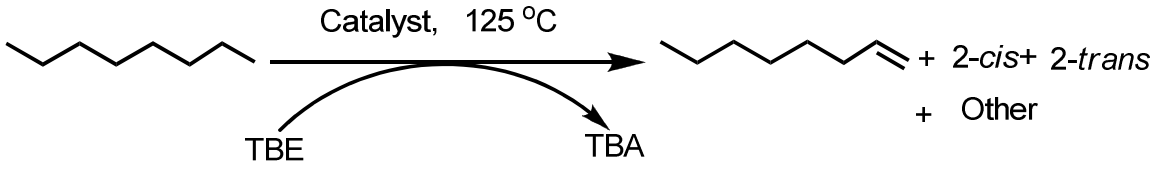

Scheme 6-3 Transfer dehydrogenation of *n*-octane using TBE

The **1d**/γ-alumina system was also effective for the transfer dehydrogenation of *n*-octane, and as with COA, more active than solution-phase **1d** (Table 6.3).

Table 6.3 *n*-Octane/TBE transfer-dehydrogenation by (Me_2N-PCP)IrH_2

	homogeneous (solution-phase)		**heterogeneous** (γ-alumina-supported)	
time (min)	1-octene (mM)	total octene (mM)	1-octene (mM)	total octene (mM)
15	4	7	2	15
30	9	22	3	30
60	15	43	3	59
120	16	73	4	99
240	16	98	4	130

6.2.3.3 *γ*-Alumina (no Ir) isomerizes 1-octene

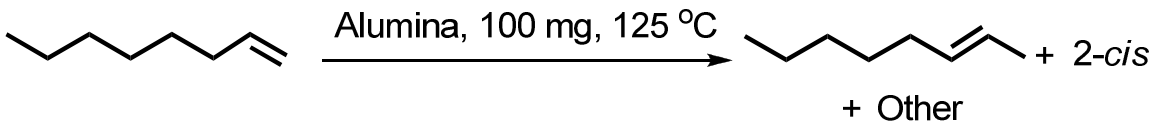

Scheme 6-4 Isomerization of 1-octene

Table 6.4 Isomerization of 1-octene by γ–alumina (no iridium present)

initial [1-octene]	time (min)	1-octene (mM)	trans-2-octene (mM)	cis-2-octene (mM)
29 mM	5	27	1	1
	10	26	2	1
	15	24	3	2
	30	20	6	3
	60	14	8	5
427 mM	5	413	8	6
	10	404	14	12
	15	393	22	15
	30	366	46	24
	60	307	88	40

The yield of 1-octene from *n*-octane with this system is much lower than with solution-phase **1d**. We initially assumed that this lower apparent selectivity was due to the isomerization of 1-octene by γ-alumina. Control experiments with γ-alumina, with no iridium present, do indeed show that 1-octene is isomerized under these conditions (Table 6.4). For example, after ca. 60 min, with an initial 1-octene concentration of 29 mM, isomerization is ca. 50 % complete with cis- and trans-2-octene being the only major products. With an initial 1-octene concentration of 427 mM, 30% isomerization is effected after 60 min. However, it does not seem that this level of isomerization activity (half-life ca. 60 min), by itself, could account for the much lower yields of 1-octene obtained from **1d**/γ-alumina vs. solution phase **1d** (e.g. 3 mM 1-octene out of 30 mM total octene product vs. 9 mM 1-octene out of 22 mM total octene, after only 30 min of catalysis).

Further work is ongoing to elucidate the reason for the relatively low yield of terminal alkene, but possible explanations include formation of a minor decomposition product on alumina that acts as a highly active isomerization catalyst, or perhaps simply increased isomerization activity from **1d** upon binding to alumina (possibly due to decreased electron-density at Ir). It should be noted, however, that even the small yields of 1-octene observed at early reaction times indicate that at least partial selectivity for dehydrogenation at the terminal position is retained upon binding to alumina (even the low 1-octene concentrations observed at early reaction times are much greater equilibrium values). Furthermore, the predominance of 2-octene, with much lower concentrations of 3- and 4-octenes, is indicative of selectivity for the terminal position followed by rapid α–β isomerization and much slower further internal isomerization.

6.2.3.4 Infrared spectroscopic characterization of the PCP complexes supported on γ-alumina

C-O stretching frequencies act as a valuable (though imperfect) indicator of small changes in electronic density at the metal center of transition metal carbonyl complexes. In order to probe the nature of the binding of the X-PCP complexes to γ-alumina, we prepared the corresponding (X-PCP)Ir(CO) complexes. All complexes appeared, visually, to be fully adsorbed by γ-alumina. The C-O stretching frequencies of the alumina-bound complexes, prepared as a nujol mull, seem to be very informative.

Table 6.5 C-O stretching frequencies of complexes (X-PCP)Ir(CO) in solution and adsorbed on γ-alumina

Compound	ν_{CO} (cm^{-1}) (solution)	ν_{CO} (cm^{-1}) (γ-alumina)
(PCP)Ir(CO)	1925.3	1925.9
(MeO-PCP)Ir(CO)	1922.6	1927.5
(Me_2N-PCP)Ir(CO)	1918.4	1928.9

Adsorption of (PCP)Ir(CO) (**1a-CO**) on alumina results in only a very slight increase in C-O stretching frequency as compared with **1a-CO** in nujol (1925.9 cm^{-1} vs. 1925.3 cm^{-1}; Table 6.5). The value of ν_{CO} of (MeO-PCP)Ir(CO) in nujol is ca. 3 cm^{-1} red-shifted versus solution-phase **1a-CO**, consistent with the electron-donating properties of the *p*-methoxy group. When bound to alumina however, ν_{CO} of **1b-CO** is 5 cm^{-1} greater than solution-phase **1b-CO** and ca. 2 cm^{-1} greater than either solution phase **1a-CO** or **1a-CO/**γ–alumina. These data strongly indicate that **1b-CO** binds to γ-alumina with the *p*-methoxy group acting as a Lewis Base toward a Lewis Acid surface site; the bound

methoxy group is then electron-withdrawing, as might be expected. Likewise, the ν_{CO} value of complex **1d-CO** in solution is 7 cm^{-1} less than that of **1a-CO**; but upon binding to alumina, ν_{CO} is blue-shifted by 10.5 cm^{-1} and is then 3 cm^{-1} higher than that of **1a-CO**/γ-alumina. Thus, as indicated by the relative binding-induced blue-shifts, the Me_2N group of **1d-CO** apparently donates significantly more electron-density to the alumina than does the MeO group of **1b-CO**; this is in accord with results of the catalytic runs which indicated that **1d** binds more strongly to γ-alumina than does **1b**.

6.2.3.5 Quantifying the strength of binding of the Me_2N-PCP unit to alumina

(Me_2N-PCP)IrH_2 (30 mg) was dissolved in 10 mL COA in the presence of 1g γ-alumina. The mixture was stirred for 15 min and then filtered; the filtrate was then evaporated in vacuo. The residue was analyzed by X-ray fluorescence and the iridium content was found to be below the detection limit of this method, which is estimated as $<1 \times 10^{-6}$ g of the initial amount of iridium.

The iridium carbonyl complexes are much more robust than the catalytically active hydrides. For this reason, (Me_2N-PCP)Ir(CO) (**1d-CO**) was used to help quantify, by UV-visible spectroscopy, the strength of binding of the (Me_2N-PCP)Ir unit to alumina. An *n*-hexane solution of **1d-CO** (2.5 mM; 3mg in 2.0 mL) has an absorbance of 1.58 at λ = 493 nm (1.0 cm path length). When 2.0 mL of the same solution was stirred in the presence of γ-alumina for 15 minutes and then filtered, the absorbance at λ = 493 nm was found to be $<1 \times 10^{-4}$. The concentration of **1d-CO** in solution under these conditions is therefore <0.006% of that present prior to the addition of alumina.

6.3 Conclusion

To summarize the above results, (PCP)IrH_2 (**1a**) shows very rapid loss of catalytic activity in the presence of γ-alumina. All three para-substituted complexes investigated in this study underwent decomposition far more slowly than **1a**, if at all. Indeed, in one case, that of complex **1c**, the binding to alumina even appears to inhibit the inter-catalyst decomposition reaction that is observed in the solution phase. In the case of catalyst **1b**, deactivation by alumina still occurs, albeit slowly, suggesting that the methoxy group does not bind as strongly as the ester or dimethyl amino groups of **1c** or **1d**, respectively. Electron-withdrawing ability of the para-substituent is correlated with catalytic TOFs in solution; consistent with the presumed binding of the Me_2N group to a Lewis Acidic surface site, the Me_2N-PCP catalyst **1d** affords increased TOFs when bound to γ-alumina. The **1d**/γ-alumina system is also found to be quite stable under catalytic conditions, and even tolerates multiple cycles of solvent removal, washing, and reuse. In the case of *n*-alkane, the product distribution from the **1d**/γ-alumina system is predominantly 2-octene, but this is likely due to increased rates of isomerization rather than selectivity for dehydrogenation at internal positions of the alkane chain. We have attempted to quantify the strength of catalyst binding to alumina by X-ray fluorescence measurements, UV-Vis spectroscopy, and other methods, none of which reveal any complex in solution under our conditions, particularly **1d**/γ-alumina. From UV-Vis studies the upper limit of iridium complex in solution is < 0.006% that bound to alumina under our conditions. [9]

6.4 Experimental

General Considerations. All reactions were carried out under argon atmosphere using standard Schlenk techniques or in an argon-filled dry box. *p*-Xylene, *p*-xylene-$d_{10,}$ THF and C_6D_6 were dried using Na/K and collected by vacuum transfer. All solvents (COA, *n*-octane, *n*-hexane) were distilled under vacuum from Na/K alloy. TBE and 1-hexene were dried under Na/K alloy and vacuum transferred under argon. $I(CH_2)_3Si(OMe)_3$ was purchased from Aldrich. 400 MHz or 500 MHz Varian instruments were used for the ^1H, ^{13}C and ^{31}P NMR experiments. The residual peak of the deuterated solvent was used as a reference for ^1H chemical shifts. ^{31}P NMR chemical shifts were referenced to PMe_3 standard, which appears at –62.2 ppm. PMe_3 internal standard in ^{31}P NMR was employed in determining the yield. (^{tBu4}PCP)IrH_2, (MeO-PCP)IrH_2, (Me_2N-PCP)IrH_2[6] and [MeOC(O)-PCP]IrH_2 was prepared as described in the literature.[5] GC analyses were carried out with a Thermal Focus GC with a flame ionization detector (FID) on Supelco Petrocol DH column (100m length × 0.25 mm ID × 0.5 μm film thickness). Calibration curves were prepared using standard samples. UV-visible spectra were recorded on a Varian Cary-50 spectrophotometer. Infrared spectra were recorded on a Thermo Nicolet 360-FT-IR instrument.

(MeO-PCP)IrHCl (6-1): Complex **6-1** was synthesized following a literature procedure.

(NBBO-PCP)IrHI (6-2): Complex **6-1** (300 mg, 0.46 mmol) was dissolved in hexane (200 mL) in a Schlenk flask under a flow of argon. 9-I-BBN (1 M in hexanes, 1.15 mL) was added, and the solution was stirred for 3 hours at room temperature. The solvent was removed at room temperature under high vacuum and the by-product 9-Cl-BBN and the

excess 9-I-BBN were removed at 100 °C under high vacuum. ^{31}Peration NMR (*p*-xylene-d_{10}, 202 MHz): δ 66.9 (s, P^{t}Bu$_2$). ^{1}H NMR (*p*-xylene-d_{10}, 500 MHz): δ – 44.72 (t, J_{PH} = 13.0 Hz, 1H, Ir-***H***).

(HO-PCP)Ir(H)(I) (6-3): Complex **6-2** (200 mg) was dissolved in a mixture of 30 mL benzene and 10 mL methanol in a Schlenk flask under a flow of argon. The solution was stirred for 2 days at 40 °C temperature. The solvent was removed under vacuum; yielding 120 mg of complex **6-3**. ^{31}P{^{1}H} NMR (*p*-xylene-d_{10}, 202 MHz): δ 66.6 (s, P^{t}Bu$_2$). ^{1}H NMR (*p*-xylene-d_{10}, 500 MHz): δ 7.12 (d, J_{HH} = 6.0 Hz, 2H, Ar, PCP), 7.09 (t, J_{HH} = 4.4 Hz, 1H, Ar, PCP), 3.67 (s, 1H, ***H***O-PCP), 3.14 (d of vt, J_{PH} = 3.7 Hz, J_{HH} = 17.5 Hz, 2H, ***CH$_2$***P^{t}Bu$_2$), 3.01 (d of vt, J_{PH} = 4.0 Hz, J_{HH} = 17.0 Hz, 2H, ***CH$_2$***P^{t}Bu$_2$), 1.35 (vt, J_{PH} = 6.5 Hz, 18H, PC(C***H***$_3$)$_3$), 1.33 (vt, J_{PH} = 6.5 Hz, 18H, PC(C***H***$_3$)$_3$), -44.8 (t, J_{PH} = 13.5 Hz, 1H, Ir-***H***).

(HO-PCP)Ir(H)(I)(CO) (6-4): Complex **6-3** (100 mg) was dissolved in 30 mL benzene in a Schlenk flask. CO was bubbled through solution for 1 h at room temperature resulting color change from dark red to yellow. The solvent was removed under vacuum to yield complex **6-4**. ^{31}P{^{1}H} NMR (*p*-xylene-d_{10}, 202 MHz): δ 49.4 (s, P^{t}Bu$_2$). ^{1}H NMR (*p*-xylene-d_{10}, 500 MHz): δ 7.23 (d, J_{HH} = 6.0 Hz, 2H, Ar, PCP), 7.14 (t, J_{HH} = 4.4 Hz, 1H, Ar, PCP), 3.73 (s, 1H, ***H***O-PCP), 2.99 (d of vt, J_{PH} = 4 Hz, J_{HH} = 17.0 Hz, 2H, ***CH$_2$***P^{t}Bu$_2$), 2.91 (d of vt, J_{PH} = 3.5 Hz, J_{HH} = 16.5 Hz, 2H, ***CH$_2$***P^{t}Bu$_2$), 1.45 (vt, J_{PH} = 7.0 Hz, 18H, PC(C***H***$_3$)$_3$), 1.31 (vt, J_{PH} = 7.0 Hz, 18H, PC(C***H***$_3$)$_3$), -9.69 (t, J_{PH} = 15.5 Hz, 1H, Ir-***H***).

(NaO-PCP)Ir(H)(I)(CO) (6-5): Complex **6-4** (50 mg, 0.067 mmol) was dissolved in 30 mL benzene in a Schlenk flask and NaH (3.2 mg, 0.134 mmol) was added at room temperature. The solution was stirred for 12 h at room temperature yielding complex **6-5**. $^{31}P\{^{1}H\}$ NMR (*p*-C_6H_6, 202 MHz): δ 49.8 (s, P^{t}Bu$_2$), ^{1}H NMR (C_6H_6, 500 MHz): -9.53 (t, J_{PH} = 16.0 Hz, 1H, Ir-***H***).

(Si(OMe)$_3$CH$_2$)$_3$O-PCP)Ir(H)(I)(CO) (6-6): To complex **6-4** (0.134 mmol) in benzene (synthesized in the previous reaction), 0.1 ml (0.536 mmol) I(CH$_2$)$_3$Si(OMe)$_3$ was added in a Schlenk at room temperature. The mixture was heated at 65 °C for 2 h. NaOMe (22 mg, 0.407 mmol) was then added to the flask inside the glove-box. The mixture was stirred at room temperature for 2 days. NaOMe reacted with the excess of I(CH$_2$)$_3$Si(OMe)$_3$ to produce NaI and CH$_2$=CHCH$_2$Si(OMe)$_3$ which is relatively easy to remove. Volatiles were then removed under high vacuum. The residue was extracted with (3 x 20) mL of pentane, and the extract was filtered into a schlenk flask. Removal of the solvent under high vacuum afforded of a red solid **6-6** in 76 % yield. $^{31}P\{^{1}H\}$ NMR (*p*-xylene-d_{10}, 202 MHz): δ 49.5 (s, P^{t}Bu$_2$). ^{1}H NMR (*p*-xylene-d_{10}, 500 MHz): 7.06 (d, J_{HH} = 5.0 Hz, 2H, Ar, PCP), 7.02 (t, J_{HH} = 4.4 Hz, 1H, Ar, PCP), 3.63 (t, J_{HH} = 5.3 Hz, 2H, O***CH$_2$***CH$_2$), 3.56 (s, 9H, Si(O***Me***)$_3$), 3.06 (d of vt, J_{PH} = 4 Hz, J_{HH} = 17.5 Hz, 2H, ***CH$_2$***P^{t}Bu$_2$), 2.96 (d of vt, J_{PH} = 3.4 Hz, J_{HH} = 16.5 Hz, 2H, ***CH$_2$***P^{t}Bu$_2$), 2.07 (q, J_{HH} = 2.3 Hz, 2H, OCH$_2$***CH$_2$***CH$_2$), 1.43 (vt, J_{PH} = 6.7 Hz, 18H, PC(C***H***$_3$)$_3$), 1.30 (vt, J_{PH} = 6.7 Hz, 18H, PC(C***H***$_3$)$_3$), 0.78 (t, J_{HH} = 2.8 Hz, 2H, OCH$_2$CH$_2$***CH$_2$***), -9.67 (t, J_{PH} = 15.5 Hz, 1H, Ir-***H***).

Complex 6-7: Complex **6-6** (50 mg), silica (1.5 g), and toluene (10 mL) were added to a Kontes flask. The toluene suspension was degassed by freeze-pump-thaw cycles. The flask was refilled with ethylene gas at -78 °C and the suspension was stirred at 120 °C for 2 days. The flask was cooled to room temperature and ethylene gas was removed by freeze-pump-thaw cycles. Excess trimethylsilyldimethylamine (3 mL, 18.7 mmol) was added in the glovebox and the flask was degassed and refilled with ethylene gas at -78 °C. The suspension was stirred at room temperature for 2 days. This supported catalyst was filtered under argon, and washed with pentane, toluene and THF three times (5 ml each), respectively. The orange solid was dried under high vacuum overnight to give 1.46 g of product.[10]

Calcination of Alumina:

γ-Al_2O_3 was calcined at 550 °C for 2 hours under a flow of O_2 and cooled to 135 °C under O_2, then cooled to room temperature under high vacuum. The solid wasbrought into the drybox under high vacuum and stored under argon.[10]

Synthesis of Alumina-supported Iridium Pincer Complexes:

Ir complexes **1(a-d)** (5 μmol) was dissolved in alkane (1mL) (cyclooctane or linear alkanes). The solution was added to 100 mg (0.98 mmol) of γ-Al_2O_3 and the suspension was stirred at room temperature. After 20 min, the original red solution turned colorless and the alumina acquired a rust-red color.

Transfer dehydrogenation of COA in heterogeneous condition:

Iridium complex **1a**, **1b**, **1c** or **1d** (5 μmol) was dissolved in COA (1mL) in a Kontes flask. γ-Al_2O_3 (100 mg, 0.98 mmol) was added to the solution and the suspension was stirred at room temperature for 20 min. TBE (70 μL, 0.54 mmol) was then added into the suspension. The flask was sealed tightly with a Teflon plug under an argon atmosphere, and the suspension was stirred in an oil bath at 125 °C. Periodically, the flask was removed from the oil bath and cooled in an ice bath. An aliquot was removed from the flask and analyzed by GC (method C). Turnover numbers were calculated for each aliquot using mesitylene as GC standard. Results are summarized in the text.

The heterogeneous catalysts can be recycled. After each cycle, the solution was syringed out and the solid was washed two times with COA. Fresh COA and TBE were then added.

Transfer dehydrogenation of COA in homogeneous condition:

A flask was charged with iridium pincer complex **1a**, **1b**, **1c** or **1d** (5 μmol), COA (1mL), and TBE (70 μL, 0.54 mmol). The flask was sealed tightly with a Teflon plug under an argon atmosphere, and the solution was stirred in an oil bath at 125 °C. Periodically, the flask was removed from the oil bath and cooled in an ice bath. An aliquot was removed from the flask and analyzed by GC (method C). Turnover numbers were calculated for each aliquot. Recycling of the homogeneous catalysts was obtained by evaporation of the solution under high vacuum and addition of fresh COA and TBE. Results are summarized in the text.

Transfer dehydrogenation of *n*-octane in heterogeneous condition:

Iridium complex **1d** (5 μmol) was dissolved in *n*-octane (1 mL) in a Kontes flask. γ-Al_2O_3 (100 mg, 0.98 mmol) was added to the solution and the suspension was stirred at room temperature for 20 min. TBE (70 μL, 0.54 mmol) was then added into the suspension. The flask was sealed tightly with a teflon plug under an argon atmosphere, and the suspension was stirred in an oil bath at 125 °C. Periodically, the flask was removed from the oil bath and cooled in an ice bath. An aliquot was removed from the flask and analyzed by GC. Turnover numbers were calculated for each aliquot using mesitylene as GC standard. Results are summarized in the text.

Transfer dehydrogenation of *n*-octane in homogeneous condition:

A flask was charged with iridium pincer complex 1d (5 μmol), n-octane (1mL), and TBE (70 μL, 0.54 mmol). The flask was sealed tightly with a Teflon plug under an argon atmosphere, and the solution was stirred in an oil bath at 125 °C. Periodically, the flask was removed from the oil bath and cooled in an ice bath. An aliquot was removed from the flask and analyzed by GC. Turnover numbers were calculated for each aliquot. Results are summarized in the text.

1-octene isomerization by Alumina:

A flask was charged with 100 mg of γ-Al_2O_3, COA (1mL), and 1-octene (4.55 μL, 29 mmol or 67 μL, 427 mmol). The flask was sealed tightly with a Teflon plug under an argon atmosphere, and the solution was stirred in an oil bath at 125 °C. Periodically, the

flask was removed from the oil bath and cooled in an ice bath. An aliquot was removed from the flask and analyzed by GC.

6.5 References

(1) Wieseman, P. *Petrochemicals*, Ellis Horwood: Chichester, England **1986**; pp 90-91.

(2) Liu, F.; Pak, E. B.; Singh, B.; Jensen, C. M.; Goldman, A. S. *J. Am. Chem. Soc.* **1999**, *121*, 4086.

(3) Gupta, M. H., C.; Flesher, R. J.; Kaska, W. C.; Jensen, C. M. *Chem. Commun.* **1996**, 2083.

(4) Gupta, M.; Hagen, C.; Kaska, W. C.; Cramer, R. E.; Jensen, C. M. *J. Am. Chem. Soc.* **1997**, *119*, 840.

(5) Krogh-Jespersen, K.; Czerw, M.; Zhu, K.; Singh, B.; Kanzelberger, M.; Darji, N.; Achord, P. D.; Renkema, K. B.; Goldman, A. S. *J. Am. Chem. Soc.* **2002**, *124*, 10797.

(6) Ray, A. *PhD thesis, Rutgers University, **2007**.*

(7) Zhu, K.; Achord, P. D.; Zhang, X.; Krogh-Jespersen, K.; Goldman, A. S. *J. Am. Chem. Soc.* **2004**, *126*, 13044.

(8) Zhang, X.; Kanzelberger, M.; Emge, T. J.; Goldman, A. S. *J. Am. Chem. Soc.* **2004**, *126*, 13192.

(9) Huang, Z.; Brookhart, M.; Goldman, A. S.; Kundu, S.; Ray, A.; Scott, S. L.; Vicente, B. C. *Adv. Synth. Catal* **2009**, *351*, 188.

(10) *This was done by Zheng Huang at UNC.*

Chapter 7

Experimental and computational studies of metal-ligand binding energies

Abstract

Using the pincer-ligated iridium fragment "(PCP)Ir", a broad range of complexes with widely varying steric and electronic effects, have been synthesized and studied. These complexes include Ir(I) complexes of the type (PCP)IrL and Ir(III) species (PCP)Ir(H)(H)L, PCP)Ir(H)(Cl)L, and (PCP)IrHX (L = various P- and N-donors, N_2, various olefins; X = various anionic ligands). The relative thermodynamics of these adducts have been detected by equilibrium measurements and calculated using DFT. The use of the B3LYP functional is found to significantly understate binding energies, while the PBE functional produces results in better agreement with experimental values for the relative bond strengths in (PCP)IrL. For example, coordination of PMe_3 or oxidative addition of Ph-H to (PCP)Ir are predicted to be endergonic additions; in fact, the corresponding products are experimentally quite stable as is predicted using the PBE functional.

7.1 Introduction

Organic molecule bond energies can be predicted with remarkable precision, either by using empirically-based methods such as Benson's Rules or computational methods. In transition metal complexes, measuring or predicting metal-ligand bond energies are so challenging, that only a limited number are known.[1,2,3,4] The ability to predict metal-ligand bond strengths with comparable accuracy would be an extremely powerful tool in catalyst design and the interpretation of many chemical and biological processes.[5, 6]

7.2 Results and Discussion

Using the pincer-ligated iridium fragment "(PCP)Ir", a broad range of complexes with widely varying steric and electronic effects, have been synthesized and studied. These complexes include Ir(I) complexes of the type (PCP)IrL and Ir(III) species (PCP)Ir(H)(H)L, PCP)Ir(H)(Cl)L, and (PCP)IrHX (L = various P- and N-donors, N_2, various olefins; X = various anionic ligands). The relative thermodynamics of these adducts have been detected by equilibrium measurements and calculated using DFT.[7]

7.2.1 Equilibrium studies with 4-coordinated (PCP)IrL

Using the pincer-ligated iridium fragment "(PCP)Ir" a broad range of complexes [(PCP)IrL] have been synthesized and studied with widely varying steric and electronic effects of the ligand L. The relative thermodynamics of these adducts have been detected by equilibrium measurements (eq. 1).

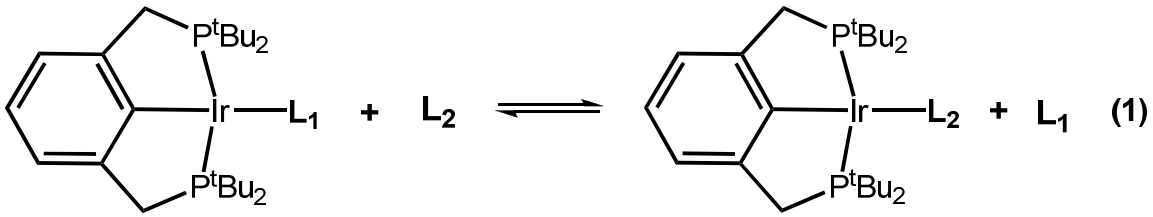

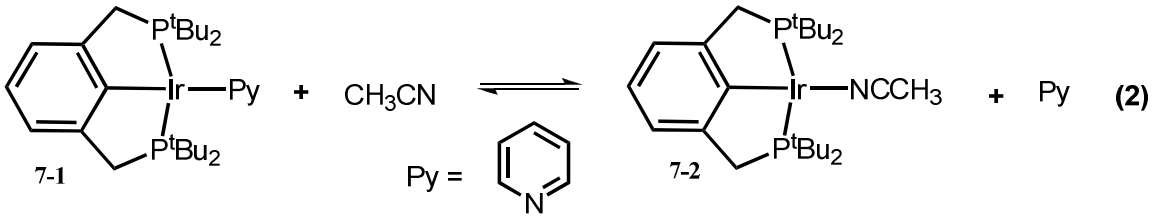

To find an anchor point to calibrate these extensive sets of relative thermodynamic data of various (PCP)IrL complexes, the displacement of pyridine by acetonitrile was investigated with varying concentrations of both pyridine and acetonitrile (eq. 2). Displacement of pyridine by acetonitrile in (eq. 2) can follow either a dissociative or an associative pathway. The dissociative reaction mechanism for this reaction is shown in Scheme **7-1**.

The results of displacement of pyridine by acetonitrile with varying concentration of both pyridine and acetonitrile are summarized in Figure 7-1. In the graph, the dots are experimental data and the lines are fitted data from the Gepasi software program. In the Gepasi fitting for these three sets of experimental data, the same listed rate constants (Figure 7-1) are used, following a dissociative mechanism. In the three graphs, the experimental data nicely fit with the gepasi-predicted data using a dissociative mechanism. The closeness of the fit indicates that this reaction follows only a dissociative mechanism (Figure 7-1).

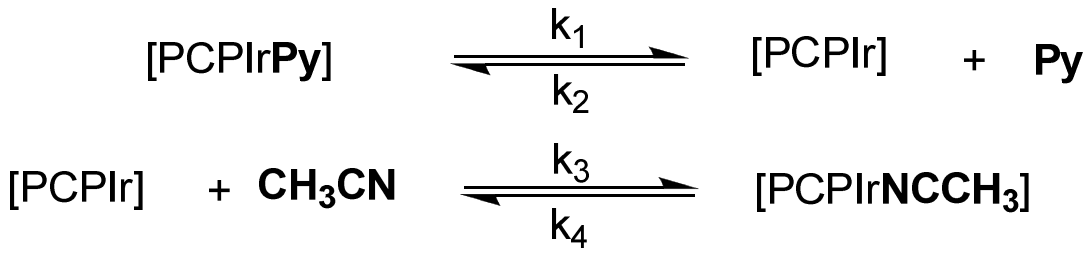

Scheme 7-1 Dissociative pathway for the displacement of pyridine by acetonitrile

From Gepasi fitting using a dissociative mechanism

k_1 = 0.11/ min
k_2 = 13750/ min
k_3 = 5000/ min
k_4 = 0.0072/ min

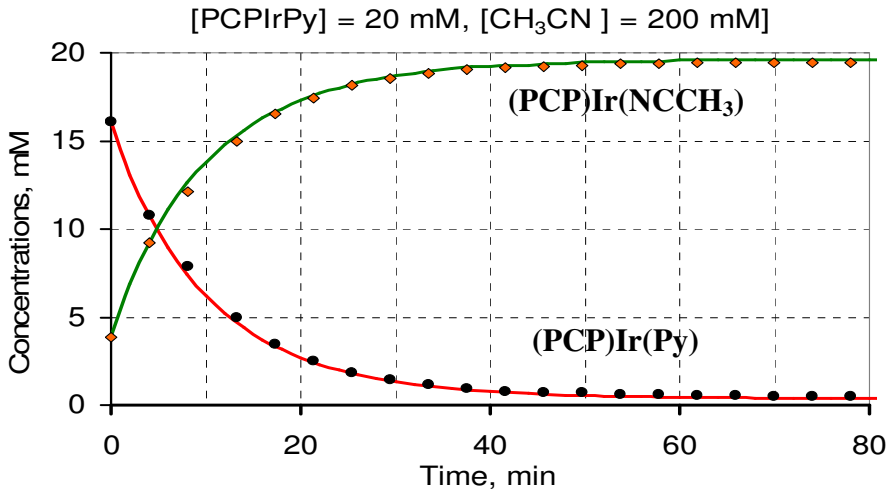

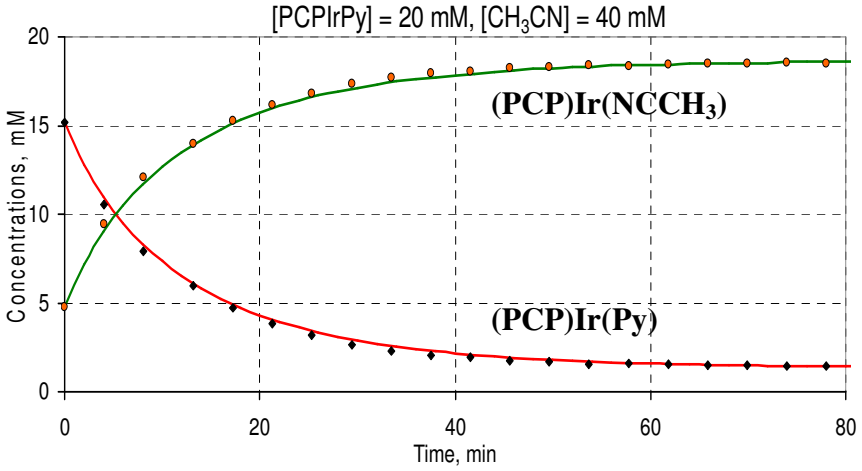

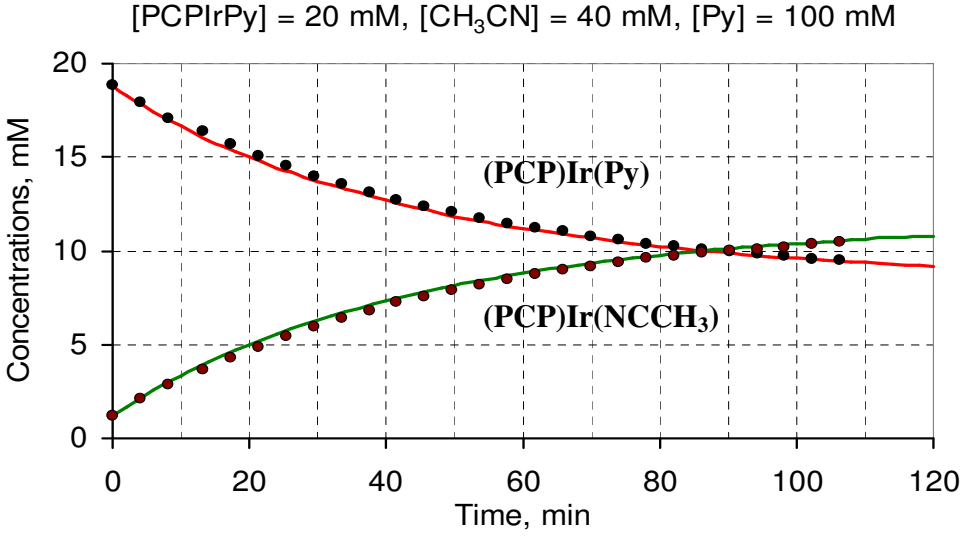

$k_1 = 0.11/$ min, $k_2 = 13750/$ min, $k_3 = 5000/$ min and $k_4 = 0.0072/$ min

Figure 7-1 Experimental and Gepasi fitting data for the displacement of pyridine

Since the displacement of pyridine by acetonitrile from (PCP)Ir(Py) followed a dissociative pathway, $\Delta H^{\neq}$ and $\Delta S^{\neq}$ were measured for k_1 using the Eyring equation (Fig 7-2). In this reaction, $\Delta H^{\neq}$ = 24.9 (1) kcal mol^{-1} and $\Delta S^{\neq}$ = 12.1 (4) cal mol^{-1} K^{-1} were measured.

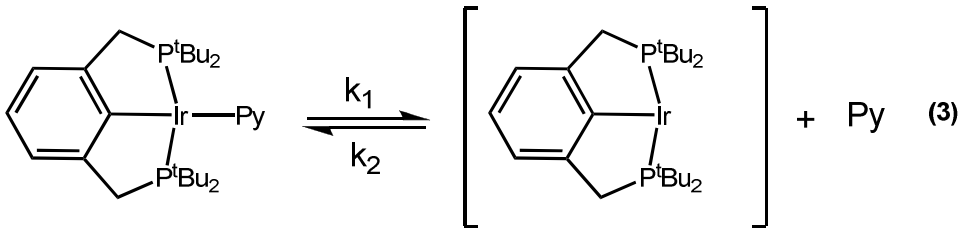

[(PCP)Ir-Py] = 20 mM, [Py] = 80 mM, [CH_3CN] = 200 mM

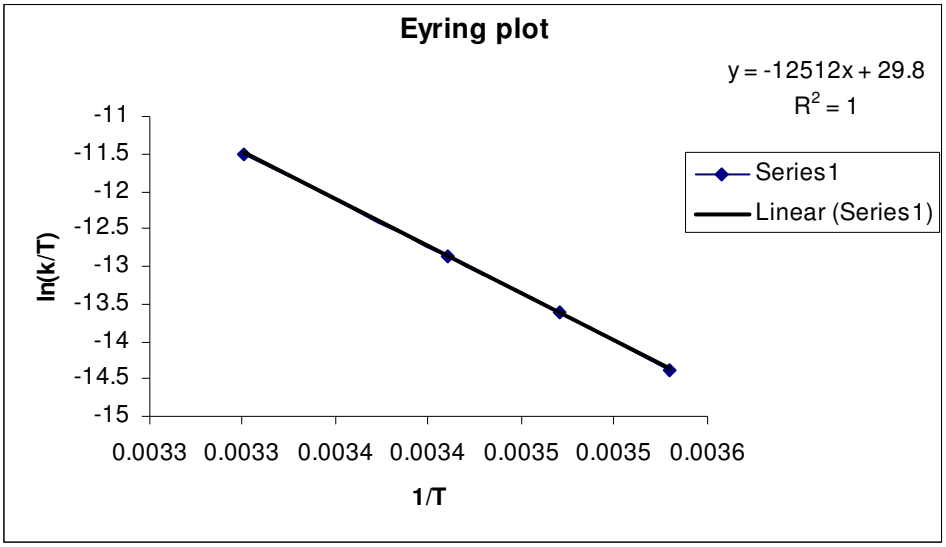

T (K)	k_1 ($M^{-1}s^{-1}$)
303	0.00308203
293	0.00076552
288	0.0003519
283	0.0001619

$\Delta H^{\neq}$ = 24.9 (1) kcal mol^{-1}, $\Delta S^{\neq}$ = 12.1 (4) cal mol^{-1} K^{-1}

Figure 7-2 Eyring plot for the displacement of pyridine

When heated, bound 1-octene in (PCP)Ir(1-octene) (**7-3**) was exchanged with free 1-octene in the solution and was detected by ^{1}H NMR spectroscopy (eq. 4). From the broadening of the C^1-H peak of bound 1-octene with increasing temperature in the ^{1}H NMR spectrum and from the gNMR-stimulated spectra, $\Delta H^{\neq}$ and $\Delta S^{\neq}$ were measured using the Eyring equation (Figure 7-3). In this exchange reaction, $\Delta H^{\neq}$ = 23.1 (5) kcal mol^{-1}, $\Delta S^{\neq}$ = 19 (1) cal mol^{-1} K^{-1} were measured.

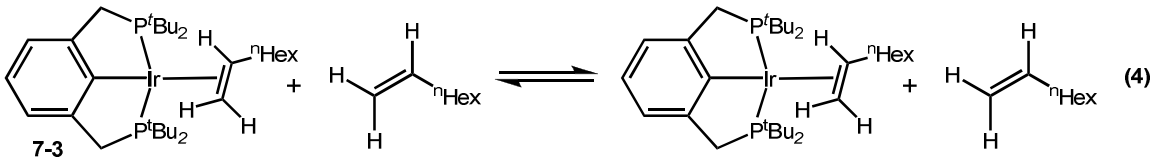

(4)

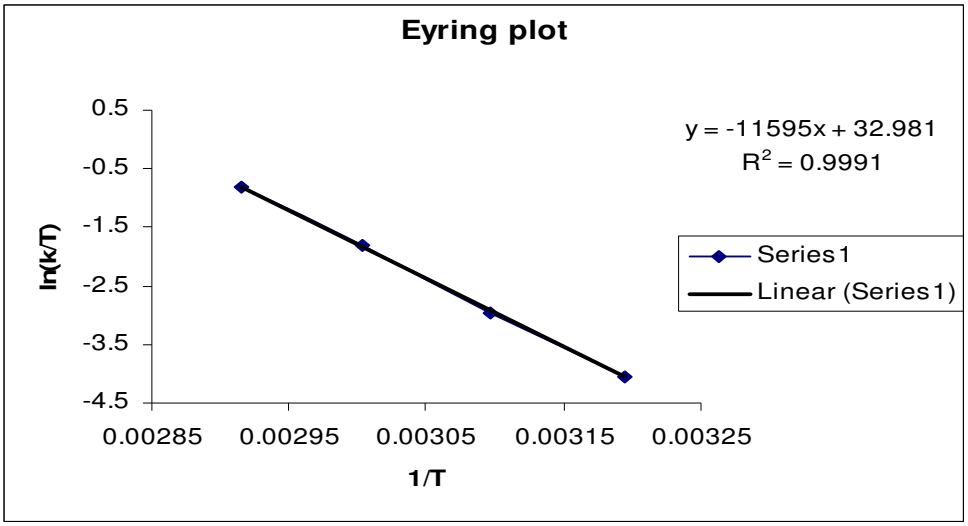

T (K)	k (s^{-1})
343	150
333	55
323	16.5
313	5.5

$\Delta H^{\neq}$ = 23.1 (5) kcal mol^{-1}, $\Delta S^{\neq}$ = 19 (1) cal mol^{-1} K^{-1}

Figure 7-3 Eyring plot for broadening of bound 1-octene (C^1-H) ^{1}H-NMR peak

Relative ΔG values of different ligands in 4-coordinate (PCP)IrL are measured by equilibrium measurements (eq. 1), and the results are summarized in Table 7.1. In Table 7.2, the relative ΔG values of these ligands with respect to pyridine are listed. Among these ligands, $P(OEt)_3$ is the strongest and norbornene (NBE) is the weakest ligand to bind "(PCP)Ir". From the Eyring plot of the displacement of pyridine from (PCP)Ir(Py), $\Delta H^{\neq}$ for this reaction was calculated. Assuming $\Delta\Delta S = 0$, the "absolute" ΔH value (24.9 kcal mol^{-1}) in (PCP)Ir(Py) was predicted. Using the relative ΔG values of other ligands with respect to pyridine, the "absolute" ΔH for other ligands were predicted. In Table 7.4, the experimentally-calculated "absolute" ΔH value is compared with theoretically-calculated ΔH value using PBE and B3LYP functionals. The PBE functional was found to produce results in better agreement with experiment as compared to the B3LYP functional.

Table7.1 Equilibrium constant and equilibrium ΔG at 298 K of different ligands

(PCP)Ir(L)	K	Equilibrium ΔG kcal mol^{-1}
1-hexene/NBE	11828	-5.6
1-hexene/COE	7454	-5.3
1-hexene/t-2-hex	1949	-4.5
Py/1-hexene	1534	-4.3
Py/DBT	189	-3.1
$PhNH_2$/Ph-H	98	-2.7
DBT/$PhNH_2$	134	-2.9
PEt_3/Py	7	-1.1
CH_3CN/Py	35	-2.1
Ethylene/CH_3CN	18	-1.7
PMe_3/PEt_3	438	-3.6
PPh_2OMe/ PMe_3	49	-2.3
$PMe(OEt)_2$/ $PPh(OEt)_2$	13	-1.5
$P(OEt)_3$/ $PMe(OEt)_2$	7	-1.1
$P(OEt)_3$/ $PPh(OEt)_2$	81	-2.6

Table7.2 Relative ΔG of different ligands in (PCP)Ir(L) with respect to pyridine

Ligands	Relative ΔG kcal mol^{-1}
NBE	9.9
COE	9.6
trans-2-hexene	8.8
Ph-H	8.7
PhNH-H	6.0
1-hexene	4.3
Dibenzothiophene	3.1
Pyridine	0.0
PEt_3	-1.0
CH_3CN	-2.1
Ethylene	-3.8
PMe_3	-4.6
PPh_2OMe	-6.9
$PPh(OEt)_2$	-7.9
$PMe(OEt)_2$	-9.4
$P(OEt)_3$	-10.4

Table7.3 Electronic parameter[8] and cone angle[8] of phosphorous ligand for addition to "(PCP)Ir"

(PCP)Ir(L)	Electronic parameter ν (cm^{-1})	Cone Angle θ (°)
PEt_3	2061.7	132
PMe_3	2064.1	118
PPh_2OMe	2072.2	132
$PPh(OEt)_2$	2074.2	116
$PMe(OEt)_2$	2072.3	107
$P(OEt)_3$	2076.3	109

Table7.4 Experimental and Computational equilibrium study in (PCP)Ir(L)[7]

Ligands	Experimental		PBE		B3LYP	
	"Absolute"ΔH (assuming ΔΔS = 0)	ΔG_{rel}	ΔH_{abs}	ΔH_{rel}	ΔH_{abs}	ΔH_{rel}
NBE	-15.0	9.9	-10.0	11.8	-1.0	-15.5
COE	-15.3	9.6	-12.2	9.6		
trans-2-hexene	-16.1	8.8	-14.1	7.7		
Ph-H	-16.2	8.7	-16.9	4.0	-10.8	5.7
$PhNH_2$	-18.9	6.0	-18.5	2.4	-15.3	1.2
1-hexene	-20.6	4.3	-17.6	4.6	-11.9	7.3
Dibenzothiophene	-21.8	3.1	-18.4	3.3	-11.4	5.1
Pyridine	-24.9	0.0	-21.8	0.0	-16.5	0.0
PEt_3	-25.9	-1.0	-24.8	1.3	-7.9	13.8
CH_3CN	-27.1	-2.1	-28.7	-6.8	-23.1	-8.8
Ethylene	-28.7	-3.8	-28.1	-3.1	-20.1	0.8
PMe_3	-29.5	-4.6	-29.6	-5.8	-13.7	5.4
PPh_2OMe	-31.8	-6.9	-29.7	-7.9		
$PMe(OEt)_2$	-34.3	-9.4	-34.7	-12.9		
$P(OEt)_3$	-35.3	-10.4	-39.3	-17.7	-31.5	-15.1

7.2.2 Equilibrium studies with 6-coordinate (PCP)Ir(H)(H)L

The equilibrium constant and energies for 6-coordinate (PCP)Ir(H)(H)L with a broad range of ligands (L) with widely varying steric and electronic properties were measured (eq. 5). When phosphorous-based ligands (phosphine, phosphinite, phosphonite, and phosphate) reacted with (PCP)IrH_4, complex **7-4** was formed immediately at room temperature, in which the two hydrides are *cis* to each other. Complex **7-4** isomerized at room temperature to form the thermodynamically more stable complex **7-5**, in which the two hydrides are *trans* to each other. Complex **7-4** was characterized by NMR spectroscopy, while complex **7-5** (L = $PPhOEt_2$) was characterized by both NMR spectroscopy and X-ray crystallography.

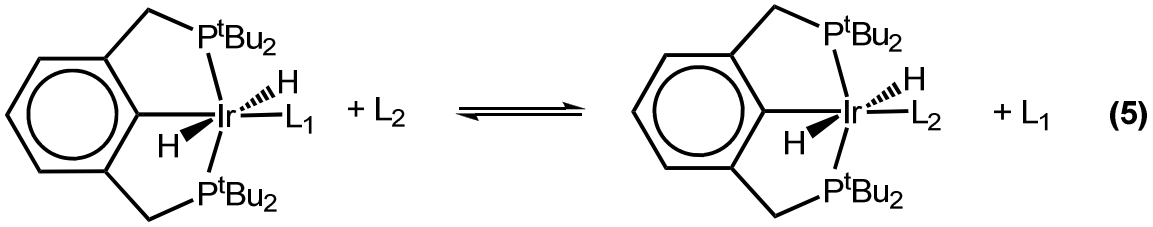

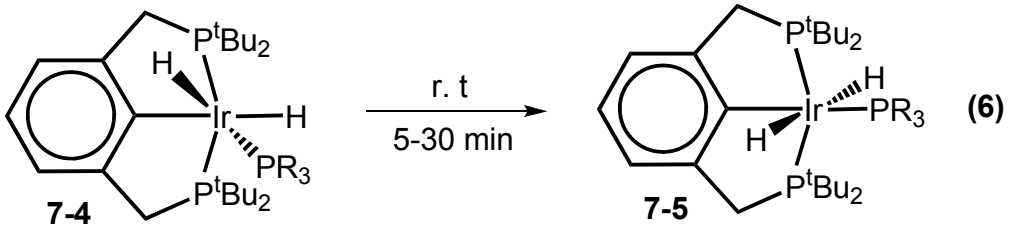

(PCP)IrH_4 reacted partially with PPh_3 at room temperature to form (PCP)Ir(H_2)(PPh_3). This reaction reached equilibrium after heating the solution at 100 °C for 10 days, and we were able to measure the equilibrium constant and ΔG (eq. 7).

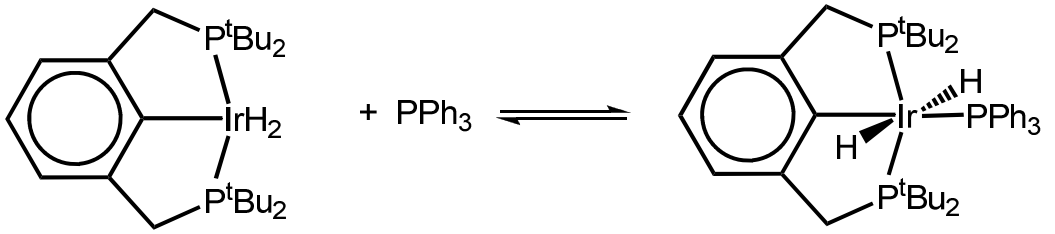

(7)

The equilibrium ΔG value of different ligands was measured by an equilibrium study and listed in Table 7.5. Using the ΔG value of (PCP)Ir(H_2)(PPh_3) and the relative equilibrium ΔG values of other ligands, the "absolute" ΔG values for other ligands in (PCP)Ir(H_2)L are predicted, which is listed in Table 7.6.

Table7.5 Equilibrium constant and equilibrium ΔG of different ligands at 298 K in (PCP)Ir(H_2)L

(PCP)Ir(H_2)L	Equilibrium constant	Equilibrium ΔG kcal mol^{-1}
PPh_3/(PCP)IrH_2	1.1	-0.1
CH_3CN/PPh_3	27.9	-2.0
$PPh(OEt)_2$/$PMe(OEt)_2$	2.5	-0.6
$P(OEt)_3$/$PMe(OEt)_2$	1.0	-0.03
PMe_3/PPh_2OMe	4.3	-0.9
$PPh(OEt)_2$/PPh_2OMe	4137	-5.0
PEt_3/Py	69.4	-2.5
Py/DBT	726	-4.0
DBT/PPh_3	5.6	-1.0
PPh_2OMe/PMe_2Ph	6.5	-1.1
$PMe(OEt)_2$/ PMe_3	409	-3.6
PMe_3/PMe_2Ph	24.8	-1.9
$P(Me)_2Ph$/PEt_3	43.3	-2.2

Table7.6 "Absolute" ΔG for addition of L to (PCP)Ir(H_2)

PCPIr(H_2)L	ΔG kcal mol^{-1}
PPh_3	-0.1
DBT	-1.1
CH_3CN	-2.1
Py	-5.0
PEt_3	-7.5
PMe_2Ph	-9.7
PPh_2OMe	-10.8
PMe_3	-11.7
$PMe(OEt)_2$	-15.2
$P(OEt)_3$	-15.3
$PPh(OEt)_2$	-15.7

Table7.7 Experimental ΔG, electronic parameter[8] and cone angle[8] of phosphorous ligand for addition to (PCP)Ir(H_2)

PCPIr(H_2)L	Exp. ΔG kcal mol^{-1}	Electronic parameter ν (cm^{-1})	Cone Angle θ (°)
PPh_3	-0.1	2068.9	145
PEt_3	-7.5	2061.7	132
PMe_2Ph	-9.7	2065.3	122
PPh_2OMe	-10.8	2072.2	132
PMe_3	-11.7	2064.1	118
$PMe(OEt)_2$	-15.2	2072.3	107
$P(OEt)_3$	-15.3	2076.3	109
$PPh(OEt)_2$	-15.7	2074.2	116

In the cases of PEt_3 and PPh_2OMe (Table 7.7), the cone angles are the same (θ = 132 °), but the experimental ΔG values to bind (PCP)Ir(H_2) favours PPh_2OMe over PEt_3 by 3.3 kcal/mol. This is due to the difference in electronic properties; PEt_3 is more electron-donating than PPh_2OMe as calculated by Tolman.[8] In the cases of PEt_3 and PMe_2Ph, PEt_3 is slightly more electron donating than PMe_2Ph, but the steric crowding in PEt_3 is much larger than PMe_2Ph (difference in cone angle is 10 °). As a result, PMe_2Ph bind stronger than PEt_3 (Table 7.7). In total, Table 7.7 indicates that the binding of a ligand to (PCP)Ir(H_2) is controlled by both electronic and steric effects.

7.2.3 Equilibrium studies with 6-coordinate (PCP)Ir(H)(Cl)(L)

The equilibrium constant and energies were measured for 6-coordinate (PCP)Ir(H)(Cl)(L) bearing a variety of ligands (L) with varying steric and electronic properties (eq. 8). When phosphorous-based ligands (phosphine, phosphinite, phosphonite, and phosphate) reacted with (PCP)Ir(H)(Cl), at room temperature complex **7-6** was formed immediately, in which the two hydrides are *cis* to each other. Complex **7-6** isomerized at room temperature to form the thermodynamically more stable complex **7-7**, in which the two hydrides are *trans* to each other. Complex **7-6** was characterized by NMR spectroscopy, while complex **7-7** (R = Me) was characterized by both NMR spectroscopy and X-ray crystallography.

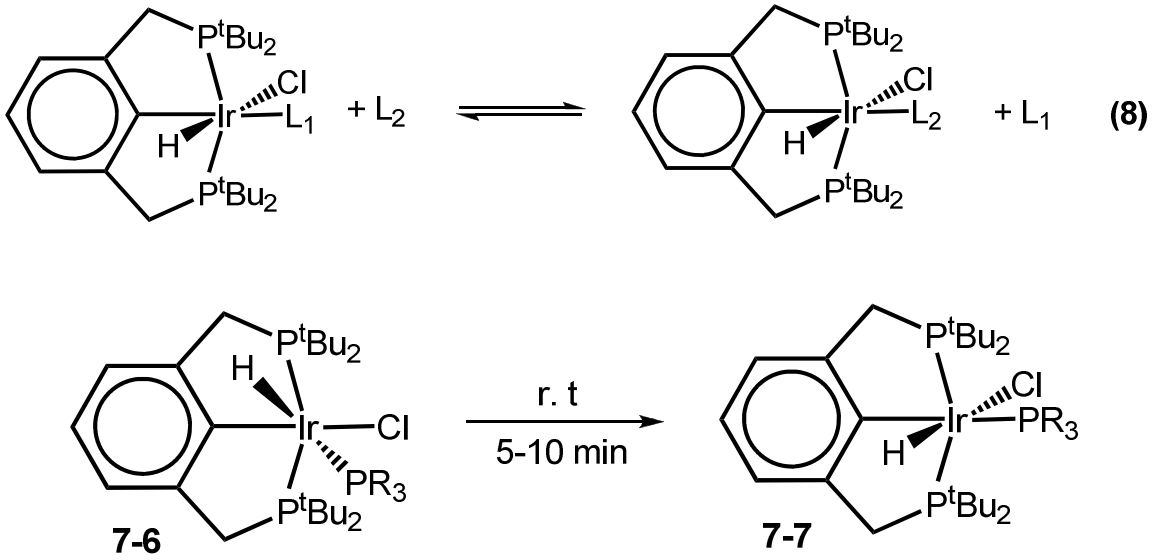

(PCP)Ir(H)(Cl) reacted partially with PEt_3 at room temperature to form (PCP)Ir(H)(Cl)(PEt_3). The reaction reached equilibrium after heating at 45 °C for 8 days and the equilibrium constant and ΔG were measured (eq. 9).

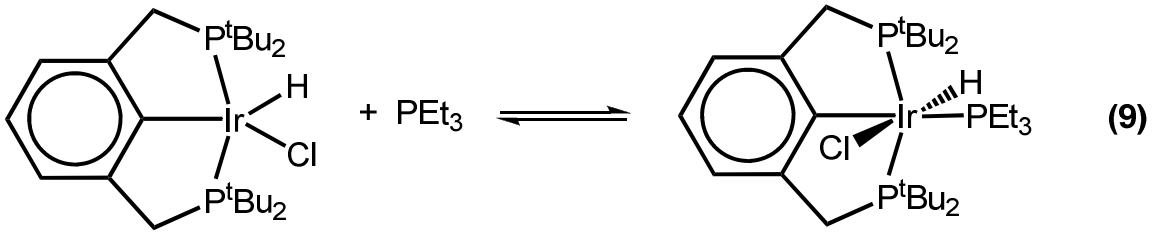

The equilibrium ΔG values of different ligands in (PCP)Ir(H)(Cl)(L) were measured by an equilibrium study and are listed in Table 7.8. Using the ΔG value of (PCP)Ir(H)(Cl)(PEt_3) and equilibrium ΔG values of other ligands, the "absolute" ΔG values for other ligands were predicted, as listed in Table 7.9.

Table7.8 Equilibrium constant and equilibrium ΔG of different ligand at 298 K in (PCP)Ir(H)(Cl)L

(PCP)Ir(H)(Cl)(L)	Equilibrium constant	Equilibrium ΔG kcal mol^{-1}
PEt_3/(PCP)Ir(H)(Cl)	1.3	-0.2
$PMe(OEt)_2$/$P(OEt)_3$	4.0	-0.8
$PMe(OEt)_2$/$PPh(OEt)_2$	21.0	-2.0
PPh_2OMe/PEt_3	246	-3.3
$P(OEt)_3$/$PPh(OEt)_2$	5.3	-1.0
$PPh(OEt)_2$/PMe_3	108	-2.8
PPh_2OMe/Py	1.7	-0.3
PMe_3/ $P(Me)_2Ph$	20.6	-1.8
$P(Me)_2Ph$ / PPh_2OMe	2.4	-0.5

Table7.9 "Absolute" ΔG for addition of L to (PCP)Ir(H)(Cl)

(PCP)Ir(H)(Cl)(L)	ΔG kcal mol^{-1}
PEt_3	-0.6
PPh_2OMe	-3.4
Py	-3.7
$P(Me)_2Ph$	-4.2
PMe_3	-6.0
$PPh(OEt)_2$	-8.8
$P(OEt)_3$	-9.8
$PMe(OEt)_2$	-10.6

Table7.10 Experimental ΔG, electronic parameter[8] and cone angle[8] of phosphorous ligand for addition to (PCP)Ir(H)(Cl)

(PCP)Ir(H)(Cl)(L)	Exp. ΔG kcal mol^{-1}	Electronic parameter ν (cm^{-1})	Cone Angle θ (°)
PEt_3	-0.6	2061.7	132
PPh_2OMe	-3.4	2072.2	132
$P(Me)_2Ph$	-4.2	2065.3	122
PMe_3	-6.0	2064.1	118
$PPh(OEt)_2$	-8.8	2074.2	116
$P(OEt)_3$	-9.8	2076.3	109
$PMe(OEt)_2$	-10.6	2072.3	107

From Table 7.10, the addition of ligand to (PCP)Ir(H)(Cl) is predicted to be controlled by both the electronic and the steric parameter of the incoming ligand. However, in overall binding, the steric parameter of the ligand plays a more dominent role than the electronic parameter. This is due to the presence of the large Cl atom in (PCP)Ir(H)(Cl).

7.3 Conclusion

The relative thermodynamics of a broad range of (PCP)Ir complexes with widely varying steric and electronic effects have been determined by equilibrium measurements and DFT calculations. In an attempt to find an anchor point to calibrate the extensive sets of relative thermodynamic data for (PCP)IrL, the displacement of pyridine by acetonitrile was investigated. This reaction appears to be an unusual example of a dissociative

substitution in a d^8 square planar complex. In all of the equilibrium studies with (PCP)IrL, (PCP)Ir(H)(H)L, or PCP)Ir(H)(Cl)L, the steric and the electronic effects of the ligand (L) play major roles. In PCP)Ir(H)(Cl)L, the steric effect of the ligand dominates over the electronic effect due to the large Cl atom.

7.4 Experimental

General Methods. All reactions were carried out under an argon atmosphere using standard Schlenk techniques or in an argon-filled dry box. Phosphine, phosphonite, phosphinite, dibenzothiophene and pyridine were purchased from Aldrich or VWR. *p*-Xylene-d_{10}, TBE, 1-hexene, 1-octene, *t*-2-hexene, cyclooctene and C_6D_6 were dried using Na/K alloy and collected by vacuum transfer. NBE was sublimed before use. 400 MHz or 500 MHz Varian instruments were used for ^1H, ^{13}C and ^{31}P NMR spectroscopy. (^{tBu4}PCP)Ir(H)(Cl) and (^{tBu4}PCP)IrH_4 were synthesized according to literature procedures.[9] The residual peak of the deuterated solvent was used as a reference for ^1H chemical shifts. ^{31}P NMR chemical shifts were referenced to a capillary PMe_3 standard (–62.2 ppm).

(^{tBu4}PCP)Ir(PMe$_3$): To a 0.5 mL *p*-xylene-d$_{10}$ solution of 5 mg (^{tBu4}PCP)IrH$_4$ (8.3 μmol) in a J-Young tube, 2.4 mg NBE (25 μmol) was added. After 3 h at room temperature, 0.85 μL PMe$_3$ (8.3 μmol) was added, and (^{tBu4}PCP)Ir(PMe$_3$) was formed in 98% yield as measured by ^{31}P{^{1}H} NMR spectroscopy. ^{31}P{^{1}H} NMR (*p*-xylene-d$_{10}$, 162 MHz): δ 68.88 (d, J_{PP} = 16.7 Hz, PCP), -46.48 (t, J_{PP} = 16.7 Hz, Ir(PMe$_3$)). ^{1}H NMR (*p*-xylene-d$_{10}$, 400 MHz): δ 7.13 (d, J_{HH} = 7.2 Hz, 2H, Ar), 7.05 (t, J_{HH} = 7.2 Hz, 1H, Ar), 3.24 (t, J_{PH} = 3.6 Hz, 4H, CH$_2$P^{t}Bu$_2$), 1.63 (d, J_{PH} = 6.0 Hz, 9H, Ir(P***Me***$_3$)), 1.20 (t, J_{PH} = 6.0 Hz, 36H, P^{t}Bu$_2$).

(^{tBu4}PCP)Ir(PEt$_3$): To a 0.5 mL *p*-xylene-d$_{10}$ solution of 5 mg (^{tBu4}PCP)IrH$_4$ (8.3 μmol) in a J-Young tube, 2.4 mg NBE (25 μmol) was added. After 3 h at room temperature, 1.3 μL PEt$_3$ (8.3 μmol) was added, and (^{tBu4}PCP)Ir(PEt$_3$) was formed in 98% yield as measured by ^{31}P{^{1}H} NMR spectroscopy. ^{31}P{^{1}H} NMR (*p*-xylene-d$_{10}$, 162 MHz): δ 66.74 (d, J_{PP} = 14.4 Hz, PCP), -6.09 (t, J_{PP} = 14.6 Hz, Ir(PEt$_3$)). ^{1}H NMR (*p*-xylene-d$_{10}$, 400 MHz): δ 7.14 (d, J_{HH} = 7.2 Hz, 2H, Ar), 7.08 (t, J_{HH} = 7.2 Hz, 1H, Ar), 3.27 (t, J_{PH} = 3.4 Hz, 4H, CH$_2$P^{t}Bu$_2$), 1.99 (qd, J_{HH} = 7.6 Hz, J_{PH} = 5.6 Hz, 6H, P(***CH$_2$***CH$_3$)$_3$), 1.22 (t, J_{PH} = 5.8 Hz, 36H, P^{t}Bu$_2$), 1.03 (dt, J_{PH} = 15.2 Hz, J_{HH} = 7.6 Hz, 9H, P(CH$_2$***CH$_3$***)$_3$).

Reaction of (^{tBu4}PCP)Ir(NBE) with P(^{i}Pr)$_3$: To a 0.5 mL *p*-xylene-d$_{10}$ solution of 5 mg (^{tBu4}PCP)IrH$_4$ (8.3 μmol) in a J-Young tube, 2.4 mg NBE (25 μmol) was added. After 3 h at room temperature, 1.5 μL P(^{i}Pr)$_3$ (8.3 μmol) was added. No (^{tBu4}PCP)Ir(P^{i}Pr$_3$) was formed, even after 5 days at room temperature. Only (^{tBu4}PCP)Ir(NBE) was present in the

solution.

(^{tBu4}PCP)Ir(P(OEt)$_3$): To a 0.5 mL *p*-xylene-d_{10} solution of 5 mg (^{tBu4}PCP)IrH_4 (8.3 μmol) in a J-Young tube, 2.4 mg NBE (25 μmol) was added. After 3 h at room temperature, 1.4 μL P(OEt)$_3$ (8.3 μmol) was added, and (^{tBu4}PCP)Ir(P(OEt)$_3$) was formed in 99% yield as measured by $^{31}P\{^1H\}$ NMR spectroscopy. $^{31}P\{^1H\}$ NMR (*p*-xylene-d_{10}, 162 MHz): δ 145.08 (t, J_{PP} = 23.2 Hz, Ir(P(OEt)$_3$)), 72.23 (d, J_{PP} = 23.2 Hz, PCP).)). ^1H NMR (*p*-xylene-d_{10}, 400 MHz): δ 7.16 (d, J_{HH} = 6.6 Hz, 2H, Ar), 7.06 (t, J_{HH} = 7.2 Hz, 1H, Ar), 3.98 (qd, J_{HH} = 7.1 Hz, J_{PH} = 5.8 Hz, 6H, P(O***CH$_2$***CH$_3$)$_3$)), 3.35 (t, J_{PH} = 3.2 Hz, 4H, $CH_2P^tBu_2$), 1.29 (t, J_{PH} = 6.1 Hz, 36H, P^tBu_2), 1.2 (t, J_{HH} = 7.1 Hz, 9H, P(OCH$_2$***CH$_3$***)$_3$).

(^{tBu4}PCP)Ir(PMe(OEt)$_2$): To a 0.5 mL *p*-xylene-d_{10} solution of 5 mg (^{tBu4}PCP)IrH_4 (8.3 μmol) in a J-Young tube, 2.4 mg NBE (25 μmol) was added. After 3 h at room temperature, 1.2 μL PMe(OEt)$_2$ (8.3 μmol) was added, and (^{tBu4}PCP)Ir(PMe(OEt)$_2$) was formed in 99% yield as measured by $^{31}P\{^1H\}$ NMR spectroscopy. $^{31}P\{^1H\}$ NMR (*p*-xylene-d_{10}, 162 MHz): δ160.77 (t, J_{PH} = 19.3 Hz, Ir(PMe(OEt)$_2$)), 72.04 (d, J_{PH} = 19.1 Hz, PCP). ^1H NMR (*p*-xylene-d_{10}, 400 MHz): δ 7.16 (d, J_{HH} = 6.8 Hz, 2H, Ar), 7.06 (t, J_{HH} = 7.6 Hz, 1H, Ar), 3.96 (m, 2H, PMe(O***CH$_2$***CH$_3$)$_2$), 3.72 (m, PMe(O***CH$_2$***CH$_3$)$_2$), 3.33 (t, J_{PH} = 3.2 Hz, 4H, $CH_2P^tBu_2$), 1.26 (t, J_{PH} = 6.0 Hz, 36H, P^tBu_2), 1.18 (t, J_{PH} = 7.1 Hz, 6H, PMe(OCH$_2$***CH$_3$***)$_2$).

(^{tBu4}PCP)Ir(Py): To a 0.5 mL *p*-xylene-d_{10} solution of 5 mg (^{tBu4}PCP)IrH_4 (8.3 μmol) in a J-Young tube, 2.4 mg NBE (25 μmol) was added. After 3 h at room temperature, 0.7 μL Py (8.3 μmol) was added, and (^{tBu4}PCP)Ir(Py) was formed in 99% yield as measured by $^{31}P\{^1H\}$ NMR spectroscopy. $^{31}P\{^1H\}$ NMR (C_6D_6, 162 MHz): δ 67.77 (s, PCP). ^1H NMR (C_6D_6, 400 MHz): δ 9.29 (d, J_{HH} = 5.2 Hz, 2H, Py), 7.25 (d, J_{HH} = 7.8 Hz, 2H, Ar), 7.19 (t, J_{HH} = 7.1 Hz, 1H, Ar), 6.65 (t, J_{HH} = 7.5 Hz, 1H, Py), 6.33 (m, 2H, Py), 2.99 (t, J_{PH} = 3.5 Hz, 4H, $CH_2P^tBu_2$), 1.15 (t, J_{PH} = 5.9 Hz, 36H, P^tBu_2). ^{13}C NMR (C_6D_6, 100 MHz): δ 160.8 (s, Ar), 157.6 (d, J_{CP} = 6.2 Hz, Ar), 152.2 (t, J_{CP} = 10.8 Hz, Ar), 132.1 (s, Ar), 124.3 (d, J_{CP} = 12Hz, Ar), 120.0 (m, Ar), 38.8 (vt, J_{CP} = 13.5 Hz, ***C***H_2P), 36.9 (vt, J_{CP} = 8.6 Hz, P***C***$(CH_3)_3$), 30.5 (vt, J_{CP} = 2.3 Hz, PC(***C***$H_3)_3$).

(^{tBu4}PCP)Ir($NCCH_3$): To a 0.5 mL *p*-xylene-d_{10} solution of 5 mg (^{tBu4}PCP)IrH_4 (8.3 μmol) in a J-Young tube, 2.4 mg NBE (25 μmol) was added. After 3 h at room temperature, 0.41 μL CH_3CN (8.3 μmol) was added, and (^{tBu4}PCP)Ir($NCCH_3$) was formed in 99% yield as measured by $^{31}P\{^1H\}$ NMR spectroscopy. $^{31}P\{^1H\}$ NMR (C_6D_6, 162 MHz): δ 69.1 (s, PCP). ^1H NMR (C_6D_6, 400 MHz): δ 7.25 (d, J_{HH} = 7.2 Hz, 2H, Ar), 7.13 (t, J_{HH} = 6.8 Hz, 1H, Ar), 3.16 (t, J_{PH} = 3.6 Hz, 4H, $CH_2P^tBu_2$), 1.40 (t, J_{PH} = 6.0 Hz, 36H, P^tBu_2). 0.93 (s, 3H, Ir($NCCH_3$)). ^{13}C NMR (C_6D_6, 125 MHz): δ 167.2 (t, J_{CP} = 3.0 Hz, Ir(N***C***CH_3)), 153.8 (d, J_{CP} = 11.6 Hz, Ar), 122.3 (s, Ar), 120.9 (s, Ar), 120.2 (t, J_{CP} = 8.6 Hz, Ar), 38.1 (vt, J_{CP} = 13.4 Hz, ***C***H_2P), 36.3 (vt, J_{CP} = 9.1 Hz, P***C***$(CH_3)_3$), 30.2 (vt, J_{CP} = 3.1 Hz, PC(***C***$H_3)_3$).

(^{tBu4}PCP)Ir(N_2): To a 0.5 mL *p*-xylene-d_{10} solution of 5 mg (^{tBu4}PCP)IrH_4 (8.3 μmol) in a J-Young tube, 2.4 mg NBE (25 μmol) was added. After 3 h at room temperature, N_2 (1atm) was added, and (^{tBu4}PCP)Ir(N_2) was formed in 99% yield, as measured by $^{31}P\{^1H\}$ NMR spectroscopy. $^{31}P\{^1H\}$ NMR (*p*-xylene-d_{10}, 162 MHz): δ 72.67 (s, PCP). ^1H NMR (*p*-xylene-d_{10}, 400 MHz): δ 6.99 (d, J_{HH} = 7.2 Hz, 2H, Ar), 6.85 (t, J_{HH} = 7.2 Hz, 1H, Ar), 3.10 (t, J_{PH} = 4.0 Hz, 4H, $CH_2P^tBu_2$), 1.24 (t, J_{PH} = 6.4 Hz, 36H, P^tBu_2).

(^{tBu4}PCP)Ir(H)(Ph): To a 0.25 mL *p*-xylene-d_{10} solution of 5 mg (^{tBu4}PCP)IrH_4 (8.3 μmol) in a J-Young tube, 2.4 mg NBE (25 μmol) was added. After 3 h at room temperature, 0.25 mL C_6H_6 was added, and (^{tBu4}PCP)Ir(H)(Ph) was formed in 94% yield as measured by $^{31}P\{^1H\}$ NMR spectroscopy. $^{31}P\{^1H\}$ NMR (*p*-xylene-d_{10}, 162 MHz): δ 67.6 (bs, PCP). ^1H NMR (*p*-xylene-d_{10}, 400 MHz): δ 3.39 (bs, 4H, $CH_2P^tBu_2$), 1.01 (bt, J_{PH} = 6.5 Hz, 36H, P^tBu_2), -45.5 (vbs, 1H, Ir-***H***).

(^{tBu4}PCP)Ir(H)(NHPh): To a 0.5 mL *p*-xylene-d_{10} solution of 5 mg (^{tBu4}PCP)IrH_4 (8.3 μmol) in a J-Young tube, 2.4 mg NBE (25 μmol) was added. After 3 h at room temperature, 0.76 μL aniline (8.3 μmol) was added, and (^{tBu4}PCP)Ir(H)(NHPh) was formed in 95% yield as measured by $^{31}P\{^1H\}$ NMR spectroscopy. $^{31}P\{^1H\}$ NMR (*p*-xylene-d_{10}, 162 MHz): δ 66.8 (s, PCP). ^1H NMR (*p*-xylene-d_{10}, 400 MHz): δ 7.10 (t, J_{HH} = 7.4 Hz, 2H, Ar), 6.9 (m, obscured by solvent, 3H, PCP), 6.75 (d, J_{HH} = 7.4 Hz, 2H, Ar), 6.56 (t, J_{HH} = 7.4 Hz, 1H, Ar), 4.85 (bs, 1H, N***H***Ph), 3.10 (d of vt, J_{PH} = 3.3 Hz, J_{HH} = 17.3 Hz, 2H, $CH_2P^tBu_2$), 2.98 (d of vt, J_{PH} = 3.3 Hz, J_{HH} = 17.2 Hz, 2H, $CH_2P^tBu_2$), 1.14

(vt, J_{PH} = 6.3 Hz, 18H, P^{t}Bu$_2$), 1.09 (vt, J_{PH} = 6.3 Hz, 18H, P^{t}Bu$_2$), -38.3 (t, J_{PH} = 12.9 Hz, 1H, Ir-***H***).

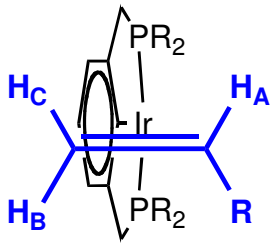

(^{tBu4}PCP)Ir(1-hexene). To 0.5 mL of a *p*-xylene-d$_{10}$ solution of (^{tBu4}PCP)IrH$_4$ (5 mg, 8.3 µmol) in a J-Young tube, 1-hexene (4.1 µL, 33.2 µmol) was added at room temperature. After 30 min solvent was removed in vacuum and the compound was characterized by NMR spectroscopy. ^{31}P{^{1}H} NMR (*p*-xylene-d_{10}, 202 MHz): δ 59.7 (s, broad, P^{t}Bu$_2$), 57.1 (s, broad, P^{t}Bu$_2$). ^{1}H NMR (*p*-xylene-d_{10}, 500 MHz): δ 7.28 (d, J_{HH} = 8 Hz, 2H, Ar), 7.16 (t, J_{HH} = 5.5 Hz, 1H, Ar), 4.52 (m, 1H, H$_A$, Ir-hexene), 3.78 (dt, J_{HH} = 12 Hz (cis), J_{HH} = 4.5 Hz, 1H, H$_C$, Ir-hexene), 3.33 (broad, 4H, CH$_2$P^{t}Bu$_2$), 2.86 (d, J_{HH} = 7.5 Hz, 1H, H$_B$, Ir-hexene), 2.32 (m, 2H, CH$_2$, Ir-hexene), 1.68 (m, 2H, CH$_2$, Ir-hexene), 1.58 (m, 2H, CH$_2$, Ir-hexene), 1.35 (broad, 18H, P^{t}Bu$_2$), 1.23 (broad, 18H, P^{t}Bu$_2$), 1.09 (t, J_{PH} = 7.2 Hz, 3H, CH$_3$, Ir-hexene).

(^{tBu4}PCP)Ir(Dibenzothiophene): To a 0.5 mL *p*-xylene-d$_{10}$ solution of 5 mg (^{tBu4}PCP)IrH$_4$ (8.3 µmol) in a J-Young tube, 2.4 mg NBE (25 µmol) was added. After 3 h at room temperature, 1.5 mg dibenzothiophene (8.3 µmol) was added, and (^{tBu4}PCP)Ir(DBT) was formed in 98% yield as measured by ^{31}P{^{1}H} NMR spectroscopy. ^{31}P{^{1}H} NMR (*p*-xylene-d_{10}, 202 MHz): δ 66.2 (s, PCP). ^{1}H NMR (*p*-xylene-d_{10}, 500

MHz): δ 8.15 (d, J_{HH} = 8.0 Hz, 2H, Ar), 7.36 (m, 4H, Ar), 7.09 (t, J_{HH} = 7.5 Hz, 2H, Ar), 3.18 (t, J_{PH} = 3.0 Hz, 4H, $CH_2P^tBu_2$), 1.20 (vt, J_{PH} = 6.0 Hz, 36H, P^tBu_2).

(^{tBu4}PCP)Ir(Ethylene): To a 0.5 mL *p*-xylene-d_{10} solution of 5 mg (^{tBu4}PCP)IrH_4 (8.3 μmol) in a J-Young tube, at room temperature, ethylene (1 atmosphere) was added, and (^{tBu4}PCP)Ir(Ethylene) was formed in 99% yield as measured by $^{31}P\{^1H\}$ NMR spectroscopy. $^{31}P\{^1H\}$ NMR (*p*-xylene-d_{10}, 202 MHz): δ 59.3 (s, PCP). ^1H NMR (*p*-xylene-d_{10}, 500 MHz): δ 7.28 (d, J_{HH} = 7.0 Hz, 2H, Ar), 7.17 (t, J_{HH} = 7.3 Hz, 1H, Ar), 3.31 (t, J_{PH} = 3.3 Hz, 4H, $CH_2P^tBu_2$), 3.29 (t, J_{PH} = 3.4 Hz, 4H, Ir(ethylene)), 1.25 (vt, J_{PH} = 6.0 Hz, 36H, P^tBu_2).

Equilibrium measurements in (^{tBu4}PCP)Ir(L):

In typical equilibrium measurements, to a 0.5 mL *p*-xylene-d_{10} solution of 5 mg (^{tBu4}PCP)IrH_4 (8.3 μmol) in a J-Young tube, 2.4 mg NBE (25 μmol) was added. After 3 h at room temperature, 8.3 μmol of two ligand were added. The solution was then heated for 7 days at 70 °C and concentrations were measured by both ^{31}P and ^1H NMR spectroscopy. In case of PMe_3, the solution was heated for 10 days at 40 °C and concentrations were measured by both ^{31}P and ^1H NMR spectroscopy.

Equilibrium between (^{tBu4}PCP)Ir(1-hexene) and (^{tBu4}PCP)Ir(COE): To a 0.45 mL *p*-xylene-d_{10} solution of 5 mg (^{tBu4}PCP)IrH_4 (8.3 μmol) in a J-Young tube, 50 μL *cis*-COE (417 μmol) and 0.5 μL 1-hexene (4.2 μmol) was added. After 5 days at room temperature, solution was reached equilibrium and concentration of each compound was

measured by ^{31}P and ^{1}H NMR spectroscopy. In $^{31}P\{^{1}H\}$ NMR sprctrum (^{tBu4}PCP)Ir(COE) appears as broad singlet at 55.1 ppm.

Equilibrium between (^{tBu4}PCP)Ir(1-hexene) and (^{tBu4}PCP)Ir(NBE): To a 0.5 mL *p*-xylene-d_{10} solution of 5 mg (^{tBu4}PCP)IrH_4 (8.3 μmol) in a J-Young tube, 48 mg NBE (500 μmol) and 0.5 μL 1-hexene (4.2 μmol) was added. After 5 days at room temperature, solution was reached equilibrium and concentration of each compound was measured by ^{31}P and ^{1}H NMR spectroscopy. In $^{31}P\{^{1}H\}$ NMR sprctrum (^{tBu4}PCP)Ir(NBE) appears as broad singlet at 62.6 ppm.

Equilibrium between (^{tBu4}PCP)Ir(1-hexene) and (^{tBu4}PCP)Ir(*trans*-2-hexene): To a 0.5 mL *p*-xylene-d_{10} solution of 5 mg (^{tBu4}PCP)IrH_4 (8.3 μmol) in a J-Young tube, 40 μL *trans*-2-hexene (318 μmol) and 1 μL 1-hexene (8.3 μmol) was added. After 5 days at room temperature, solution was reached equilibrium and concentration of each compound was measured by ^{31}P and ^{1}H NMR spectroscopy.

(^{tBu4}PCP)Ir(H_2)(PMe(OEt)$_2$): To a 0.5 mL *p*-xylene-d_{10} solution of 5 mg (^{tBu4}PCP)IrH_4 (8.3 μmol) in a J-Young tube, 1.34 μL $PMe(OEt)_2$ (8.3 μmol) (Alfa Aesar) was added. An immediate color change from dark red to colorless was observed.
(^{tBu4}PCP)Ir(H_2)(PMe(OEt)$_2$) (hydrides are *cis*): $^{31}P\{^{1}H\}$ NMR (*p*-xylene-d_{10}, 202 MHz): δ 136.5 (bt, Ir(H_2)(PMe(OEt)$_2$), 66.0 (d, J_{PP} = 13.4 Hz, PCP). ^{1}H NMR (*p*-xylene-d_{10}, 500 MHz): δ 7.10 (d, J_{PH} = 15.0 Hz, 2H, Ar), 7.05 (m, 1H, Ar-*H*), 3.98 (m, 2H, P(O***CH$_2$***CH_3)), 3.67 (m, 2H, P(O***CH$_2$***CH_3)), 3.54 (broad d of vt, J_{HH} = 16.5 Hz, 2H,

$CH_2P^tBu_2$), 3.46 (d of vt, J_{PH} = 4.0 Hz, J_{HH} = 16.5 Hz, 2H, $CH_2P^tBu_2$), 1.43 (vt, J_{PH} = 6.0 Hz, 18H, P^tBu_2), 1.32 (vt, J_{PH} = 6.0 Hz, 18H, P^tBu_2),), 1.17 (t, J_{HH} = 6.8 Hz, 6H, $P(OCH_2\boldsymbol{CH_3})_2$), 1.16 (d, 3H, P***Me***), -12.75 (dq, J_{PH} = 13 Hz, J_{HH} = 4.5 Hz, 1H, Ir(***H***)(H)($PMeOEt_2$), H is *cis* to $PMeOEt_2$), -13.49 (dtd, J_{PH} = 168.0 Hz, J_{PH} = 20.5 Hz, J_{HH} = 4.5 Hz,1H, Ir(***H***)(H)($PMeOEt_2$), H is *trans* to $PMeOEt_2$).

(^{tBu4}PCP)Ir(H_2)(PMe(OEt)$_2$) (hydrides are *trans*): $^{31}P\{^1H\}$ NMR (*p*-xylene-d_{10}, 202 MHz): δ 133.6 (t, J_{PP} = 18.4 Hz, Ir(H_2)(PMe(OEt)$_2$), 62.2 (d, J_{PP} = 18.4 Hz, PCP). ^1H NMR (*p*-xylene-d_{10}, 500 MHz): 7.09 (m, 2H, Ar), 7.04 (m, 1H, Ar-*H*), 4.01 (m, 2H, $P(O\boldsymbol{CH_2}CH_3)$), 3.64 (m, 2H, $P(O\boldsymbol{CH_2}CH_3)$), 3.45 (vt, J_{PH} = 3.5 Hz, 4H, $CH_2P^tBu_2$), 2.02 (d, J_{PH} = 5.0 Hz, 3H, PMe), 1.37 (vt, J_{PH} = 6.3 Hz, 36H, P^tBu_2), 1.24 (t, J_{HH} = 7.0 Hz, 6H, $P(OCH_2\boldsymbol{CH_3})_2$), -10.98 (q, J_{PH} = 15.0 Hz, 2H, Ir(***H*****$_2$**))($PMeOEt_2$)).

(^{tBu4}PCP)Ir(H_2)((PPh(OEt)$_2$) (hydrides are *cis*): To a 0.5 mL *p*-xylene-d_{10} solution of 5 mg (^{tBu4}PCP)IrH_4 (8.3 μmol) in a J-Young tube, 1.54 μL $PPh(OEt)_2$ (8.3 μmol) (Aldrich) was added. An immediate color change from dark red to colorless was observed. NMR spectrum was recorded immediately. $^{31}P\{^1H\}$ NMR (*p*-xylene-d_{10}, 202 MHz): δ 123.4 (broad, Ir(H_2)($PPh(OEt)_2$), 64.5 (broad d, J_{PP} = 11.5 Hz, PCP). ^1H NMR (*p*-xylene-d_{10}, 500 MHz): -12.71 (m, 1H, Ir(***H***)(H)($PMeOEt_2$), H is *cis* to $PPhOEt_2$), -13.39 (dtd, J_{PH} = 166.5 Hz, J_{PH} = 20.0 Hz, J_{HH} = 4.5 Hz,1H, Ir(H)(***H***)(PR_3, H is *trans* to $PPhOEt_2$).

(^{tBu4}PCP)Ir(H_2)((PPh(OEt)$_2$) (hydrides are *trans*): $^{31}P\{^1H\}$ NMR (*p*-xylene-d_{10}, 202 MHz): δ 129.4 (t, J_{PP} = 18.1 Hz, Ir(H_2)($PPh(OEt)_2$), 60.3 (d, J_{PP} = 18.1 Hz, PCP). ^1H NMR (*p*-xylene-d_{10}, 500 MHz): 8.31 (t, J_{HH} = 8.0 Hz, 2H, Ar), 7.29 (t, J_{HH} = 7.7 Hz, J_{HH} 3H, Ar), 7.18 (m, 2H, Ar), 7.04 (m, 1H, Ar-*H*), 4.07 (m, 2H, $P(O\boldsymbol{CH_2}CH_3)$), 3.59 (m,

2H, P(O***CH₂***CH_3)), 3.48 (vt, J_{PH} = 3.8 Hz, 4H, $CH_2P^tBu_2$), 1.27 (vt, J_{PH} = 6.3 Hz, 36H, P^tBu_2), 1.11 (t, J_{HH} = 7.0 Hz, 6H, P(OCH_2***CH_3***$)_2$), -10.69 (q, J_{PH} = 15.0 Hz, 2H, Ir(***H_2***)(PPhOEt_2)). An X-ray quality crystal was formed from hexane solution. Figure 7-6 shows an ORTEP of (PCP)Ir(H_2)(PPh($OEt)_2$), refinement parameters are given in Table 7.15 and bond angles and bond distances are listed in Table 7.16.

(^{tBu4}PCP)Ir(H_2)((P($OEt)_3$): To a 0.5 mL *p*-xylene-d_{10} solution of 5 mg (^{tBu4}PCP)IrH_4 (8.3 μmol) in a J-Young tube, 1.4 μL P($OEt)_3$ (8.3 μmol) (Aldrich) was added. An immediate color change from dark red to colorless was observed.

(^{tBu4}PCP)Ir(H_2)(P($OEt)_3$)) (hydrides are *cis*) : $^{31}P\{^1H\}$ NMR (*p*-xylene-d_{10}, 202 MHz): δ 111.3 (t, J_{PP} = 15.5 Hz, Ir(H_2)(P($OEt)_3$), 64.2 (d, J_{PP} = 15.5 Hz, PCP). ^1H NMR (*p*-xylene-d_{10}, 500 MHz): 7.08 (d, J_{HH} = 8.0 Hz, 2H, Ar), 6.97 (t, J_{HH} = 7.3 Hz, 1H, Ar), 3.78 (m, 6H, P(O***CH₂***CH_3)), 3.68 (d of vt, J_{PH} = 3.8 Hz, J_{HH} = 15.5 Hz, 2H, $CH_2P^tBu_2$), 3.44 (d of vt, J_{PH} = 4.3 Hz, J_{HH} = 15.5 Hz, 2H, $CH_2P^tBu_2$), 1.44(vt, J_{PH} = 6.5 Hz, 18H, P^tBu_2), 1.32 (vt, J_{PH} = 6.5 Hz, 18H, P^tBu_2), 1.14 (t, J_{HH} = 7.0 Hz, 9H, P(OCH_2***CH_3***$)_2$, -12.84 (dq, J_{PH} = 13.5 Hz, J_{HH} = 4.5 Hz, 1H, Ir(***H***)(H)($POEt_3$), H is *cis* to $POEt_3$), -13.49 (dtd, J_{PH} = 197.3 Hz, J_{PH} = 21.3 Hz, J_{HH} = 4.5 Hz,1H, Ir(***H***)(H)($POEt_3$), H is *trans* to $POEt_3$).

(^{tBu4}PCP)Ir(H_2)(P($OEt)_3$)) (hydrides are *trans*) : $^{31}P\{^1H\}$ NMR (*p*-xylene-d_{10}, 202 MHz): δ 114.1 (t, J_{PP} = 22.4 Hz, Ir(H_2)(P($OEt)_3$), 61.4 (d, J_{PP} = 22.4 Hz, PCP). ^1H NMR (*p*-xylene-d_{10}, 500 MHz): 7.09 (m, 2H, Ar), 7.04 (m, 1H, Ar-*H*), 4.00 (m, 6H, P(O***CH₂***CH_3)), 3.46 (vt, J_{PH} = 3.5 Hz, 4H, $CH_2P^tBu_2$), 1.38 (vt, J_{PH} = 6.3 Hz, 36H,

P^tBu_2), 1.27 (t, J_{HH} = 7.0 Hz, 9H, $P(OCH_2\boldsymbol{CH_3})_2$, -10.92 (q, J_{PH} = 15.3 Hz, 2H, $Ir(\boldsymbol{H_2})(POEt_3)$).

(^{tBu4}PCP)Ir(H_2)(PPh_2(OMe)): To a 0.5 mL *p*-xylene-d_{10} solution of 5 mg (^{tBu4}PCP)IrH_4 (8.3 μmol) in a J-Young tube, 1.67 μL PPh_2(OMe) (8.3 μmol) (Aldrich) was added. An immediate color change from dark red to colorless was observed.

(^{tBu4}PCP)Ir(H_2)(PPh_2(OMe)) (hydrides are *cis*) : $^{31}P\{^1H\}$ NMR (*p*-xylene-d_{10}, 202 MHz): δ 103.2 (t, J_{PP} = 12.1 Hz, $Ir(H_2)(PPh_2(OMe))$, 66.2 (d, J_{PP} = 12.1 Hz, PCP). ^1H NMR (*p*-xylene-d_{10}, 500 MHz): 7.55 (t, J_{HH} = 5.3 Hz, 2H, Ar), 7.18 (m, 7H, Ar), 7.13 (m, 4H, Ar), 3.55 (m, 2H, $CH_2P^tBu_2$), 3.29 (m, 2H, $CH_2P^tBu_2$), 2.85 (d, J_{PH} = 10.0 Hz, 3H, P-O***Me***), 1.36 (vt, J_{PH} = 5.0 Hz, 18H, P^tBu_2), 1.17 (vt, J_{PH} = 5.0 Hz, 18H, P^tBu_2), -12.11 (dq, J_{PH} = 12.5 Hz, J_{HH} = 4.5 Hz, 1H, Ir(***H***)(H)($POEt_3$), H is *cis* to PPh_2OMe), -13.49 (dtd, J_{PH} = 148.8 Hz, J_{PH} = 19.3 Hz, J_{HH} = 4.5 Hz,1H, Ir(***H***)(H)(PPh_2OMe), H is *trans* to PPh_2OMe).

(^{tBu4}PCP)Ir(H_2)(PPh_2(OMe)) (hydrides are *trans*) : $^{31}P\{^1H\}$ NMR (*p*-xylene-d_{10}, 202 MHz): δ 109.8 (t, J_{PP} = 16.2 Hz, $Ir(H_2)(PPh_2(OMe))$, 60.7 (d, J_{PP} = 16.2 Hz, PCP). ^1H NMR (*p*-xylene-d_{10}, 500 MHz): δ 8.26 (t, J_{HH} = 8.0 Hz, 4H, Ar), 7.55 (m, 1H, Ar), 7.31 (t, J_{HH} = 7.8 Hz, 4H, Ar), 7.21 (m, 2H, Ar), 7.06 (m, 2H, Ar), 3.48 (vt, J_{PH} = 3.5 Hz, 4H, $CH_2P^tBu_2$), 3.01 (d, J_{PH} = 10.0 Hz, 3H, P-O***Me***), 1.17 (t, J_{HH} = 6.0 Hz, 36H, P^tBu_2), -10.47 (q, J_{PH} = 15.0 Hz, 2H, Ir(***H_2***)(PPh_2(OMe)).

(^{tBu4}PCP)Ir(H_2)(Py) (hydrides are *trans*) : To a 0.5 mL *p*-xylene-d_{10} solution of 5 mg (^{tBu4}PCP)IrH_4 (8.3 μmol) in a J-Young tube, 0.72 μL Py (8.3 μmol) (Aldrich) was added.

An immediate color change from dark red to colorless was observed. $^{31}P\{^{1}H\}$ NMR (*p*-xylene-d_{10}, 202 MHz): δ 64.5 (s, PCP). ^{1}H NMR (*p*-xylene-d_{10}, 500 MHz): δ 9.59 (d, J_{HH} = 5.0 Hz, 2H, Py), 8.54 (m, 1H, Py), 6.95 (d, J_{HH} = 7.5 Hz, 2H, PCP), 6.85 (t, J_{HH} = 7.5 Hz, 1H, PCP), 6.37 (m, 2H, Py), 3.27 (vt, J_{PH} = 3.5 Hz, 4H, $CH_2P^tBu_2$), 1.31 (t, J_{HH} = 6.0 Hz, 36H, P^tBu_2), -7.86 (t, J_{PH} = 14.8 Hz, 2H, Ir(***H₂***)(Py)). An X-ray quality crystal was formed from hexane solution. Figure 7-4 shows an ORTEP of (PCP)Ir(H_2)(Py), refinement parameters are given in Table 7.11 and bond angles and bond distances are listed in Table 7.12.

(^{tBu4}PCP)Ir(H_2)($NCCH_3$) (hydrides are *trans*) : To a 0.5 mL *p*-xylene-d_{10} solution of 5 mg (^{tBu4}PCP)IrH_4 (8.3 μmol) in a J-Young tube, 0.41 μL CH_3CN (8.3 μmol) was added. An immediate color change from dark red to colorless was observed. At room temperature after 5 h, 1: 1 mixture of (^{tBu4}PCP)Ir(H_2)($NCCH_3$) and (^{tBu4}PCP)Ir($NCCH_3$) was present.

$^{31}P\{^{1}H\}$ NMR (*p*-xylene-d_{10}, 202 MHz): δ 70.2 (s, PCP). ^{1}H NMR (*p*-xylene-d_{10}, 500 MHz): δ 6.93 (d, J_{HH} = 7.5 Hz, 2H, PCP), 6.88 (t, J_{HH} = 6.5 Hz, 1H, PCP), 3.14 (vt, J_{PH} = 4.8 Hz, 4H, $CH_2P^tBu_2$), 1.43 (t, J_{HH} = 7.5 Hz, 36H, P^tBu_2), -9.02 (t, J_{PH} = 18 Hz, 2H, Ir(***H₂***)($NCCH_3$)).

(^{tBu4}PCP)Ir(H_2)(Dibenzothiophene) (hydrides are *trans*): To a 0.5 mL *p*-xylene-d_{10} solution of 5 mg (^{tBu4}PCP)IrH_4 (8.3 μmol) in a J-Young tube, 1.5 mg DBT (dibenzothiophene) (8.3 μmol) (Aldrich) was added. An immediate color change from dark red to very light red was observed. $^{31}P\{^{1}H\}$ NMR (*p*-xylene-d_{10}, 202 MHz): δ 60.9

(s, PCP). ^{1}H NMR (*p*-xylene-d_{10}, 500 MHz): δ 8.34 (d, J_{HH} = 8.0 Hz, 2H, Ar), 7.80 (d, J_{HH} = 8.0 Hz, 2H, Ar), 7.38 (t, J_{HH} = 7.5 Hz, 2H, Ar), 7.25 (m, 2H, Ar), 7.08 (d, J_{HH} = 7.5 Hz, 2H, Ar), 6.97 (t, J_{HH} = 7.5 Hz, 1H, Ar), 3.23 (vt, J_{PH} = 3.3 Hz, 4H, $CH_2P^tBu_2$), 1.19 (vt, J_{PH} = 6.2 Hz, 36H, P^tBu_2), -8.89 (t, J_{PH} = 14.5 Hz, Ir(***H₂***)).

(^{tBu4}PCP)Ir(H_2)(PEt_3) (hydrides are *trans*): To a 0.5 mL *p*-xylene-d_{10} solution of 5 mg (^{tBu4}PCP)IrH_4 (8.3 μmol) in a J-Young tube, 1.22 μL PEt_3 (8.3 μmol) (Aldrich) was added. An immediate color change from dark red to colorless was observed. $^{31}P\{^{1}H\}$ NMR (*p*-xylene-d_{10}, 202 MHz): δ 56.5 (d, J_{PP} = 15.9 Hz, PCP), -24.9 (t, J_{PP} = 15.9 Hz, Ir(H_2)(PEt_3)). ^{1}H NMR (*p*-xylene-d_{10}, 500 MHz): δ 7.06 (d, J_{HH} = 7.5 Hz, 2H, Ar), 7.03 (t, J_{HH} = 7.0 Hz, 1H, Ar), 3.45 (vt, J_{PH} = 3.8 Hz, 4H, $CH_2P^tBu_2$), 1.81 (dq, J_{PH} = 7.5 Hz, J_{HH} = 7.3 Hz, 6H, P(***CH₂***$CH_3)_3$), 1.33 (vt, J_{PH} = 5.8 Hz, 36H, P^tBu_2), 1.09 (dt, J_{HH} = 8.0 Hz, J_{PH} = 2.0 Hz, 9H, $P(CH_2$***CH₃***$)_3$), -11.56 (q, J_{PH} = 15.2 Hz, Ir(***H₂***)).

(^{tBu4}PCP)Ir(H_2)(PMe_3) (hydrides are *trans*): To a 0.5 mL *p*-xylene-d_{10} solution of 5 mg (^{tBu4}PCP)IrH_4 (8.3 μmol) in a J-Young tube, 0.85 μL PMe_3 (8.3 μmol) (Aldrich) was added. An immediate color change from dark red to colorless was observed. $^{31}P\{^{1}H\}$ NMR (*p*-xylene-d_{10}, 202 MHz): δ 60.5 (d, J_{PP} = 18.2 Hz, PCP), -75.4 (t, J_{PP} = 18.2 Hz, Ir(H_2)(PMe_3)). ^{1}H NMR (*p*-xylene-d_{10}, 500 MHz): δ 7.08 (d, J_{HH} = 7.5 Hz, 2H, Ar), 7.03 (t, J_{HH} = 7.0 Hz, 1H, Ar), 3.42 (vt, J_{PH} = 3.8 Hz, 4H, $CH_2P^tBu_2$), 1.71 (d, J_{PH} = 7.5 Hz, 9H, P(***CH₃***$)_3$), 1.33 (vt, J_{PH} = 6.0 Hz, 36H, P^tBu_2), -11.42 (q, J_{PH} = 15.2 Hz, Ir(***H₂***)).

(^{tBu4}PCP)Ir(H_2)(PMe_2Ph) (hydrides are *trans*): To a 0.5 mL *p*-xylene-d_{10} solution of 5 mg (^{tBu4}PCP)IrH_4 (8.3 μmol) in a J-Young tube, 1.3 μL PMe_3 (8.3 μmol) (Aldrich) was added. An immediate color change from dark red to colorless was observed. $^{31}P\{^1H\}$ NMR (*p*-xylene-d_{10}, 202 MHz): δ 58.6 (d, J_{PP} = 17.2 Hz, PCP), -75.4 (t, J_{PP} = 17.2 Hz, Ir(H_2)(PMe_3)). ^1H NMR (*p*-xylene-d_{10}, 500 MHz): δ 7.92 (t, J_{HH} = 9.0 Hz, 2H, Ar), 7.26 (dt, J_{HH} = 7.8 Hz, J_{HH} = 1.5 Hz, 2H, Ar), 7.14 (m, 1H, Ar), 7.06 (m, 2H, Ar), 7.03 (m, 1H, Ar), 3.43 (vt, J_{PH} = 3.8 Hz, 4H, $CH_2P^tBu_2$), 1.97 (d, J_{PH} = 7.0 Hz, 6H, P(***CH₃***)$_2$Ph), 1.24 (vt, J_{PH} = 6.0 Hz, 36H, P^tBu_2), -11.10 (q, J_{PH} = 15.0 Hz, Ir(***H₂***)).

(^{tBu4}PCP)Ir(H_2)(PPh_3) (hydrides are *trans*): To a 0.5 mL *p*-xylene-d_{10} solution of 5 mg (^{tBu4}PCP)IrH_4 (8.3 μmol) in a J-Young tube, 2.2 mg PPh_3 (8.3 μmol) (Aldrich) was added. Solution was reached equilibrium after heating for 10 days at 45 °C. In the solution (PCP)IrH_2, (PCP)IrH_4 and (PCP)Ir(H_2)(PPh_3) and PPh_3 were present. **(^{tBu4}PCP)Ir(H_2)(PPh_3):** $^{31}P\{^1H\}$ NMR (*p*-xylene-d_{10}, 202 MHz): δ 51.1 (d, J_{PP} = 17.5 Hz, PCP), 7.40 (t, J_{PP} = 17.5 Hz, Ir(H_2)(PPh_3)). ^1H NMR (*p*-xylene-d_{10}, 500 MHz): δ 3.48 (vt, J_{PH} = 4.3 Hz, 4H, $CH_2P^tBu_2$), 0.96 (vt, J_{PH} = 7.5 Hz, 36H, P^tBu_2), -10.24 (q, J_{PH} = 17.8 Hz, Ir(***H₂***)).

Equilibrium measurements with (^{tBu4}PCP)Ir(H)(H): In typical equilibrium measurements, to a 0.5 mL *p*-xylene-d_{10} solution of 5 mg (^{tBu4}PCP)IrH_4 (8.3 μmol) in a J-Young tube, 8.3 μmol of two ligands were added. One atmosphere H_2 was added to the solution and heated for 10 days at 90 °C. Concentration of all the species was measured

by both ^{31}P and ^{1}H NMR spectroscopy. In case of PMe_3, the solution was heated for 10 days at 40 °C and concentrations were measured by both ^{31}P and ^{1}H NMR spectroscopy.

Equilibrium between (^{tBu4}PCP)Ir(H_2) and (^{tBu4}PCP)Ir(H_2)(PPh_3): To a 0.5 mL *p*-xylene-d_{10} solution of 5 mg (^{tBu4}PCP)IrH_4 (8.3 μmol) in a J-Young tube, 2.2 mg PPh_3 (8.3 μmol) (Aldrich) was added. Solution was reached equilibrium after heating for 10 days at 45 °C. In the solution (PCP)IrH_2, (PCP)IrH_4 and (PCP)Ir(H_2)(PPh_3) and PPh_3 were present.

(^{tBu4}PCP)Ir(H)(Cl)(($P(OEt)_3$)(H and Cl are cis): To a 0.5 mL C_6D_6 solution of 5 mg (^{tBu4}PCP)IrHCl (8.9 μmol) in a J-Young tube, 1.5 μL $P(OEt)_3$ (8.9 μmol) (Aldrich) was added. An immediate color change from dark red to colorless was observed. $^{31}P\{^{1}H\}$ NMR (C_6D_6, 162 MHz): δ 86.9 (dt, J_{PP} = 17.0 Hz, J_{PH} = 234.8 Hz, Ir($P(OEt)_3$), 48.6 (d, J_{PP} = 15.9 Hz, PCP). ^{1}H NMR (C_6D_6, 400 MHz): δ 6.87 (bs, 3H, Ar), 3.78 (q, J_{HH} = 7.2 Hz, 6H, $P(O\boldsymbol{CH_2}CH_3)_3$), 3.43 (d of vt, J_{PH} = 4.0 Hz, J_{HH} = 16.0 Hz, 2H, $CH_2P^tBu_2$), 2.95 (d of vt, J_{PH} = 4.0 Hz, J_{HH} = 16.0 Hz, 2H, $CH_2P^tBu_2$), 1.63 (t, J_{PH} = 6.8 Hz, 18H, P^tBu_2), 1.36 (broad singlet, 18H, P^tBu_2), 0.98 (t, J_{HH} = 6.6 Hz, 9H, $P(OCH_2\boldsymbol{CH_3})_3$), -10.58 (dt, J_{PH} = 17.0 Hz, J_{PH} = 234.8 Hz, 1H, Ir-***H***).

(^{tBu4}PCP)Ir(H)(Cl)(($P(OEt)_3$) (H and Cl are trans): To a 0.5 mL C_6D_6 solution of 5 mg (^{tBu4}PCP)IrHCl (8.9 μmol) in a J-Young tube, 1.5 μL $P(OEt)_3$ (8.9 μmol) (Aldrich) was added. An immediate color change from dark red to colorless was observed. NMR was recorded after this solution was heated 10 h 80 °C. $^{31}P\{^{1}H\}$ NMR (C_6D_6, 162 MHz): δ 95.8 (t, J_{PP} = 22.4 Hz, Ir($P(OEt)_3$), 50.9 (d, J_{PP} = 22.4 Hz, PCP). ^{1}H NMR (C_6D_6, 400

MHz): δ 7.17 (PCP aromatic proton peak overlap with solvent C_6D_6 peak), 4.05 (q, J_{HH} = 6.4 Hz, 6H, P(O***CH₂***$CH_3)_3$), 3.88 (d of vt, J_{PH} = 4.1 Hz, J_{HH} = 15.6 Hz, 2H, $CH_2P^tBu_2$), 3.20 (d of vt, J_{PH} = 4.1 Hz, J_{HH} = 15.6 Hz, 2H, $CH_2P^tBu_2$), 1.51 (t, J_{PH} = 6.2 Hz, 18H, P^tBu_2), 1.17 (t, J_{PH} = 6.2 Hz, 18H, P^tBu_2), 1.07 (t, J_{HH} = 7.0 Hz, 9H, $P(OCH_2CH_3)_3$), -22.02 (q, J_{PH} = 14.8 Hz, 1H, Ir-***H***).

(^{tBu4}PCP)Ir(H)(Cl)((PMe(OEt)$_2$)(H and Cl are cis): To a 0.5 mL C_6D_6 solution of 5 mg (^{tBu4}PCP)IrHCl (8.9 μmol) in a J-Young tube, 1.34 μL $PMe(OEt)_2$ (8.9 μmol) (VWR) was added. An immediate color change from dark red to colorless was observed. $^{31}P\{^1H\}$ NMR (C_6D_6, 162 MHz): δ 133.7 (broad, $Ir(PMe(OEt)_2)$), 50.5 (broad, PCP). ^1H NMR (C_6D_6, 400 MHz): δ 6.86 (bs, 3H, Ar-*H*), 3.3 (broad, 4H, P(O***CH₂***$CH_3)_2$), 3.14 (broad, 2H, $CH_2P^tBu_2$), 2.98 (d of vt, J_{PH} = 3.8 Hz, J_{HH} = 16.0 Hz, 2H, $CH_2P^tBu_2$), 1.57 (t, J_{PH} = 6.6 Hz, 18H, P^tBu_2), 1.34 (broad singlet, 18H, P^tBu_2), 1.08 (broad, 3H, P***Me***), 0.91 (broad, 6H, $P(OCH_2CH_3)_2$), -10.62 (broad doublet, J_{PH} = 196.0 Hz, 1H, Ir-***H***).

(^{tBu4}PCP)Ir(H)(Cl)((PMe(OEt)$_2$) (H and Cl are trans): To a 0.5 mL C_6D_6 solution of 5 mg (^{tBu4}PCP)IrHCl (8.9 μmol) in a J-Young tube, 1.34 μL $PMe(OEt)_2$ (8.9 μmol) (VWR) was added. An immediate color change from dark red to colorless was observed. NMR was recorded after this solution was heated 10 h 80 °C. $^{31}P\{^1H\}$ NMR (C_6D_6, 162 MHz): δ 134.6 (t, J_{PP} = 17.2 Hz, $Ir(PMe(OEt)_2)$), 50.1 (d, J_{PP} = 17.2 Hz, PCP). ^1H NMR (C_6D_6, 400 MHz): δ 7.17 (PCP aromatic proton peak overlap with solvent C_6D_6 peak), 3.98 (d of vt, J_{PH} = 3.6 Hz, J_{HH} = 14.6 Hz, 2H, $CH_2P^tBu_2$), 3.94 (m, 2H, P(O***CH₂***CH_3)), 3.61 (m, 2H, P(O***CH₂***CH_3)), 3.19 (d of vt, J_{PH} = 4.0 Hz, J_{HH} = 15.6 Hz, 2H, $CH_2P^tBu_2$),

2.09 (d, J_{PH} = 4.8 Hz, 3H, P***Me***), 1.47 (t, J_{PH} = 6.4 Hz, 18H, P^{t}Bu$_2$), 1.11 (t, J_{PH} = 6.4 Hz, 18H, P^{t}Bu$_2$), 1.07 (t, J_{HH} = 7.2 Hz, 6H, P(OCH$_2$***CH$_3$***)$_2$), -22.16 (q, J_{PH} = 14.5 Hz, 1H, Ir-***H***).

(^{tBu4}PCP)Ir(H)(Cl)((PPh(OEt)$_2$)(H and Cl are cis): To a 0.5 mL C_6D_6 solution of 5 mg (^{tBu4}PCP)IrHCl (8.9 μmol) in a J-Young tube, 1.7 μL PPh(OEt)$_2$ (8.9 μmol) (Aldrich) was added. An immediate color change from dark red to colorless was observed. $^{31}P\{^1H\}$ NMR (C_6D_6, 162 MHz): δ 104.4 (broad, Ir(PPh(OEt)$_2$), 47.8 (broad, PCP). ^{1}H NMR (C_6D_6, 400 MHz): δ 1.59 (broad singlet, 18H, P^{t}Bu$_2$), 1.34 (broad singlet, 18H, P^{t}Bu$_2$), -11.02 (broad doublet, J_{PH} = 198.5 Hz, 1H, Ir-***H***).

(^{tBu4}PCP)Ir(H)(Cl)((PPh(OEt)$_2$) (H and Cl are trans): To a 0.5 mL C_6D_6 solution of 5 mg (^{tBu4}PCP)IrHCl (8.9 μmol) in a J-Young tube, 1.7 μL PPh(OEt)$_2$ (8.9 μmol) (Aldrich) was added. An immediate color change from dark red to colorless was observed. NMR was recorded after this solution was heated 10 h 80 ℃. $^{31}P\{^1H\}$ NMR (C_6D_6, 162 MHz): δ 116.4 (t, J_{PP} = 16.9 Hz, Ir(PPh(OEt)$_2$), 49.4 (d, J_{PP} = 16.9 Hz, PCP). ^{1}H NMR (C_6D_6, 400 MHz): δ 8.38 (J_{HH} = 7.8 Hz, 2H, Ar), 7.24 (m, 3H, Ar), 4.01 (d of vt, J_{PH} = 3.6 Hz, J_{HH} = 14.4 Hz, 2H, CH$_2$P^{t}Bu$_2$), 3.96 (m, 2H, P(O***CH$_2$***CH$_3$)), 3.50 (m, 2H, P(O***CH$_2$***CH$_3$)), 3.19 (d of vt, J_{PH} = 4.0 Hz, J_{HH} = 15.6 Hz, 2H, CH$_2$P^{t}Bu$_2$), 1.34 (t, J_{PH} = 6.4 Hz, 18H, P^{t}Bu$_2$), 1.11 (t, J_{PH} = 6.4 Hz, 18H, P^{t}Bu$_2$), 1.01 (t, J_{HH} = 7.2 Hz, 6H, P(OCH$_2$***CH$_3$***)$_2$), -22.0 (q, J_{PH} = 14.4 Hz, 1H, Ir-***H***).

(^{tBu4}PCP)Ir(H)(Cl)(PMe_2Ph): To a 0.5 mL C_6D_6 solution of 5 mg (^{tBu4}PCP)IrHCl (8.9 μmol) in a J-Young tube, 1.3 μL PMe_2Ph (8.9 μmol) (Aldrich) was added. An immediate color change from dark orange to colorless was observed. $^{31}P\{^1H\}$ NMR (C_6D_6, 162 MHz): δ 46.0 (d, J_{PP} = 15.1 Hz, PCP), -48.6 (t, J_{PP} = 15.1 Hz, Ir(PMe_2Ph). ^1H NMR (C_6D_6, 400 MHz): δ 7.80 (m, 2H, Ar), 7.37 (m, 2H, Ar), 7.12 (d, J_{HH} = 7.6 Hz, 2H, Ar-*H*), 7.08 (m, 1H, Ar), 7.02 (m, 1H, Ar), 4.04 (d of vt, J_{PH} = 3.0 Hz, J_{HH} = 14.4 Hz, 2H, $CH_2P^tBu_2$), 3.12 (d of vt, J_{PH} = 4.0 Hz, J_{HH} = 14.8 Hz, 2H, $CH_2P^tBu_2$), 2.02 (d, J_{PH} = 7.2 Hz, 6H, P***Me₂***Ph), 1.29 (t, J_{PH} = 6.2 Hz, 18H, P^tBu_2), 0.93 (t, J_{PH} = 6.2 Hz, 18H, P^tBu_2), -22.97 (dt, J_{PH} = 15.6 Hz, J_{PH} = 10.2 Hz, 1H, Ir-***H***).

^{tBu4}PCP)Ir(H)(Cl)($NCCH_3$): To a 0.5 mL *p*-xylene-d_{10} solution of 5 mg (^{tBu4}PCP)IrHCl (8.9 μmol) in a J-Young tube, 0.44 μL $NCCH_3$ (8.9 μmol) (Aldrich) was added. An immediate color change from dark orange to light orange was observed at room temperature, while at 75 °C, it became dark orange. Room temperature: $^{31}P\{^1H\}$ NMR (*p*-xylene-d_{10}, 202 MHz): δ 56.5 (s, broad, PCP). ^1H NMR (*p*-xylene-d_{10}, 500 MHz): δ 6.97 (d, J_{HH} = 7.5 Hz, 2H, Ar), 6.89 (t, J_{HH} = 7.3 Hz, 1H, Ar), 3.17 (d of vt, J_{PH} = 3.0 Hz, J_{HH} = 16.5 Hz, 2H, $CH_2P^tBu_2$), 3.06 (d of vt, J_{PH} = 3.7 Hz, J_{HH} = 16.5 Hz, 2H, $CH_2P^tBu_2$), 1.47 (t, J_{PH} = 6.2 Hz, 18H, P^tBu_2), 1.38 (t, J_{PH} = 6.2 Hz, 18H, P^tBu_2), 0.88 (s, CH_3CN), -25.56 (broad singlet, 1H, Ir-***H***).

At 75 °C: $^{31}P\{^1H\}$ NMR (*p*-xylene-d_{10}, 202 MHz): δ 65.7 (broad singlet, PCP). ^1H NMR (*p*-xylene-d_{10}, 500 MHz): δ 6.98 (d, J_{HH} = 7.5 Hz, 2H, Ar), 6.87 (t, J_{HH} = 7.5 Hz, 1H, Ar), 3.24 (d of vt, J_{PH} = 3.5 Hz, J_{HH} = 17.0 Hz, 2H, $CH_2P^tBu_2$), 3.13 (d of vt, J_{PH} = 4.0 Hz,

J_{HH} = 17.0 Hz, 2H, $CH_2P^tBu_2$), 1.42 (t, J_{PH} = 6.2 Hz, 18H, P^tBu_2), 1.36 (t, J_{PH} = 6.2 Hz, 18H, P^tBu_2), 1.03 (s, CH_3CN), -38.93 (broad singlet, 1H, Ir-***H***).

(^{tBu4}PCP)Ir(H)(Cl)(PMe_3): To a 0.5 mL C_6D_6 solution of 5 mg (^{tBu4}PCP)IrHCl (8.9 µmol) in a J-Young tube, 0.92 µL PMe_3 (8.9 µmol) (Aldrich) was added. An immediate color change from dark orange to colorless was observed. $^{31}P\{^1H\}$ NMR (C_6D_6, 162 MHz): δ 46.0 (d, J_{PP} = 14.9 Hz, PCP), -65.0 (t, J_{PP} = 16.3 Hz, Ir(PMe_3). ^1H NMR (C_6D_6, 400 MHz): δ 7.15 (d, J_{HH} = 7.3 Hz, 2H, Ar), 7.08 (t, J_{HH} = 7.3 Hz, 1H, Ar), 3.87 (d of vt, J_{PH} = 3.2 Hz, J_{HH} = 15.6 Hz, 2H, $CH_2P^tBu_2$), 3.13 (d of vt, J_{PH} = 4.0 Hz, J_{HH} = 15.2 Hz, 2H, $CH_2P^tBu_2$), 1.63 (d, J_{PH} = 7.6 Hz, 9H, P***Me₃***), 1.39 (t, J_{PH} = 6.2 Hz, 18H, P^tBu_2), 1.02 (t, J_{PH} = 6.2 Hz, 18H, P^tBu_2), -23.28 (dt, J_{PH} = 15.6 Hz, J_{PH} = 11.6 Hz, 1H, Ir-***H***). An X-ray quality crystal was formed from hexane solution. Figure 7-7 shows an ORTEP of (PCP)Ir(H)(Cl)(PMe_3), refinement parameters are given in Table 7.17 and bond angles and bond distances are listed in Table 7.18.

(^{tBu4}PCP)Ir(H)(Cl)(PEt_3): To a 0.5 mL C_6D_6 solution of 5 mg (^{tBu4}PCP)IrHCl (8.9 µmol) in a J-Young tube, 1.3 µL PEt_3 (8.9 µmol) (Aldrich) was added. Solution was reached equilibrium after heating for 8 days at 45 °C. In solution free (^{tBu4}PCP)IrHCl, (^{tBu4}PCP)Ir(HCl)((PEt_3), and free PEt_3 was present. $^{31}P\{^1H\}$ NMR (C_6D_6, 162 MHz): δ 43.4 (d, J_{PP} = 13.8 Hz, PCP), -36.1 (t, J_{PP} = 13.8 Hz, Ir(PEt_3). ^1H NMR (C_6D_6, 500 MHz): δ 7.06 (m, 2H, Ar), 7.02 (1H, Ar), 4.05 (d of vt, J_{PH} = 3.3 Hz, J_{HH} = 15.0 Hz, 2H, $CH_2P^tBu_2$), 3.06 (d of vt, J_{PH} = 4.0 Hz, J_{HH} = 17.0 Hz, 2H, $CH_2P^tBu_2$), 1.81 (dq, J_{PH} = 7.5 Hz, J_{HH} = 7.2 Hz, 6H, P(***CH₂***$CH_3)_3$), 1.41 (t, J_{PH} = 6.2 Hz, 18H, P^tBu_2), 1.06 (t, J_{PH} = 6.2

Hz, 18H, P^{t}Bu$_2$), 0.96 (dt, J_{HH} = 8.0 Hz, J_{PH} = 2.0 Hz, 9H, P(CH$_2$***CH$_3$***)$_3$), -23.5 (dt, J_{PH} = 14.8 Hz, J_{PH} = 12.5 Hz, 1H, Ir-***H***).

(^{tBu4}PCP)Ir(H)(Cl)((PPh$_2$(OMe)): To a 0.5 mL C_6D_6 solution of 5 mg (^{tBu4}PCP)IrHCl (8.9 μmol) in a J-Young tube, 1.8 μL PPh$_2$(OMe) (8.9 μmol) (Aldrich) was added. An immediate color change from dark orange to colorless was observed. ^{31}P{^{1}H} NMR (C_6D_6, 162 MHz): δ 98.4 (t, J_{PP} = 14.6 Hz, Ir(PPh$_2$(OMe)), 51.3 (broad, PCP). ^{1}H NMR (C_6D_6, 400 MHz): δ 8.05 (t, J_{HH} = 8.0 Hz, 4H, Ar), 7.19 (d, J_{HH} = 6.5 Hz, 2H, Ar), 7.17 ((t, J_{HH} = 6.1 Hz, 1H, Ar), 7.10 (m, 4H, Ar), 7.04 (t, J_{HH} = 7.0 Hz, 2H, Ar-*H*), 4.16 (d of vt, J_{PH} = 3.2 Hz, J_{HH} = 15.2 Hz, 2H, CH$_2$P^{t}Bu$_2$), 3.14 (d of vt, J_{PH} = 3.8 Hz, J_{HH} = 14.8 Hz, 2H, CH$_2$P^{t}Bu$_2$), 3.06 (d, J_{PH} = 10.4 Hz, 3H, PO***Me***), 1.23 (t, J_{PH} = 6.2 Hz, 18H, P^{t}Bu$_2$), 1.04 (t, J_{PH} = 6.0 Hz, 18H, P^{t}Bu$_2$), -23.28 (dt, J_{PH} = 15.4 Hz, J_{PH} = 13.2 Hz, 1H, Ir-***H***).

(^{tBu4}PCP)Ir(H)(Cl)(Py): To a 0.5 mL *p*-xylene-d$_{10}$ solution of 5 mg (^{tBu4}PCP)IrHCl (8.9 μmol) in a J-Young tube, 0.72 μL Py (8.9 μmol) (Aldrich) was added. An immediate color change from dark orange to colorless was observed. ^{31}P{^{1}H} NMR (*p*-xylene-d$_{10}$, 202 MHz): δ 46.6. ^{1}H NMR (*p*-xylene-d$_{10}$, 500 MHz): δ 10.45 (d, J_{HH} = 5.5 Hz, 2H, Py), 9.14 (d, J_{HH} = 5.5, 1H, Py), 7.05 (d, J_{HH} = 7.0 Hz, 2H, PCP), 6.84 (m, 1H, PCP), 6.46 (m, 2H, Py), 2.98 (d of vt, J_{PH} = 3.0 Hz, J_{HH} = 16.5 Hz, 2H, CH$_2$P^{t}Bu$_2$), 2.93 (d of vt, J_{PH} = 3.0 Hz, J_{HH} = 16.5 Hz, 2H, CH$_2$P^{t}Bu$_2$), 1.41 (t, J_{HH} = 6.0 Hz, 18H, P^{t}Bu$_2$), 1.04 (t, J_{HH} = 6.0 Hz, 18H, P^{t}Bu$_2$), -21.46 (t, J_{PH} = 16.8 Hz, 1H, Ir-***H***).

Equilibrium measurements with (^{tBu4}PCP)Ir(H)(Cl):

In typical equilibrium measurements, to a 0.5 mL *p*-xylene-d_{10} solution of 5 mg (^{tBu4}PCP)IrHCl (8.9 μmol) in a J-Young tube, 8.9 μmol of two ligands were added. The solution was then heated for 10 days at 90 °C and concentrations were measured by both ^{31}P and ^{1}H NMR spectroscopy. In case of PMe_3, the solution was heated for 10 days at 40 °C and concentrations were measured by both ^{31}P and ^{1}H NMR spectroscopy.

Equilibrium between (^{tBu4}PCP)Ir(HCl) and (^{tBu4}PCP)Ir(HCl)(PEt_3): To a 0.5 mL *p*-xylene-d_{10} solution of 5 mg (^{tBu4}PCP)IrHCl (8.9 μmol) in a J-Young tube, 1.3 μL PEt_3 (8.9 μmol) (Aldrich) was added. This solution was heated 20 days at 90 °C and concentration of free (^{tBu4}PCP)IrHCl, (^{tBu4}PCP)Ir(HCl)((PEt_3), and free PEt_3 were measure by both ^{31}P and ^{1}H NMR spectroscopy.

7.5 References

(1) Hoff, C. D. In *Progress in Inorganic Chemistry*; Stephen, J. L., Ed. **1992**, p 503-561.
(2) King, W. A.; Di Bella, S.; Gulino, A.; Lanza, G.; Fragala, I. L.; Stern, C. L.; Marks, T. J. *J. Am. Chem. Soc.* **1999**, *121*, 355.
(3) Schock, L. E.; Marks, T. J. *J. Am. Chem. Soc.* **1988**, *110*, 7701.
(4) Simoes, J. A. M.; Beauchamp, J. L. *Chem. Rev.* **1990**, *90*, 629.
(5) Fey, N.; Harvey, J. N.; Lloyd-Jones, G. C.; Murray, P.; Orpen, A. G.; Osborne, R.; Purdie, M. *Organometallics* **2008**, *27*, 1372-1383.
(6) Clot, E.; MeÌgret, C.; Eisenstein, O.; Perutz, R. N. *J. Am. Chem. Soc.* **2009**, *131*, 7817.
(7) Choliy, Y.; Krogh-Jespersen, K., Unpublished work
(8) Tolman, C. A. *Chem. Rev.* **1977**, *77*, 313.

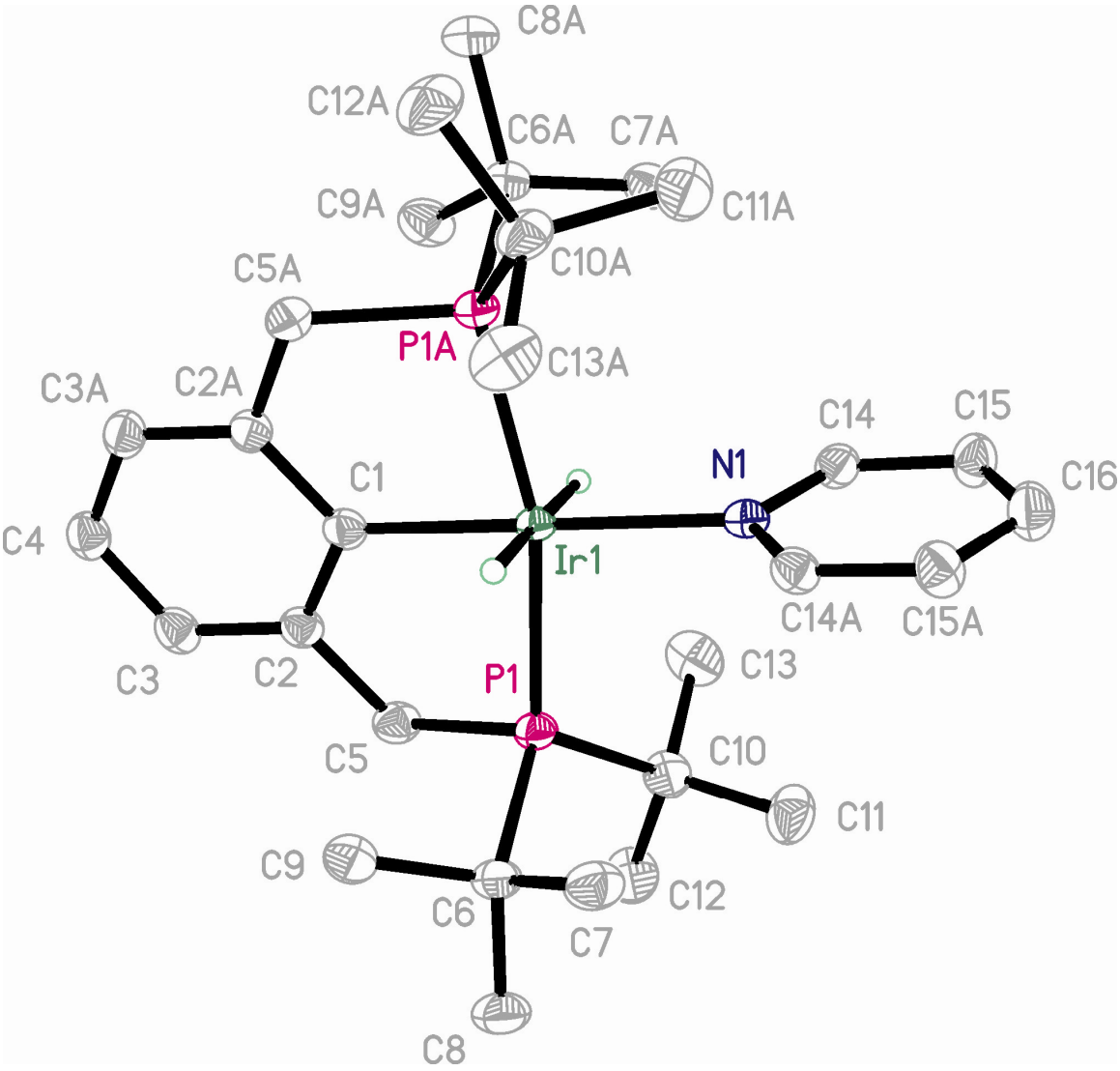

Figure 7-4 Crystal structure of (PCP)Ir(H_2)(Py)

Table 7.11 Crystal data and structure refinement for (PCP)Ir(H_2)(Py)

Empirical formula	C29 H50 Ir N P2	
Formula weight	666.84	
Temperature	100(2) K	
Wavelength	0.71073 Å	
Crystal system	Monoclinic	
Space group	C2/c	
Unit cell dimensions	a = 9.4580(5) Å	□= 90°.
	b = 15.4864(8) Å	□= 97.307(1)°.
	c = 20.8417(11) Å	□ = 90°.
Volume	3027.9(3) $Å^3$	
Z	4	
Density (calculated)	1.463 Mg/m^3	
Absorption coefficient	4.532 mm^{-1}	
F(000)	1352	
Crystal size	0.25 x 0.15 x 0.03 mm^3	
Theta range for data collection	2.54 to 31.55°.	
Index ranges	-13<=h<=13, -13<=k<=22, -25<=l<=30	
Reflections collected	19258	
Independent reflections	5055 [R(int) = 0.0268]	
Completeness to theta = 31.55°	99.8 %	
Absorption correction	Numerical	
Max. and min. transmission	0.8951 and 0.3971	
Refinement method	Full-matrix least-squares on F^2	
Data / restraints / parameters	5055 / 1 / 162	
Goodness-of-fit on F^2	1.001	
Final R indices [I>2sigma(I)]	R1 = 0.0236, wR2 = 0.0554	
R indices (all data)	R1 = 0.0254, wR2 = 0.0562	
Largest diff. peak and hole	2.557 and -1.000 $e.Å^{-3}$	

Table 7.12 Selective bond lengths [Å] and angles [°] for (PCP)Ir(H_2)(Py)

Ir(1)-C(1)	2.034(3)	C(3)-C(4)	1.393(3)
Ir(1)-N(1)	2.172(3)	C(6)-C(8)	1.530(3)
Ir(1)-P(1)	2.2926(6)	C(6)-C(7)	1.534(3)
Ir(1)-H(1)	1.56(3)	C(6)-C(9)	1.536(4)
P(1)-C(5)	1.838(2)	C(10)-C(12)	1.537(4)
P(1)-C(10)	1.896(2)	C(10)-C(11)	1.537(4)
P(1)-C(6)	1.896(2)	C(10)-C(13)	1.538(4)
C(1)-C(2)	1.417(3)	N(1)-C(14)	1.351(2)
C(2)-C(3)	1.395(3)	C(14)-C(15)	1.387(3)
C(2)-C(5)	1.509(3)	C(15)-C(16)	1.384(3)
C(1)-Ir(1)-N(1)	180.000(1)	C(6)-C(8)-H(8A)	109.5
C(1)-Ir(1)-P(1)	82.457(14)	C(6)-C(8)-H(8B)	109.5
N(1)-Ir(1)-P(1)	97.543(14)	H(8A)-C(8)-H(8B)	109.5
C(1)-Ir(1)-H(1)	90.9(13)	C(6)-C(8)-H(8C)	109.5
N(1)-Ir(1)-H(1)	89.1(13)	H(8A)-C(8)-H(8C)	109.5
P(1)-Ir(1)-H(1)	86(2)	H(8B)-C(8)-H(8C)	109.5
C(5)-P(1)-C(10)	103.28(11)	C(6)-C(9)-H(9A)	109.5
C(5)-P(1)-C(6)	103.10(10)	C(6)-C(9)-H(9B)	109.5
C(10)-P(1)-C(6)	109.63(11)	H(9A)-C(9)-H(9B)	109.5
C(5)-P(1)-Ir(1)	102.26(7)	C(6)-C(9)-H(9C)	109.5
C(10)-P(1)-Ir(1)	119.46(7)	H(9A)-C(9)-H(9C)	109.5
C(6)-P(1)-Ir(1)	116.42(8)	H(9B)-C(9)-H(9C)	109.5
C(2)-C(1)-Ir(1)	121.92(14)	C(12)-C(10)-C(11)	109.3(2)
C(3)-C(2)-C(1)	121.7(2)	C(12)-C(10)-C(13)	106.8(2)
C(3)-C(2)-C(5)	120.2(2)	C(11)-C(10)-C(13)	108.5(2)
C(1)-C(2)-C(5)	118.08(19)	C(12)-C(10)-P(1)	114.54(17)
C(4)-C(3)-C(2)	120.9(2)	C(11)-C(10)-P(1)	109.79(17)
C(2)-C(5)-P(1)	108.49(15)	C(13)-C(10)-P(1)	107.69(17)
C(8)-C(6)-C(7)	109.43(19)	C(10)-C(11)-H(11A)	109.5
C(8)-C(6)-C(9)	108.1(2)	C(10)-C(11)-H(11B)	109.5
C(7)-C(6)-C(9)	107.0(2)	H(11A)-C(11)-H(11B)	109.5
C(8)-C(6)-P(1)	115.08(18)	C(10)-C(11)-H(11C)	109.5
C(7)-C(6)-P(1)	110.24(16)	C(10)-C(12)-H(12A)	109.5
C(9)-C(6)-P(1)	106.69(15)		

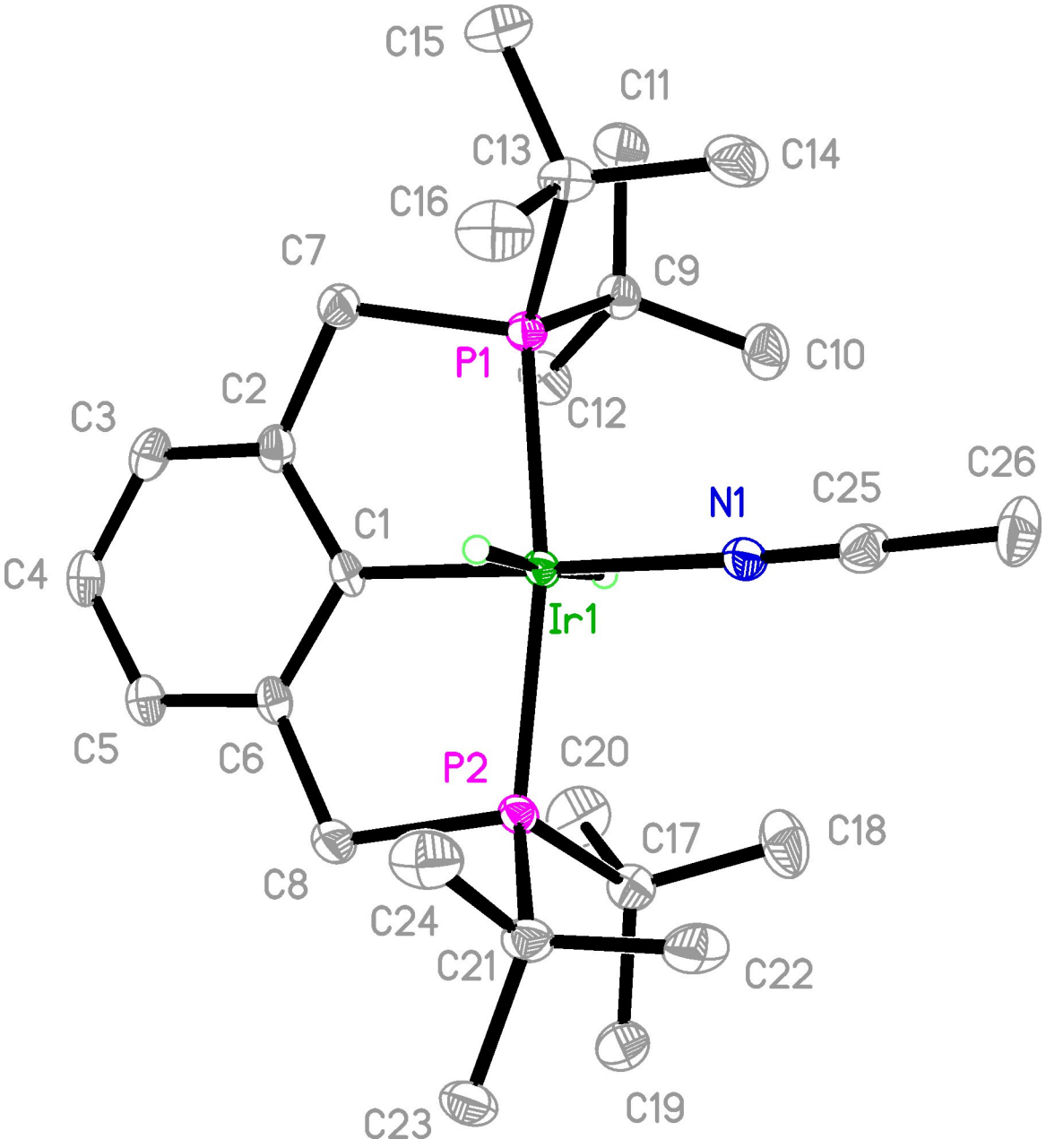

Figure 7-5 Crystal structure of (PCP)Ir(H_2)($NCCH_3$)

Table 7.13 Crystal data and structure refinement for (PCP)Ir(H_2)($NCCH_3$)

Empirical formula	C26 H48 Ir N P2	
Formula weight	628.79	
Temperature	100(2) K	
Wavelength	0.71073 Å	
Crystal system	Monoclinic	
Space group	P2(1)/c	
Unit cell dimensions	a = 12.0953(8) Å	□= 90°.
	b = 15.6071(11) Å	□= 104.696(1)°.
	c = 14.9896(10) Å	□ = 90°.
Volume	2737.1(3) $Å^3$	
Z	4	
Density (calculated)	1.526 Mg/m^3	
Absorption coefficient	5.008 mm^{-1}	
F(000)	1272	
Crystal size	0.44 x 0.34 x 0.04 mm^3	
Theta range for data collection	2.18 to 31.57°.	
Index ranges	-17<=h<=17, -22<=k<=22, -22<=l<=22	
Reflections collected	33843	
Independent reflections	9124 [R(int) = 0.0456]	
Completeness to theta = 31.57°	99.7 %	
Absorption correction	Semi-empirical from equivalents	
Max. and min. transmission	0.825 and 0.217	
Refinement method	Full-matrix least-squares on F^2	
Data / restraints / parameters	9124 / 2 / 290	
Goodness-of-fit on F^2	1.004	
Final R indices [I>2sigma(I)]	R1 = 0.0300, wR2 = 0.0688	
R indices (all data)	R1 = 0.0382, wR2 = 0.0721	
Largest diff. peak and hole	2.948 and -1.079 e.$Å^{-3}$	

Table 7.14 Selective bond lengths [Å] and angles [°] for (PCP)Ir(H_2)($NCCH_3$)

Ir(1)-C(1)	2.021(2)	C(3)-C(4)	1.387(4)
Ir(1)-N(1)	2.036(2)	C(4)-C(5)	1.390(4)
Ir(1)-P(1)	2.2685(7)	C(5)-C(6)	1.393(4)
Ir(1)-P(2)	2.2744(7)	C(6)-C(8)	1.510(4)
Ir(1)-H(1)	1.575(17)	C(9)-C(10)	1.532(4)
Ir(1)-H(2)	1.581(17)	C(9)-C(11)	1.534(4)
P(1)-C(7)	1.836(3)	C(9)-C(12)	1.538(4)
P(1)-C(13)	1.887(3)	C(13)-C(14)	1.526(5)
P(1)-C(9)	1.889(3)	C(13)-C(15)	1.537(4)
P(2)-C(8)	1.842(3)	C(13)-C(16)	1.540(4)
P(2)-C(17)	1.882(3)	C(17)-C(18)	1.525(4)
P(2)-C(21)	1.886(3)	C(17)-C(19)	1.534(4)
C(1)-C(6)	1.418(4)	C(17)-C(20)	1.544(4)
C(1)-C(2)	1.427(4)	C(21)-C(22)	1.531(4)
C(2)-C(3)	1.399(4)	C(21)-C(24)	1.532(4)
C(2)-C(7)	1.507(4)	C(21)-C(23)	1.533(4)
C(1)-Ir(1)-N(1)	177.19(10)	C(7)-P(1)-Ir(1)	104.22(9)
C(1)-Ir(1)-P(1)	82.98(8)	C(13)-P(1)-Ir(1)	119.41(9)
N(1)-Ir(1)-P(1)	96.34(7)	C(9)-P(1)-Ir(1)	112.61(9)
C(1)-Ir(1)-P(2)	83.42(8)	C(8)-P(2)-C(17)	104.83(14)
N(1)-Ir(1)-P(2)	97.63(7)	C(8)-P(2)-C(21)	102.75(13)
P(1)-Ir(1)-P(2)	164.11(3)	C(17)-P(2)-C(21)	110.81(13)
C(1)-Ir(1)-H(1)	87.7(12)	C(8)-P(2)-Ir(1)	104.51(10)
N(1)-Ir(1)-H(1)	94.9(12)	C(17)-P(2)-Ir(1)	112.26(10)
P(1)-Ir(1)-H(1)	82.5(12)	C(21)-P(2)-Ir(1)	119.86(10)
P(2)-Ir(1)-H(1)	88.8(12)	C(6)-C(1)-C(2)	115.3(2)
C(1)-Ir(1)-H(2)	93.8(12)	C(6)-C(1)-Ir(1)	122.6(2)
N(1)-Ir(1)-H(2)	83.5(12)	C(2)-C(1)-Ir(1)	122.02(19)
P(1)-Ir(1)-H(2)	94.0(12)	C(3)-C(2)-C(1)	121.7(3)
P(2)-Ir(1)-H(2)	95.1(12)	C(3)-C(2)-C(7)	119.4(3)
H(1)-Ir(1)-H(2)	176.0(16)	C(1)-C(2)-C(7)	118.8(2)
C(7)-P(1)-C(13)	103.97(13)	C(4)-C(3)-C(2)	121.1(3)
C(7)-P(1)-C(9)	104.14(13)	C(3)-C(4)-C(5)	118.6(3)
C(13)-P(1)-C(9)	110.68(13)	C(4)-C(5)-C(6)	121.0(3)

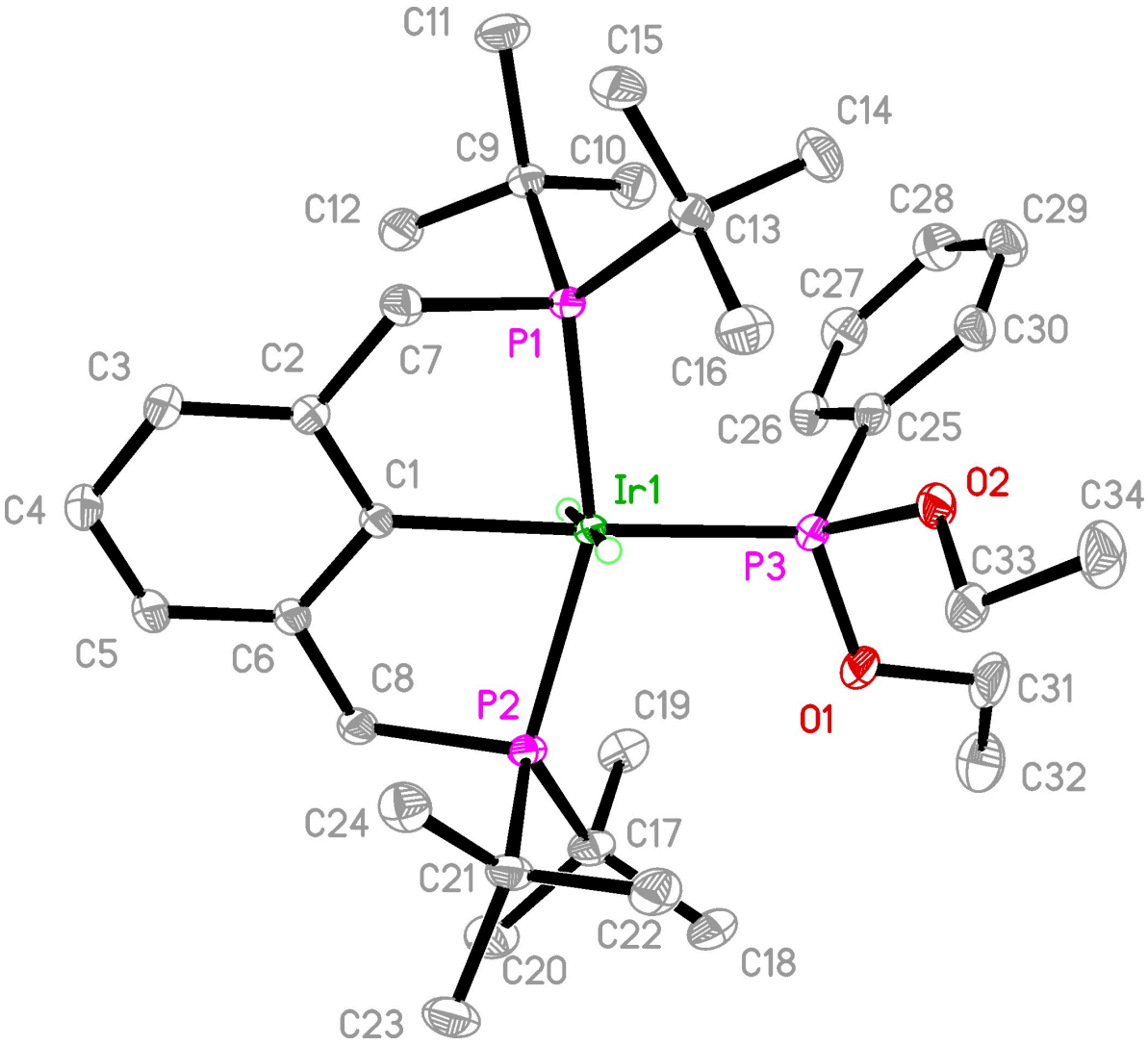

Figure 7-6 Crystal structure of (PCP)Ir(H_2)(PPhOEt_2)

Table 7.15 Crystal data and structure refinement for (PCP)Ir(H_2)(PPhOEt_2)

Empirical formula	C34 H60 Ir O2 P3	
Formula weight	785.93	
Temperature	100(2) K	
Wavelength	0.71073 Å	
Crystal system	Triclinic	
Space group	P-1	
Unit cell dimensions	a = 10.3024(6) Å	□= 91.522(1)°.
	b = 11.5351(6) Å	□= 107.357(1)°.
	c = 16.8658(9) Å	□ = 111.562(1)°.
Volume	1758.11(17) $Å^3$	
Z	2	
Density (calculated)	1.485 Mg/m^3	
Absorption coefficient	3.961 mm^{-1}	
F(000)	804	
Crystal size	0.36 x 0.05 x 0.03 mm^3	
Theta range for data collection	1.92 to 31.56°.	
Index ranges	-15<=h<=15, -16<=k<=16, -24<=l<=24	
Reflections collected	22063	
Independent reflections	11402 [R(int) = 0.0161]	
Completeness to theta = 31.56°	97.0 %	
Absorption correction	Semi-empirical from equivalents	
Max. and min. transmission	0.999 and 0.528	
Refinement method	Full-matrix least-squares on F^2	
Data / restraints / parameters	11402 / 2 / 383	
Goodness-of-fit on F^2	1.001	
Final R indices [I>2sigma(I)]	R1 = 0.0205, wR2 = 0.0500	
R indices (all data)	R1 = 0.0221, wR2 = 0.0508	
Largest diff. peak and hole	2.039 and -1.714 e.$Å^{-3}$	

Table 7.16 Selective bond lengths [Å] and angles [°] for (PCP)Ir(H_2)(PPhOEt_2)

Ir(1)-C(1)	2.1273(17)	C(3)-C(4)	1.385(3)
Ir(1)-P(3)	2.2733(5)	C(4)-C(5)	1.392(3)
Ir(1)-P(1)	2.3373(4)	C(5)-C(6)	1.393(2)
Ir(1)-P(2)	2.3418(5)	C(6)-C(8)	1.501(3)
Ir(1)-H(1)	1.593(10)	C(9)-C(11)	1.532(3)
Ir(1)-H(2)	1.598(10)	C(9)-C(10)	1.531(3)
P(1)-C(7)	1.8314(18)	C(9)-C(12)	1.539(3)
P(1)-C(9)	1.8949(18)	C(13)-C(14)	1.525(3)
P(1)-C(13)	1.8984(19)	C(13)-C(16)	1.536(3)
P(2)-C(8)	1.8381(18)	C(13)-C(15)	1.546(3)
P(2)-C(21)	1.8977(18)	C(17)-C(19)	1.536(3)
P(2)-C(17)	1.9027(19)	C(17)-C(18)	1.538(3)
C(1)-C(2)	1.406(2)	C(17)-C(20)	1.545(3)
C(1)-C(6)	1.408(2)	C(21)-C(22)	1.534(3)
C(2)-C(3)	1.396(2)	C(21)-C(24)	1.539(3)
C(2)-C(7)	1.494(2)	C(21)-C(23)	1.542(3)
C(1)-Ir(1)-P(3)	176.40(5)	C(9)-P(1)-C(13)	109.62(8)
C(1)-Ir(1)-P(1)	78.98(5)	C(7)-P(1)-Ir(1)	102.28(6)
P(3)-Ir(1)-P(1)	100.060(17)	C(9)-P(1)-Ir(1)	117.04(6)
C(1)-Ir(1)-P(2)	78.44(5)	C(13)-P(1)-Ir(1)	121.80(6)
P(3)-Ir(1)-P(2)	102.787(17)	C(8)-P(2)-C(21)	104.33(9)
P(1)-Ir(1)-P(2)	156.865(16)	C(8)-P(2)-C(17)	99.47(9)
C(1)-Ir(1)-H(1)	90.1(12)	C(21)-P(2)-C(17)	108.41(8)
P(3)-Ir(1)-H(1)	86.6(12)	C(8)-P(2)-Ir(1)	101.79(6)
P(1)-Ir(1)-H(1)	100.4(13)	C(21)-P(2)-Ir(1)	113.42(6)
P(2)-Ir(1)-H(1)	84.6(13)	C(17)-P(2)-Ir(1)	125.87(6)
C(1)-Ir(1)-H(2)	87.2(11)	C(2)-C(1)-C(6)	115.97(15)
P(3)-Ir(1)-H(2)	96.0(11)	C(2)-C(1)-Ir(1)	122.16(12)
P(1)-Ir(1)-H(2)	78.7(11)	C(6)-C(1)-Ir(1)	121.87(13)
P(2)-Ir(1)-H(2)	95.3(11)	C(3)-C(2)-C(1)	122.08(16)
H(1)-Ir(1)-H(2)	177.3(14)	C(3)-C(2)-C(7)	120.49(16)
C(7)-P(1)-C(9)	102.45(8)	C(1)-C(2)-C(7)	117.42(15)
C(7)-P(1)-C(13)	99.51(8)	C(4)-C(3)-C(2)	120.55(17)

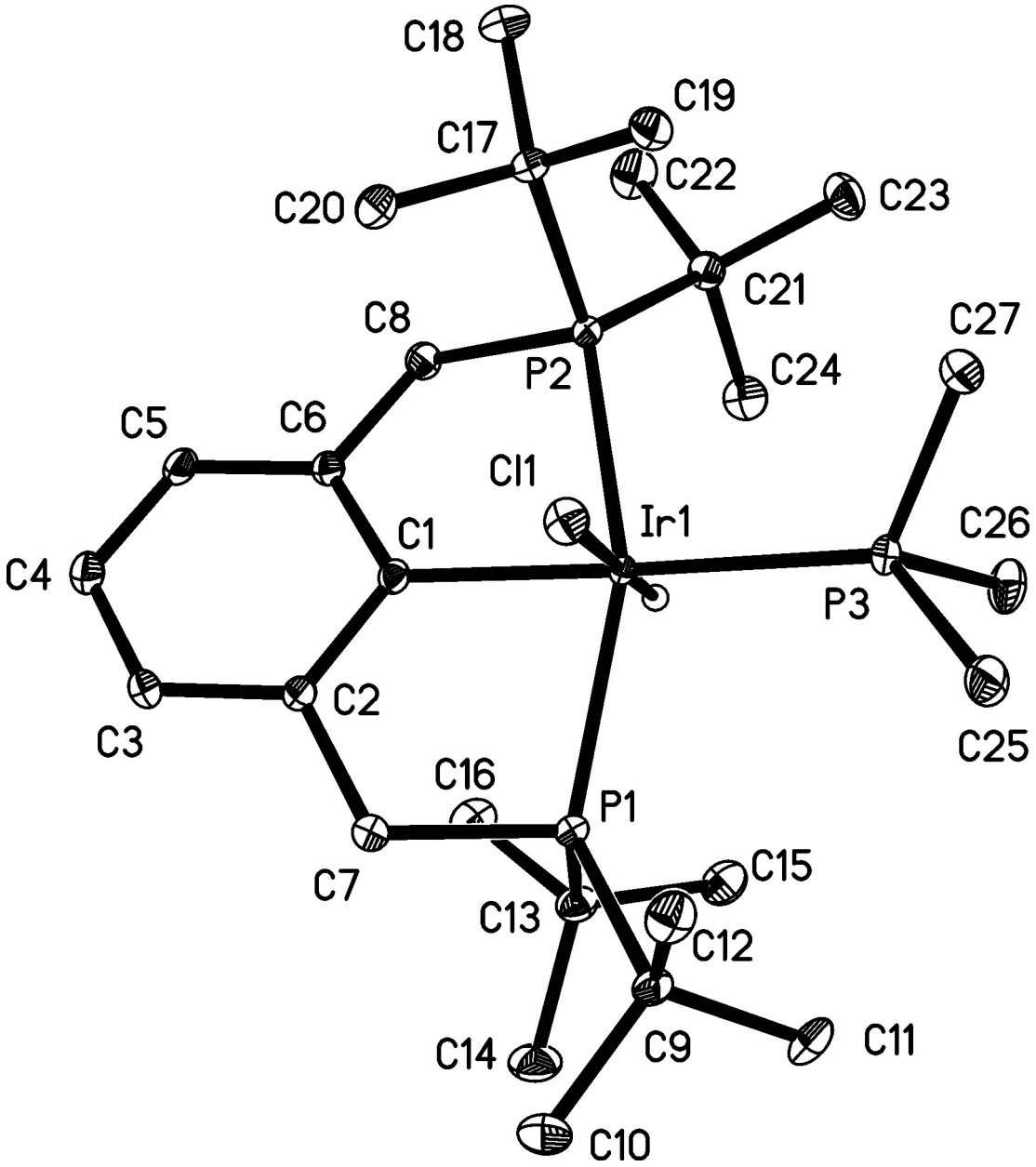

Figure 7-7 Crystal structure of (PCP)Ir(H)(Cl)(PMe_3)

Table 7.17 Crystal data and structure refinement for (PCP)Ir(H)(Cl)(PMe_3)

Empirical formula	C27 H53 Cl Ir P3	
Formula weight	698.25	
Temperature	100(2) K	
Wavelength	0.71073 Å	
Crystal system	Triclinic	
Space group	P-1	
Unit cell dimensions	a = 8.8621(4) Å	α= 75.239(1)°.
	b = 10.6164(5) Å	β= 76.134(1)°.
	c = 17.0269(8) Å	γ = 80.188(1)°.
Volume	1493.70(12) $Å^3$	
Z	2	
Density (calculated)	1.552 Mg/m^3	
Absorption coefficient	4.733 mm^{-1}	
F(000)	708	
Crystal size	0.41 x 0.23 x 0.19 mm^3	
Theta range for data collection	2.00 to 31.51°.	
Index ranges	-12<=h<=12, -14<=k<=15, -25<=l<=23	
Reflections collected	18860	
Independent reflections	9700 [R(int) = 0.0168]	
Completeness to theta = 31.51°	97.6 %	
Absorption correction	Semi-empirical from equivalents	
Max. and min. transmission	0.466 and 0.247	
Refinement method	Full-matrix least-squares on F^2	
Data / restraints / parameters	9700 / 1 / 309	
Goodness-of-fit on F^2	1.001	
Final R indices [I>2sigma(I)]	R1 = 0.0209, wR2 = 0.0488	
R indices (all data)	R1 = 0.0219, wR2 = 0.0493	
Extinction coefficient	0.00262(16)	
Largest diff. peak and hole	1.865 and -2.566 $e.Å^{-3}$	

Table 7.18 Selective bond lengths [Å] and angles [°] for (PCP)Ir(H)(Cl)(PMe_3)

Ir(1)-C(1)	2.1020(19)	C(2)-C(7)	1.502(3)
Ir(1)-P(2)	2.3625(5)	C(3)-C(4)	1.389(3)
Ir(1)-P(1)	2.3639(5)	C(3)-H(3)	0.9500
Ir(1)-P(3)	2.3754(5)	C(4)-C(5)	1.390(3)
Ir(1)-Cl(1)	2.5069(5)	C(5)-C(6)	1.398(3)
Ir(1)-H(1)	1.587(10)	C(5)-H(5)	0.9500
P(1)-C(7)	1.834(2)	C(6)-C(8)	1.495(3)
P(1)-C(9)	1.901(2)	C(9)-C(12)	1.536(3)
P(1)-C(13)	1.905(2)	C(9)-C(11)	1.540(3)
P(2)-C(8)	1.838(2)	C(9)-C(10)	1.547(3)
P(2)-C(17)	1.903(2)	C(13)-C(16)	1.536(3)
P(2)-C(21)	1.906(2)	C(13)-C(14)	1.540(3)
P(3)-C(27)	1.830(2)	C(13)-C(15)	1.541(3)
P(3)-C(26)	1.832(2)	C(17)-C(18)	1.534(3)
P(3)-C(25)	1.837(2)	C(17)-C(19)	1.535(3)
C(1)-C(6)	1.406(3)	C(17)-C(20)	1.537(3)
C(1)-C(2)	1.409(3)	C(21)-C(23)	1.533(3)
C(2)-C(3)	1.399(3)	C(21)-C(24)	1.537(3)
C(1)-Ir(1)-P(2)	79.96(5)	C(7)-P(1)-C(9)	99.45(9)
C(1)-Ir(1)-P(1)	78.41(5)	C(7)-P(1)-C(13)	106.50(9)
P(2)-Ir(1)-P(1)	154.714(17)	C(9)-P(1)-C(13)	108.26(9)
C(1)-Ir(1)-P(3)	176.42(5)	C(7)-P(1)-Ir(1)	101.07(7)
P(2)-Ir(1)-P(3)	99.501(18)	C(9)-P(1)-Ir(1)	127.83(7)
P(1)-Ir(1)-P(3)	102.880(18)	C(13)-P(1)-Ir(1)	110.85(7)
C(1)-Ir(1)-Cl(1)	90.16(5)	C(8)-P(2)-C(17)	101.30(9)
P(2)-Ir(1)-Cl(1)	99.720(17)	C(8)-P(2)-C(21)	99.18(9)
P(1)-Ir(1)-Cl(1)	93.302(17)	C(17)-P(2)-C(21)	110.71(9)
P(3)-Ir(1)-Cl(1)	86.437(17)	C(8)-P(2)-Ir(1)	101.22(7)
C(1)-Ir(1)-H(1)	90.4(12)	C(17)-P(2)-Ir(1)	119.23(7)
P(2)-Ir(1)-H(1)	80.5(13)	C(21)-P(2)-Ir(1)	120.12(7)
P(1)-Ir(1)-H(1)	86.7(13)	C(27)-P(3)-C(26)	102.52(11)
P(3)-Ir(1)-H(1)	93.0(12)	C(27)-P(3)-C(25)	94.41(10)
Cl(1)-Ir(1)-H(1)	179.4(13)	C(26)-P(3)-C(25)	99.38(11)

Chapter 8

Cleavage of alkyl carbon-oxygen bonds in esters by (PCP)Ir: C-O bond cleavage proceeding via oxidative addition of C-H bonds

Abstract

We herein report that precursors of "(PCP)Ir" (PCP = κ^3-2,6-(^{t}Bu$_2$PCH$_2$)$_2$C$_6$H$_3$) cleaves sp^3 C–O bonds of various esters (RCO$_2$R$_1$, R$_1$= alkyl) to give (PCP)Ir(R$_1$)(O$_2$CR) or, in cases where R$_1$ has a β-hydrogen, (PCP)Ir(H)(O$_2$CR) plus the corresponding alkene derived from R$_1$. Although the net reaction is a formal oxidative addition of the C-O bond (or what appears to be C-O oxidative addition followed by β-H elimination in the cases where R$_1$ has a β-hydrogen), the reaction does not proceed via simple oxidative addition of R$_1$–O$_2$CR to the iridium center. Instead, the reaction is proposed to proceed via a multi-step pathway that begins with C-H bond addition, and is followed by α or β-acetate elimination.

8.1 Introduction

Carbon–oxygen bond activation in esters promoted by transition-metal complexes has been interesting subject to organic and organometallic chemists.[1] While numerous studies of allyl–O bond cleavages in allyl esters and their applications (e.g. Tsuji–Trost reaction) have been reported, unreactive alkyl C–O cleavage has been relatively unexplored and is still challenging.[2, 3]

In allyl alkynoate, allyl–O cleavage is relatively facile due to the stability of π-allyl palladium intermediates formed in the oxidative addition of allylic alkynoate to the palladium center (Scheme 8-1).[4, 5]

To our knowledge, there are only two examples of alkyl C–O activation in esters by a transition-metal complex. In 1978, Tolman and Ittel reported that $Fe(Me_2PCH_2CH_2PMe_2)_2$ cleaves a C-O bond in certain esters to afford products from the HFe(naphthyl) ($Me_2PCH_2CH_2PMe_2$).[6] In the case of ethyl acetate, only C-H bond activation αto the ester carbonyl (complex **8-1a,** Fig 9-1) and for methyl acetate only 25% C-O bond cleavage (75% **8-1b** and 25 % **8-2a**) was observed. For methyl benzoate, only 70% C-O bond cleavage (complex **8-2b)** and for ethyl benzoate no C-O bond cleavage was reported.

Recently, Chirik *et al*. reported that (^{ipr}PDI)$Fe(N_2)_2$ (^{ipr}PDI = 2,6-(2,6-$^{i}Pr_2$-$C_6H_3N{=}CMe)_2C_5H_3N$)) cleaves the C–O bonds in alkyl-substituted esters via oxidative addition and proposed this reaction as a major catalyst decomposition pathway during catalytic olefin hydrogenation by this iron complex (Scheme 8-2).[7]

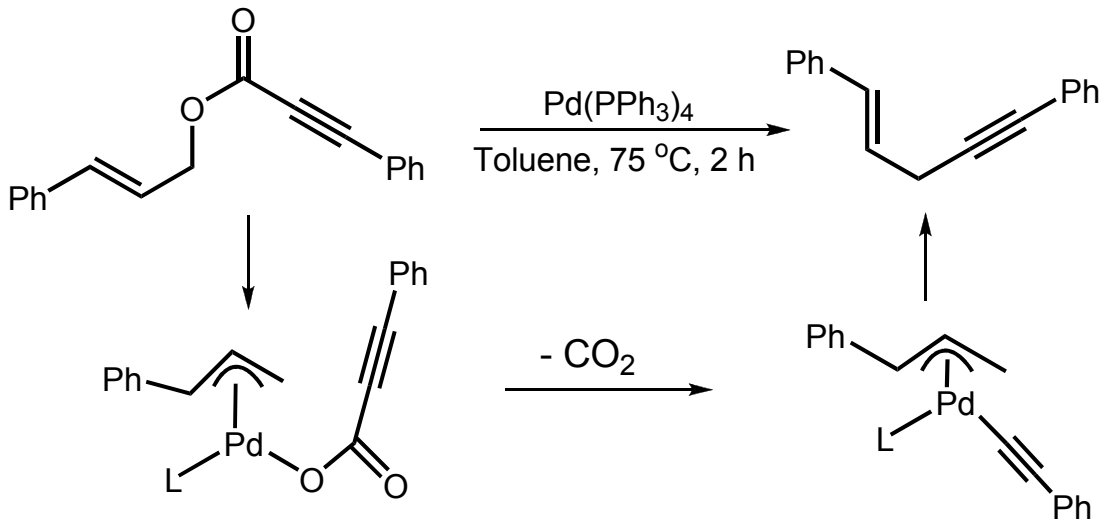

Scheme 8-1 Palladium-catalyzed allylic C-O bond activation in esters[4]

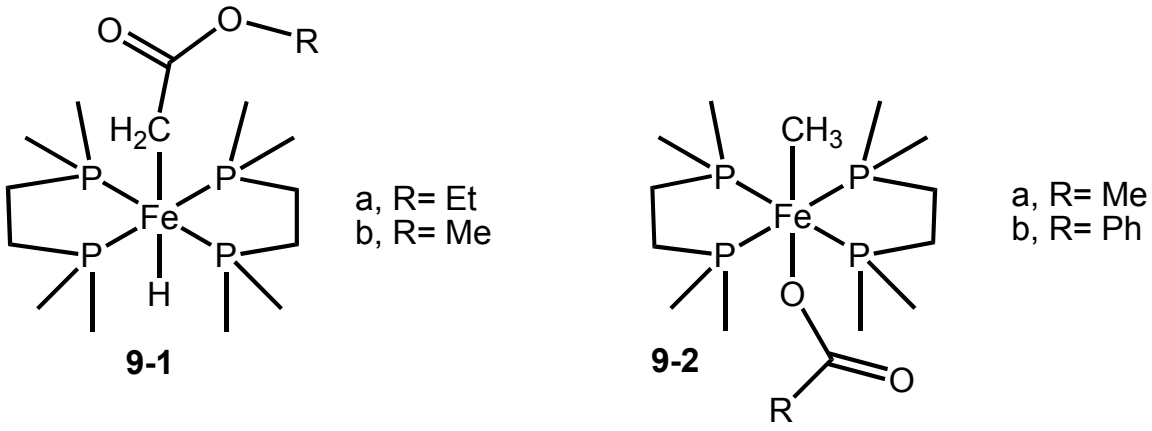

Figure 8-1 C-O and C-H activation using $Fe(Me_2PCH_2CH_2PMe_2)_2$[6]

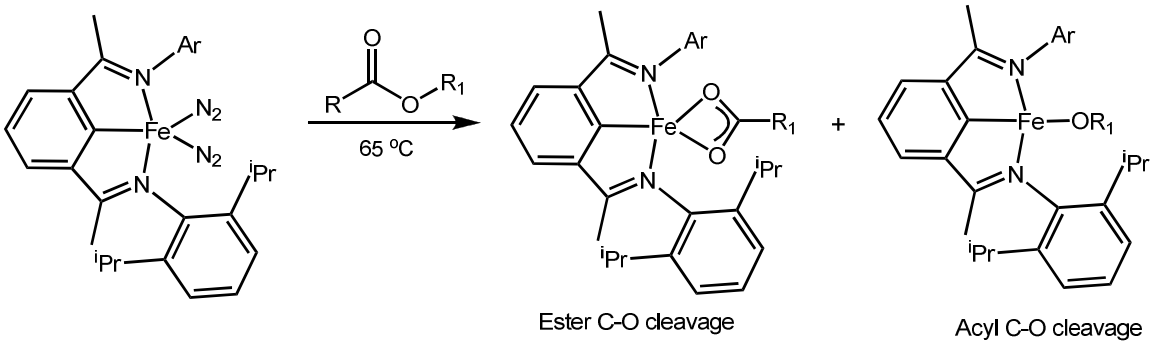

Scheme 8-2 Iron-catalyzed C-O bond activation[7]

In this chapter we discuss alkyl C–O bond cleavage in esters by a (PCP)Ir complex. Mechanistic investigations suggest that the reaction does not proceed via simple oxidative addition of $R_1–O_2CR$ to the iridium center; the reaction instead proceeds via a multi- step pathway.

8.2 Results

8.2.1 Reaction of (PCP)Ir with methyl benzoate and methyl acetate

The precursor complex (PCP)Ir(NBE) (NBE = norbornene) complex reacts with methyl benzoate and methyl acetate at room temperature to form the C-H activated 6-coordinate complexes **8-6** and **8-7** respectively (Scheme 8-3). Complexes **8-6** and **8-7** were characterized by NMR spectroscopy. Complex **8-6** is presumably formed by C-H activation of the sp^2 C-H bond (more easily to activate than sp^3 C-H bonds) and coordination of ester oxygen to the metal center (Scheme 8-3). In contrast, complex **8-7** presumably results from C-H activation of the acyl methyl group followed by coordination of ester oxygen to the metal center (Scheme 8-3). Heating complexes **8-6**

and **8-7** at 80 °C generated complexes **8-4a** and **8-4b,** most likely formed by cleavage of the ester H_3C-O bond followed by inserting into (PCP) *ipso*-carbon and iridium center (Scheme 8-4).

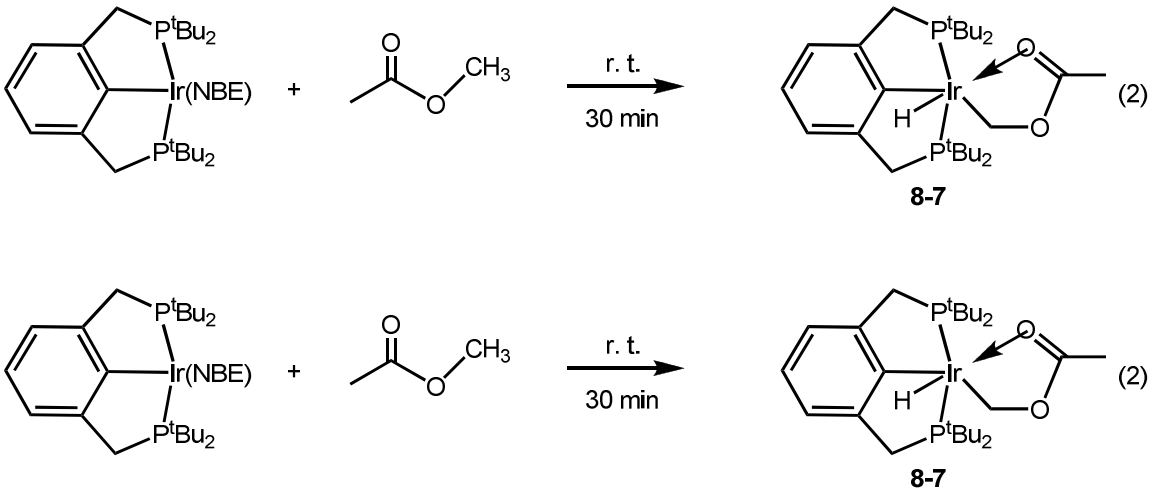

Scheme 8-3 Initial reaction of (PCP)Ir(NBE) with methyl benzoate and methyl acetate

Complexes **8-4a** and **8-4b** were characterized by NMR spectroscopy and X-ray crystallography. In the ^{1}H NMR spectrum, the signal Ir-**CH_2-**Ar appeared as a triplet at 2.28 ppm (J_{PH} = 9.8 Hz) (**8-4a**) or 2.17 ppm (J_{PH} = 9.5 Hz) (**8-4b**), and in the ^{13}C NMR spectrum as a triplet at –17.7 ppm (J_{CP} = 5.2 Hz) (**8-4a**) or –17.9 ppm (J_{CP} = 5.1 Hz) (**8-4b**). Hydride appeared as triplet at –32.8 ppm (J_{PH} = 12.5 Hz) (**8-4a**), –32.9 ppm (J_{PH} = 12.9 Hz) (**8-4b**).

Complex **8-4a** was crystallized from *n*-hexane/benzene solution and the structure was confirmed by X-ray crystallography. Figure 8-2 displays an ORTEP diagram of this

complex, structure refinement parameters are given in Table 8.1 and selected bond angles and bond distances are listed in Table 8.2.[8]

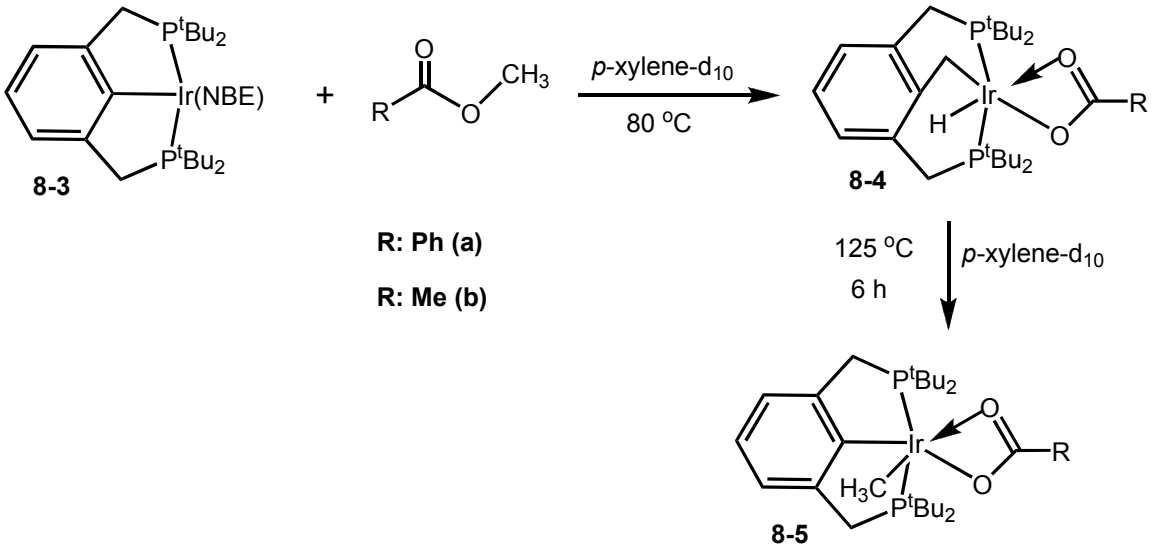

Scheme 8-4 Overall reaction

Heating complexes **8-4 (a, b)** at 125 °C results in cleavage of C-C bond and generation of complexes **8-5 (a, b)**. Complexes **8-5 (a, b),** were characterized by NMR spectroscopy and X-ray crystallography. In the ^{1}H NMR spectrum, the Ir-***CH$_3$*** signal appears as triplet at 1.45 ppm (J_{PH} = 4.8 Hz) (**8-5a**) or 1.30 ppm (J_{PH} = 4.7 Hz) (**8-5b**), and in the ^{13}C NMR spectrum as a triplet at –29.1 ppm (J_{CP} = 4.6 Hz) (**8-5a**). Complex **8-5a** was crystallized from *n*-hexane and the structure was confirmed by X-ray crystallography. Figure 8-3 displays the ORTEP of this complex, refinement parameters are given in Table 8.3 and selected bond angles and bond distance are listed in Table 8.4.[8]

In 1996, Milstein *et al*. reported that at room temperature in benzene, [Ir(COE)$_2$Cl]$_2$ reacts with 1,3-bis[(di-*tert*-butylphosphino)methyl]-2,4,6-trimethylbenzene (**8-12**) to form two products, **8-13** which was the C-H activated complex and **8-14** (the C-C activated complex), in 2:1 ratio (Scheme 8-4).[9] Complex **8-13** was converted to

complex **8-14**, by heating at 100 °C in benzene which is similar to the conversion of complex **8-4** to complex **8-5** by heating.

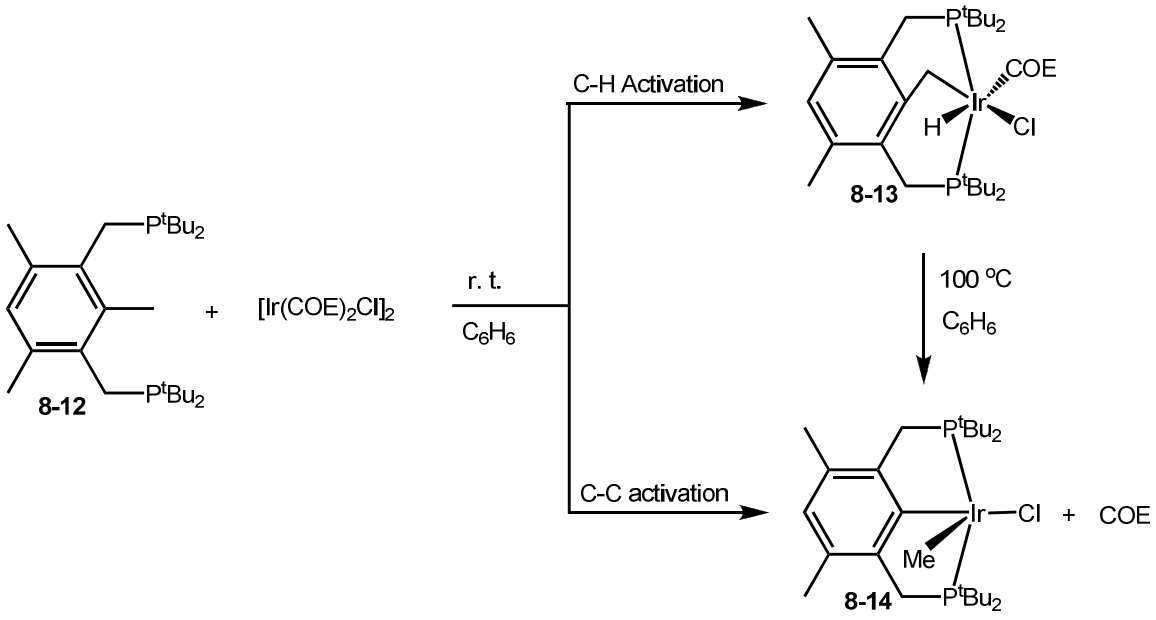

Scheme 8-5 Reaction of $[Ir(COE)_2Cl]_2$ with **8-12**

8.2.2 Reaction of (PCP)IrH$_4$ with ethyl acetate and ethyl benzoate

At room temperature, in *p*-xylene-d_{10}, PCP)IrH$_4$ in the presence of t-butyl ethylene (TBE) reacts with the esters having β-hydrogen, ethyl acetate and ethyl benzoate to form ethylene and complexes **8-8** and **8-9** respectively (eq. 3 and 4). Ethylene was identified by G.C. and NMR spectroscopy, while complexes **8-8** and **8-9** were characterized by NMR spectroscopy and X-ray crystallography.

In the ^{1}H NMR spectrum, the Ir-H signal appeared as a triplet at -29.76 ppm (J_{PH} = 13.3 Hz) (**8-8**), -29.56 ppm (J_{PH} = 13.3 Hz) (**8-9**), while in the ^{31}P NMR spectrum, complexes **8-8** and **8-9** appeared as singlets at 60.4 and 60.5 ppm. Complexes **8-8** and **8-9**

were crystallized from *n*-hexane and the structure was confirmed by X-ray crystallography. Figure 8-4 and 8-5 displays the ORTEPs of complexes **8-8** and **8-9**, respectively, refinement parameters are given in Tables 8.5 and 8.7 and selected bond angles and bond distances are listed in Tables 8.6 and 8.8.

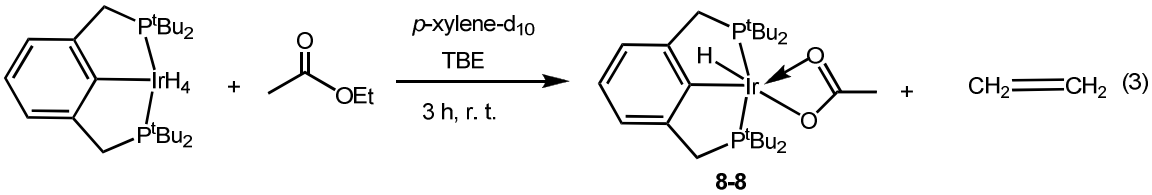

8-8

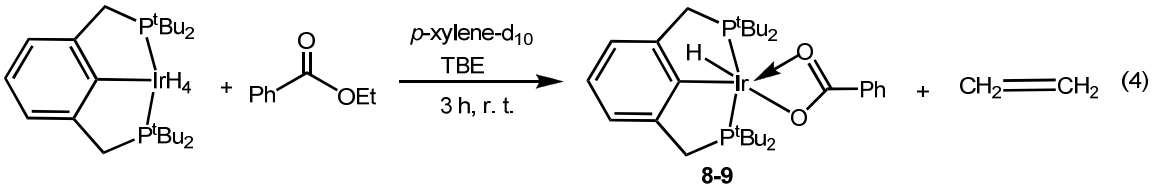

8-9

8.2.3 Reaction of (PCP)IrH$_4$ with other esters having β-hydrogen

We have tested various other esters possessing β-C–H bonds to react with (PCP)Ir such as *iso*-propyl, *iso*-butyl, cyclohexyl acetate and *tert*-butyl acetate. All these esters react with (PCP)Ir to form complex **8-8** and corresponding alkenes (Scheme 8-5). After 3 h heating at 70 °C, respectively 50 % and 70 % conversion of starting (PCP)IrH$_4$ was observed in case of t*ert*-butyl and *iso*-butyl acetate; this rate of reaction was slower than *iso*-propyl acetate (100 % conversion at room temperature after 3 h). In the same condition (3 h heating at 70 °C) only 5 % C-O bond cleavage was observed in case of cyclohexyl acetate. Complex **8-8** was characterized by NMR spectroscopy and X-ray crystallography and all alkenes were identified by GC.

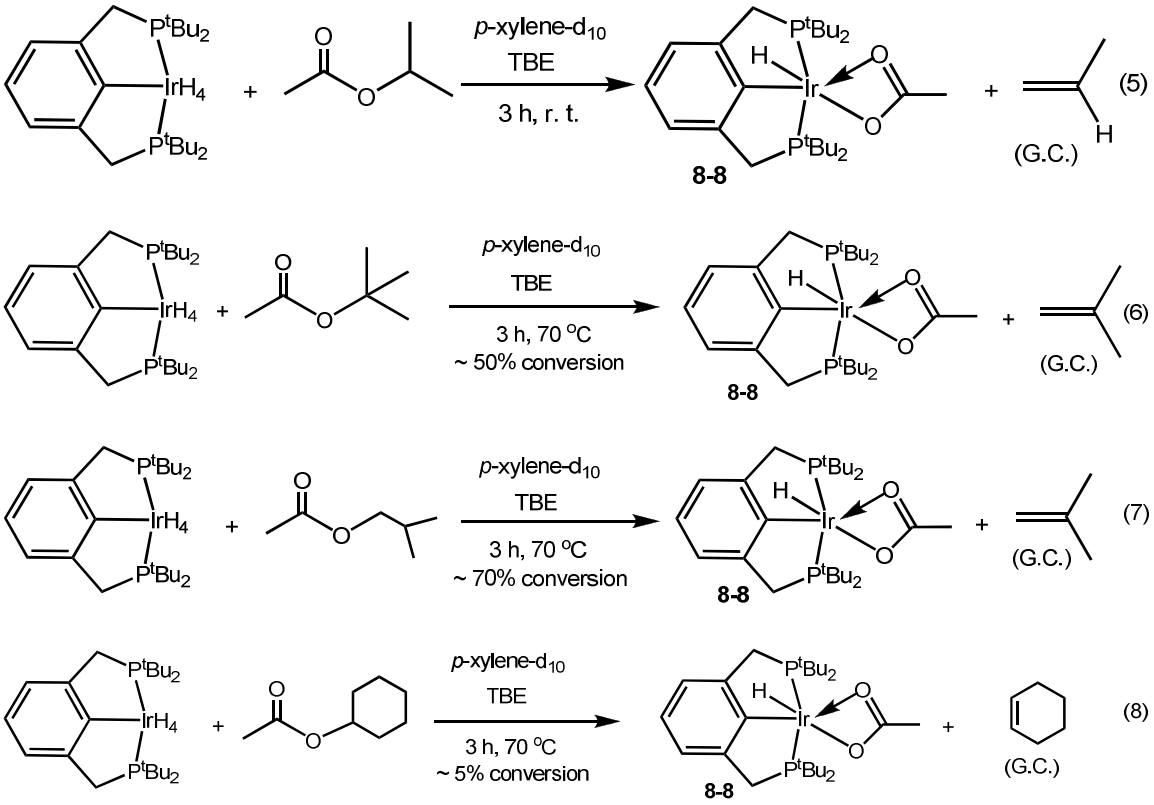

Scheme 8-6 Reaction of (PCP)IrH$_4$ with other esters

8.2.4 Reaction of (PCP)Ir with benzyl acetate

(PCP)IrH$_4$ in the presence of t-butyl ethylene (TBE) reacts with benzyl acetate at room temperature to form complex **8-10** (eq. 9). No intermediate was observed. Complex **8-10** was characterized by NMR spectroscopy. In the ^{1}H NMR spectroscopy, Ir-***CH$_2$***Ph signal appeared as triplet at 3.13 ppm (J_{PH} = 3.2 Hz) and in the ^{13}C NMR spectrum as a triplet at -16.8 (J_{CP} = 5.3 Hz).

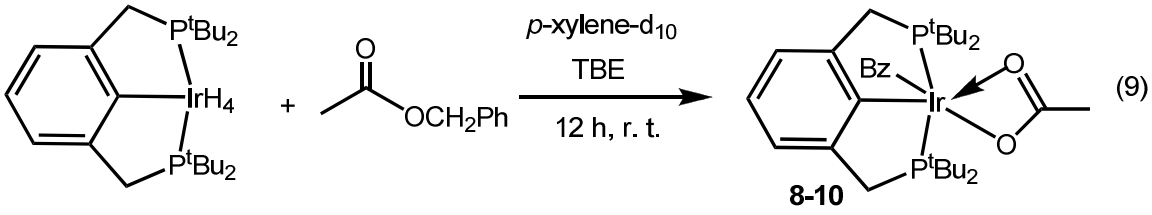

(9)

8.2.5 Reaction of (PCP)IrH$_4$ with phenyl acetate

(PCP)IrH$_4$ in the presence of t-butyl ethylene (TBE) reacts with phenyl acetate at room temperature to afford complex **8-11**, presumably formed by C-H activation of the phenyl ring and coordination of the ester carbonyl group to the metal center (Scheme 8-6). Complex **8-11** was characterized by NMR spectroscopy and X-ray crystallography. No identifiable C-O bond activated product was observed even after heating **8-11** at 100 °C for two hours, though unknown compounds were observed in low concentrations. In the ^{1}H NMR spectrum, Ir-***H*** signal appeared as a triplet at -27.27 ppm (J_{PH} = 16.4 Hz) and in the ^{31}P NMR spectrum, **8-11** appeared as a singlet at 55.6 ppm. Complex **8-11** was crystallized from hexane and the structure was confirmed by X-ray crystallography. The ORTEP is given in Figure 8-6 and refined parameters and bond angles and distances are listed in Tables 8.9 and 8.10, respectively.

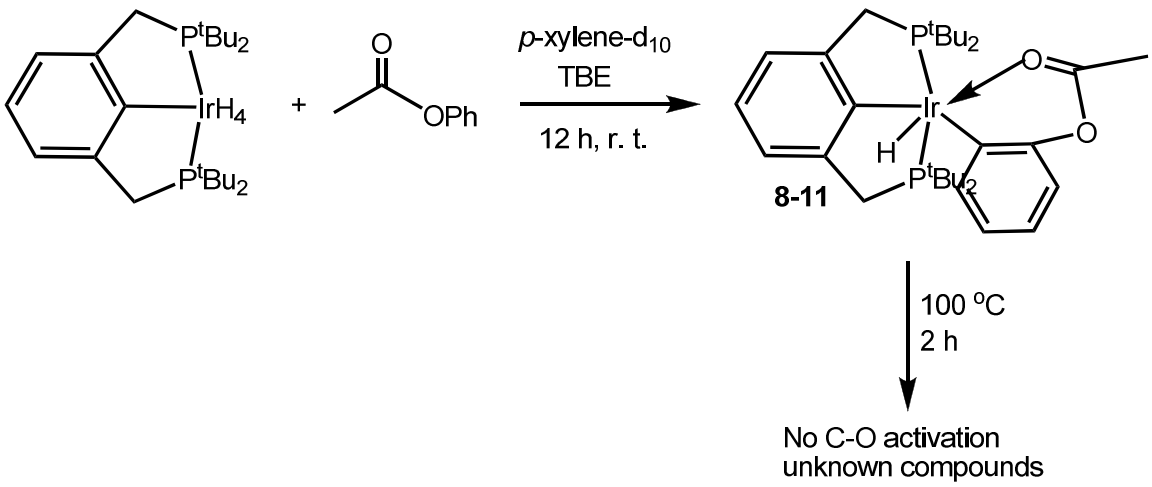

Scheme 8-7 Reaction of (PCP)IrH$_4$ with phenyl acetate

8.3 Discussion

Reaction of (PCP)Ir with ester having β-hydrogen is different from ester having no β-hydrogen. In case of ester having β-hydrogen, the reaction [with (PCP)Ir] is fast, no intermediate was detected and we observed complex **8-8** and corresponding alkene. In contrast, ester having no β-hydrogen, initially chelated product (**8-7**) was detected. Heating this complex results in formation of complex **8-5b**. This indicates presumably different mechanism is involved in the reaction of these types of esters (having β-hydrogen or having no β-hydrogen).

A competition experiment was carried out with a 1:1 mixture of methyl acetate and ethyl acetate in order to determine which ester reacts faster. In this experiment only complex **8-8** and ethylene were observed; this clearly indicates C-O bond activation of

ethyl acetate is much faster than methyl acetate (eq. 10). Competitive reaction was done with complex **8-7** (formed initially with methyl acetate) to rule out the possibility that due to stable intermediate (**8-7**) methyl acetate reacts slowly (Scheme 8-7).[8]

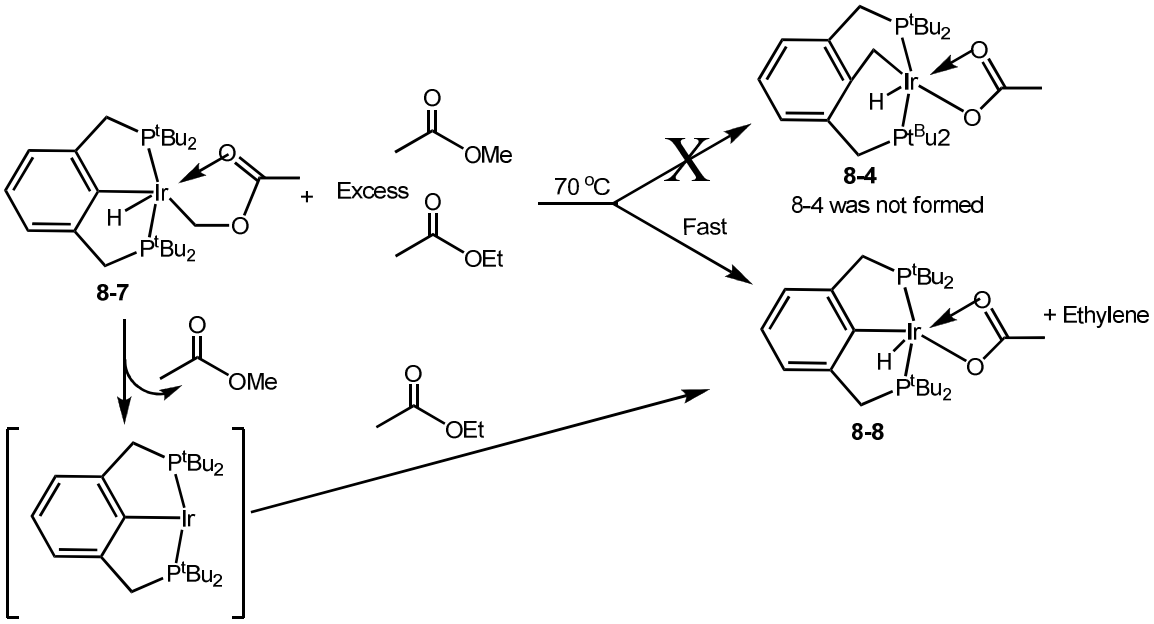

Scheme 8-8 Competition experiment with mixture of methyl acetate and ethyl acetate

In the C-O bond activation of ester having a β-hydrogen two mechanisms are possible; one is direct C-O bond activation followed by β-hydrogen elimination and the other is C-H activation followed by β-acetate elimination.

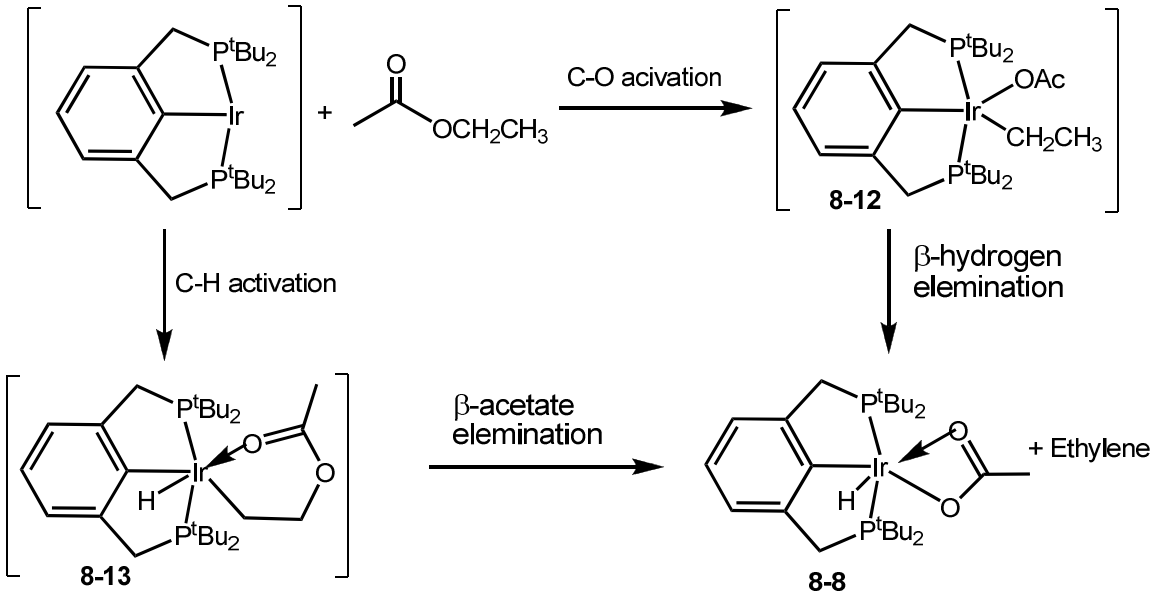

Scheme 8-9 Possible mechanism for ester having β-hydrogen

C-O activation of ester having no β-hydrogen can proceed via two possible pathways; α–acetate elimination (Scheme 8-9) or direct C-O activation (Scheme 8-10). In α–acetate elimination, initial C-H activation is followed by slow α-acetate elimination to form carbene intermediate. The methylidine group then inserts into the PCP-Ir bond, and finally, C-C bond cleavage generated the final product **8-5b** (Scheme 8-9). The other possible mechanism is direct C-O bond activation followed by C-H activation to form carbene intermediate. The methylidine group then inserts into the PCP-Ir bond (Scheme 8-10). In reaction of methyl acetate with (PCP)IrH_4 in presence of TBE, after heating 5 h at 80 °C, only complex **8-4b** was observed. Heating complexes **8-4b** 4 h at 125 °C results in cleavage of C-C bond and generation of complexes **8-5b**. This clearly indicates that complexes **8-5b** is thermodynamically more stable that complexes **8-4b**. So formation of

complexes **8-4b** from complexes **8-5b** is not possible; thus we can rule out direct C-O activation mechanism.

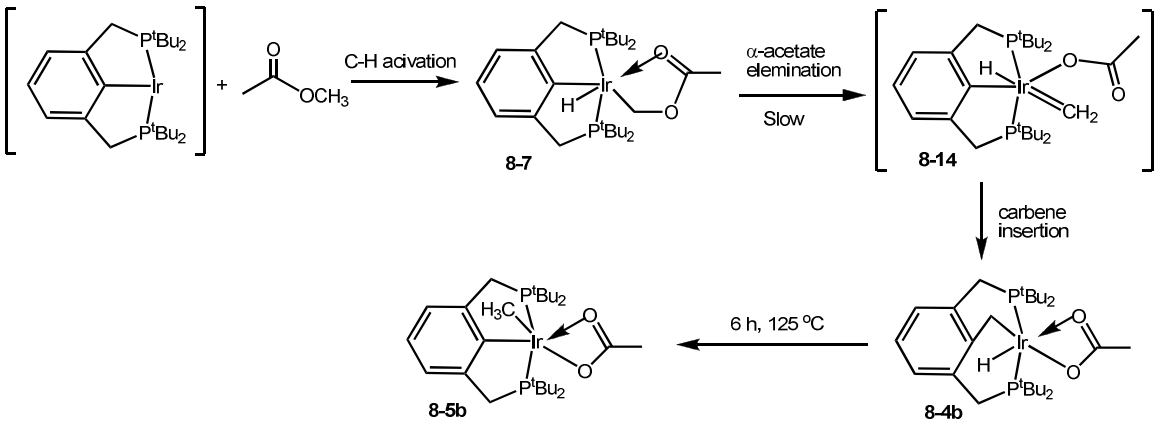

Scheme 8-10 Proposed α–acetate elimination

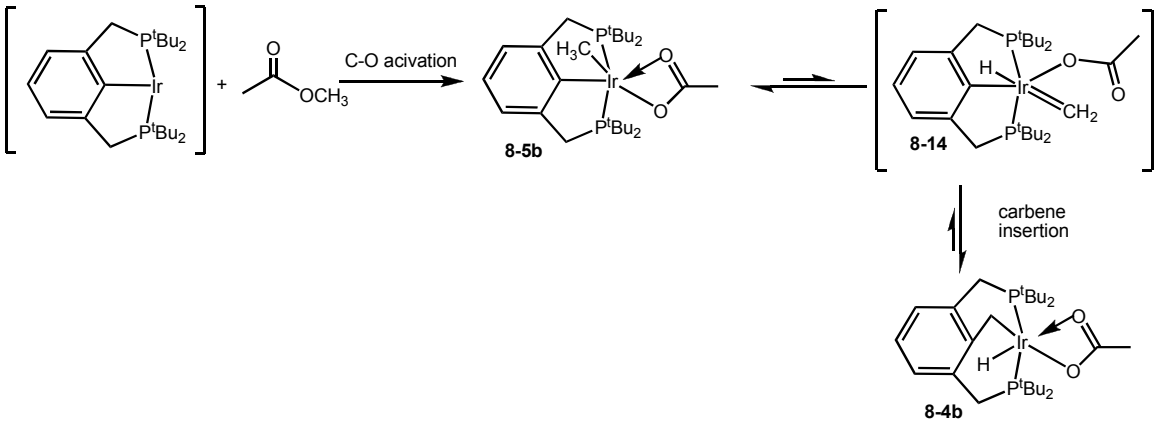

Scheme 8-11 Proposed direct C-O activation

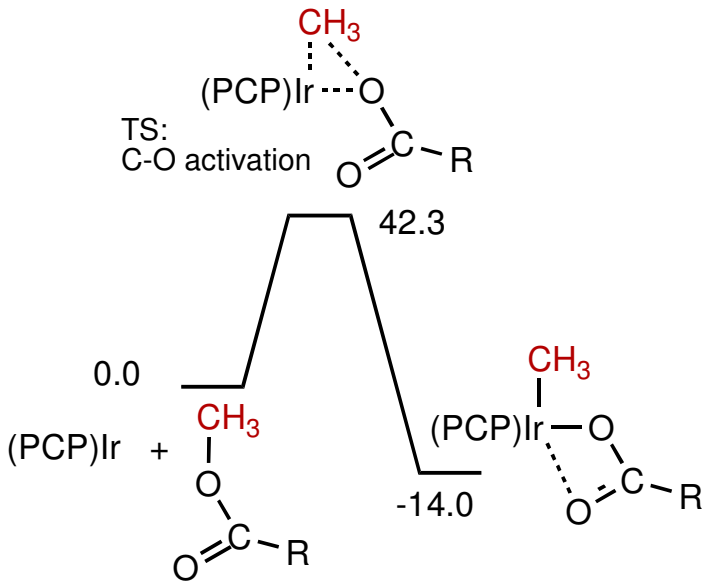

Scheme 8-12 Barrier for direct C-O bond activation[10]

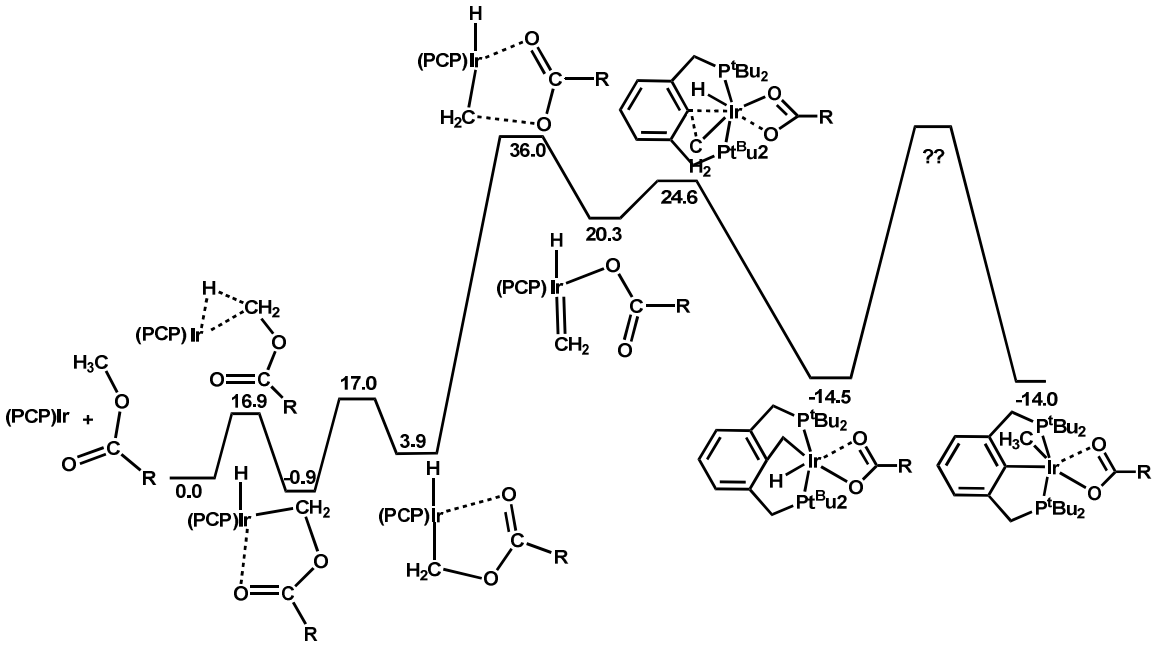

Scheme 8-13 DFT calculation for C-O bond cleavage in ester having no β-hydrogen[10]

The calculated free energy barrier for direct C-O bond activation of methyl acetate is quite high, 42.3 kcal/mol (Scheme 8-11). In the DFT calculation, overall free energy barrier for direct C-O bond activation of methyl acetate,e following α-acetate elimination, is 37 kcal/mol (Scheme 8-11), which is much lower than direct C-O bond activation.

In order to test the hypothesis that a carbene intermediate is formed in the reaction of ester having no β-hydrogen, methoxymethyl acetate was used as a substrate, as it contains no β-hydrogens and possesses an electron donating methoxy group which would stabilize the carbene intermediate (**8-14**). At room temperature in presence of TBE, (PCP)IrH_4 was allowed to react with 0.5 equivalents of $MeOCH_2OAc$ and approximately 1:1 ratio of complexes **8-8** and **8-15** were formed (Scheme 8-13). Complex **8-8** is presumably formed by reaction of acetic acid (generated from intermediate **8-14**) with the starting complex, (PCP)Ir(H)(TBV) (formed by binding TBE to (PCP)IrH_4). The carbene complex **8-15** was characterized by NMR (^{1}H, ^{13}C and NOE) spectroscopy.[8]

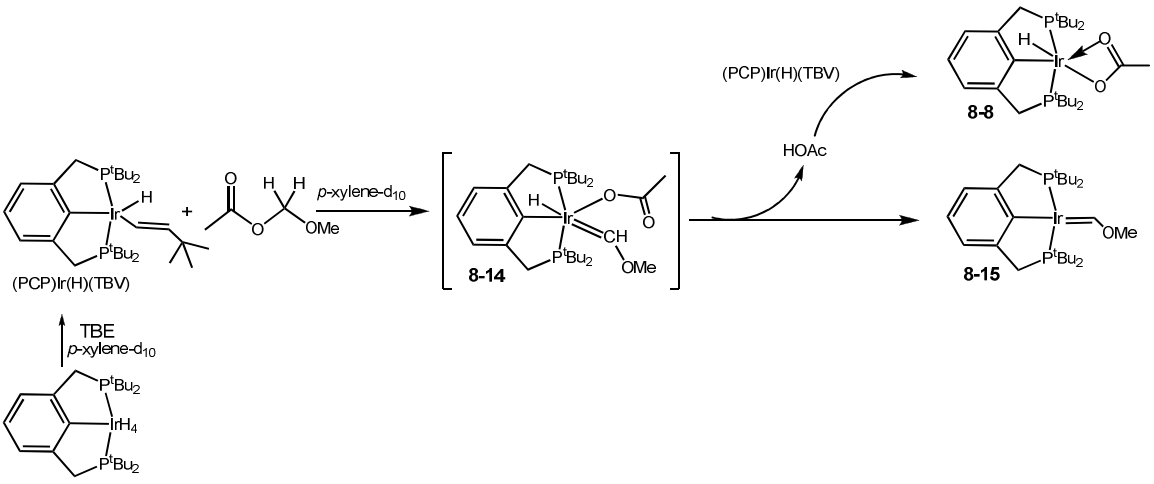

Scheme 8-14 Reaction with methoxymethyl acetate

In contrast to the stable carbene generated from methoxymethyl acetate, the use of acetoxy acetone should produce an acetyl carbene, which would be destabilized relative to the Schrock carbenes. At room temperature, (PCP)Ir(H)(TBV) was found to react with acetoxy acetone to yield the C-H activated complex **8-16** (Scheme 8-15), yet no C-O activated product was observed, even after heating complex **8-16** 4 days at 125 °C. Complex **8-16** was characterized by NMR spectroscopy and X-ray crystallography. Figure 8-6 shows an ORTEP of this complex, refinement parameters are given in Table 8.11 and bond angles and bond distances are listed in Table 8.12.

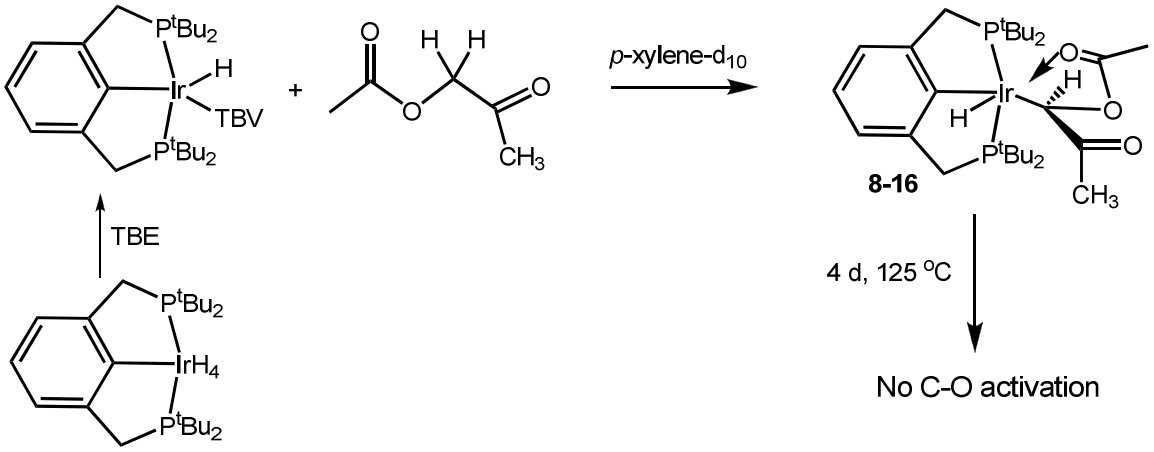

Scheme 8-15 Reaction with acetoxy acetone

Brookhart *et al.* have reported a study in which a series of Ni complexes containing β-acetate groups decomposed at much faster rates than Ni complexes containing α-acetate group.[11] This suggests that β-acetate elimination is much faster than α-acetate elimination. This explains why ester having a β-hydrogen reacts so fast

compared to ester having no β-hydrogen. Cyclohexyl and *tert*-butyl acetate reacts slowly although they have β-hydrogen, due to steric hindrance by the bulky cyclohexyl and *tert*-butyl groups. The reaction with benzyl acetate is faster than the methyl acetate, although both of them follow α-acetate elimination. This is due to absence of stable chelation intermediate in benzyl acetate to slow down the reaction and the formation of relatively more stable transient metal carbene complex (**8-17**).

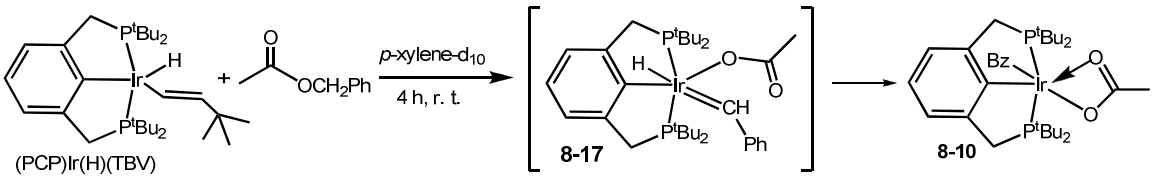

Scheme 8-16 Proposed reaction mechanism with benzyl acetate

8.4 Experimental

General Methods. All reactions were carried out under an argon atmosphere using standard Schlenk techniques or in an argon-filled dry box. All esters were purchased from Aldrich and degassed by sparging with argon. *p*-Xylene, *p*-xylene-d_{10}, TBE and C_6D_6 were dried using Na/K alloy and collected by vacuum transfer. TBE was dried under Na/K alloy and vacuum transferred under argon. All esters were degassed and used. NBE was sublimed before use. 400 MHz or 500 MHz Varian instruments were used for ^{1}H, ^{13}C and ^{31}P NMR spectroscopy. The residual peak of the deuterated solvent was used as a reference for ^{1}H chemical shifts. ^{31}P NMR chemical shifts were referenced to a capillary PMe_3 standard (–62.2 ppm). (^{tBu4}PCP)IrH_4 was prepared as described in the literature.[12]

(PCP)-CH_2-Ir(H)(O_2CPh) (**8-4a**): To a 0.5 mL *p*-xylene-d_{10} solution of 5 mg (PCP)IrH_4 (0.0083 mmol) in a J-Young tube, 2.4 mg NBE (0.025 mmol) and 1.1 μL methyl benzoate (0.0083 mmol) were added. After 30 minutes at r. t., complex **8-6** was quantitatively formed. The mixture was subsequently heated at 80 °C for 5 h. The solvent was then removed under vacuum. The bright yellow powder was obtained in quantitative yield. This powder was washed with a minimal amount of hexane twice and dried under vacuum. An X-ray quality crystal was obtained by slow evaporation of a hexane/benzene mixture. ^{31}P NMR (C_6D_6, 202 MHz): δ 84.82 (d, 11.8 Hz) ^{1}H NMR (C_6D_6, 500 MHz): δ 8.31 (d, 2H, Ar), 7.10 (m, 3H, Ar), 6.88 (d, 2H, PCP), 6.73 (t, 1H, PCP), 2.92 (d of vt, J_{PH} = 3.5 Hz, J_{HH} =14.5 Hz, 2H, C***H***$_2$P), 2.83 (d of vt, J_{PH} = 3.5 Hz, J_{HH} = 14.5 Hz, 2H, C***H***$_2$P), 2.28 (t, J_{PH} = 9.8 Hz, 2H, C***H***$_2$Ir), 1.34 (t, 6.0 Hz, 18H, PC(C***H***$_3$)$_3$), 1.08 (t, 6.0 Hz, 18H, PC(C***H***$_3$)$_3$), -32.76 (t, 12.5 Hz, 1H, Ir***H***) ^{13}C NMR (C_6D_6, 100 MHz): δ 179.2 (s, ***C***(O)), 158.8 (t, 5.8 Hz, PCP), 136.4 (s, Ar), 131.2 (s, Ar), 129.7 (t, 2.4 Hz, PCP), 128.8 (s, Ar), 127.7 (t, 2.9 Hz, PCP), 119.9 (s, PCP), 38.2 (vt, J_{CP} = 4.7 Hz, P***C***$(CH_3)_3$), 38.0 (vt, J_{CP} = 9.8 Hz, P***C***$(CH_3)_3$), 29.9 (vt, J_{CP} = 2.4 Hz, PC(***C***$H_3)_3$), 29.3 (vt, J_{CP} = 2.5 Hz, PC(***C***$H_3)_3$), 29.0 (vt, J_{CP} = 12.2 Hz, ***C***H_2P), -17.7 (t, J_{CP} = 5.2 Hz, PCP–***C***H_2–Ir).

(PCP)-CH_2-Ir(H)(O_2CMe) (**8-4b**): To a 0.5 mL *p*-xylene-d_{10} solution of 5 mg (PCP)IrH_4 (0.0083 mmol) in a J-Young tube, 2.4 mg NBE (0.025 mmol) and 0.7μL methyl acetate (0.0083 mmol) were added. After 30 minutes at r. t., complex **9-7** was formed. The solution was then heated at 80 °C for 5 h and then the solvent was removed under vacuum to yield a bright yellow powder that was washed with a minimal amount of

hexane twice and dried under vacuum. An X-ray quality crystal was obtained by slow evaporation of a hexane/benzene mixture (3:1). ^{31}P NMR (*p*-xylene-d_{10}, 161.9 MHz): δ 84.51 (d, 10.0 Hz) ^{1}H NMR (C_6D_6, 500 MHz): δ 6.86 (d, 2H, PCP), 6.71 (t, 1H, PCP), 2.91 (d of vt, J_{PH} = 3.5 Hz, J_{HH} = 14.5 Hz, 2H, C***H***$_2$P), 2.79 (d of vt, J_{PH} = 3.5 Hz, J_{HH} = 14.5 Hz, 2H, C***H***$_2$P), 2.17 (t, 9.5 Hz, 2H, C***H***$_2$Ir), 1.87 (s, 3H, C(O)C***H***$_3$), 1.40 (t, 6.0 Hz, 18H, PC(C***H***$_3$)$_3$), 1.05 (t, 6.0 Hz, 18H, PC(C***H***$_3$)$_3$), -32.90 (t, 12.5 Hz, 1H, Ir***H***) ^{13}C NMR (C_6D_6, 100 MHz): δ 183.3 (s, ***C***(O)), 158.8 (t, 5.8 Hz, PCP), 129.5 (t, 2.4 Hz, PCP), 127.6 (t, 2.9 Hz, PCP), 119.8 (s, PCP), 38.1 (vt, J_{CP} = 4.5 Hz, P***C***(CH$_3$)$_3$), 38.0 (vt, $J_{C\,P}$= 9.9 Hz, P***C***(CH$_3$)$_3$), 29.9 (vt, J_{CP} = 2.3 Hz, PC(***C***H$_3$)$_3$), 29.3 (vt, J_{CP} = 2.5 Hz, PC(***C***H$_3$)$_3$), 29.0 (vt, J_{CP} = 12.3 Hz, ***C***H$_2$P), 25.2 (s, C(O)***C***H$_3$), -17.9 (t, J_{CP} = 5.1 Hz, PCP–***C***H$_2$–Ir).

(PCP)Ir(CH$_3$)(O$_2$CPh) (8-5a): A 0.5 mL *p*-xylene-d_{10} solution of **8-4a** (5 mg) was placed in a J-Young tube and heated at 125 °C for 5 hours, at which point **9-4a** had completely converted to **9-5a** (85 % yield by ^{31}P NMR). An X-ray quality crystal was obtained from slow evaporation of a hexane solution. ^{31}P NMR (C_6D_6, 202 MHz): δ 35.57 (s) ^{1}H NMR (C_6D_6, 500 MHz): δ 8.33 (d, 2H, Ar), 7.17 (m, 1H, Ar), 7.11 (m, 2H, Ar), 7.01 (d, 2H, PCP), 6.91 (t, 1H, PCP), 3.05 (d of vt, J_{PH} = 3.8 Hz, J_{HH} = 16.5 Hz, 2H, C***H***$_2$P), 2.98 (d of vt, J_{PH} = 4.0 Hz, J_{HH} = 16.5 Hz, 2H, C***H***$_2$P), 1.45 (t, 4.8 Hz, 3H, IrC***H***$_3$), 1.31 (t, 6.0 Hz, 18H, PC(C***H***$_3$)$_3$), 1.21 (t, 6.3 Hz, 18H, PC(C***H***$_3$)$_3$) ^{13}C NMR (C_6D_6, 125 MHz): δ 176.9 (s, ***C***(O)), 148.4 (t, 7.3 Hz, PCP), 142.4 (s), 136.5 (s), 131.3 (s), 129.3 (s), 121.1 (s), 121.0 (t, 8.1 Hz, PCP), 38.6 (vt, J_{CP} = 11.0 Hz, P***C***(CH$_3$)$_3$), 36.0 (vt, J_{CP} = 8.3 Hz, P***C***(CH$_3$)$_3$), 32.2 (vt, J_{CP} = 12.5 Hz, ***C***H$_2$P) 31.1 (vt, J_{CP} = 2.3 Hz, PC(***C***H$_3$)$_3$), 30.2 (vt, J_{CP} = 2.3 Hz, PC(***C***H$_3$)$_3$), -29.1 (t, J_{CP} = 4.6 Hz, Ir–***C***H$_3$).

(PCP)Ir(CH_3)(O_2CMe) (8-5b): A 0.5 mL *p*-xylene-d_{10} solution of **8-4b** (5 mg) was placed in a J-Young tube and heated at 125 °C for 5 hours. The reaction was monitored by ^{31}P NMR until ~ 50 % of **8-4b** had been converted to **8-5b**. The reaction has not further monitored because of the concomitant formation of metallacycle product **8-5b′** generated by the loss of CH_4 from **8-5b**. Complex **8-5b** was characterized from the 1:1 mixture of **8-4b** and **8-5b**. ^{31}P NMR (C_6D_6, 161.9 MHz): δ 34.97 (s) ^{1}H NMR (C_6D_6, 400 MHz): δ 6.99 (d, 2H, PCP), 6.89 (t, 1H, PCP), 2.97~3.01 (m, 4H, C***H***$_2$P), 1.82 (s, 3H, C(O)C***H***$_3$), 1.31 (t, 6.0 Hz, 18H, PC(C***H***$_3$)$_3$), 1.30 (t, 3H, IrC***H***$_3$), 1.25 (t, 6.0 Hz,18H, PC(C***H***$_3$)$_3$).

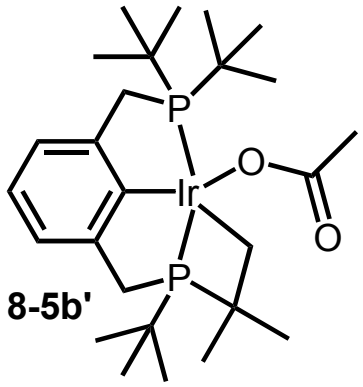

8-5b'

(PCP)Ir(CH_2Ph)(OAc) (**8-10**): To a 0.5 mL *p*-xylene-d_{10} solution of 5 mg (PCP)IrH_4 (0.0083 mmol) in a J-Young tube, 3.2 μL TBE (0.025 mmol) and 1.1μL BzOAc (0.0083 mmol) were added. After two hours at room temperature, ^{1}H and ^{31}P NMR showed the clean formation of (PCP)Ir(CH_2Ph)(O_2CMe) (**8-10**). ^{31}P NMR (*p*-xylene-d_{10}, 202 MHz): δ 29.96 (s). ^{1}H NMR (C_6D_6, 400 MHz): δ 8.06 (d, 2 H, J_{HH} = 7.6 Hz, Ar), 7.27 (t, J_{HH} = 7.6 Hz, 2H, Ar), 3.21 (d of vt, J_{PH} = 4.4Hz, J_{HH}=16.8 Hz, 2H, C***H***$_2$P), 3.13 (t, J_{PH} = 3.2Hz,

2H, C***H***$_2$Ph), 2.96 (d of vt, J_{PH} = 3.8 Hz, J_{HH} = 18.4 Hz, 2H, C***H***$_2$P), 1.81 (s, 3H, C(O)C***H***$_3$), 1.30 (t, 5.4Hz, 18H, PC(C***H***$_3$)$_3$), 1.14 (t, 7.0Hz, 18H, PC(C***H***$_3$)$_3$). ^{13}C NMR (C_6D_6, 125 MHz): δ 182.77 (s, ***C***(O)), 150.65 (s, Ar), 149.37 (t, J_{CP} = 5.2 Hz, Ar),148.34 (t, J_{CP} = 8.5 Hz, PCP), 141.10 (s, Ar), 131.01 (s, Ar), 124.53 (s, PCP), 122.1 (s, PCP), 121.57 (t, J_{CP} = 9.5 Hz, PCP), 38.85 (vt, J_{CP} = 13.8 Hz, P***C***(CH$_3$)$_3$), 36.26 (vt, J_{CP} = 9.9 Hz, P***C***(CH$_3$)$_3$), 31.94 (vt, J_{CP} = 15.7 Hz, ***C***H$_2$P), 29.9 (vt, J_{CP} = 2.6 Hz, PC(***C***H$_3$)$_3$), 29.8 (vt, J_{CP} = 2.4 Hz, PC(***C***H$_3$)$_3$), 26.3 (s, C(O)***C***H$_3$), -16.8 (t, J_{CP} = 5.3 Hz, ***CH$_2$***Ph)

Reaction of (PCP)Ir with ethyl, *iso*-propyl, *iso*-butyl, cyclohexyl, and *tert*-butyl acetate: In a typical reaction To a 0.5 mL *p*-xylene-d_{10} solution of 5 mg (PCP)IrH$_4$ (0.0083 mmol) in a J-Young tube, 3.2 μL TBE (0.025 mmol) and ester (0.0083 mmol) were added. Depending on the reaction substrate, the reaction was held a given temperature for a number of hours (see Scheme 8-5). ^{1}H and ^{31}P NMR spectroscopy showed the formation of (PCP)Ir(H)(O$_2$CMe) (**8-8**) complex in all cases. The generation of the corresponding olefins (e.g. ethylene, propylene or 2-methylpropylene) was confirmed by GC or NMR spectroscopy.

(PCP)Ir(H)(O$_2$CMe) (8-8): ^{31}P NMR (*p*-xylene-d_{10}, 202 MHz): δ 60.40 (d, 10.5 Hz) ^{1}H NMR (C_6D_6, 500 MHz): δ 6.94 (s, 3H, PCP), 3.17 (d of vt, J_{PH} = 3.3 Hz, J_{HH} = 17.0 Hz, 2H, C***H***$_2$P), 2.90 (d of vt, J_{PH}=4.0 Hz, J_{HH}=16.5 Hz, 2H, C***H***$_2$P), 1.86 (s, 3H, C(O)C***H***$_3$), 1.31 (t, 6.3 Hz, 18H, PC(C***H***$_3$)$_3$), 1.22 (t, 6.5 Hz, 18H, PC(C***H***$_3$)$_3$), -29.76 (t, 13.3 Hz, 1H, Ir***H***) ^{13}C NMR (C_6D_6, 125 MHz): δ 183.2 (s, ***C***(O)), 149.0 (t, J_{CP} = 8.2 Hz, PCP), 128.3 (s, PCP), 121.8 (s, PCP), 120.9 (t, J_{CP} = 7.7 Hz, PCP), 36.9 (vt, J_{CP} = 9.3 Hz, P***C***(CH$_3$)$_3$),

35.6 (vt, J_{CP} = 11.4 Hz, P***C***$(CH_3)_3$), 35.2 (vt, J_{CP} = 14.1 Hz, ***C***H_2P) 29.9 (vt, J_{CP} = 2.6 Hz, PC(***C***$H_3)_3$), 29.8 (vt, J_{CP} = 2.4 Hz, PC(***C***$H_3)_3$), 26.3 (s, C(O)***C***H_3).

(PCP)Ir(H)(O_2CPh) (8-9): ^{31}P NMR (*p*-xylene-d_{10}, 202 MHz): δ 60.48 (s, PCP) ^{1}H NMR (C_6D_6, 500 MHz): δ 8.22 (m, 2H, Ar), 7.19 (m, 4H, Ar), 6.92 (s, 2H, Ar), 3.24 (d of vt, J_{PH} = 3.3 Hz, J_{HH} = 17.0 Hz, 2H, C***H***$_2$P), 2.97 (d of vt, J_{PH} = 4.0 Hz, J_{HH} = 16.5 Hz, 2H, C***H***$_2$P), 1.30 (t, 6.3 Hz, 18H, PC(C***H***$_3)_3$), 1.24 (t, 6.5 Hz, 18H, PC(C***H***$_3)_3$), -29.56 (t, 13.3 Hz, 1H, Ir***H***).

Complex (8-11): To a 0.5 mL *p*-xylene-d_{10} solution of 5 mg (PCP)IrH_4 (0.0083 mmol) in a J-Young tube, 3.2 μL TBE (0.025 mmol) and 1.1μL PhOAc (0.0083 mmol) were added. After two hours at room temperature, ^{1}H and ^{31}P NMR spectroscopy showed the formation of complex **8-11.** An X-ray quality crystal was obtained by slow evaporation of a hexane solution. ^{31}P NMR (*p*-xylene-d_{10}, 202 MHz): δ 55.6 (s), ^{1}H NMR (C_6D_6, 400 MHz): δ 8.32 (m, 1H, Ph), 7.22 (d, J_{HH} = 7.2 Hz, 2H, Ar), 7.14 (t, J_{HH} = 7.2 Hz, 1H, Ar), 6.97 (m, 2H, Ph), 6.89 (m, 1H, Ph), 3.43 (d of vt, J_{PH} = 2.8 Hz, J_{HH} = 16.0 Hz, 2H, C***H***$_2$P), 3.27 (d of vt, J_{PH} = 3.8 Hz, J_{HH} = 16.4 Hz, 2H, C***H***$_2$P), 1.56 (s, 3H, C(O)C***H***$_3$), 1.15 (t, J_{PH} = 6.2 Hz, 18H, PC(C***H***$_3)_3$), 1.02 (t, J_{PH} = 6.0 Hz, 18H, PC(C***H***$_3)_3$), -27.27 (t, J_{PH} = 16.4 Hz, 1H, Ir***H***). ^{13}C NMR (C_6D_6, 100 MHz): δ 169.3 (s, ***C***(O)), 165.7 (s, Ar), 158.4 (t, PCP), 150.3 (s, Ar), 150.0 (t, J_{CP} = 6.1 Hz, Ar), 138.2 (t, J_{CP} = 5.6 Hz, Ar), 124.9 (s, Ar), 123.3 (s, Ar), 122.1 (s, Ar), 120.2 (t, J_{CP} = 5.8 Hz, PCP), 116.6 (s, Ar), 40.9 (vt, J_{CP} = 11.1 Hz, ***C***H_2P), 36.5 (vt, J_{CP} = 6.4 Hz, P***C***$(CH_3)_3$), 36.4 (vt, J_{CP} = 9.8 Hz,

P***C***$(CH_3)_3$), 30.2 (vt, J_{CP} = 1.7 Hz, PC(***C***$H_3)_3$), 29.9 (vt, J_{CP} = 1.7 Hz, PC(***C***$H_3)_3$), 23.4 (s, ***C***H_3(CO)).

(PCP)Ir(H)(*κ*^{2}-C,O-$CH_2OC(O)CH_3$) (**8-7**): To a 0.5 mL *p*-xylene-d_{10} solution of 5 mg (PCP)IrH_4 (0.0083 mmol) in a J-Young tube, 2.4 mg NBE (0.025 mmol) and 0.7μL methyl acetate (0.0083 mmol) were added. After 30 minutes at room temperature, complex **8-7** was formed in quantitative yield. Removal of the solvent under vacuum, afford a dark brown powder. ^{31}P NMR (*p*-xylene-d_{10}, 202 MHz): δ 51.54 (d, 8.2 Hz) ^{1}H NMR (*p*-xylene-d_{10}, 500 MHz): δ 7.13 (d, 2H, PCP), 7.05 (t, 1H, PCP), 6.81 (t, 8.0 Hz, 2H, IrC***H***$_2$O), 3.40 (d of vt, J_{PH} = 2.5 Hz, J_{HH} = 16.0 Hz, 2H, PC***H***$_2$), 3.21 (d of vt, J_{PH} = 4.0 Hz, J_{HH} = 16.0 Hz, 2H, PC***H***$_2$), 1.80 (s, 3H, C(O)C***H***$_3$), 1.18 (t, 6.0 Hz, 18H, PC(C***H***$_3)_3$), 1.14 (t, 5.8 Hz, 18H, PC(C***H***$_3)_3$), -25.90 (t, 16.3 Hz, 1H, Ir***H***).

Reaction of (PCP)Ir with Methoxymethyl Acetate: To a 0.5 mL *p*-xylene-d_{10} solution of (PCP)Ir(TBE)(H), made from 5 mg (PCP)IrH_4 (0.0083 mmol) and 3.2 μL TBE (0.025 mmol), 0.5 eqiv. of methoxymethyl acetate was added. An immediate color change to dark-brown was observed. Removal of the solvent afforded a dark-brown waxy solid. ^{1}H and ^{31}P NMR spectroscopy showed the formation of (PCP)Ir=C(H)(OMe) (**8-15**) and (PCP)Ir(H)(OAc) (**8-8**) with 1:1 ratio. The formation of compound **8-15** was confirmed by NOE and HMQC. Enhancement of OCH_3 was observed by saturation of the proton on the carbene. An attempt to isolate the compound **8-15** was unsuccessful.

(PCP)Ir=C(H)(OMe) (**8-15**): ^{31}P NMR (C_6D_6, 162 MHz): δ 69.65 (br s). ^{1}H NMR (C_6D_6, 400 MHz): δ 14.89 (t, J_{PH} = 4.2 Hz, 1H, Ir=C***H***(OMe)), 7.39 (d, 2H, PCP), 7.07 (t,

1H, PCP), 3.63 (vt, J_{PH} = 3.6 Hz, 4H, C***H***$_2$P), 1.32 (t, J_{PH} = 6.2 Hz, 36H, PC(C***H***$_3$)$_3$). ^{13}C NMR (C_6D_6, 100 MHz): δ 254.8 (br s, Ir=***C***H(OMe)).

Complex (**8-16**): To a 0.5 mL *p*-xylene-d_{10} solution of 5 mg (PCP)IrH_4 (0.0083 mmol) in a J-Young tube, 3.2 μL TBE (0.025 mmol) and 0.9μL methyl acetate (0.0083 mmol) were added. After 4 h at r. t., complex **8-16** was formed. The solvent was removed under vacuum to yield a brown powder that (yield 95%). An X-ray quality crystal was obtained by slow evaporation of a hexane. ^{31}P NMR (C_6D_6, 162 MHz): δ 48.51 (d, J_{PP} = 18.5 Hz). ^{1}H NMR (C_6D_6, 400 MHz): δ 7.64 (t, J_{HH} = 8.4 Hz, 1H, PCP), 7.10 (d, J_{HH} = 6.4 Hz, 1H, PCP), 3.39 (m, 2H, PC***H***$_2$), 3.25 (m, 2H, PC***H***$_2$), 3.16 (m, 1H, Ir-C***H***(COCH$_3$)(OCOCH$_3$)), 2.95 (m, 1H, PC***H***$_2$), 2.25 (s, 3H, OCO***CH$_3$***), 1.74 (s, 3H, CO***CH$_3$***), 1.28 (q, J_{PH} = 7.6, PC(C***H***$_3$)$_3$), 1.18 (q, J_{PH} = 7.6, 9H, PC(C***H***$_3$)$_3$), 1.01 (q, J_{PH} = 7.6, 9H, PC(C***H***$_3$)$_3$), 0.94(q, J_{PH} = 7.6, 9H, PC(C***H***$_3$)$_3$) -26.34 (t, J_{PH} = 16.2, Ir-***H***).

8.5 Conclusion

We have demonstrated that "(PCP)Ir" cleaves sp^3-alkyl C–O bonds of various esters (RCO_2R_1) to give (PCP)Ir(R_1)(O_2CR) or, in cases where R_1 has a β-hydrogen, (PCP)Ir(H)(O_2CR) and the corresponding alkenes. The reaction does not proceed via simple oxidative addition of R_1–O_2CR to the iridium center. Rather the reaction is proposed to proceed via a multi- step pathway. In cases where R_1 has a no β-hydrogen, initially C-H activation is followed by slow α-acetate elimination form carbene intermediate. The methilydine group then inserts into the PCP-Ir bond and finally C-C bond cleavage generated the final product. In cases where R_1 has a β-hydrogen, C-H

activation followed by β-acetate elimination generated the final product complex **9-8** and corresponding alkene.

8.6 References

(1) Lin, Y.-S.; Yamamoto, A., In Activation of Unreactvie Bonds and Organic Synthesis Murai, S., Ed.; Springer: Berlin, 1999; pp 161-192.
(2) Trost, B. M. C., M. L. *Chem. Rev* **2003**, *103*, 2921.
(3) Trost, B. M. V. V., D. L. *Chem. Rev* **1996**, *96*, 395.
(4) Rayabarapu, D. K.; Tunge, J. A. *J. Am. Chem. Soc.* **2005**, *127*, 13510.
(5) Yamamoto, T. I., J.; Yamamoto, A. *J. Am. Chem. Soc.* **1981**, *103*, 6863.
(6) Ittel, S. D. T., C. A.; English, A. D.; Jesson, J. P. *J. Am. Chem. Soc.* **1978**, *100*, 7577.
(7) Trovitch, R. J. L., E.; Bouwkamp, M. W.; Chirik, P. J. *Organometallics* **2008**, *27*, 6264.
(8) Choi, J., Unpublished work
(9) Rybtchinski, B. V., A.; Ben-David, Y.; Milstein, D. *J. Am. Chem. Soc.* **1996**, *118*, 12406.
(10) Choliy, Y.; Krogh-Jespersen, K., Unpublished work
(11) Williams, B. S. L., M. D.; White, P. S.; Brookhart, M. *J. Am. Chem. Soc.* **2005**, *127*.
(12) Gupta, M.; Hagen, C.; Flesher, R. J.; Kaska, W. C.; Jensen, C. M. *Chem. Commun.* **1996**, 2083.

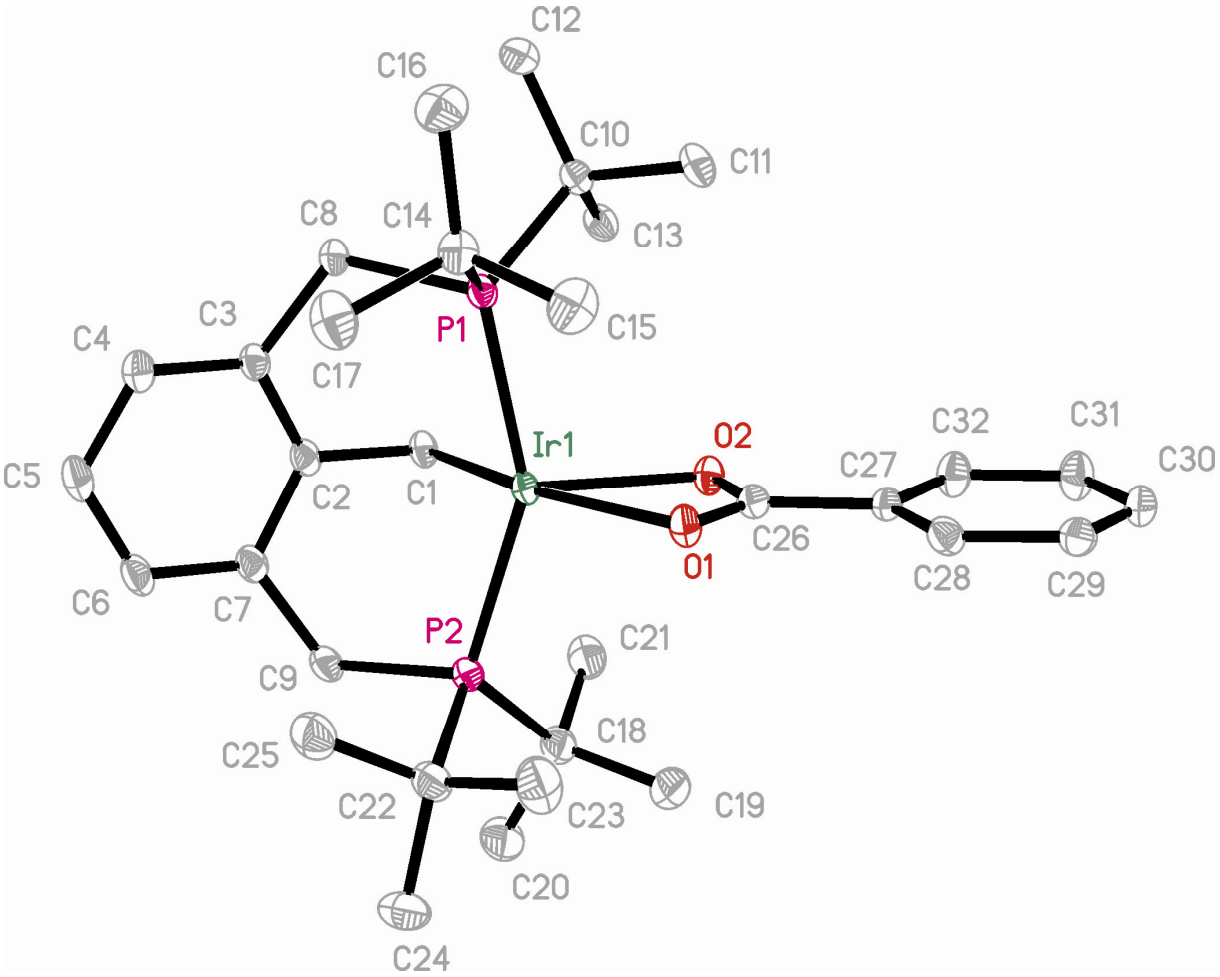

Figure 8-2 Crystal structure of complex **8-4a**

Table 8.1 Crystal data and structure refinement for complex **8-4a**

Empirical formula	C31 H44 Ir O2 P2	
Formula weight	702.80	
Temperature	100(2) K	
Wavelength	0.71073 Å	
Crystal system	Triclinic	
Space group	P-1	
Unit cell dimensions	a = 10.597(2) Å	α= 97.612(6)°.
	b = 10.845(2) Å	β= 96.676(6)°.
	c = 15.489(3) Å	γ = 109.943(6)°.
Volume	1633.5(6) $Å^3$	
Z	2	
Density (calculated)	1.429 Mg/m^3	
Absorption coefficient	4.208 mm^{-1}	
F(000)	706	
Crystal size	0.18 x 0.07 x 0.04 mm^3	
Theta range for data collection	2.03 to 28.28°.	
Index ranges	-14<=h<=12, -14<=k<=14, -20<=l<=20	
Reflections collected	14368	
Independent reflections	7867 [R(int) = 0.0213]	
Completeness to theta = 28.28°	97.0 %	
Absorption correction	Semi-empirical from equivalents	
Max. and min. transmission	0.8497 and 0.5180	
Refinement method	Full-matrix least-squares on F^2	
Data / restraints / parameters	7867 / 0 / 347	
Goodness-of-fit on F^2	0.969	
Final R indices [I>2sigma(I)]	R1 = 0.0348, wR2 = 0.0913	
R indices (all data)	R1 = 0.0426, wR2 = 0.1152	
Extinction coefficient	0.0000(3)	
Largest diff. peak and hole	4.202 and -1.392 $e.Å^{-3}$	

Table 8.2 Selected bond lengths [Å] and angles [°] for complex **8-4a**

Ir(1)-C(1)	2.040(5)	C(3)-C(4)	1.400(8)
Ir(1)-C(25)	2.122(6)	C(4)-C(5)	1.400(8)
Ir(1)-O(1)	2.207(4)	C(5)-C(6)	1.395(8)
Ir(1)-P(1)	2.3624(14)	C(6)-C(8)	1.517(7)
Ir(1)-P(2)	2.3630(14)	C(9)-C(11)	1.535(9)
Ir(1)-O(2)	2.429(4)	C(9)-C(12)	1.539(9)
P(1)-C(7)	1.848(6)	C(9)-C(10)	1.545(10)
P(1)-C(13)	1.908(6)	C(13)-C(14)	1.499(9)
P(1)-C(9)	1.940(6)	C(13)-C(15)	1.517(11)
P(2)-C(8)	1.855(6)	C(13)-C(16)	1.522(12)
P(2)-C(17)	1.891(6)	C(17)-C(18)	1.561(9)
P(2)-C(21)	1.934(6)	C(17)-C(19)	1.553(9)
C(1)-C(2)	1.418(8)	C(17)-C(20)	1.552(9)
C(1)-C(6)	1.431(7)	C(21)-C(24)	1.542(8)
C(2)-C(3)	1.397(8)	C(21)-C(22)	1.550(8)
C(2)-C(7)	1.525(7)	C(21)-C(23)	1.555(8)
C(1)-Ir(1)-C(25)	77.7(2)	C(7)-P(1)-Ir(1)	100.67(17)
C(1)-Ir(1)-O(1)	175.53(19)	C(13)-P(1)-Ir(1)	121.92(19)
C(25)-Ir(1)-O(1)	98.0(2)	C(9)-P(1)-Ir(1)	114.14(18)
C(1)-Ir(1)-P(1)	82.96(16)	C(8)-P(2)-C(17)	107.2(3)
C(25)-Ir(1)-P(1)	93.50(17)	C(8)-P(2)-C(21)	102.8(3)
O(1)-Ir(1)-P(1)	96.24(11)	C(17)-P(2)-C(21)	109.4(3)
C(1)-Ir(1)-P(2)	82.48(16)	C(8)-P(2)-Ir(1)	100.49(18)
C(25)-Ir(1)-P(2)	94.28(17)	C(17)-P(2)-Ir(1)	120.2(2)
O(1)-Ir(1)-P(2)	99.12(11)	C(21)-P(2)-Ir(1)	114.53(17)
P(1)-Ir(1)-P(2)	161.63(5)	C(2)-C(1)-C(6)	116.8(5)
C(1)-Ir(1)-O(2)	127.51(18)	C(2)-C(1)-Ir(1)	121.5(4)
C(25)-Ir(1)-O(2)	154.80(19)	C(6)-C(1)-Ir(1)	121.4(4)
O(1)-Ir(1)-O(2)	56.84(15)	C(3)-C(2)-C(1)	120.7(5)
P(1)-Ir(1)-O(2)	91.33(10)	C(3)-C(2)-C(7)	120.1(5)
P(2)-Ir(1)-O(2)	88.69(10)	C(1)-C(2)-C(7)	118.9(5)
C(7)-P(1)-C(13)	105.6(3)	C(2)-C(3)-C(4)	121.1(5)
C(7)-P(1)-C(9)	103.0(3)	C(3)-C(4)-C(5)	118.9(5)
C(13)-P(1)-C(9)	108.9(3)	C(3)-C(4)-H(4)	120.6

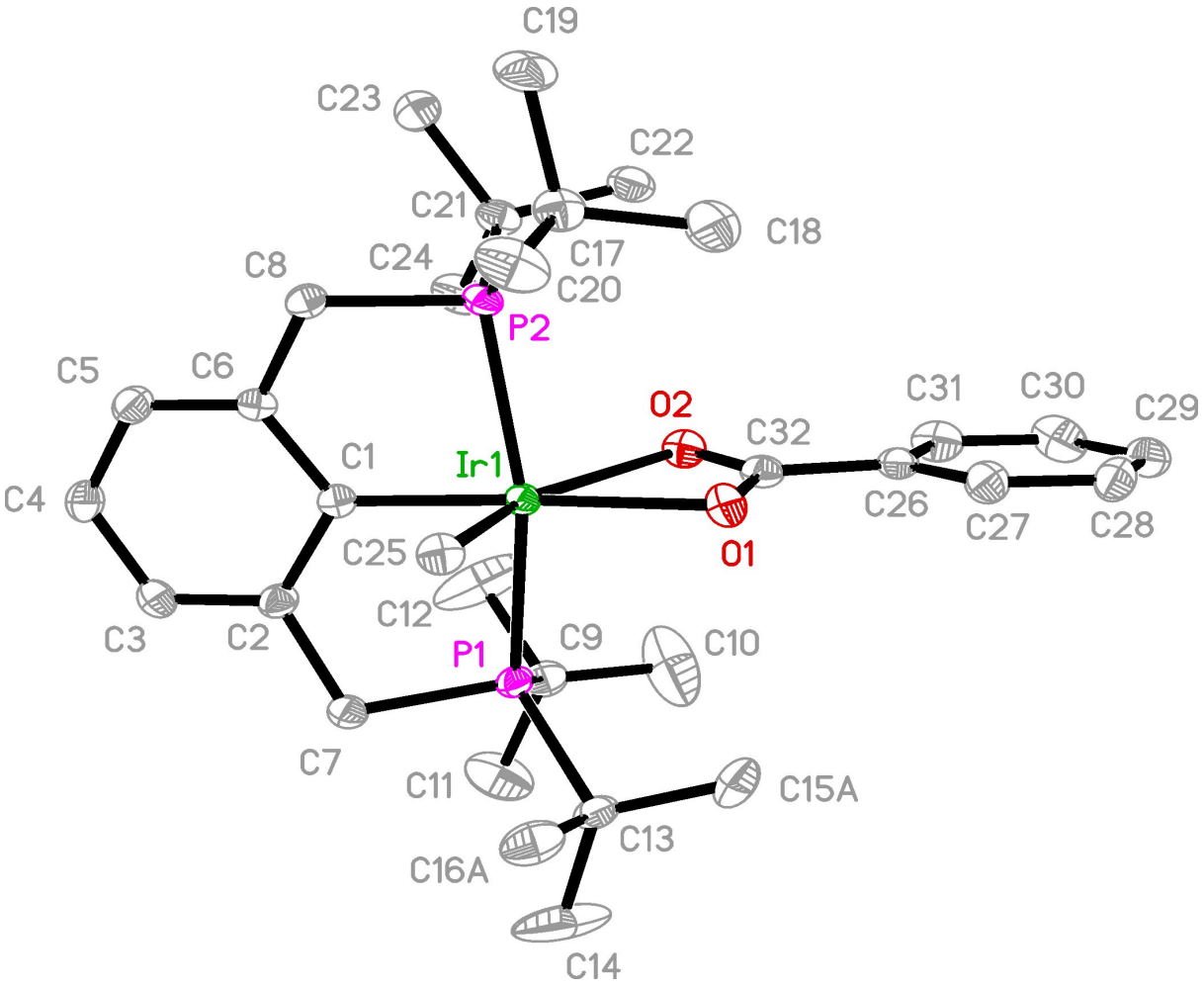

Figure 8-3 Crystal structure of complex **8-5a**

Table 8.3 Crystal data and structure refinement for complex **8-5a**

Empirical formula	C32 H50 Ir O2 P2	
Formula weight	720.86	
Temperature	100(2) K	
Wavelength	0.71073 Å	
Crystal system	Monoclinic	
Space group	P2(1)/n	
Unit cell dimensions	a = 8.5618(5) Å	α= 90°.
	b = 18.9460(10) Å	β= 100.961(1)°.
	c = 19.7697(10) Å	γ = 90°.
Volume	3148.4(3) $Å^3$	
Z	4	
Density (calculated)	1.521 Mg/m^3	
Absorption coefficient	4.368 mm^{-1}	
F(000)	1460	
Crystal size	0.34 x 0.14 x 0.05 mm^3	
Theta range for data collection	2.10 to 31.56°.	
Index ranges	-12<=h<=12, -27<=k<=27, -29<=l<=29	
Reflections collected	39186	
Independent reflections	10484 [R(int) = 0.0259]	
Completeness to theta = 31.56°	99.4 %	
Absorption correction	Numerical	
Max. and min. transmission	0.8112 and 0.3182	
Refinement method	Full-matrix least-squares on F^2	
Data / restraints / parameters	10484 / 0 / 346	
Goodness-of-fit on F^2	1.004	
Final R indices [I>2sigma(I)]	R1 = 0.0259, wR2 = 0.0587	
R indices (all data)	R1 = 0.0298, wR2 = 0.0600	
Largest diff. peak and hole	2.588 and -1.469 e.$Å^{-3}$	

Table 8.4 Selected bond lengths [Å] and angles [°] for complex **8-5a**

Ir(1)-C(1)	2.097(2)	C(4)-C(5)	1.394(4)
Ir(1)-O(1)	2.2299(17)	C(5)-C(6)	1.393(4)
Ir(1)-O(2)	2.2683(17)	C(6)-C(7)	1.391(3)
Ir(1)-P(2)	2.3253(6)	C(7)-C(9)	1.516(4)
Ir(1)-P(1)	2.3279(6)	C(10)-C(12)	1.535(4)
P(1)-C(8)	1.887(2)	C(10)-C(11)	1.537(3)
P(1)-C(10)	1.888(3)	C(10)-C(13)	1.545(4)
P(1)-C(14)	1.901(3)	C(14)-C(16)	1.532(4)
P(2)-C(22)	1.892(3)	C(14)-C(15)	1.534(4)
P(2)-C(18)	1.893(3)	C(14)-C(17)	1.539(4)
P(2)-C(9)	1.895(2)	C(18)-C(19)	1.535(4)
C(1)-C(2)	1.469(3)	C(18)-C(21)	1.538(4)
C(2)-C(7)	1.404(3)	C(18)-C(20)	1.541(4)
C(2)-C(3)	1.405(3)	C(22)-C(23)	1.535(4)
C(3)-C(4)	1.390(3)	C(22)-C(25)	1.536(4)
C(3)-C(8)	1.522(3)	C(22)-C(24)	1.538(4)
C(1)-Ir(1)-O(1)	163.91(8)	C(18)-P(2)-C(9)	102.08(12)
C(1)-Ir(1)-O(2)	105.41(8)	C(22)-P(2)-Ir(1)	113.77(9)
O(1)-Ir(1)-O(2)	58.50(6)	C(18)-P(2)-Ir(1)	117.36(9)
C(1)-Ir(1)-P(2)	81.88(7)	C(9)-P(2)-Ir(1)	109.06(8)
O(1)-Ir(1)-P(2)	101.02(5)	C(2)-C(1)-Ir(1)	102.63(15)
O(2)-Ir(1)-P(2)	104.48(5)	C(2)-C(1)-H(1A)	111.2
C(1)-Ir(1)-P(1)	81.60(7)	Ir(1)-C(1)-H(1A)	111.2
O(1)-Ir(1)-P(1)	101.29(5)	C(2)-C(1)-H(1B)	111.2
O(2)-Ir(1)-P(1)	102.20(5)	Ir(1)-C(1)-H(1B)	111.2
P(2)-Ir(1)-P(1)	151.51(2)	C(7)-C(2)-C(3)	120.4(2)
C(8)-P(1)-C(10)	100.90(11)	C(7)-C(2)-C(1)	119.2(2)
C(8)-P(1)-C(14)	103.29(11)	C(3)-C(2)-C(1)	118.9(2)
C(10)-P(1)-C(14)	109.43(11)	C(4)-C(3)-C(2)	119.0(2)
C(8)-P(1)-Ir(1)	108.59(8)	C(4)-C(3)-C(8)	123.4(2)
C(10)-P(1)-Ir(1)	118.82(8)	C(2)-C(3)-C(8)	117.1(2)
C(14)-P(1)-Ir(1)	113.85(9)	C(3)-C(4)-C(5)	120.3(2)
C(22)-P(2)-C(18)	110.39(13)	C(5)-C(4)-H(4)	119.8
C(22)-P(2)-C(9)	102.40(12)	C(6)-C(5)-C(4)	120.2(2)

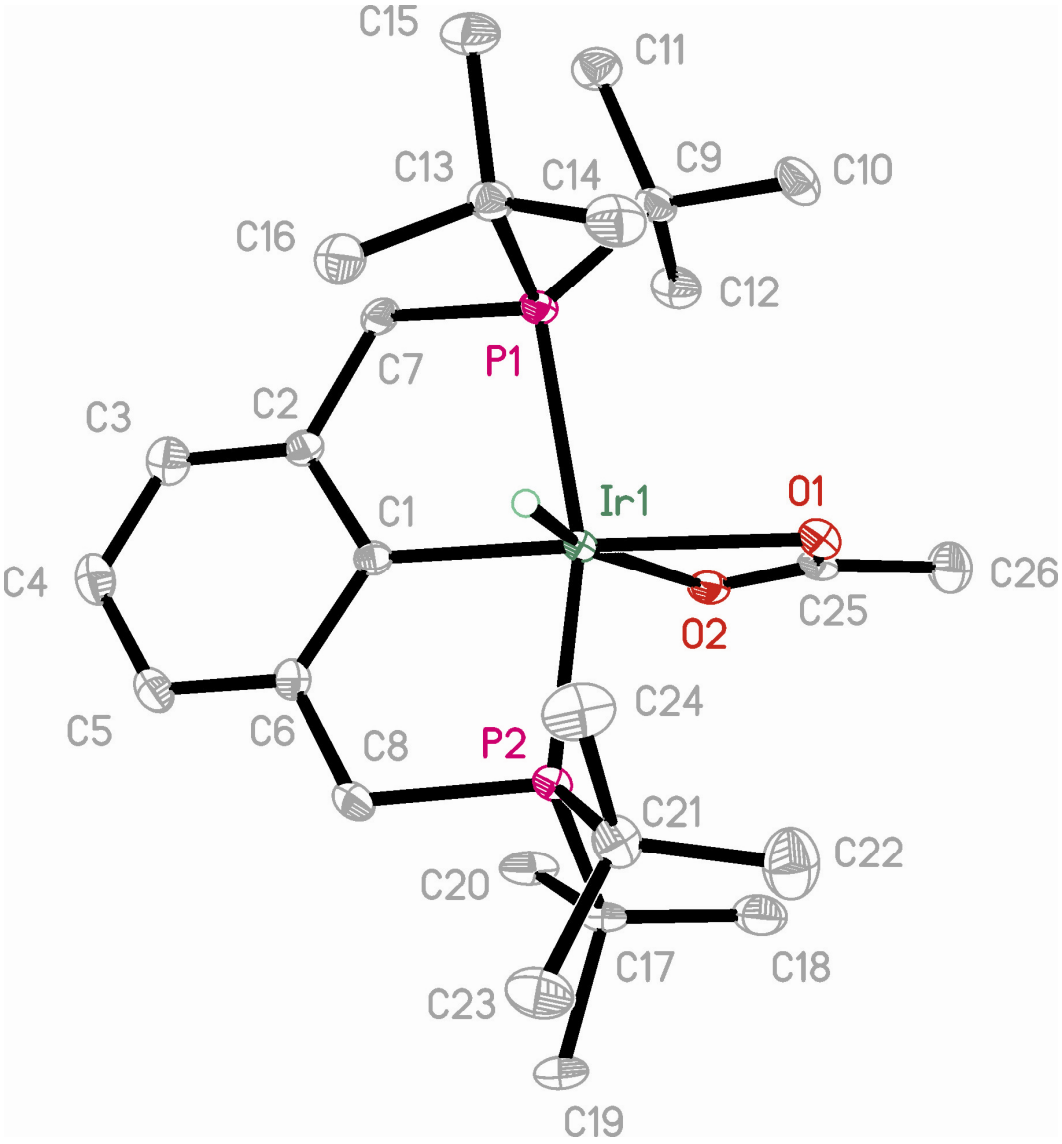

Figure 8-4 Crystal structure of complex **8-8**

Table 8.5 Crystal data and structure refinement for complex **8-8**

Empirical formula	C26 H47 Ir O2 P2	
Formula weight	645.78	
Temperature	100(2) K	
Wavelength	0.71073 Å	
Crystal system	Triclinic	
Space group	P-1	
Unit cell dimensions	a = 12.0304(8) Å	α= 89.576(1)°.
	b = 18.5067(12) Å	β= 74.350(1)°.
	c = 19.0177(13) Å	γ = 88.380(1)°.
Volume	4075.6(5) $Å^3$	
Z	6	
Density (calculated)	1.579 Mg/m^3	
Absorption coefficient	5.052 mm^{-1}	
F(000)	1956	
Crystal size	0.35 x 0.13 x 0.03 mm^3	
Theta range for data collection	2.05 to 30.53°.	
Index ranges	-17<=h<=17, -25<=k<=26, -27<=l<=27	
Reflections collected	49968	
Independent reflections	24513 [R(int) = 0.0306]	
Completeness to theta = 30.53°	98.3 %	
Absorption correction	Semi-empirical from equivalents	
Max. and min. transmission	0.8632 and 0.2709	
Refinement method	Full-matrix least-squares on F^2	
Data / restraints / parameters	24513 / 4 / 889	
Goodness-of-fit on F^2	1.004	
Final R indices [I>2sigma(I)]	R1 = 0.0356, wR2 = 0.0766	
R indices (all data)	R1 = 0.0489, wR2 = 0.0813	
Largest diff. peak and hole	4.233 and -1.041 $e.Å^{-3}$	

Table 8.6 Selected bond lengths [Å] and angles [°] for complex **8-8**

Ir(1)-C(1)	2.017(3)	C(3)-C(4)	1.371(5)
Ir(1)-O(1)	2.255(3)	C(4)-C(5)	1.388(5)
Ir(1)-O(2)	2.294(3)	C(5)-C(6)	1.406(5)
Ir(1)-P(2)	2.3119(9)	C(6)-C(8)	1.512(5)
Ir(1)-P(1)	2.3230(9)	C(9)-C(10)	1.532(5)
Ir(1)-H(1I)	1.597(5)	C(9)-C(12)	1.537(5)
P(1)-C(7)	1.834(4)	C(9)-C(11)	1.541(5)
P(1)-C(9)	1.885(4)	C(13)-C(14)	1.531(5)
P(1)-C(13)	1.898(4)	C(13)-C(16)	1.533(5)
P(2)-C(8)	1.839(4)	C(13)-C(15)	1.541(5)
P(2)-C(17)	1.884(4)	C(17)-C(18)	1.528(5)
P(2)-C(21)	1.889(4)	C(17)-C(20)	1.533(5)
C(1)-C(6)	1.410(5)	C(17)-C(19)	1.538(5)
C(1)-C(2)	1.415(5)	C(21)-C(24)	1.522(6)
C(2)-C(3)	1.401(5)	C(21)-C(22)	1.526(6)
C(2)-C(7)	1.512(5)	C(21)-C(23)	1.539(5)
C(1)-Ir(1)-O(1)	169.47(12)	C(7)-P(1)-Ir(1)	102.20(12)
C(1)-Ir(1)-O(2)	111.82(12)	C(9)-P(1)-Ir(1)	122.81(12)
O(1)-Ir(1)-O(2)	57.66(10)	C(13)-P(1)-Ir(1)	110.52(12)
C(1)-Ir(1)-P(2)	84.08(10)	C(8)-P(2)-C(17)	102.82(18)
O(1)-Ir(1)-P(2)	97.30(7)	C(8)-P(2)-C(21)	104.11(17)
O(2)-Ir(1)-P(2)	97.02(7)	C(17)-P(2)-C(21)	111.30(17)
C(1)-Ir(1)-P(1)	82.11(10)	C(8)-P(2)-Ir(1)	101.73(12)
O(1)-Ir(1)-P(1)	98.39(7)	C(17)-P(2)-Ir(1)	118.41(12)
O(2)-Ir(1)-P(1)	98.79(7)	C(21)-P(2)-Ir(1)	115.84(13)
P(2)-Ir(1)-P(1)	162.01(3)	C(6)-C(1)-C(2)	116.8(3)
C(1)-Ir(1)-H(1I)	84.6(14)	C(6)-C(1)-Ir(1)	121.2(3)
O(1)-Ir(1)-H(1I)	105.9(14)	C(2)-C(1)-Ir(1)	122.0(3)
O(2)-Ir(1)-H(1I)	163.5(14)	C(3)-C(2)-C(1)	121.1(3)
P(2)-Ir(1)-H(1I)	85.6(15)	C(3)-C(2)-C(7)	119.5(3)
P(1)-Ir(1)-H(1I)	81.7(15)	C(1)-C(2)-C(7)	119.4(3)
C(7)-P(1)-C(9)	103.55(17)	C(4)-C(3)-C(2)	120.7(4)
C(7)-P(1)-C(13)	105.88(17)	C(3)-C(4)-C(5)	119.9(4)
C(9)-P(1)-C(13)	110.02(17)	C(3)-C(4)-H(4)	120.1(4)

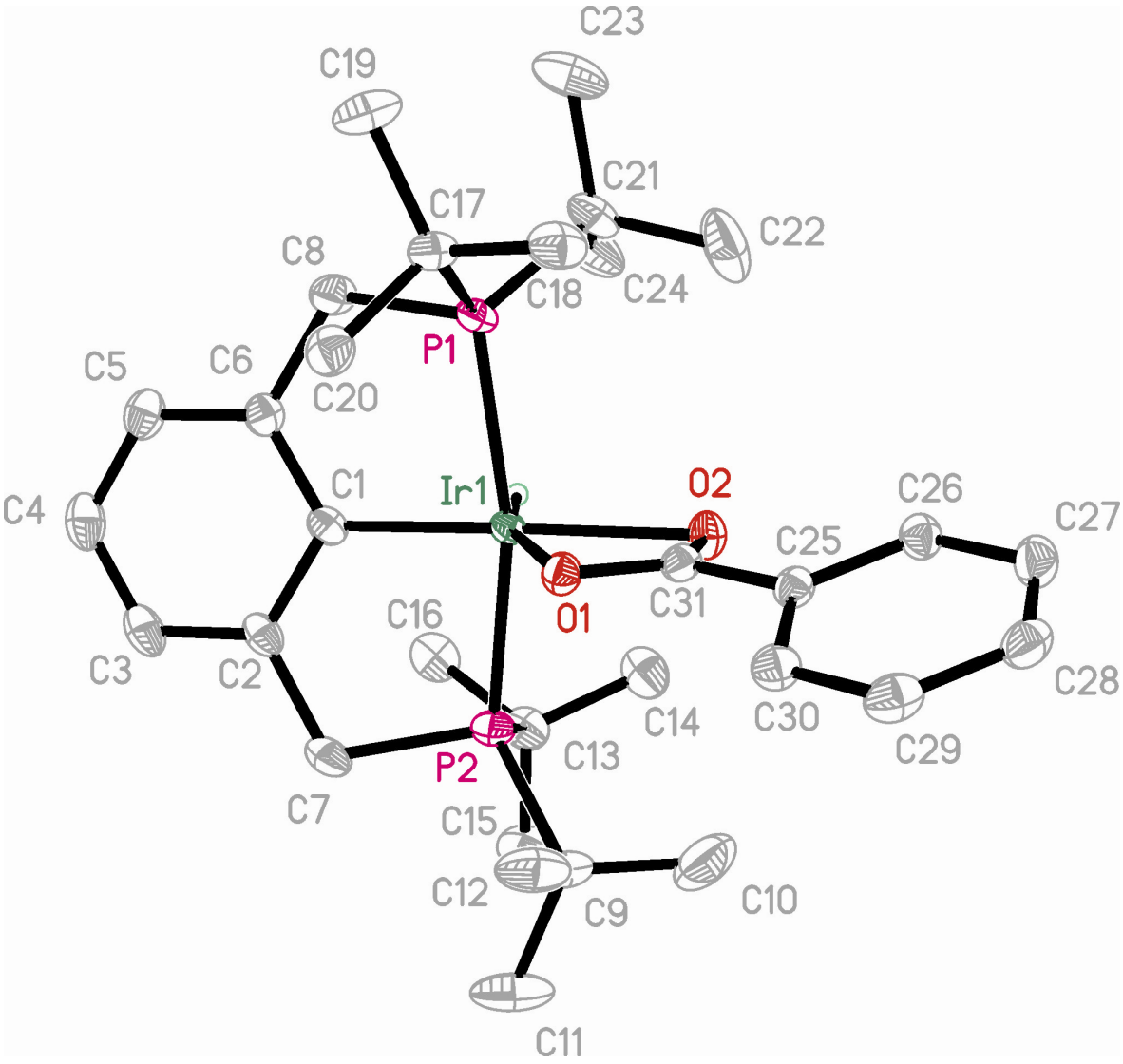

Figure 8-5 Crystal structure of complex **8-9**

Table 8.7 Crystal data and structure refinement for complex **8-9**

Empirical formula	C31 H49 Ir O2 P2	
Formula weight	707.84	
Temperature	100(2) K	
Wavelength	0.71073 Å	
Crystal system	Triclinic	
Space group	P-1	
Unit cell dimensions	a = 10.7671(6) Å	α= 84.888(1)°.
	b = 11.7049(7) Å	β= 73.086(1)°.
	c = 12.9622(7) Å	γ = 86.327(1)°.
Volume	1555.47(15) $Å^3$	
Z	2	
Density (calculated)	1.511 Mg/m^3	
Absorption coefficient	4.420 mm^{-1}	
F(000)	716	
Crystal size	0.25 x 0.17 x 0.04 mm^3	
Theta range for data collection	1.75 to 32.13°.	
Index ranges	-15<=h<=16, -17<=k<=17, -19<=l<=19	
Reflections collected	20170	
Independent reflections	10496 [R(int) = 0.0187]	
Completeness to theta = 32.13°	96.1 %	
Absorption correction	Semi-empirical from equivalents	
Max. and min. transmission	0.860 and 0.404	
Refinement method	Full-matrix least-squares on F^2	
Data / restraints / parameters	10496 / 1 / 341	
Goodness-of-fit on F^2	1.001	
Final R indices [I>2sigma(I)]	R1 = 0.0231, wR2 = 0.0546	
R indices (all data)	R1 = 0.0257, wR2 = 0.0558	
Largest diff. peak and hole	1.997 and -0.779 $e.Å^{-3}$	

Table 8.8 Selected bond lengths [Å] and angles [°] for complex **8-9**

Ir(1)-C(1)	2.024(2)	C(3)-C(4)	1.386(4)
Ir(1)-O(2)	2.2151(15)	C(4)-C(5)	1.389(3)
Ir(1)-P(1)	2.3129(5)	C(5)-C(6)	1.396(3)
Ir(1)-O(1)	2.3144(15)	C(6)-C(8)	1.515(3)
Ir(1)-P(2)	2.3315(5)	C(9)-C(10)	1.520(4)
Ir(1)-H(1)	1.594(10)	C(9)-C(12)	1.539(4)
P(1)-C(8)	1.840(2)	C(9)-C(11)	1.540(4)
P(1)-C(21)	1.883(2)	C(13)-C(16)	1.532(3)
P(1)-C(17)	1.890(2)	C(13)-C(14)	1.539(3)
P(2)-C(7)	1.829(2)	C(13)-C(15)	1.547(3)
P(2)-C(13)	1.893(2)	C(17)-C(18)	1.536(3)
P(2)-C(9)	1.893(2)	C(17)-C(20)	1.542(3)
C(1)-C(6)	1.415(3)	C(17)-C(19)	1.543(3)
C(1)-C(2)	1.421(3)	C(21)-C(23)	1.529(4)
C(2)-C(3)	1.393(3)	C(21)-C(24)	1.532(4)
C(2)-C(7)	1.512(3)	C(21)-C(22)	1.538(4)
C(1)-Ir(1)-O(2)	175.12(7)	C(8)-P(1)-Ir(1)	101.52(7)
C(1)-Ir(1)-P(1)	83.32(6)	C(21)-P(1)-Ir(1)	115.64(8)
O(2)-Ir(1)-P(1)	97.03(4)	C(17)-P(1)-Ir(1)	117.41(7)
C(1)-Ir(1)-O(1)	117.20(7)	C(7)-P(2)-C(13)	105.28(11)
O(2)-Ir(1)-O(1)	57.92(5)	C(7)-P(2)-C(9)	103.71(11)
P(1)-Ir(1)-O(1)	94.86(4)	C(13)-P(2)-C(9)	110.04(11)
C(1)-Ir(1)-P(2)	82.21(6)	C(7)-P(2)-Ir(1)	101.36(7)
O(2)-Ir(1)-P(2)	98.00(4)	C(13)-P(2)-Ir(1)	111.30(8)
P(1)-Ir(1)-P(2)	163.88(2)	C(9)-P(2)-Ir(1)	122.98(8)
O(1)-Ir(1)-P(2)	98.04(4)	C(6)-C(1)-C(2)	116.57(19)
C(1)-Ir(1)-H(1)	80.1(13)	C(6)-C(1)-Ir(1)	121.55(15)
O(2)-Ir(1)-H(1)	104.8(13)	C(2)-C(1)-Ir(1)	121.71(15)
P(1)-Ir(1)-H(1)	85.8(14)	C(3)-C(2)-C(1)	121.1(2)
O(1)-Ir(1)-H(1)	162.7(13)	C(3)-C(2)-C(7)	120.24(19)
P(2)-Ir(1)-H(1)	84.8(14)	C(1)-C(2)-C(7)	118.64(19)
C(8)-P(1)-C(21)	105.80(11)	C(4)-C(3)-C(2)	120.9(2)
C(8)-P(1)-C(17)	103.02(11)	C(3)-C(4)-C(5)	119.4(2)
C(21)-P(1)-C(17)	111.30(10)	C(4)-C(5)-C(6)	120.3(2)

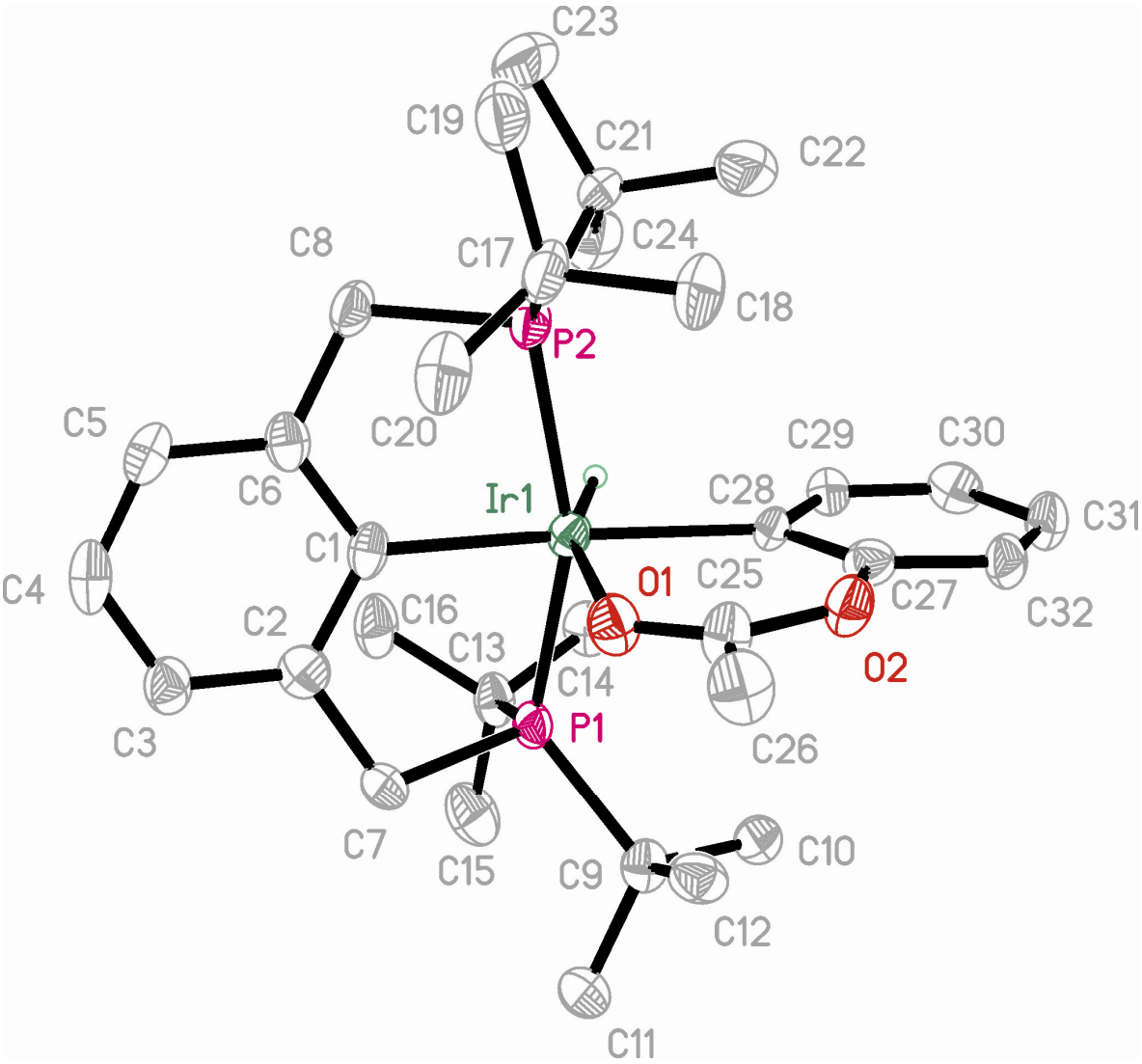

Figure 8-6 Crystal structure of complex **8-11**

Table 8.9 Crystal data and structure refinement for complex **8-11**

Empirical formula	C32 H51 Ir O2 P2	
Formula weight	721.87	
Temperature	100(2) K	
Wavelength	0.71073 Å	
Crystal system	Orthorhombic	
Space group	Pbca	
Unit cell dimensions	a = 13.7789(12) Å	α= 90°.
	b = 15.4011(13) Å	β= 90°.
	c = 29.526(3) Å	γ = 90°.
Volume	6265.7(9) $Å^3$	
Z	8	
Density (calculated)	1.530 Mg/m^3	
Absorption coefficient	4.390 mm^{-1}	
F(000)	2928	
Crystal size	0.09 x 0.04 x 0.02 mm^3	
Theta range for data collection	2.02 to 26.46°.	
Index ranges	-17<=h<=17, -19<=k<=19, -36<=l<=36	
Reflections collected	52363	
Independent reflections	6446 [R(int) = 0.1078]	
Completeness to theta = 26.46°	99.6 %	
Absorption correction	Semi-empirical from equivalents	
Max. and min. transmission	0.917 and 0.693	
Refinement method	Full-matrix least-squares on F^2	
Data / restraints / parameters	6446 / 1 / 351	
Goodness-of-fit on F^2	1.014	
Final R indices [I>2sigma(I)]	R1 = 0.0608, wR2 = 0.1325	
R indices (all data)	R1 = 0.0909, wR2 = 0.1468	
Largest diff. peak and hole	4.530 and -1.832 e.$Å^{-3}$	

Table 8.10 Selected bond lengths [Å] and angles [°] for complex **8-11**

Ir(1)-C(1)	2.080(9)	C(3)-C(4)	1.382(15)
Ir(1)-C(28)	2.108(9)	C(4)-C(5)	1.372(15)
Ir(1)-O(1)	2.242(6)	C(5)-C(6)	1.417(13)
Ir(1)-P(2)	2.312(3)	C(6)-C(8)	1.506(14)
Ir(1)-P(1)	2.317(3)	C(9)-C(11)	1.518(14)
Ir(1)-H(1)	1.594(10)	C(9)-C(10)	1.530(13)
P(1)-C(7)	1.836(9)	C(9)-C(12)	1.558(13)
P(1)-C(13)	1.868(10)	C(13)-C(14)	1.513(13)
P(1)-C(9)	1.905(10)	C(13)-C(15)	1.544(15)
P(2)-C(8)	1.839(10)	C(13)-C(16)	1.556(14)
P(2)-C(17)	1.881(11)	C(17)-C(18)	1.541(13)
P(2)-C(21)	1.901(11)	C(17)-C(20)	1.544(16)
C(1)-C(6)	1.402(14)	C(17)-C(19)	1.545(16)
C(1)-C(2)	1.407(14)	C(21)-C(24)	1.527(17)
C(2)-C(3)	1.388(14)	C(21)-C(23)	1.531(14)
C(2)-C(7)	1.512(14)	C(21)-C(22)	1.546(15)
C(1)-Ir(1)-C(28)	176.5(4)	C(17)-P(2)-C(21)	109.7(5)
C(1)-Ir(1)-O(1)	92.2(3)	C(8)-P(2)-Ir(1)	101.4(3)
C(28)-Ir(1)-O(1)	84.8(3)	C(17)-P(2)-Ir(1)	119.6(4)
C(1)-Ir(1)-P(2)	82.0(3)	C(21)-P(2)-Ir(1)	117.6(3)
C(28)-Ir(1)-P(2)	100.0(3)	C(6)-C(1)-C(2)	116.2(8)
O(1)-Ir(1)-P(2)	95.2(2)	C(6)-C(1)-Ir(1)	121.9(7)
C(1)-Ir(1)-P(1)	80.0(3)	C(2)-C(1)-Ir(1)	121.9(7)
C(28)-Ir(1)-P(1)	98.6(3)	C(3)-C(2)-C(1)	122.1(10)
O(1)-Ir(1)-P(1)	96.3(2)	C(3)-C(2)-C(7)	120.1(9)
P(2)-Ir(1)-P(1)	158.91(8)	C(1)-C(2)-C(7)	117.8(8)
C(7)-P(1)-C(13)	105.9(5)	C(4)-C(3)-C(2)	119.9(10)
C(7)-P(1)-C(9)	102.7(4)	C(5)-C(4)-C(3)	120.5(9)
C(13)-P(1)-C(9)	108.6(4)	C(4)-C(5)-C(6)	119.2(10)
C(7)-P(1)-Ir(1)	102.1(3)	C(1)-C(6)-C(5)	121.8(9)
C(13)-P(1)-Ir(1)	113.9(4)	C(1)-C(6)-C(8)	117.1(8)
C(9)-P(1)-Ir(1)	121.6(3)	C(5)-C(6)-C(8)	121.0(9)
C(8)-P(2)-C(17)	102.5(5)	C(2)-C(7)-P(1)	108.5(7)
C(8)-P(2)-C(21)	102.8(5)	C(6)-C(8)-P(2)	109.6(7)

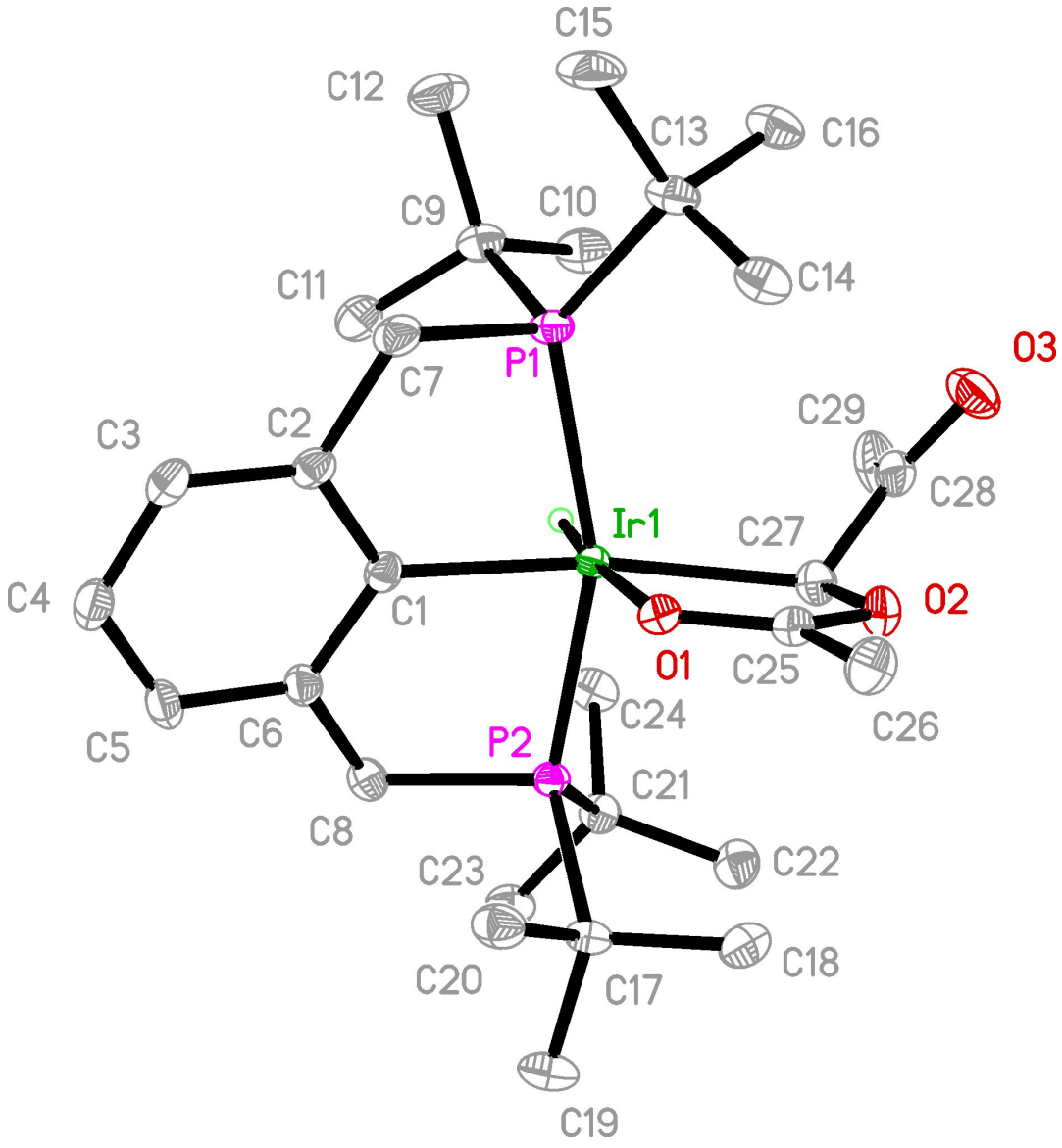

Figure 8-7 Crystal structure of complex **8-14**

Table 8.11 Crystal data and structure refinement for complex **8-14**

Empirical formula	C29 H51 Ir O3 P2	
Formula weight	701.84	
Temperature	100(2) K	
Wavelength	0.71073 Å	
Crystal system	Triclinic	
Space group	P1	
Unit cell dimensions	a = 10.6670(7) Å	α= 68.759(1)°.
	b = 11.0680(7) Å	β= 69.935(1)°.
	c = 14.7045(9) Å	γ = 72.729(1)°.
Volume	1490.07(16) $Å^3$	
Z	2	
Density (calculated)	1.564 Mg/m^3	
Absorption coefficient	4.615 mm^{-1}	
F(000)	712	
Crystal size	0.18 x 0.10 x 0.04 mm^3	
Theta range for data collection	2.01 to 30.55°.	
Index ranges	-14<=h<=15, -15<=k<=15, -21<=l<=21	
Reflections collected	18378	
Independent reflections	8988 [R(int) = 0.0208]	
Completeness to theta = 30.55°	98.3 %	
Absorption correction	Semi-empirical from equivalents	
Max. and min. transmission	0.8369 and 0.4905	
Refinement method	Full-matrix least-squares on F^2	
Data / restraints / parameters	8988 / 1 / 334	
Goodness-of-fit on F^2	1.001	
Final R indices [I>2sigma(I)]	R1 = 0.0252, wR2 = 0.0587	
R indices (all data)	R1 = 0.0287, wR2 = 0.0601	
Largest diff. peak and hole	1.812 and -0.602 e.$Å^{-3}$	

Table 8.12 Selected bond lengths [Å] and angles [°] for complex **8-14**

Ir(1)-C(1)	2.074(2)	C(1)-C(6)	1.408(3)
Ir(1)-C(27)	2.191(3)	C(2)-C(3)	1.394(4)
Ir(1)-O(1)	2.2049(18)	C(2)-C(7)	1.506(4)
Ir(1)-P(2)	2.3317(6)	C(3)-C(4)	1.386(4)
Ir(1)-P(1)	2.3439(7)	C(4)-C(5)	1.387(4)
Ir(1)-H(1)	1.584(10)	C(5)-C(6)	1.394(4)
P(1)-C(7)	1.844(3)	C(6)-C(8)	1.509(4)
P(1)-C(9)	1.898(3)	C(9)-C(10)	1.532(4)
P(1)-C(13)	1.903(3)	C(9)-C(11)	1.539(4)
P(2)-C(8)	1.840(3)	C(9)-C(12)	1.542(4)
P(2)-C(17)	1.890(3)	C(13)-C(14)	1.533(4)
P(2)-C(21)	1.892(3)	C(13)-C(16)	1.537(4)
O(1)-C(25)	1.230(3)	C(13)-C(15)	1.545(4)
O(2)-C(25)	1.306(3)	C(17)-C(18)	1.533(4)
O(2)-C(27)	1.490(3)	C(17)-C(19)	1.536(4)
O(3)-C(28)	1.229(3)	C(17)-C(20)	1.540(4)
C(1)-C(2)	1.408(3)	C(21)-C(22)	1.535(4)
C(1)-Ir(1)-C(27)	166.41(9)	C(8)-P(2)-C(21)	101.73(12)
C(1)-Ir(1)-O(1)	91.69(8)	C(17)-P(2)-C(21)	109.30(12)
C(27)-Ir(1)-O(1)	75.85(8)	C(8)-P(2)-Ir(1)	101.63(9)
C(1)-Ir(1)-P(2)	81.96(7)	C(17)-P(2)-Ir(1)	118.79(8)
C(27)-Ir(1)-P(2)	94.35(7)	C(21)-P(2)-Ir(1)	118.87(9)
O(1)-Ir(1)-P(2)	98.49(5)	C(25)-O(1)-Ir(1)	114.09(16)
C(1)-Ir(1)-P(1)	80.18(7)	C(25)-O(2)-C(27)	117.5(2)
C(27)-Ir(1)-P(1)	105.61(7)	C(2)-C(1)-C(6)	116.1(2)
O(1)-Ir(1)-P(1)	93.47(5)	C(2)-C(1)-Ir(1)	121.69(18)
P(2)-Ir(1)-P(1)	158.75(2)	C(6)-C(1)-Ir(1)	122.01(19)
C(7)-P(1)-C(9)	104.33(13)	C(3)-C(2)-C(1)	121.8(2)
C(7)-P(1)-C(13)	100.49(12)	C(3)-C(2)-C(7)	120.4(2)
C(9)-P(1)-C(13)	108.90(12)	C(1)-C(2)-C(7)	117.8(2)
C(7)-P(1)-Ir(1)	100.50(9)	C(4)-C(3)-C(2)	120.7(2)
C(9)-P(1)-Ir(1)	112.53(9)	C(3)-C(4)-C(5)	118.9(2)
C(13)-P(1)-Ir(1)	126.49(9)	C(4)-C(5)-C(6)	120.4(3)
C(8)-P(2)-C(17)	103.21(12)	C(5)-C(6)-C(1)	122.0(2)

Chapter 9

Other Reactions

9.1 Introduction

Reactivity of iridium pincer complexes in presence of some other substrates were also studied. Some of these reactions showed interesting phenomena which have not been reported yet. Although these projects are not finished, they are still worth mentioning in this thesis.

9.2 Results and discussion

9.2.1 Reaction of (PCP)Ir(NBE) with (methoxymethyl)benzene

(PCP)IrH_4 in presence of NBE at room temperature formed (PCP)Ir(NBE) complex. Addition of one and a half equivalent (methoxymethyl)benzene to (PCP)Ir(NBE) in *p*-xylene-d_{10}, yields a new complex **9-2** after 20 minutes at room temperature. Complex **9-2** was characterized by ^{31}P and ^{1}H NMR spectroscopy. In the ^{31}P NMR spectrum, complex **9-2** appeared as a singlet at 53.1 ppm. In the ^{1}H NMR spectrum, there was a hydride signal at -29.16 ppm (t, J_{PH} = 17.5 Hz), which is characteristic of a 6-coordinate iridium complex, in which hydride is *cis* to carbon atom.[1]

At -30 °C, (PCP)Ir(NBE) in mesitylene-d_{12} reacted with (methoxymethyl)benzene to yield complex **9-1** along with three 5-coordinated aromatic C-H bond activated complexes. In the ^{31}P NMR spectrum at -30 °C, complex **9-1** appeared as a singlet at 53.3

ppm. In the ^{1}H NMR spectrum at -30 °C, there was a hydride signal at -8.93 ppm (t, J_{PH} = 18.0 Hz), which is characteristic of 6-coordinate iridium complex in which hydride is *trans* to carbon atom.[1] When this solution was brought back to room temperature, only complex **9-2** was formed after 5 minutes.

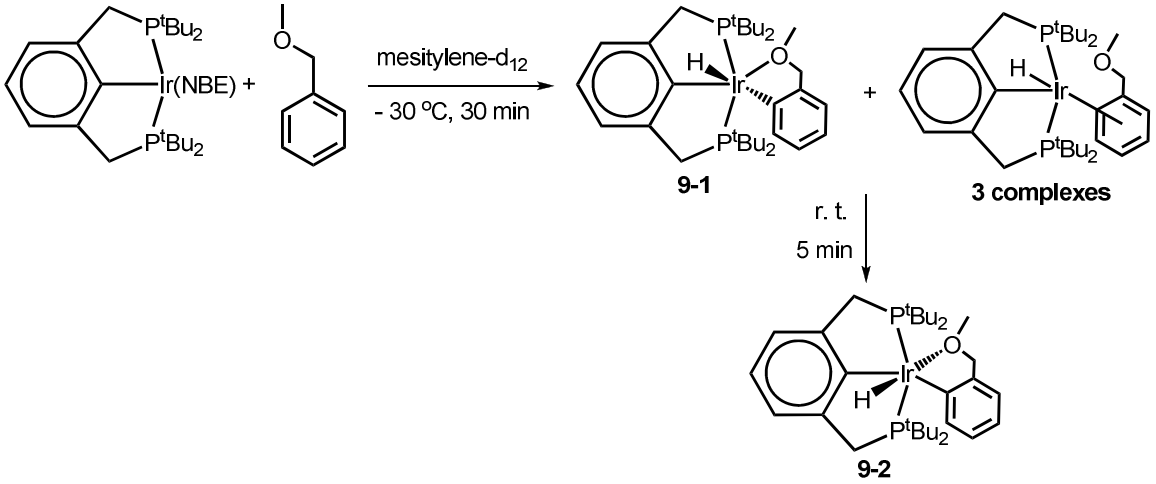

Scheme 9-1 Reaction of (PCP)Ir(NBE) with (methoxymethyl)benzene

9.2.2 Reaction of (PCP)Ir(NBE) with 1-methoxynaphthalene

(PCP)IrH$_4$ in presence of NBE at room temperature formed (PCP)Ir(NBE) complex. Addition of one and a half equivalent 1-methoxynaphthalene to (PCP)Ir(NBE) in *p*-xylene-d$_{10}$, after 20 minutes at room temperature yields complexes **9-3** and **9-4** in 1:1 ratio. The ratio of complexes **9-3** and **9-4** did not change after keeping the solution at room temperature for 2 days. Complex **9-3** was characterized by ^{31}P and ^{1}H NMR spectroscopy. In the ^{31}P NMR spectrum, complex **9-3** appeared as a singlet at 53.1 ppm. In the ^{1}H NMR spectrum, there was a hydride signal at -8.23 ppm (t, J_{PH} = 18.5 Hz), which is characteristic of 6-cordinate iridium complex in which hydride is *trans* to carbon

atom.[1] In the ^{31}P NMR spectrum, complex **9-4** appeared as a broad singlet at 67.4 ppm. In the ^{1}H NMR spectrum, there is a broad hydride signal at -45.56 ppm, which is characteristic of 5-coordinate aromatic C-H bond activated complexes.[1]

The solution containing complexes **9-3** and **9-4,** after 10 h heating at 70 °C in *p*-xylene-d_{10}, yields complexes **9-5** and **9-6** in 4:1 ratio. Complexes **9-5** and **9-6** were characterized by ^{31}P and ^{1}H NMR spectroscopy. From this mixture, complex **9-5** was crystallized from hexane and was characterized by X-ray crystallography. In the ^{31}P NMR spectrum, complex **9-5** appeared as a singlet at 50.8 ppm. In the ^{1}H NMR spectrum, there was a hydride signal at -28.58 ppm (t, J_{PH} = 17.0 Hz,), which is characteristic of 6-cordinate iridium complex, in which hydride is *cis* to carbon atom.[1]

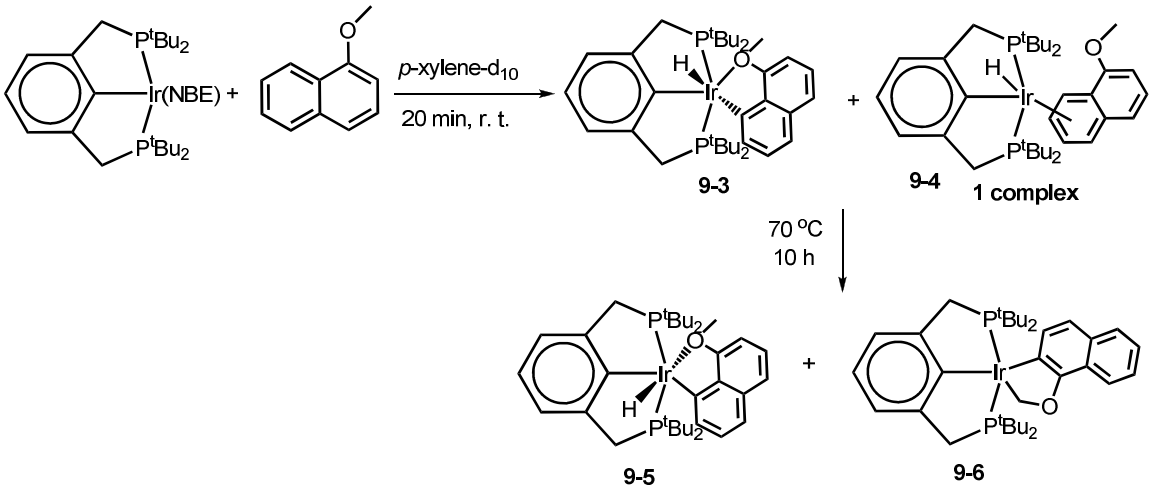

Scheme 9-2 Reaction of (PCP)Ir(NBE) with 1-methoxynaphthalene

9.2.3 Reaction of (PCP)Ir(NBE) with N,N-dimethyl-1-phenylmethanamine and N,N-dimethylnaphthalen-1-amine

(PCP)IrH_4 in presence of NBE, at room temperature formed (PCP)Ir(NBE) complex. Addition of one and a half equivalent N,N-dimethyl-1-phenylmethanamine to (PCP)Ir(NBE) in *p*-xylene-d_{10}, yields complexes **9-7** and **9-8**, after 5 hours at room temperature (Scheme 9-3). While addition of one and a half equivalent N,N-dimethylnaphthalen-1-amine to (PCP)Ir(NBE) yields complex **9-9** (Scheme 9-3). Complexes **9-7**, **9-8** and **9-9** were characterized by ^{31}P and ^{1}H NMR spectroscopy. In separate experiments, the complexes **9-7** and **9-9**, after 1 h heating at 110 °C in *p*-xylene-d_{10}, yield (PCP)IrH_2 along with uncharacterized organic products.

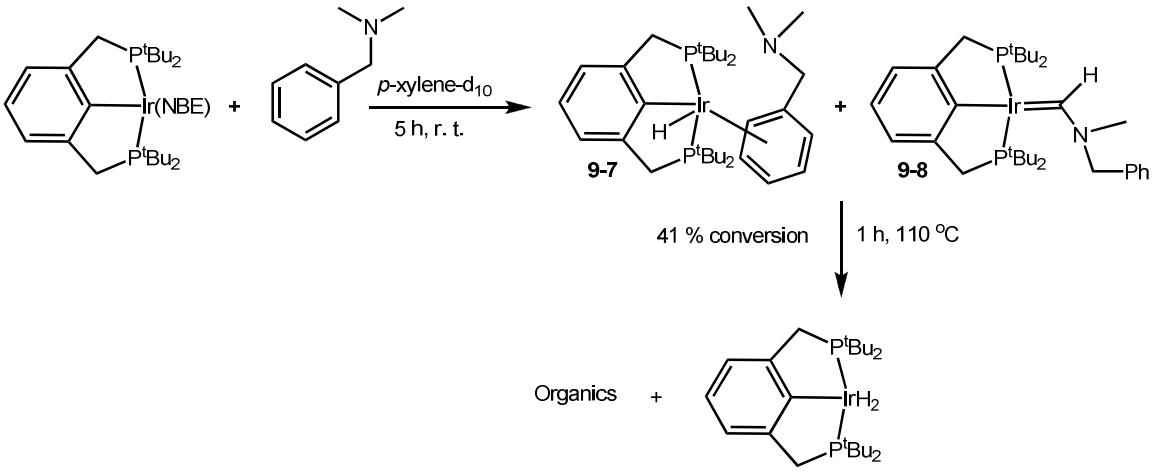

Scheme 9-3 Reaction of (PCP)Ir(NBE) with N,N-dimethyl-1-phenylmethanamine

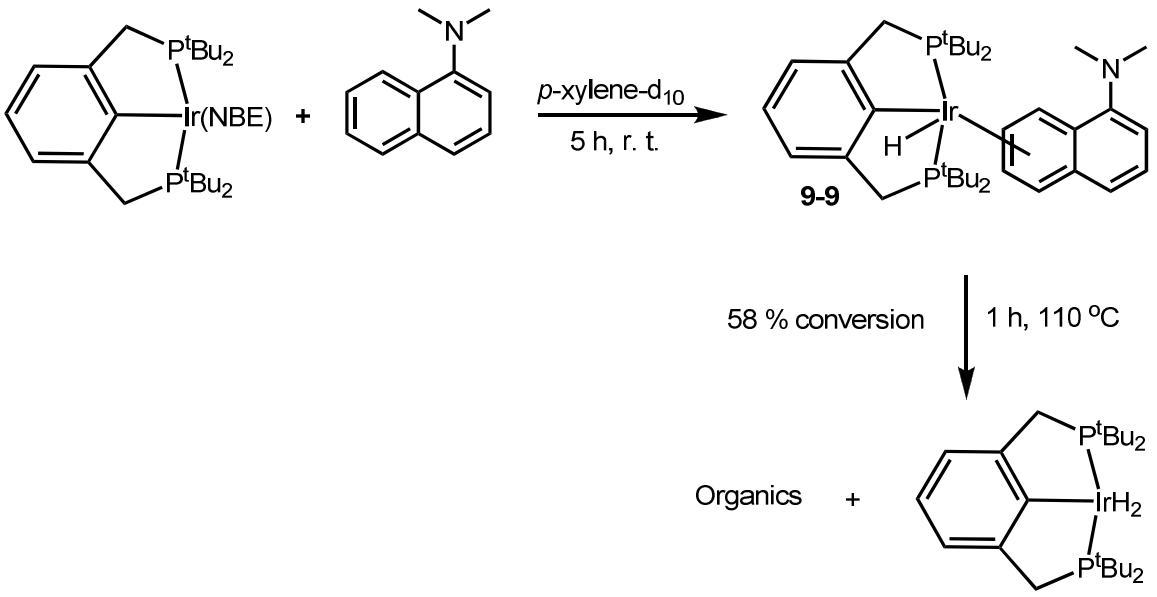

Scheme 9-4 Reaction of (PCP)Ir(NBE) with N,N-dimethylnaphthalen-1-amine

9.2.4 Reaction of (PCP)Ir(NBE) with 1-p-tolylpropan-2-one and 1,1,1-trifluoro-3-phenylpropan-2-one

Addition of one and a half equivalent 1-*p*-tolylpropan-2-one to (PCP)Ir(NBE) in *p*-xylene-d_{10}, yields complexes **9-10** and its isomer (in 2.6:1 ratio), after 12 hours at room temperature (Scheme 9-5). Complexes **9-10** and its isomer were characterized by ^{31}P and ^{1}H NMR spectroscopy. In the ^{31}P NMR spectrum, complex **9-10** and its isomer appear as a singlet at 68.9 and 68.1 ppm, respectively. In the ^{1}H NMR spectrum, there were hydride signals at -39.49 ppm (t, J_{PH} = 13.0 Hz, complex **9-10**) and -39.65 ppm (t, J_{PH} = 13.0 Hz, isomer of **9-10**). 1,1,1-trifluoro-3-phenylpropan-2-one also reacted with (PCP)Ir(NBE) in *p*-xylene-d_{10}, in a similar fashion. After 12 hours at room temperature, three complexes (in 1:5:2 ratio) were observed and all of them had a hydride signal. After addition of CO, CO adduct of enol activated complex was crystallized and characterized by X-ray crystallography (Figure 9-5). Heating this solution at 120 °C for 24 hours, yields complex

9-11 along with (PCP)IrH_2, (PCP)Ir(CO) in 7:2:1 ratio (Scheme 9-6). After addition of CO, CO adduct of complex **9-11** was crystallized from the solution (Figure 9-6).

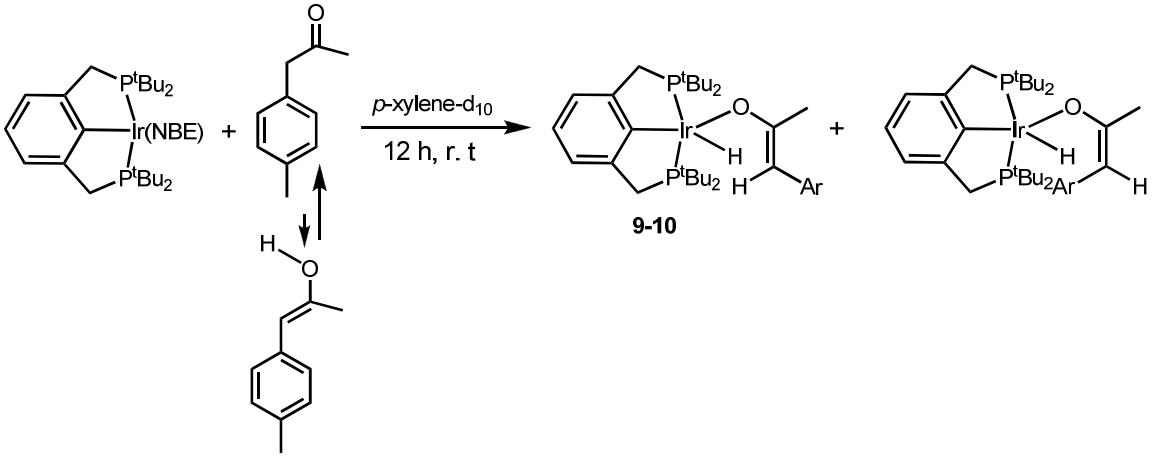

Scheme 9-5 Reaction of (PCP)Ir(NBE) with 1-*p*-tolylpropan-2-one

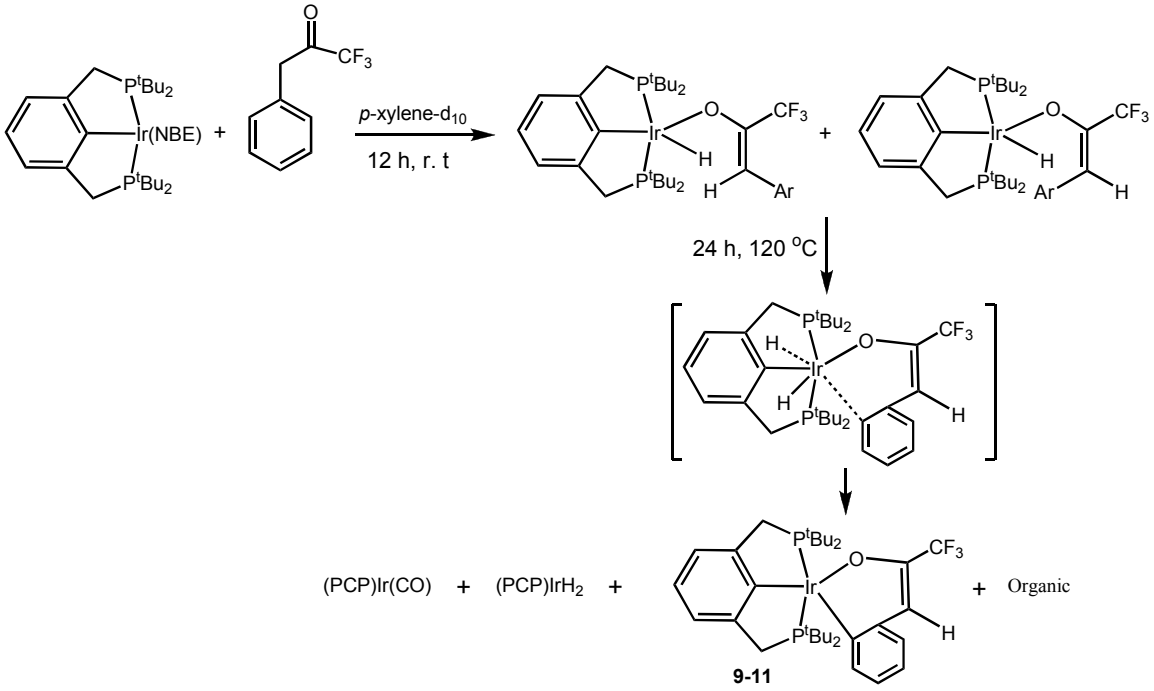

Scheme 9-6 Reaction of (PCP)Ir(NBE) with 1,1,1-trifluoro-3-phenylpropan-2-one

9.2.5 Reaction of (PCP)Ir(NBE) with 4,4,4-trifluorobutan-2-one

Addition of one and a half equivalent 4,4,4-trifluorobutan-2-one to (PCP)Ir(NBE) in *p*-xylene-d_{10} yields three complexes (PCP)Ir(H)(F) and **9-12** and enol activated complex (in 2:1:1 ratio), after 12 hours at room temperature (Scheme 9-7). Only (PCP)Ir(H)(F) and **9-12** were observed (in 1:1 ratio) after 2 hour heating at 100 °C. (PCP)Ir(H)(F) and **9-12** were characterized by ^{31}P, ^{1}H and ^{19}F NMR spectroscopy.

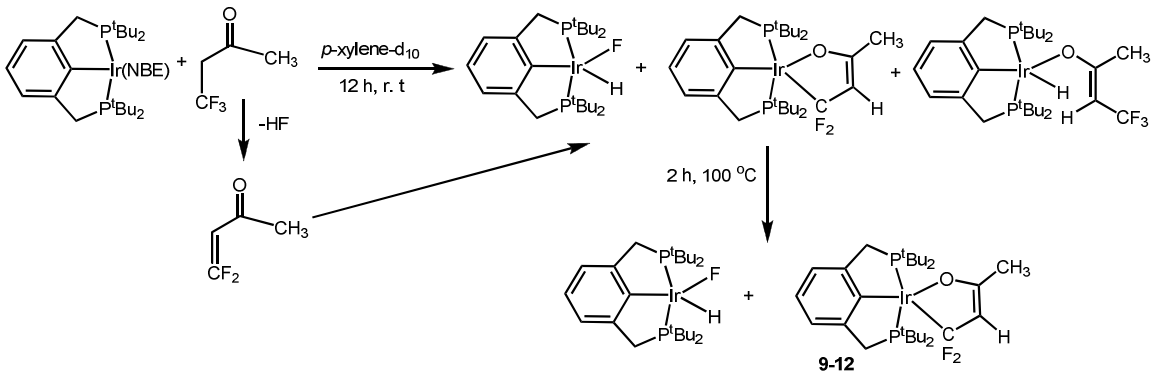

Scheme 9-7 Reaction of (PCP)Ir(NBE) with 4,4,4-trifluorobutan-2-one

9.2.6 Reaction of (PCP)Ir(NBE) with 1-fluorooctane

In the previous reaction of (PCP)Ir(NBE) with 4,4,4-trifluorobutan-2-one, dehydrofluorination was observed. Addition of one equivalent of 1-fluorooctane to (PCP)Ir(NBE) in *p*-xylene-d_{10} yields complexes (PCP)Ir(H)(F), one uncharacterized complex and (PCP)Ir(alkene), after 12 hours at room temperature (Scheme 9-8). (PCP)Ir(H)(F) and one uncharacterized complex were observed (in 5:1 ratio) after 1 hour heating at 100 °C (Scheme 9-8). (PCP)Ir(H)(F) were characterized by ^{31}P, ^{1}H and ^{19}F NMR spectroscopy.

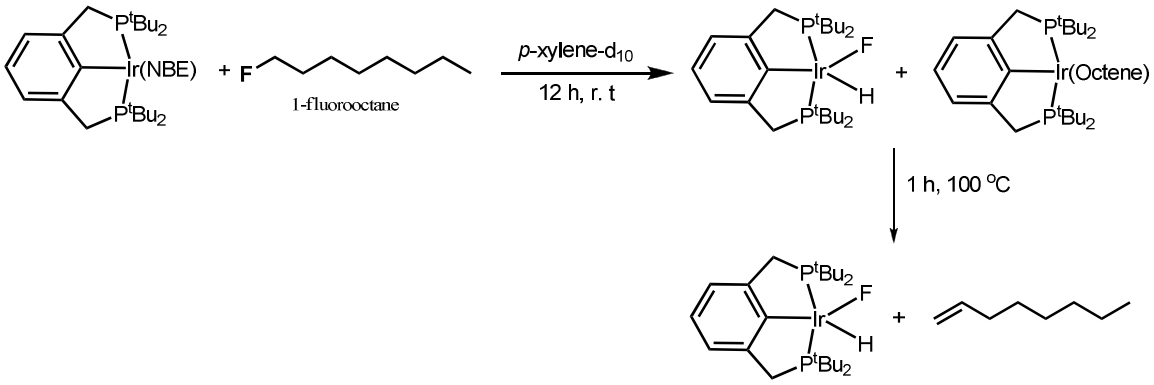

Scheme 9-8 Reaction of (PCP)Ir(NBE) with 1-fluorooctane

9.2.7 N-H reductive elimination from (PCP)Ir(H)(NPh$_2$)

Addition of one equivalent of diphenylamine to (PCP)Ir(NBE) in *p*-xylene-d$_{10}$ yields complexes (PCP)Ir(H)(NPh$_2$) (**9-13**), after 3 hours at room temperature (eq. 1). Addition of aniline and benzene to (PCP)Ir(H)(NPh$_2$) (**9-13**) after 1 day at room temperature, yields complex **9-14** and **9-15**, respectively. But, in both cases reaction did not reach equilibrium even after 5 days at room temperature (Scheme 9-9). In a separate experiment when benzene was added to complex **9-14**, reaction was fast upon mixing and reached equilibrium after 12 hours at room temperature (Scheme 9-9). The N-H reductive elimination from complex **9-13** was very slow, probably due to elimination in the transition state, where the NPh$_2$ group has to rotate around the Ir-N bond which is severely hindered by steric crowding of the ^{t}Bu group in the phosphorous atom.

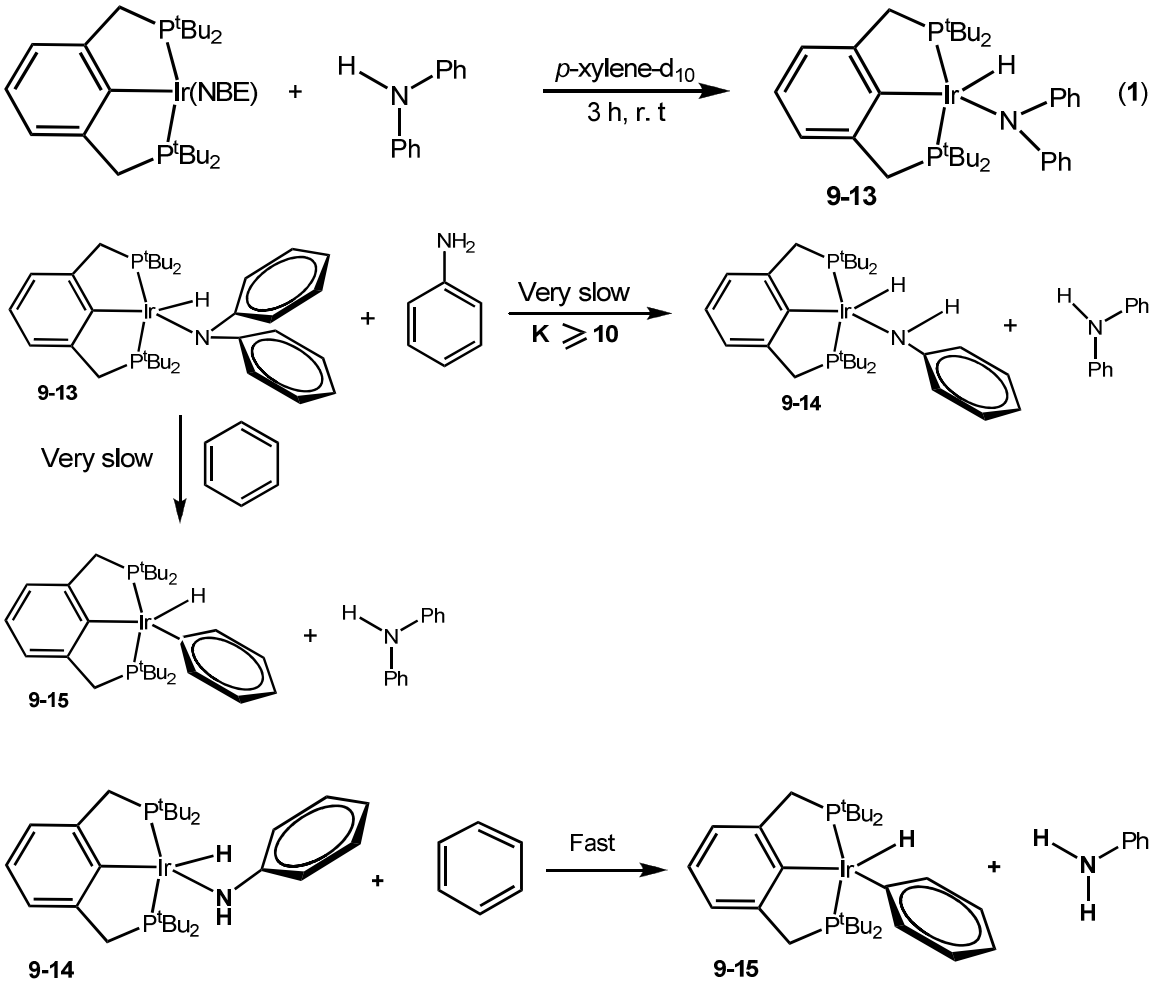

Scheme 9-9 N-H reductive elimination from (PCP)Ir(H)(NPh_2) and (PCP)Ir(H)(NHPh)

The elimination of diphenylamine by pyridine with varying concentration of both pyridine and diphenylamine was studied to find out if N-H reductive elimination from complex **9-13** follows a dissociative pathway (Scheme 9-9) and to measure $\Delta S^{\neq}$ for the reaction. The results are summarized in Figure 9-1. In the graph, the dots are experimental data and the lines are fitted data from the Gepasi software program. Following a dissociative mechanism, k_1 increased with increasing concentration of pyridine; while other three rate constant (k_2, k_3 and k_4) remained same. This is probably

due to H-bonding between pyridine nitrogen and proton in diphenylamine in the transition state favoring the elimination of diphenylamine from the complex **9-13**. In ^{1}H NMR spectra, H-bonding between pyridine nitrogen and proton in free diphenylamine in the solution was observed. In future, other substrates will be tested in the N-H elimination of diphenylamine, so that H-bonding will not possible.

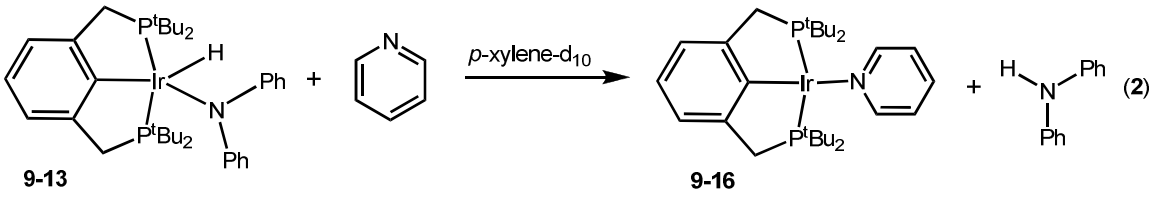

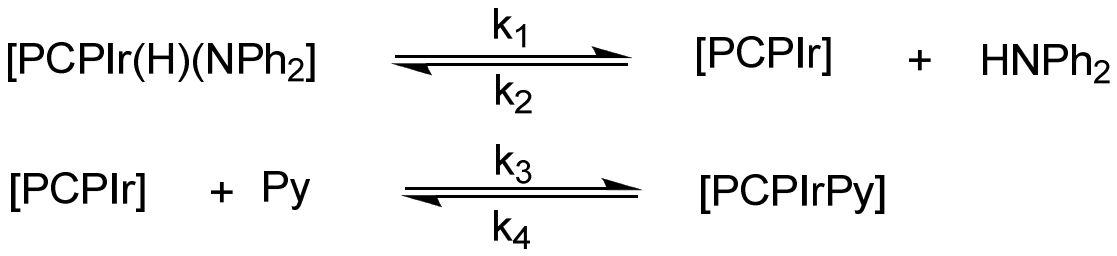

Scheme 9-10 Dissociative pathway for N-H reductive elimination by Py

[PCPIr(H)(NPh_2] = 10 mM, [$HNPh_2$] = 38 mM, [py] = 72 mM

k_1 =10.1E-5/sec, k_2 = 5E4/sec, k_3 = 5E5/sec, k_4 = 2E-6/sec

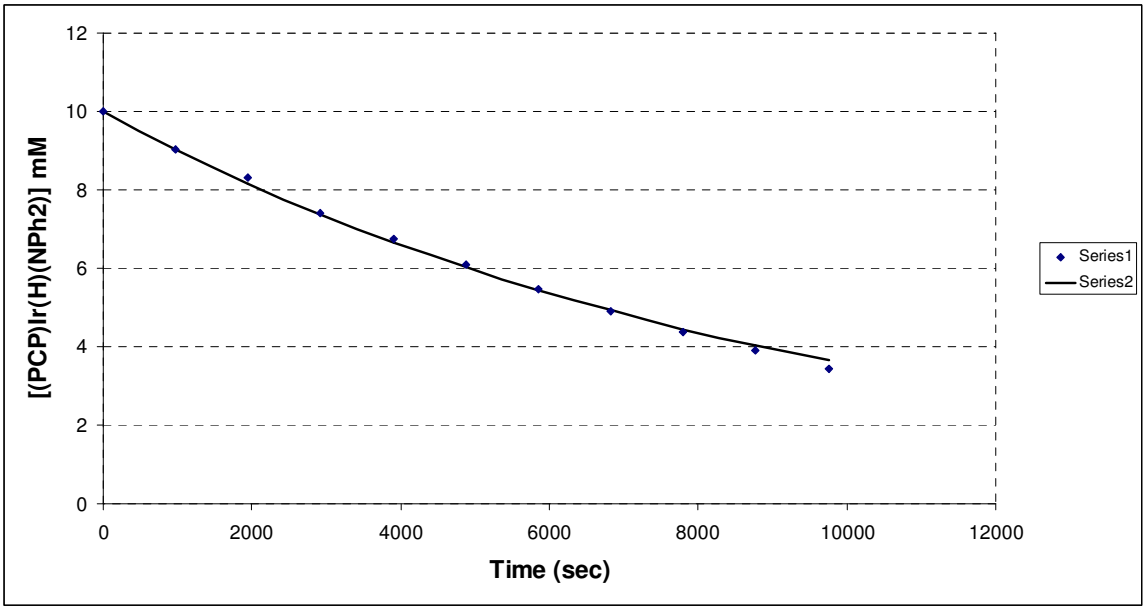

[PCPIr(H)(NPh_2] = 10 mM, [$HNPh_2$] = 34 mM, [py] = 13 mM

k_1 =6.8E-5/sec, k_2 = 5E4/sec, k_3 = 5E5/sec, k_4 = 2E-6/sec

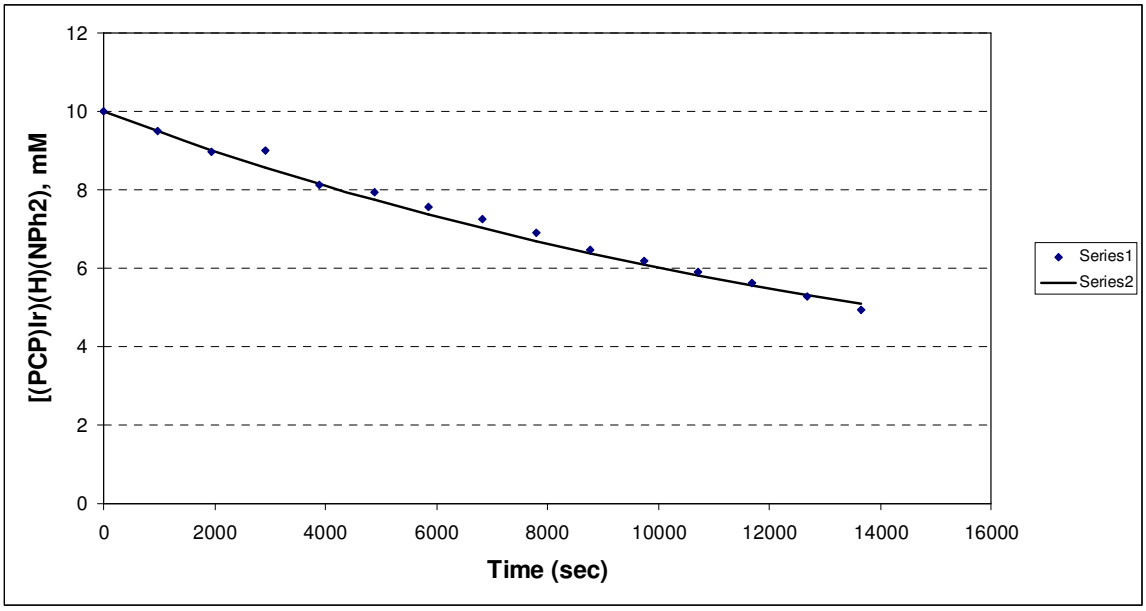

[PCPIr(H)(NPh_2] = 10 mM, [$HNPh_2$] = 117 mM, [py] = 47 mM

k_1 =3.8E-5/sec, k_2 = 5E4/sec, k_3 = 5E5/sec, k_4 = 2E-6/sec

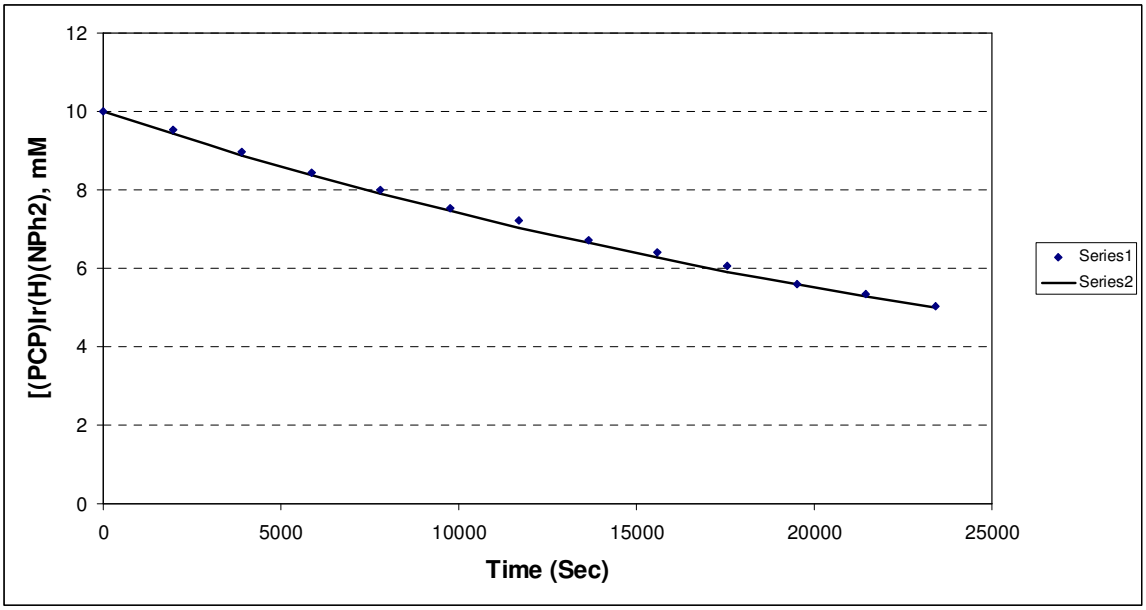

Figure 9-1 Experimental and Gepasi fitting data for N-H reductive elimination from complex **9-13**

9.2.8 Hydrogenation of *trans*-5-decene using (^{tBu4}PCP)IrH$_2$ and (^{tBu4}POCOP)IrH$_2$

In alkane metathesis of *n*-hexane using (^{tBu4}PCP)IrH$_2$ catalyst, hydrogenation of *trans*-5-decene was proposed to be the slowest step.[2] Hydrogenation of *trans*-5-decene was performed using 24 mM iridium complex ((^{tBu4}PCP)IrH$_2$ and (^{tBu4}POCOP)IrH$_2$) and 144 mM *trans*-5-decene in 0.5 mL mesitylene at different temperatures (Scheme 9-11). The reaction was monitored by ^{31}P NMR spectroscopy. (^{tBu4}PCP)Ir(*trans*-5-decene) was characterized by ^{1}H and ^{31}P NMR spectroscopy, while (^{tBu4}POCOP)Ir(*trans*-5-decene) was characterized by ^{1}H and ^{31}P NMR spectroscopy and X-ray crystallography. From the Eyring plot in case of using (^{tBu4}PCP)IrH$_2$, $\Delta H^{\neq}$ = 3.2(4) kcal mol^{-1} and $\Delta S^{\neq}$ = - 60(1) cal mol^{-1} K^{-1} were measured (Figure 9-2). Such high entropy of activation has no presidence and further study is needed to find out if the reaction involved tunneling or not. From the Eyring plot, in case of using (^{tBu4}POCOP)IrH$_2$, $\Delta H^{\neq}$ = 8.2(4) kcal mol^{-1} and $\Delta S^{\neq}$ = - 38(1) cal mol^{-1} K^{-1} were measured (Figure 9-3). In the case using (^{tBu4}POCOP)IrH$_2$ hydrogenation of *trans*-5-decene was much faster and entropy of activation was much lower than (^{tBu4}PCP)IrH$_2$.

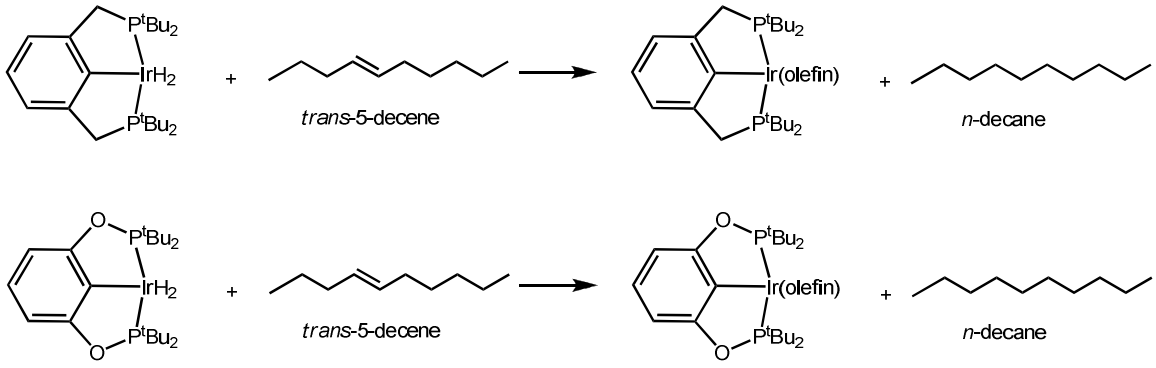

Scheme 9-11 Hydrogenation of *trans*-5-decene

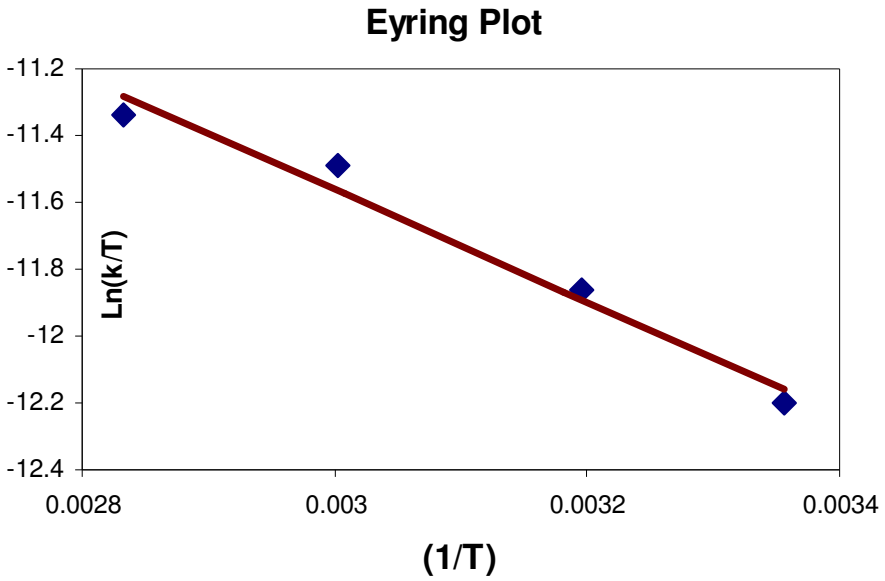

T (°C)	k ($M^{-1}s^{-1}$)
25	1.5E-03
40	2.2E-03
60	3.4E-03
80	4.2E-03

$\Delta H^{\neq}$ = 3.2(4) kcal mol^{-1} $\Delta S^{\neq}$ = - 60(1) cal mol^{-1} K^{-1}

Figure 9-2 Eyring plot for hydrogenation of *trans*-5-decene using (^{tBu4}PCP)IrH_2

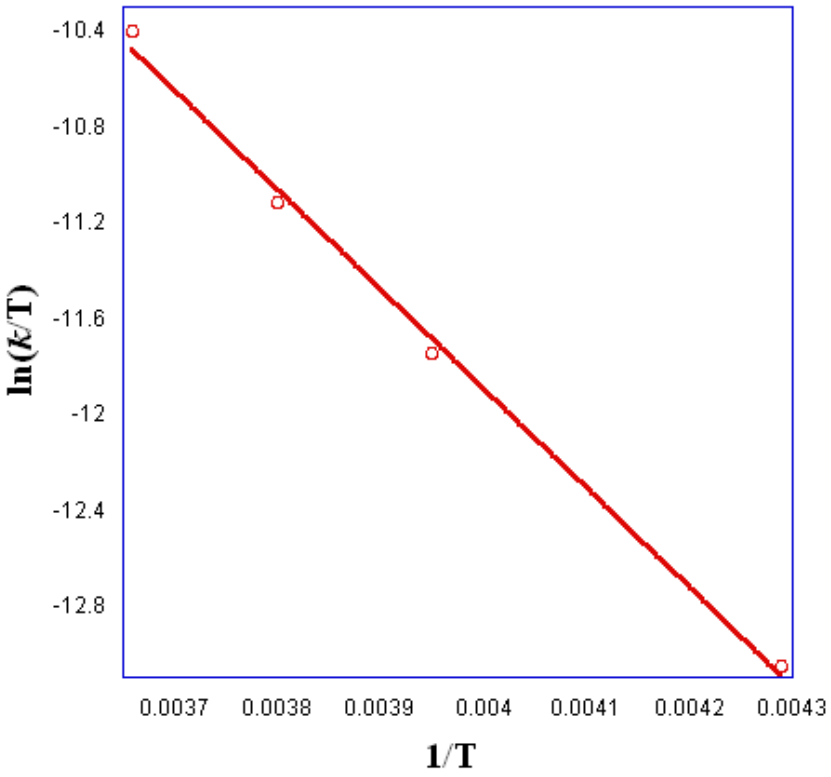

T (°C)	k ($M^{-1}s^{-1}$)
- 40	0.5E-03
- 20	2.0E-03
- 10	3.9E-03
0	8.3E-03

$\Delta H^{\neq}$ = 8.2(4) kcal mol^{-1} $\Delta S^{\neq}$ = - 38(1) cal mol^{-1} K^{-1}

Figure 9-3 Eyring plot for hydrogenation of *trans*-5-decene using (^{tBu4}POCOP)IrH_2

9.2.9 Checking metalloaromaticity in (PCP)Ir complexes

In 1945 Calvin and Wilson first introduced the idea of metalloaromaticity to explain the stability of Cu(II)–1,3-diketonate complexes.[3] In synthesis and theory, of organometallic compounds, there has been a lot of interest in the past decade about the concept of metalloaromaticity.[4] Complex **9-17** was synthesized as reported by our group.[1] Addition of CO to complex **9-17** in C_6D_6 followed by 2 hours reflux yields (PCP)Ir(CO), (PCP)Ir(D)(CO)(C_6D_5) and complex **9-18**. But complex **9-18** did not react with CO, even after heating for 3 days at 100 °C (Scheme 9-12). This indicates high stability of complex **9-18**, probably due to metalloaromaticity. Addition of one equivalent phenylacetate to (PCP)Ir(NBE) in *p*-xylene-d_{10} yields complexes **9-19**, after 4 hours at room temperature. Addition of CO to complex **9-19** followed by 1 day heating at 70 °C yields (PCP)Ir(CO) and complex **9-20** (Scheme 9-13). Complex **9-19** did not show high stability because the cyclometalated ring in complexes **9-19** had $8e^-$. CO reacts with complex **9-3**, after 12 hours at room temperature and 92% conversion of complex **9-3** was observed while only 35% conversion of complex **9-5** was observed after 1 day heating at 100 °C in presence of CO (Scheme 9-14). Addition of one equivalent pentane-2,4-dione to (PCP)Ir(NBE) in *p*-xylene-d_{10} yields complexes **9-21**, after 12 hours at room temperature. Complex **9-21** was characterized by NMR spectroscopy and X-ray crystallography. Complex **9-21** was highly stable, only 31% conversion of complex **9-21** was observed after 6 days heating at 90 °C in presence of CO (Scheme 9-15). Complex **9-21** showed high stability although the cyclometalated ring in complex **9-21** had $8e^-$.

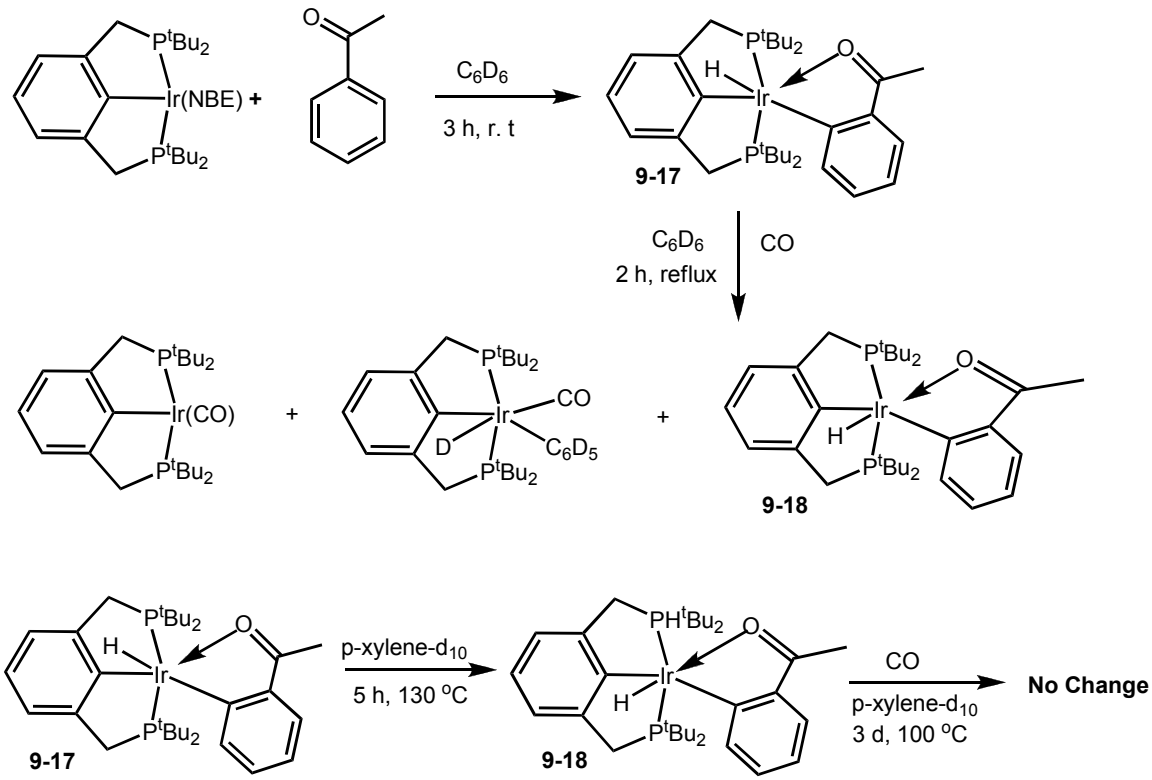

Scheme 9-12 Addition of CO to complexes **9-17** and **9-18**

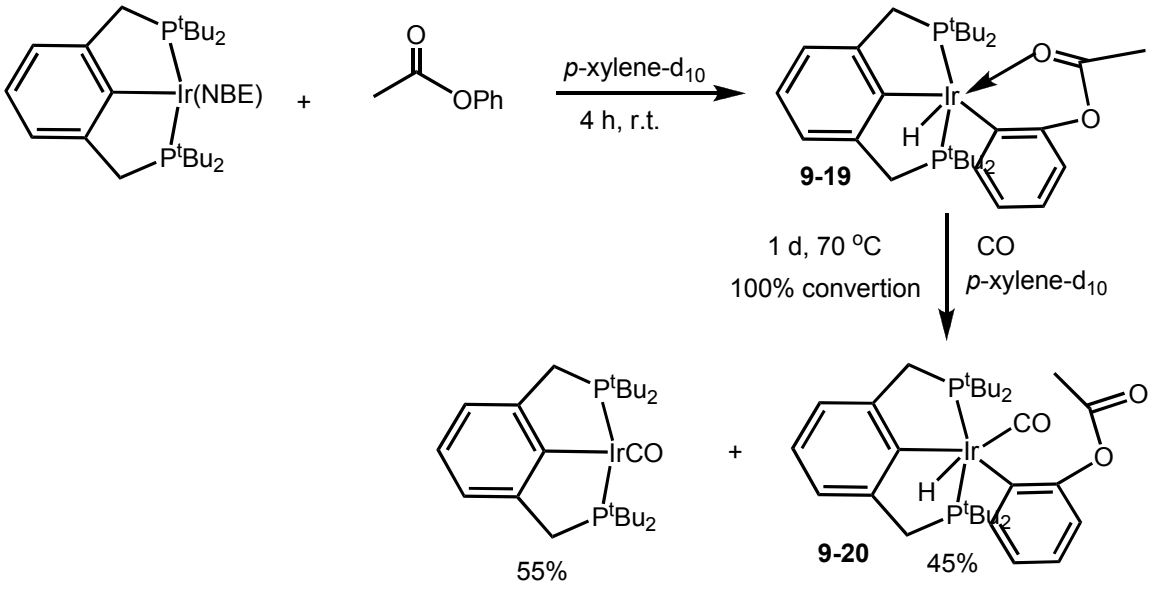

Scheme 9-13 Addition of CO to complex **9-19**

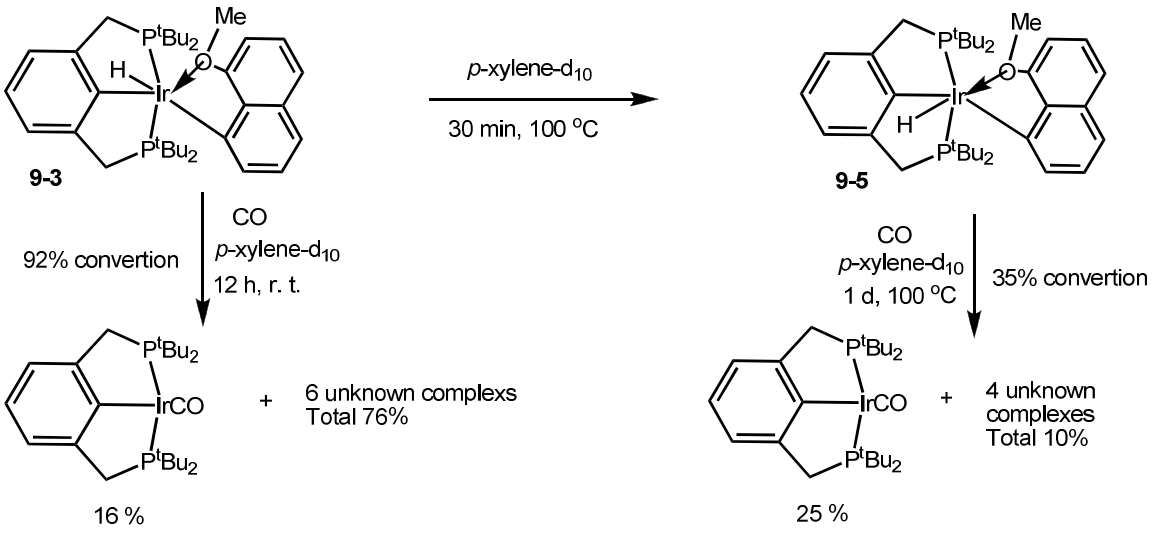

Scheme 9-14 Addition of CO to complexes **9-3** and **9-5**

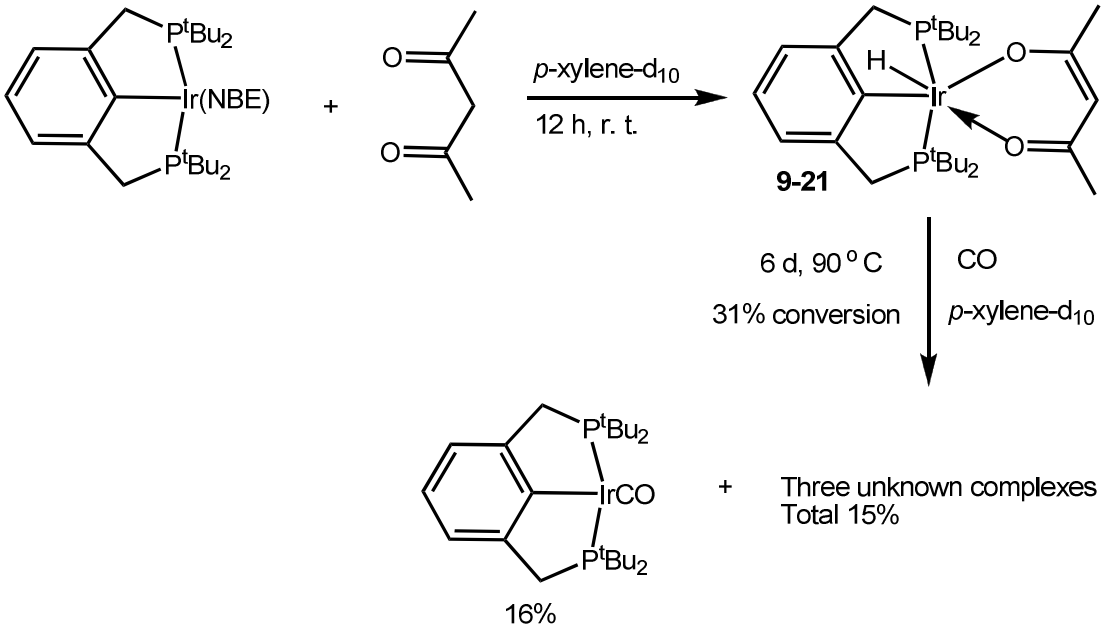

Scheme 9-15 Addition of CO to complex **9-21**

9.3 Experimental

General Methods. All reactions were carried out under an argon atmosphere using standard Schlenk techniques or in an argon-filled dry box. *p*-Xylene-d_{10}, TBE, 1-hexene, *t*-5-decene, cyclooctene and C_6D_6 were dried using Na/K alloy and collected by vacuum transfer. (methoxymethyl)benzene, 1-methoxynaphthalene, N,N-dimethyl-1-phenylmethanamine, N,N-dimethylnaphthalen-1-amine, 1-p-tolylpropan-2-one, 1,1,1-trifluoro-3-phenylpropan-2-one, 4,4,4-trifluorobutan-2-one, and 1-fluorooctane were degassed by sparging with argon and used. NBE was sublimed before use. 400 MHz or 500 MHz Varian instruments were used for ^{1}H, ^{13}C and ^{31}P NMR spectroscopy. (^{tBu4}PCP)IrH_4 was synthesized according to literature procedure.[5] The residual peak of the deuterated solvent was used as a reference for ^{1}H chemical shifts. ^{31}P NMR chemical shifts were referenced to a capillary PMe_3 standard (–62.2 ppm).

Complex 9-1: To a 0.5 mL mesitylene-d12 solution of 5 mg (^{tBu4}PCP)IrH_4 (8.3 μmol) in a J-Young tube, 2.34 mg NBE (25 μmol) was added. After 10 hours at room temperature (PCP)Ir(NBE) was formed, 1.55μL (0.012 mmol) (methoxymethyl)benzene was then added and immediately the solution was frozen in liquid nitrogen. The NMR spectra at -30 °C indicated formation of complex **9-1** along with three 5-coordinate aromatic C-H bond activated complexes. In ^{31}P NMR spectroscopy at -30 °C, three peaks at 68.2 ppm (broad), 67.5 ppm (broad), and 66.9 ppm (broad) in 1:2:8 were observed, respectively. **Complex 9-1:** ^{31}Pw NMR (mesitylene-d_{12}, -30 °C, 202 MHz): δ 53.32 (s, PCP). ^{1}H NMR (mesitylene-d_{12}, -30 °C, 500 MHz): δ -8.93 (t, J_{PH} = 18.0 Hz, 1H, Ir-***H***).

Complex 9-2: To a 0.5 mL *p*-xylene-d_{10} solution of 5 mg (^{tBu4}PCP)IrH_4 (8.3 μmol) in a J-Young tube, 2.34 mg NBE (25 μmol) was added. After 10 hours at room temperature (PCP)Ir(NBE) complex was formed, then 1.55 μL (12 μmol) (methoxymethyl)benzene was added to the solution. After 15 min at room temperature solvent was removed and NMR spectrum was recorded. $^{31}P\{^1H\}$ NMR (*p*-xylene-d_{10}, 202 MHz): δ 53.13 (s, PCP). ^{1}H NMR (*p*-xylene-d_{10}, 500 MHz): δ 8.07 (d, J_{HH} = 7.5 Hz,1H, Ar), 7.28 (m, 1H, Ar), 7.22 (d, J_{HH} = 7.5 Hz, 2H, Ar), 7.01 (d, J_{HH} = 7.3 Hz, 1H, Ar), 6.94 (m, 2H, Ar), 4.68 (s, 2H, ***CH₂***Ar), 3.40 (d of vt, J_{PH} = 4.0 Hz, J_{HH} = 16.5 Hz, 2H, ***CH₂***P^{t}Bu$_2$), 3.26 (d of vt, J_{PH} = 2.5 Hz, J_{HH} = 17.0 Hz, 2H, ***CH₂***P^{t}Bu$_2$), 2.75 (s, 2H, CH$_2$O***CH₃***), 1.23 (t, J_{PH} = 6.3 Hz, 18H, PC(C***H***$_3$)$_3$), 1.05 (t, J_{PH} = 6.3 Hz, 18H, PC(C***H***$_3$)$_3$), -29.16 (t, J_{PH} = 17.5 Hz, 1H, Ir-***H***).

Complex 9-3: To a 0.5 mL *p*-xylene-d_{10} solution of 5 mg (^{tBu4}PCP)IrH_4 (8.3 μmol) in a J-Young tube, 2.34 mg NBE (25 μmol) was added. After 10 hours at room temperature (PCP)Ir(NBE) was formed, then 1.8 μL (12 μmol) 1-methoxynaphthalene was added to the solution. After 20 minute at room temperature, solvent was removed and NMR was recorded; complex **9-3** and **9-4** were observed in 1: 1 ratio. $^{31}P\{^1H\}$ NMR (*p*-xylene-d_{10}, 202 MHz): δ 53.1 (s, PCP). ^{1}H NMR (*p*-xylene-d_{10}, 500 MHz): δ 4.13 (s, 3H, O-***CH₃***), 3.19 (broad d of vt, J_{PH} = 3.3 Hz, J_{HH} = 12.0 Hz, 2H, ***CH₂***P^{t}Bu$_2$), 2.91 (broad d of vt, J_{PH} = 2.5 Hz, J_{HH} = 16.0 Hz, 2H, ***CH₂***P^{t}Bu$_2$), 1.35 (t, J_{PH} = 6.3 Hz, 18H, PC(C***H***$_3$)$_3$), 0.65 (t, J_{PH} = 6.3 Hz, 18H, PC(C***H***$_3$)$_3$), -8.23 (t, J_{PH} = 18.5 Hz, 1H, Ir-***H***).

Complex 9-4: $^{31}P\{^{1}H\}$ NMR (*p*-xylene-d_{10}, 202 MHz): δ 67.4 (bs, PCP). ^{1}H NMR (*p*-xylene-d_{10}, 500 MHz): 3.48 (bs, 4H, ***CH₂***P^{t}Bu$_2$), 3.34 (bs, 3H, O-***CH₃***), 1.07 (vt, J_{PH} = 5.5 Hz, 36H, PC(C***H***$_3$)$_3$), -45.56 (bs, 1H, Ir-***H***).

Complex 9-5: 5 mg mixtures of complex **9-3** and **9-4** in a 0.5 mL *p*-xylene-d_{10} was heated 10 hours at 70 °C. Complex **9-5** and **9-6** was formed in 4 : 1 ratio as characterized by NMR spectroscopy. $^{31}P\{^{1}H\}$ NMR (*p*-xylene-d_{10}, 202 MHz): δ 50.8 (s, PCP). ^{1}H NMR (*p*-xylene-d_{10}, 500 MHz): δ 8.14 (d, J_{HH} = 6.0 Hz,1H, Ar), 7.40 (m, 3H, Ar),7.16 (m, 2H, Ar), 7.12 (m, 2H, Ar), 6.18 (d, J_{HH} = 7.5 Hz, 1H, Ar), 3.45 (d of vt, J_{PH} = 4.0 Hz, J_{HH} = 17.0 Hz, 2H, ***CH₂***P^{t}Bu$_2$), 3.31 (s, 3H, O-***CH₃***), 3.26 (d of vt, J_{PH} = 2.5 Hz, J_{HH} = 17.0 Hz, 2H, ***CH₂***P^{t}Bu$_2$), 1.27 (t, J_{PH} = 6.3 Hz, 18H, PC(C***H***$_3$)$_3$), 0.75 (t, J_{PH} = 6.3 Hz, 18H, PC(C***H***$_3$)$_3$), -28.58 (t, J_{PH} = 17.0 Hz, 1H, Ir-***H***).

Complex 9-6: $^{31}P\{^{1}H\}$ NMR (*p*-xylene-d_{10}, 202 MHz): δ 45.2 (s, PCP). ^{1}H NMR (*p*-xylene-d_{10}, 500 MHz): δ 8.36 (d, J_{HH} = 8.5 Hz, 1H, Ar), 8.10 (d, J_{HH} = 7.5 Hz, 1H, Ar), 7.86 (d, J_{HH} = 8.0 Hz, 1H, Ar), 7.42 (m, 2H, Ar), 7.25 (m, 1H, Ar), 6.92 (m, 2H, Ar), 6.84 (m, 1H, Ar), 5.31 (t, J_{PH} = 9.0 Hz, 2H, Ir-***CH₂***O), 3.40 (vt, J_{PH} = 3.3 Hz, 4H, ***CH₂***P^{t}Bu$_2$), 1.01 (t, J_{PH} = 6.3 Hz, 18H, PC(C***H***$_3$)$_3$), 0.96 (t, J_{PH} = 6.3 Hz, 18H, PC(C***H***$_3$)$_3$).

Reaction of (PCP)Ir(NBE) with N,N-dimethyl-1-phenylmethanamine:

To a 0.5 mL *p*-xylene-d_{10} solution of 5 mg (^{tBu4}PCP)IrH$_4$ (8.3 μmol) in a J-Young tube, 2.34 mg NBE (25 μmol) was added. After 10 hours at room temperature (PCP)Ir(NBE) was formed, then 1.8 μL (12 μmol) N,N-dimethyl-1-phenylmethanamine was added to

the solution. After 5 hours at room temperature, solvent was removed and three complexes in 2:2:1 ratios were observed in ^{31}P NMR spectroscopy. $^{31}P\{^{1}H\}$ NMR (*p*-xylene-d_{10}, 202 MHz): δ 73.6 (bs), 67.5 (bs), 66.3 (bs) (in 2:2:1). ^{1}H NMR (*p*-xylene-d_{10}, 500 MHz): δ -45.43 (bt, 1H, Ir-***H***), -45.60 (bt, 1H, Ir-***H***). After 1 hour heating this solution at 110 °C in *p*-xylene-d_{10} yields (PCP)IrH_2 and some uncharacterized organic product.

(PCP)Ir=C(H)(N(Me)CH$_2$Ph) (**9-8**) (60 °C): $^{31}P\{^{1}H\}$ NMR (*p*-xylene-d_{10}, 202 MHz): δ 73.6 (s). ^{1}H NMR (*p*-xylene-d_{10}, 500 MHz): δ 13.42 (s, 1H, Ir=C(***H***)(N(Me)CH_2Ph)), 3.50 (bt, 4H, C***H***$_2$P), 1.14 (bt, 36H, PC(C***H***$_3$)$_3$). Further characterization is needed to confirm it.

Reaction of (PCP)Ir(NBE) with N,N-dimethylnaphthalen-1-amine: To a 0.5 mL *p*-xylene-d_{10} solution of 5 mg (^{tBu4}PCP)IrH_4 (8.3 μmol) in a J-Young tube, 2.34 mg NBE (25 μmol) was added. After 10 hours at room temperature (PCP)Ir(NBE) was formed, then 2.1 μL (12 μmol) N,N-dimethylnaphthalen-1-amine was added to the solution. After 5 hours at room temperature, complex **9-9** and nitrogen complex were observed in ^{31}P NMR spectroscopy. $^{31}P\{^{1}H\}$ NMR (*p*-xylene-d_{10}, 202 MHz): δ 67.7 (bs). ^{1}H NMR (*p*-xylene-d_{10}, 500 MHz): δ -45.51 (bt, 1H, Ir-***H***). After 1 hour heating this solution at 110 °C in *p*-xylene-d_{10} yields (PCP)IrH_2 and uncharacterized organic products.

Reaction of (PCP)Ir(NBE) with 1-p-tolylpropan-2-one:

To a 0.5 mL *p*-xylene-d_{10} solution of 5 mg (^{tBu4}PCP)IrH_4 (8.3 μmol) in a J-Young tube, 2.34 mg NBE (25 μmol) was added. After 10 hours at room temperature (PCP)Ir(NBE)

was formed, then 1.9 μL (12 μmol) 1-p-tolylpropan-2-one was added to the solution. After 12 hours at room temperature, complexes **9-9** and **9-10** in 2:1 ratio were observed in ^{1}H and ^{31}P NMR spectroscopy. $^{31}P\{^{1}H\}$ NMR (*p*-xylene-d_{10}, 202 MHz): δ 68.9 (s) and 68.1 (s) (2: 1). ^{1}H NMR (*p*-xylene-d_{10}, 500 MHz): δ 5.51 (s, 1H, Ir-OC(CH_3)=C***H***-Ar, complex 9-9), 5.48 (s, 1H, Ir-OC(CH_3)=C***H***-Ar, complex 9-10), -39.49 (t, J_{PH} = 13.0 Hz, complex **9-9**), -39.65 (t, J_{PH} = 13.0 Hz, complex **9-10**).

Reaction of (PCP)Ir(NBE) with 1,1,1-trifluoro-3-phenylpropan-2-one: To a 0.5 mL *p*-xylene-d_{10} solution of 5 mg (^{tBu4}PCP)IrH_4 (8.3 μmol) in a J-Young tube, 2.34 mg NBE (25 μmol) was added. After 10 hours at room temperature (PCP)Ir(NBE) was formed, then 1.9 μL (12 μmol) 1,1,1-trifluoro-3-phenylpropan-2-one was added to the solution. After 12 hours at room temperature three complexes (in 1:5:2 ratio) were observed and all of them had hydride signal. $^{31}P\{^{1}H\}$ NMR (*p*-xylene-d_{10}, 202 MHz): δ 70.3 (s), 68.0 (s), 66.0 (s) (in 1:5:2). ^{1}H NMR (*p*-xylene-d_{10}, 500 MHz): δ 6.09, 5.89, 5.75 (s, 1H, Ir-OC(CF_3)=C***H***-Ar) (in 5: 2: 1), 1.27, 1.22, 1.10 (t, J_{PH} = 6.6 Hz, 36H, PC(C***H***$_3$)$_3$) (in 2: 5: 1), -37.08 (t, J_{PH} = 13.4 Hz, 1H, Ir-***H***), -39.77 (t, J_{PH} = 13.4 Hz, 1H, Ir-***H***), -41.64 (t, J_{PH} = 13.2 Hz, 1H, Ir-***H***) (in 2:5:1).

After addition of CO: $^{31}P\{^{1}H\}$ NMR (*p*-xylene-d_{10}, 202 MHz): δ 60.0 (s), 59.6 (s), 59.3 (s) 5:2:1). ^{1}H NMR (*p*-xylene-d_{10}, 500 MHz): δ 6.11, 6.06, 5.61 (s, 1H, Ir-OC(CF_3)=C***H***-Ar) (in 2:5:1), -5.64 (t, J_{PH} = 15.0 Hz, 1H, Ir-***H***), -5.90 (t, J_{PH} = 14.2 Hz, 1H, Ir-***H***), -6.19 (t, J_{PH} = 15.4 Hz, 1H, Ir-***H***) (in 5:2:1).

Complex 9-11: Heating this solution (before adding CO) at 120 °C for 24 hours yields complex **9-11** along with (PCP)IrH_2 and (PCP)Ir(CO) in 7:2:1 ratio (Scheme 9-6).

$^{31}P\{^1H\}$ NMR (*p*-xylene-d_{10}, 202 MHz): δ 43.1 (s, complex **9-11**).

After addition of CO: $^{31}P\{^1H\}$ NMR (*p*-xylene-d_{10}, 202 MHz): δ 40.4 (s).

Reaction of (PCP)Ir(NBE) with 4,4,4-trifluorobutan-2-one:

To a 0.5 mL *p*-xylene-d_{10} solution of 5 mg (^{tBu4}PCP)IrH_4 (8.3 μmol) in a J-Young tube, 2.34 mg NBE (25 μmol) was added. After 10 hours at room temperature (PCP)Ir(NBE) was formed, then 1.4 μL (12 μmol) 4,4,4-trifluorobutan-2-one was added to the solution. After 12 hours at room temperature, three complexes (PCP)Ir(H)(F), complex **9-12** and enol activated complex (2:1:1) were observed in ^{31}P NMR spectroscopy. Only (PCP)Ir(H)(F) and complex **9-12** were observed (1:1) after 2 hour heating at 100 °C.

(PCP)Ir(H)(F): $^{31}P\{^1H\}$ NMR (*p*-xylene-d_{10}, 202 MHz): δ 69.0 (t, J_{PF} = 5.9 Hz, PCP). ^1H NMR (*p*-xylene-d_{10}, 500 MHz): δ 8.36 (d, J_{HH} = 8.5 Hz, 1H, Ar), 6.90 (m, 3H, Ar), 3.00 (d of vt, J_{PH} = 4.0 Hz, J_{HH} = 17.5 Hz, 2H, ***CH*****$_2$**P^{t}Bu$_2$), 2.95 (d of vt, J_{PH} = 4.0 Hz, J_{HH} = 17.5 Hz, 2H, ***CH*****$_2$**P^{t}Bu$_2$), 1.40 (t, J_{PH} = 6.5 Hz, 18H, PC(C***H***$_3$)$_3$), 1.30 (t, J_{PH} = 6.3 Hz, 18H, PC(C***H***$_3$)$_3$), -35.26 (dt, J_{PH} = 6.5 Hz, J_{FH} = 31.0 Hz, 1H, Ir(*H*)(F)). ^{19F} NMR (*p*-xylene-d_{10}, 470.2 MHz): δ -225.61 (dt, J_{PF} = 5.9 Hz, J_{FH} = 31.0 Hz, 1H, Ir(H)(***F***)).

Reaction of (PCP)Ir(NBE) with 1-fluorooctane:

To a 0.5 mL *p*-xylene-d_{10} solution of 5 mg (^{tBu4}PCP)IrH_4 (8.3 μmol) in a J-Young tube, 2.34 mg NBE (25 μmol) was added. After 10 hours at room temperature (PCP)Ir(NBE)

was formed, then 1.4 μL (8.3 μmol) one equivalent 1-fluorooctane was added to the solution. After 12 hours at room temperature, (PCP)Ir(H)(F), one uncharacterized complex and (PCP)Ir(alkene), were observed. After 1 hour heating at 100 °C yields (PCP)Ir(H)(F) and one uncharacterized in 5:1 ratio, respectively. 1-octene and isomers of 1-octene were characterized by ^{1}H NMR spectroscopy.

Complex 9-12: $^{31}P\{^{1}H\}$ NMR (*p*-xylene-d_{10}, 202 MHz): δ 50.8 (t, J_{PF} = 27.5Hz, PCP). ^{19F} NMR (*p*-xylene-d_{10}, 470.2 MHz): δ -324.4 (dt, J_{PF} = 27.5 Hz, J_{FH} = 65.0.0 Hz, 1H, Ir(C***F*****$_2$**CH=C)).

(^{tBu4}PCP)Ir(H)(NPh_2) (9-13): To a 0.5 mL *p*-xylene-d_{10} solution of 5 mg (^{tBu4}PCP)IrH_4 (8.3 μmol) in a J-Young tube, 2.4 mg NBE (25 μmol) was added. After 3 h at room temperature, 1.4 mg (8.3 μmol) was added, (^{tBu4}PCP)Ir(H)(NPh_2) was formed in 97% yield measured by $^{31}P\{^{1}H\}$ NMR spectroscopy. $^{31}P\{^{1}H\}$ NMR (*p*-xylene-d_{10}, 202 MHz): δ 68.0 (s, PCP). ^{1}H NMR (*p*-xylene-d_{10}, 500 MHz): δ 7.43 (m, 4H, Ar), 7.22 (t, J_{HH} = 8.0 Hz, 3H, Ar), 6.97 (m, obscured by solvent, 3H, PCP), 6.75 (d, J_{HH} = 7.4 Hz, 3H, Ar), 6.56 (t, J_{HH} = 7.4 Hz, 1H, Ar), 4.85 (bs, 1H, N***H***Ph), 3.26 (d of vt, J_{PH} = 3.3 Hz, J_{HH} = 15.5 Hz, 2H, $CH_2P^tBu_2$), 3.14 (d of vt, J_{PH} = 3.5 Hz, J_{HH} = 16.0 Hz, 2H, $CH_2P^tBu_2$), 1.12 (vt, J_{PH} = 6.3 Hz, 18H, P^tBu_2), 0.90 (vt, J_{PH} = 6.3 Hz, 18H, P^tBu_2), -36.40 (t, J_{PH} = 15.0 Hz, 1H, Ir-***H***).

(^{tBu4}PCP)Ir(H)(NHPh) (9-14): To a 0.5 mL *p*-xylene-d_{10} solution of 5 mg (^{tBu4}PCP)IrH_4 (8.3 μmol) in a J-Young tube, 2.4 mg NBE (25 μmol) was added. After 3 h at room

temperature, 0.76 μL aniline (8.3 μmol) was added, (^{tBu4}PCP)Ir(H)(NHPh) was formed in 95 % yield measured by $^{31}P\{^{1}H\}$ NMR spectroscopy. $^{31}P\{^{1}H\}$ NMR (*p*-xylene-d_{10}, 162 MHz): δ 66.8 (s, PCP). ^{1}H NMR (*p*-xylene-d_{10}, 400 MHz): δ 7.10 (t, J_{HH} = 7.4 Hz, 2H, Ar), 6.9 (m, obscured by solvent, 3H, PCP), 6.75 (d, J_{HH} = 7.4 Hz, 2H, Ar), 6.56 (t, J_{HH} = 7.4 Hz, 1H, Ar), 4.85 (bs, 1H, N***H***Ph), 3.10 (d of vt, J_{PH} = 3.3 Hz, J_{HH} = 17.3 Hz, 2H, $CH_2P^tBu_2$), 2.98 (d of vt, J_{PH} = 3.3 Hz, J_{HH} = 17.2 Hz, 2H, $CH_2P^tBu_2$), 1.14 (vt, J_{PH} = 6.3 Hz, 18H, P^tBu_2), 1.09 (vt, J_{PH} = 6.3 Hz, 18H, P^tBu_2), -38.3 (t, J_{PH} = 12.9 Hz, 1H, Ir-***H***).

(^{tBu4}PCP)Ir(H)(Ph) (9-15): To a 0.25 mL *p*-xylene-d_{10} solution of 5 mg (^{tBu4}PCP)IrH_4 (8.3 μmol) in a J-Young tube, 2.4 mg NBE (25 μmol) was added. After 3 h at room temperature, 0.25 mL C_6H_6 was added, (^{tBu4}PCP)Ir(H)(Ph) was formed in 94 % yield measured by $^{31}P\{^{1}H\}$ NMR spectroscopy. $^{31}P\{^{1}H\}$ NMR (*p*-xylene-d_{10}, 162 MHz): δ 67.6 (bs, PCP). ^{1}H NMR (*p*-xylene-d_{10}, 400 MHz): δ 3.39 (bs, 4H, $CH_2P^tBu_2$), 1.01 (bt, J_{PH} = 6.5 Hz, 36H, P^tBu_2), -45.5 (vbs, 1H, Ir-***H***).

(^{tBu4}PCP)Ir(Py) (9-16): To a 0.5 mL *p*-xylene-d_{10} solution of 5 mg (^{tBu4}PCP)IrH_4 (8.3 μmol) in a J-Young tube, 2.4 mg NBE (25 μmol) was added. After 3 h at room temperature, 0.7 μL Py (8.3 μmol) was added, (^{tBu4}PCP)Ir(Py) was formed in 99 % yield measured by $^{31}P\{^{1}H\}$ NMR spectroscopy. $^{31}P\{^{1}H\}$ NMR (C_6D_6, 162 MHz): δ 67.77 (s, PCP). ^{1}H NMR (C_6D_6, 400 MHz): δ 9.29 (d, J_{HH} = 5.2 Hz, 2H, Py), 7.25 (d, J_{HH} = 7.8 Hz, 2H, Ar), 7.19 (t, J_{HH} = 7.1 Hz, 1H, Ar), 6.65 (t, J_{HH} = 7.5 Hz, 1H, Py), 6.33 (m, 2H, Py), 2.99 (t, J_{PH} = 3.5 Hz, 4H, $CH_2P^tBu_2$), 1.15 (t, J_{PH} = 5.9 Hz, 36H, P^tBu_2). ^{13}C NMR (C_6D_6,

100 MHz): δ 160.8 (s, Ar), 157.6 (d, J_{CP} = 6.2 Hz, Ar), 152.2 (t, J_{CP} = 10.8 Hz, Ar), 132.1 (s, Ar), 124.3 (d, J_{CP} = 12Hz, Ar), 120.0 (m, Ar), 38.8 (vt, J_{CP} = 13.5 Hz, ***C***H_2P), 36.9 (vt, J_{CP} = 8.6 Hz, P***C***$(CH_3)_3$), 30.5 (vt, J_{CP} = 2.3 Hz, PC(***C***$H_3)_3$).

Hydrogenation of *trans*-5-decene using (^{tBu4}PCP)IrH$_2$ and (^{tBu4}POCOP)IrH$_2$:

In a J-Young tube, 0.5 mL mesitylene and of 12 μmol Ir complex [(^{tBu4}PCP)IrH$_2$ or (^{tBu4}POCOP)IrH$_2$] was added and was cooled at -48 °C; under the cold condition 13.6 μL *trans*-5-decene (72 μmol) was added and immediately the J-Young tube was frozen in liquid nitrogen. In different time interval, concentration of (^{tBu4}PCP)IrH$_2$ or (^{tBu4}POCOP)IrH$_2$ was measured by ^{31}P NMR spectroscopy.

9.4 References

(1) Zhang, X.; Kanzelberger, M.; Emge, T. J.; Goldman, A. S. *J. Am. Chem. Soc.* **2004**, *126*, 13192.
(2) Goldman, A. S.; Roy, A. H.; Huang, Z.; Ahuja, R.; Schinski, W.; Brookhart, M. *Science* **2006**, *312*, 257.
(3) Calvin, M.; Wilson, K. W. *J. Am. Chem. Soc.* **1945**, *67*, 2003.
(4) Masui, H. *Coord. Chem. Rev.* **2001**, *219*, 957.
(5) Gupta, M.; Hagen, C.; Flesher, R. J.; Kaska, W. C.; Jensen, C. M. *Chem. Commun.* **1996**, 2083.

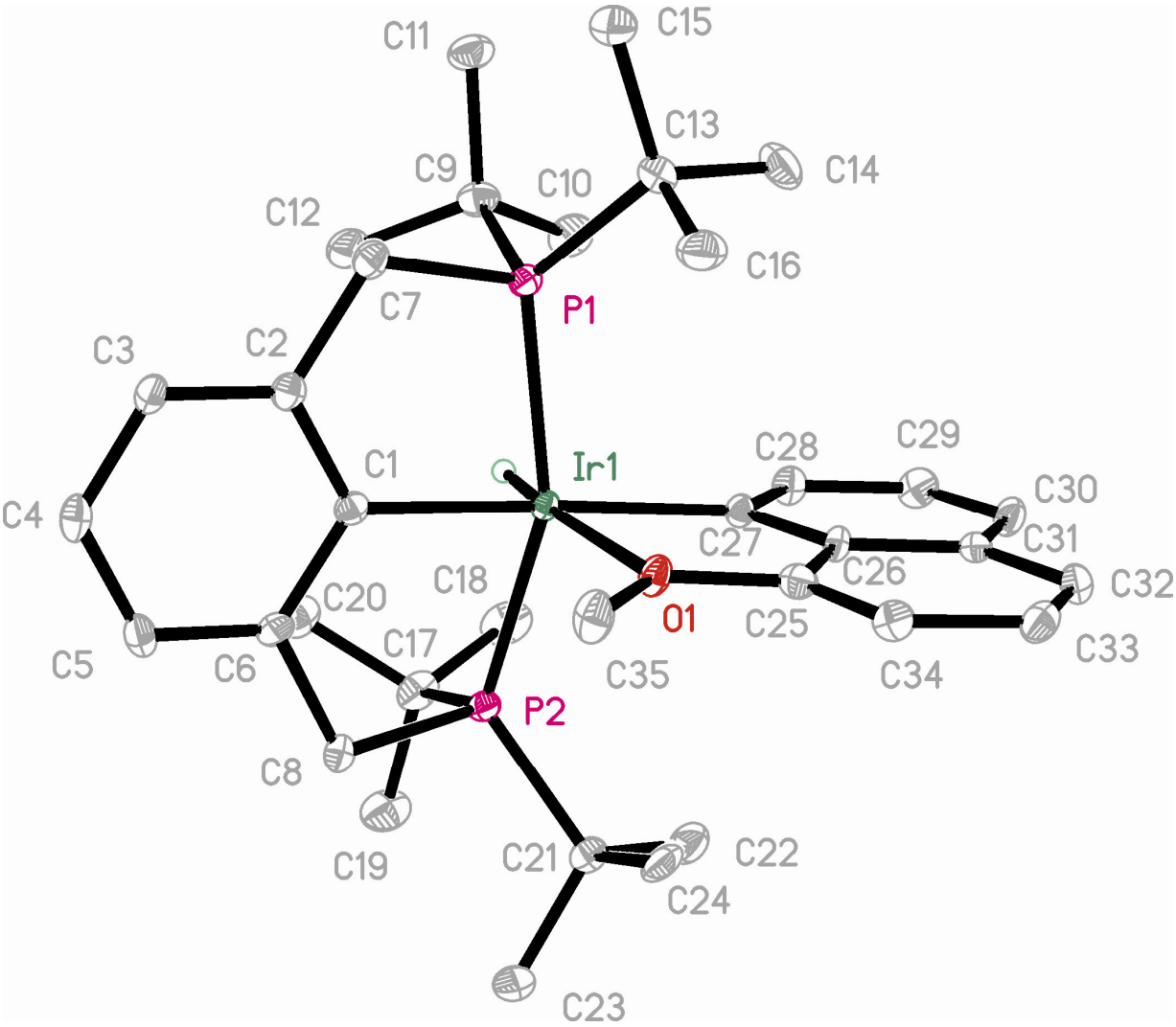

Figure 9-4 Crystal structure of complex **9-5**

Table 9.1 Crystal data and structure refinement for complex **9-5**

Empirical formula	C35 H53 Ir O P2	
Formula weight	743.91	
Temperature	100(2) K	
Wavelength	0.71073 Å	
Crystal system	Monoclinic	
Space group	P2(1)/c	
Unit cell dimensions	a = 15.7281(7) Å	α= 90°.
	b = 11.4349(5) Å	β= 91.990(1)°.
	c = 18.1602(8) Å	γ = 90°.
Volume	3264.1(2) $Å^3$	
Z	4	
Density (calculated)	1.514 Mg/m^3	
Absorption coefficient	4.214 mm^{-1}	
F(000)	1512	
Crystal size	0.24 x 0.07 x 0.03 mm^3	
Theta range for data collection	2.20 to 31.55°.	
Index ranges	-23<=h<=23, -16<=k<=16, -26<=l<=26	
Reflections collected	40463	
Independent reflections	10872 [R(int) = 0.0283]	
Completeness to theta = 31.55°	99.6 %	
Absorption correction	Numerical	
Max. and min. transmission	0.884 and 0.431	
Refinement method	Full-matrix least-squares on F^2	
Data / restraints / parameters	10872 / 1 / 376	
Goodness-of-fit on F^2	1.004	
Final R indices [I>2sigma(I)]	R1 = 0.0218, wR2 = 0.0469	
R indices (all data)	R1 = 0.0278, wR2 = 0.0487	
Largest diff. peak and hole	1.337 and -0.418 e.$Å^{-3}$	

Table 9.2 Selective bond lengths [Å] and angles [°] for complex **9-5**

Ir(1)-C(27)	2.091(3)	C(6)-C(8)	1.519(4)
Ir(1)-C(1)	2.096(3)	C(9)-C(11)	1.531(4)
Ir(1)-O(1)	2.289(2)	C(9)-C(12)	1.541(5)
Ir(1)-P(2)	2.3124(8)	C(9)-C(10)	1.544(4)
Ir(1)-P(1)	2.3167(8)	C(13)-C(14)	1.532(4)
Ir(1)-H(1)	1.20(4)	C(13)-C(15)	1.535(4)
P(1)-C(7)	1.849(3)	C(13)-C(16)	1.538(5)
P(1)-C(13)	1.890(3)	C(14)-H(14A)	0.9800
P(1)-C(9)	1.896(3)	C(14)-H(14B)	0.9800
P(2)-C(8)	1.848(3)	C(14)-H(14C)	0.9800
P(2)-C(21)	1.892(3)	C(15)-H(15A)	0.9800
P(2)-C(17)	1.895(3)	C(15)-H(15B)	0.9800
C(1)-C(2)	1.412(4)	C(15)-H(15C)	0.9800
C(1)-C(6)	1.419(4)	C(16)-H(16A)	0.9800
C(2)-C(3)	1.397(4)	C(16)-H(16B)	0.9800
C(2)-C(7)	1.516(4)	C(16)-H(16C)	0.9800
C(3)-C(4)	1.385(4)	C(17)-C(18)	1.532(5)
C(3)-H(3)	0.9500	C(17)-C(19)	1.536(5)
C(4)-C(5)	1.387(4)	C(17)-C(20)	1.538(4)
C(4)-H(4)	0.9500	C(21)-C(24)	1.529(5)
C(5)-C(6)	1.397(4)	C(21)-C(23)	1.535(5)
C(5)-H(5)	0.9500	C(21)-C(22)	1.537(4)
C(27)-Ir(1)-C(1)	171.02(11)	O(1)-Ir(1)-H(1)	174(2)
C(27)-Ir(1)-O(1)	76.43(10)	P(2)-Ir(1)-H(1)	83.8(19)
C(1)-Ir(1)-O(1)	94.62(10)	P(1)-Ir(1)-H(1)	80.1(19)
C(27)-Ir(1)-P(2)	99.38(8)	C(7)-P(1)-C(13)	102.67(14)
C(1)-Ir(1)-P(2)	82.27(8)	C(7)-P(1)-C(9)	103.22(14)
O(1)-Ir(1)-P(2)	97.65(6)	C(13)-P(1)-C(9)	109.40(15)
C(27)-Ir(1)-P(1)	98.91(8)	C(7)-P(1)-Ir(1)	104.27(10)
C(1)-Ir(1)-P(1)	81.82(8)	C(13)-P(1)-Ir(1)	122.74(10)
O(1)-Ir(1)-P(1)	100.03(6)	C(9)-P(1)-Ir(1)	112.08(10)
P(2)-Ir(1)-P(1)	157.05(3)	C(8)-P(2)-C(21)	102.93(14)
C(27)-Ir(1)-H(1)	97.8(19)	C(8)-P(2)-C(17)	103.93(15)
C(1)-Ir(1)-H(1)	91.2(19)	C(21)-P(2)-C(17)	108.57(14)

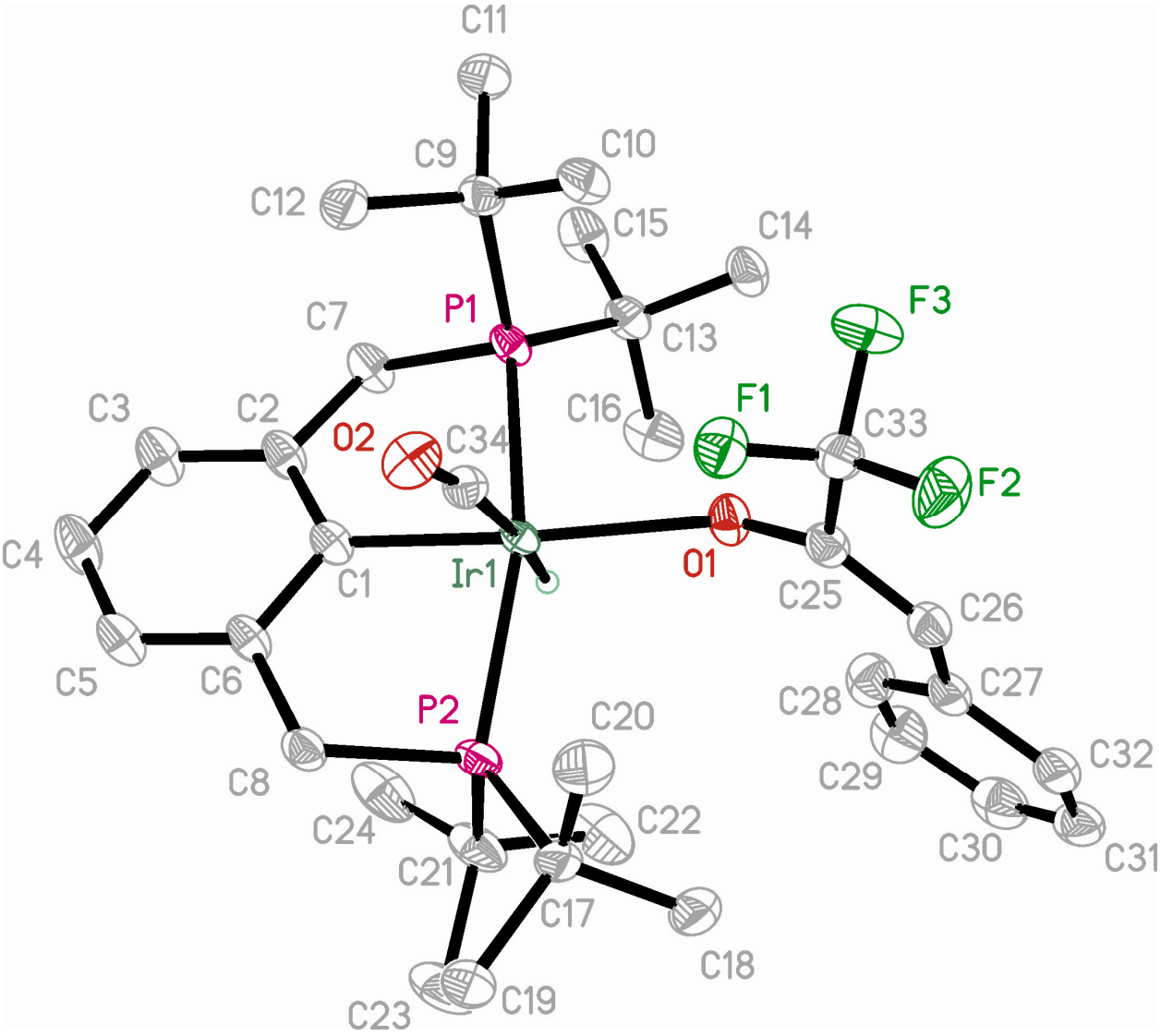

Figure 9-5 Crystal structure of complex (PCP)Ir(H)(CO)(OC(CF_3)C(H)Ph)

Table 9.3 Crystal data and structure refinement for (PCP)Ir(H)(CO)(OC(CF_3)C(H)Ph)

Empirical formula	C34 H50 F3 Ir O2 P2	
Formula weight	801.88	
Temperature	100(2) K	
Wavelength	0.71073 Å	
Crystal system	Monoclinic	
Space group	C2/c	
Unit cell dimensions	a = 23.8376(16) Å	α= 90°.
	b = 22.5927(15) Å	β= 127.650(1)°.
	c = 16.0473(11) Å	γ = 90°.
Volume	6842.6(8) $Å^3$	
Z	8	
Density (calculated)	1.557 Mg/m^3	
Absorption coefficient	4.041 mm^{-1}	
F(000)	3232	
Crystal size	0.24 x 0.14 x 0.12 mm^3	
Theta range for data collection	2.16 to 31.51°.	
Index ranges	-35<=h<=35, -32<=k<=33, -23<=l<=22	
Reflections collected	33431	
Independent reflections	11320 [R(int) = 0.0194]	
Completeness to theta = 31.51°	99.2 %	
Absorption correction	Semi-empirical from equivalents	
Max. and min. transmission	0.6427 and 0.4439	
Refinement method	Full-matrix least-squares on F^2	
Data / restraints / parameters	11320 / 1 / 395	
Goodness-of-fit on F^2	1.003	
Final R indices [I>2sigma(I)]	R1 = 0.0310, wR2 = 0.0777	
R indices (all data)	R1 = 0.0355, wR2 = 0.0805	
Largest diff. peak and hole	8186 and -2.283 e.$Å^{-3}$	

Table 9.4 Selective bond lengths [Å] and angles [°] of (PCP)Ir(H)(CO)(OC(CF_3)C(H)Ph)

Ir(1)-C(34)	1.923(3)	C(4)-C(5)	1.390(5)
Ir(1)-C(1)	2.044(3)	C(4)-H(4)	0.9500
Ir(1)-O(1)	2.205(2)	C(5)-C(6)	1.396(4)
Ir(1)-P(1)	2.3507(7)	C(5)-H(5)	0.9500
Ir(1)-P(2)	2.3602(7)	C(6)-C(8)	1.511(4)
Ir(1)-H(1)	1.589(10)	C(9)-C(11)	1.532(4)
P(1)-C(7)	1.836(3)	C(9)-C(10)	1.534(4)
P(1)-C(13)	1.882(3)	C(9)-C(12)	1.540(4)
P(1)-C(9)	1.885(3)	C(13)-C(16)	1.531(5)
P(2)-C(8)	1.837(3)	C(13)-C(14)	1.535(4)
P(2)-C(17)	1.885(4)	C(13)-C(15)	1.544(4)
P(2)-C(21)	1.893(3)	C(17)-C(20)	1.534(5)
C(1)-C(6)	1.407(4)	C(17)-C(18)	1.537(5)
C(1)-C(2)	1.411(4)	C(17)-C(19)	1.544(4)
C(2)-C(3)	1.399(4)	C(21)-C(24)	1.530(6)
C(2)-C(7)	1.510(4)	C(21)-C(22)	1.533(5)
C(3)-C(4)	1.390(5)	C(21)-C(23)	1.546(5)
C(34)-Ir(1)-C(1)	86.94(11)	C(7)-P(1)-C(9)	104.69(15)
C(34)-Ir(1)-O(1)	100.10(10)	C(13)-P(1)-C(9)	110.32(14)
C(1)-Ir(1)-O(1)	171.01(9)	C(7)-P(1)-Ir(1)	100.06(10)
C(34)-Ir(1)-P(1)	99.95(9)	C(13)-P(1)-Ir(1)	117.58(11)
C(1)-Ir(1)-P(1)	83.08(8)	C(9)-P(1)-Ir(1)	117.21(9)
O(1)-Ir(1)-P(1)	90.15(6)	C(8)-P(2)-C(17)	104.48(14)
C(34)-Ir(1)-P(2)	92.80(9)	C(8)-P(2)-C(21)	104.27(16)
C(1)-Ir(1)-P(2)	80.68(8)	C(17)-P(2)-C(21)	110.72(18)
O(1)-Ir(1)-P(2)	104.36(6)	C(8)-P(2)-Ir(1)	98.47(10)
P(1)-Ir(1)-P(2)	158.75(3)	C(17)-P(2)-Ir(1)	121.63(11)
C(34)-Ir(1)-H(1)	174.5(18)	C(21)-P(2)-Ir(1)	114.30(12)
C(1)-Ir(1)-H(1)	88.0(18)	C(6)-C(1)-C(2)	118.4(3)
O(1)-Ir(1)-H(1)	85.1(18)	C(6)-C(1)-Ir(1)	120.6(2)
P(1)-Ir(1)-H(1)	81.7(18)	C(2)-C(1)-Ir(1)	121.0(2)
P(2)-Ir(1)-H(1)	84.1(18)	C(3)-C(2)-C(1)	120.4(3)
C(7)-P(1)-C(13)	104.63(14)	C(3)-C(2)-C(7)	120.6(3)

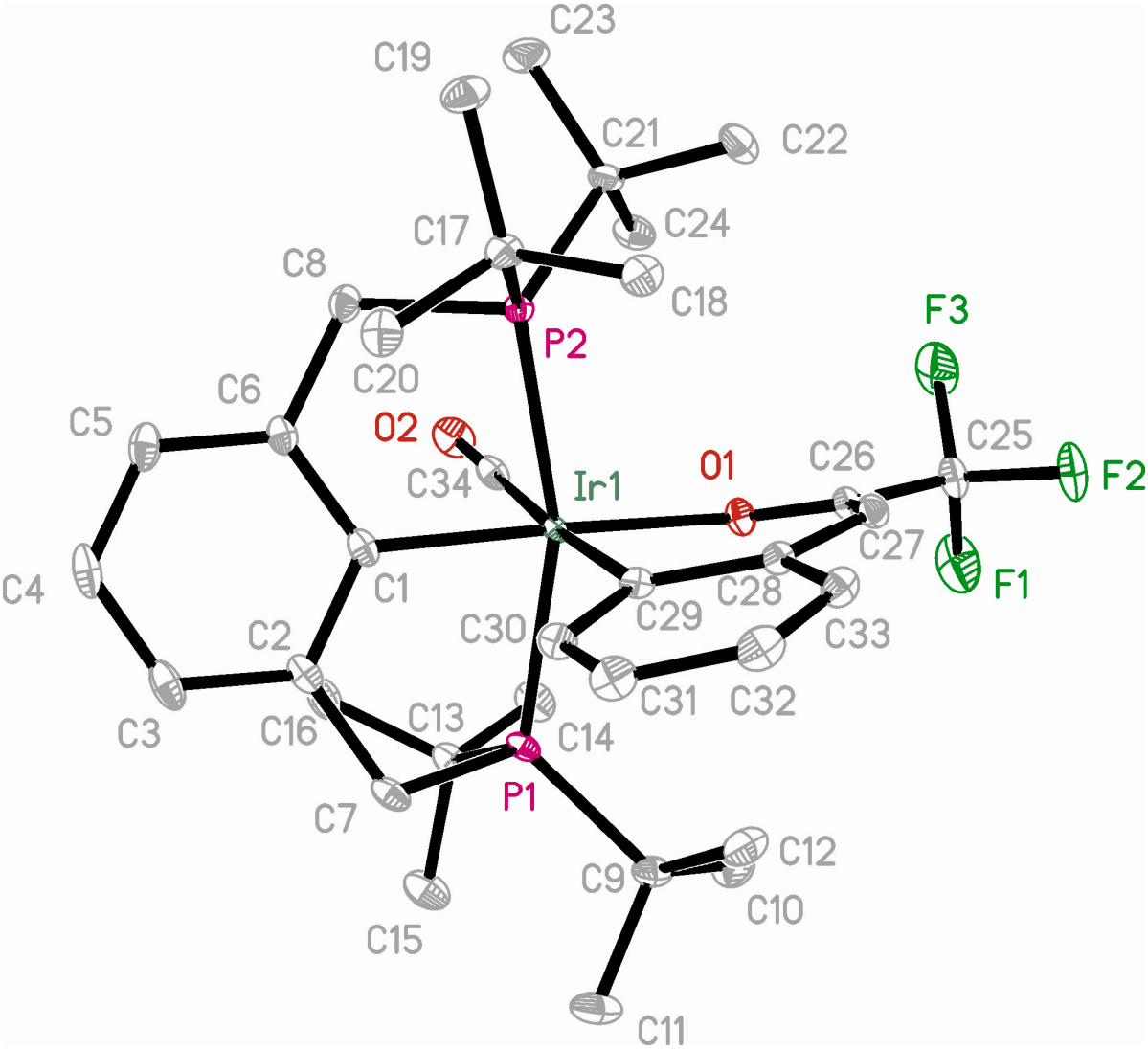

Figure 9-6 Crystal structure of CO adduct of complex **9-11**

Table 9.5 Crystal data and structure refinement for CO adduct of complex **9-11**

Empirical formula	C34 H48 F3 Ir O2 P2	
Formula weight	799.86	
Temperature	100(2) K	
Wavelength	0.71073 Å	
Crystal system	Triclinic	
Space group	P-1	
Unit cell dimensions	a = 9.4798(5) Å	α= 73.629(1)°.
	b = 11.1246(6) Å	β= 86.685(1)°.
	c = 17.3743(9) Å	γ = 69.364(1)°.
Volume	1643.44(15) $Å^3$	
Z	2	
Density (calculated)	1.616 Mg/m^3	
Absorption coefficient	4.206 mm^{-1}	
F(000)	804	
Crystal size	0.44 x 0.35 x 0.25 mm^3	
Theta range for data collection	2.30 to 31.50°.	
Index ranges	-13<=h<=13, -16<=k<=16, -25<=l<=25	
Reflections collected	21413	
Independent reflections	10708 [R(int) = 0.0186]	
Completeness to theta = 31.50°	97.9 %	
Absorption correction	Semi-empirical from equivalents	
Max. and min. transmission	0.4195 and 0.2591	
Refinement method	Full-matrix least-squares on F^2	
Data / restraints / parameters	10708 / 0 / 392	
Goodness-of-fit on F^2	1.002	
Final R indices [I>2sigma(I)]	R1 = 0.0231, wR2 = 0.0560	
R indices (all data)	R1 = 0.0242, wR2 = 0.0564	
Extinction coefficient	0.00297(18)	
Largest diff. peak and hole	2.305 and -2.888 e.$Å^{-3}$	

Table 9.6 Selective bond lengths [Å] and angles [°] of CO adduct of complex **9-11**

Ir(1)-C(34)	1.925(2)	C(3)-H(3)	0.9500
Ir(1)-C(1)	2.048(2)	C(4)-C(5)	1.390(3)
Ir(1)-C(29)	2.113(2)	C(5)-C(6)	1.398(3)
Ir(1)-O(1)	2.1377(15)	C(5)-H(5)	0.9500
Ir(1)-P(1)	2.3855(5)	C(6)-C(8)	1.519(3)
Ir(1)-P(2)	2.4123(5)	C(9)-C(12)	1.534(3)
P(1)-C(7)	1.840(2)	C(9)-C(10)	1.539(3)
P(1)-C(9)	1.890(2)	C(9)-C(11)	1.540(3)
P(1)-C(13)	1.892(2)	C(13)-C(15)	1.541(3)
P(2)-C(8)	1.846(2)	C(13)-C(14)	1.547(3)
P(2)-C(21)	1.900(2)	C(13)-C(16)	1.548(3)
P(2)-C(17)	1.912(2)	C(17)-C(19)	1.537(3)
C(1)-C(6)	1.409(3)	C(17)-C(18)	1.538(3)
C(1)-C(2)	1.415(3)	C(17)-C(20)	1.541(3)
C(2)-C(3)	1.398(3)	C(21)-C(24)	1.535(3)
C(2)-C(7)	1.514(3)	C(21)-C(22)	1.535(3)
C(3)-C(4)	1.388(3)	C(21)-C(23)	1.536(3)
C(34)-Ir(1)-C(1)	86.90(8)	C(9)-P(1)-C(13)	108.34(10)
C(34)-Ir(1)-C(29)	175.69(8)	C(7)-P(1)-Ir(1)	98.95(7)
C(1)-Ir(1)-C(29)	94.69(8)	C(9)-P(1)-Ir(1)	122.06(7)
C(34)-Ir(1)-O(1)	87.58(7)	C(13)-P(1)-Ir(1)	114.28(7)
C(1)-Ir(1)-O(1)	173.26(7)	C(8)-P(2)-C(21)	107.34(10)
C(29)-Ir(1)-O(1)	91.10(7)	C(8)-P(2)-C(17)	100.91(10)
C(34)-Ir(1)-P(1)	92.28(6)	C(21)-P(2)-C(17)	108.68(9)
C(1)-Ir(1)-P(1)	81.12(6)	C(8)-P(2)-Ir(1)	95.59(7)
C(29)-Ir(1)-P(1)	91.92(5)	C(21)-P(2)-Ir(1)	116.58(7)
O(1)-Ir(1)-P(1)	95.26(4)	C(17)-P(2)-Ir(1)	123.97(7)
C(34)-Ir(1)-P(2)	87.75(6)	C(6)-C(1)-C(2)	119.11(19)
C(1)-Ir(1)-P(2)	80.65(6)	C(6)-C(1)-Ir(1)	119.44(15)
C(29)-Ir(1)-P(2)	88.56(5)	C(2)-C(1)-Ir(1)	121.17(15)
O(1)-Ir(1)-P(2)	102.98(4)	C(3)-C(2)-C(1)	119.7(2)
P(1)-Ir(1)-P(2)	161.743(19)	C(3)-C(2)-C(7)	121.52(19)
C(7)-P(1)-C(9)	106.92(10)	C(1)-C(2)-C(7)	118.75(18)
C(7)-P(1)-C(13)	104.01(10)	C(4)-C(3)-C(2)	120.5(2)

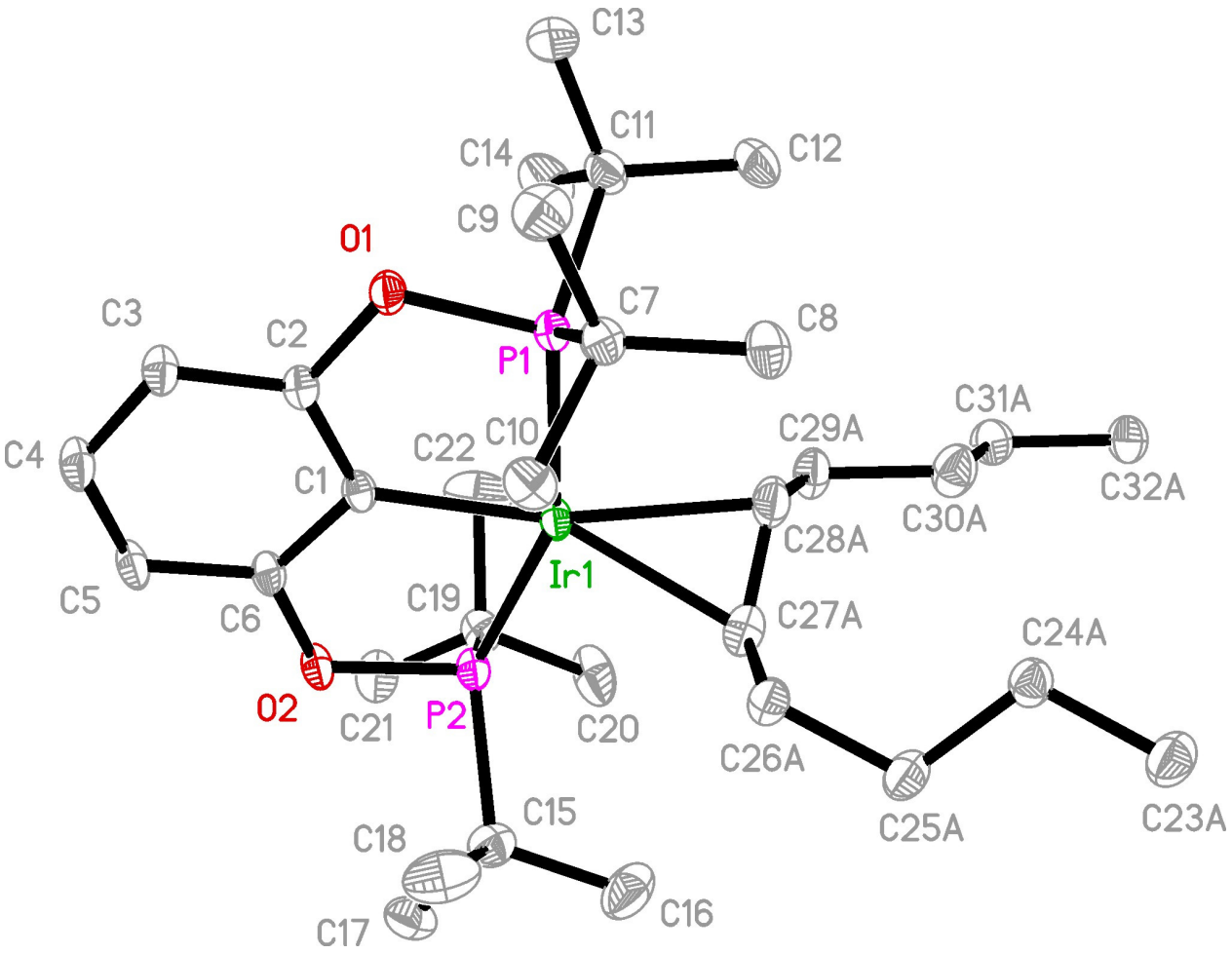

Figure 9-7 Crystal structure of (^{tBu4}POCOP)Ir(*trans*-5-decene)

Table 9.7 Crystal data and structure refinement for (^{tBu4}POCOP)Ir(*trans*-5-decene)

Empirical formula	C32 H59 Ir O2 P2	
Formula weight	729.93	
Temperature	100(2) K	
Wavelength	0.71073 Å	
Crystal system	Monoclinic	
Space group	P2(1)/c	
Unit cell dimensions	a = 12.5226(7) Å	α= 90°.
	b = 13.0103(8) Å	β= 101.265(1)°.
	c = 20.8285(12) Å	γ = 90°.
Volume	3328.1(3) Å^3	
Z	4	
Density (calculated)	1.457 Mg/m^3	
Absorption coefficient	4.133 mm^{-1}	
F(000)	1496	
Crystal size	0.29 x 0.19 x 0.05 mm^3	
Theta range for data collection	1.99 to 30.56°.	
Index ranges	-17<=h<=17, -18<=k<=18, -29<=l<=29	
Reflections collected	38730	
Independent reflections	10178 [R(int) = 0.0230]	
Completeness to theta = 30.56°	99.8 %	
Absorption correction	Numerical	
Max. and min. transmission	0.68 and 0.33	
Refinement method	Full-matrix least-squares on F^2	
Data / restraints / parameters	10178 / 803 / 437	
Goodness-of-fit on F^2	1.006	
Final R indices [I>2sigma(I)]	R1 = 0.0347, wR2 = 0.0779	
R indices (all data)	R1 = 0.0399, wR2 = 0.0806	
Largest diff. peak and hole	3.012 and -2.099 e.Å^{-3}	

Table 9.8 Selective bond lengths [Å] and angles [°] of (^{tBu4}POCOP)Ir(*trans*-5-decene)

Ir(1)-C(1)	2.030(3)	C(3)-C(4)	1.391(5)
Ir(1)-C(28B)	2.209(6)	C(3)-H(3)	0.9500
Ir(1)-C(28A)	2.222(6)	C(4)-C(5)	1.386(5)
Ir(1)-C(27A)	2.235(6)	C(4)-H(4)	0.9500
Ir(1)-C(27B)	2.250(6)	C(5)-C(6)	1.391(4)
Ir(1)-P(2)	2.2864(8)	C(5)-H(5)	0.9500
Ir(1)-P(1)	2.2964(8)	C(7)-C(8)	1.535(5)
P(2)-O(2)	1.656(2)	C(7)-C(10)	1.537(5)
P(2)-C(15)	1.877(4)	C(7)-C(9)	1.540(5)
P(2)-C(19)	1.882(4)	C(11)-C(12)	1.533(5)
P(1)-O(1)	1.659(2)	C(11)-C(14)	1.539(6)
P(1)-C(11)	1.864(4)	C(11)-C(13)	1.542(6)
P(1)-C(7)	1.878(3)	C(15)-C(16)	1.528(6)
O(1)-C(2)	1.383(4)	C(15)-C(18)	1.537(6)
O(2)-C(6)	1.384(4)	C(15)-C(17)	1.541(6)
C(1)-C(6)	1.396(4)	C(19)-C(21)	1.526(5)
C(1)-C(2)	1.403(4)	C(19)-C(20)	1.529(5)
C(2)-C(3)	1.389(4)	C(19)-C(22)	1.543(6)

C(1)-Ir(1)-C(28B)	163.7(2)	C(1)-Ir(1)-P(1)	78.32(9)
C(1)-Ir(1)-C(28A)	166.6(2)	C(28B)-Ir(1)-P(1)	89.4(2)
C(28B)-Ir(1)-C(28A)	13.9(3)	C(28A)-Ir(1)-P(1)	88.7(2)
C(1)-Ir(1)-C(27A)	153.9(2)	C(27A)-Ir(1)-P(1)	111.0(2)
C(28B)-Ir(1)-C(27A)	26.0(3)	C(27B)-Ir(1)-P(1)	113.0(2)
C(28A)-Ir(1)-C(27A)	35.9(2)	P(2)-Ir(1)-P(1)	156.24(3)
C(1)-Ir(1)-C(27B)	159.8(2)	O(2)-P(2)-C(15)	96.19(16)
C(28B)-Ir(1)-C(27B)	36.3(2)	O(2)-P(2)-C(19)	98.60(15)
C(28A)-Ir(1)-C(27B)	28.1(3)	C(15)-P(2)-C(19)	111.15(17)
C(27A)-Ir(1)-C(27B)	39.9(3)	O(2)-P(2)-Ir(1)	106.28(9)
C(1)-Ir(1)-P(2)	78.27(9)	C(15)-P(2)-Ir(1)	122.10(13)
C(28B)-Ir(1)-P(2)	114.4(2)	C(19)-P(2)-Ir(1)	116.91(12)
C(28A)-Ir(1)-P(2)	114.4(2)	O(1)-P(1)-C(11)	98.25(15)
C(27A)-Ir(1)-P(2)	92.0(2)	O(1)-P(1)-C(7)	96.67(14)
C(27B)-Ir(1)-P(2)	88.3(2)	C(11)-P(1)-C(7)	112.47(16)

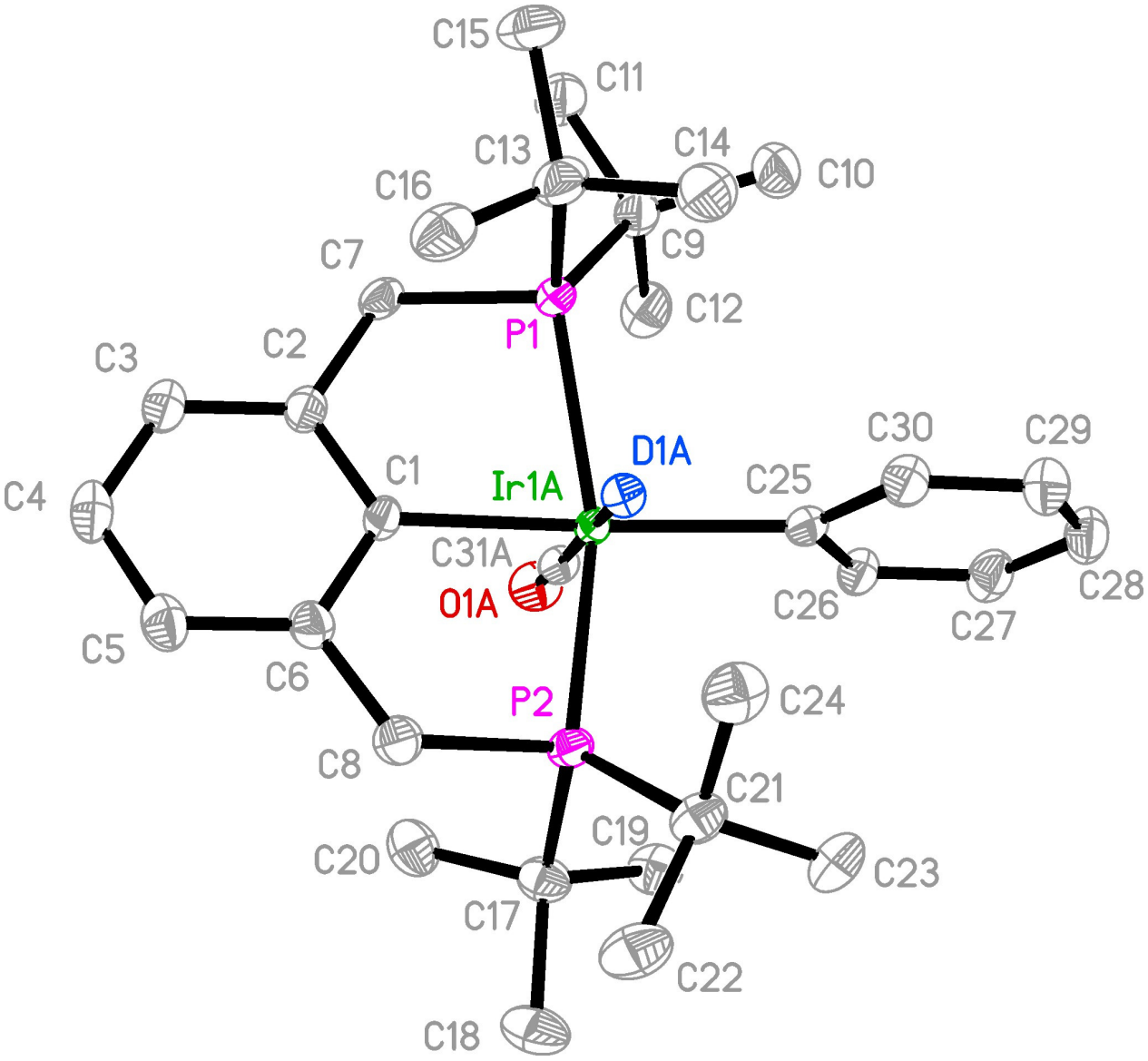

Figure 9-8 Crystal structure of (^{tBu4}PCP)Ir(D)(CO)(C_6D_5)

Table 9.9 Crystal data and structure refinement for (^{tBu4}PCP)Ir(D)(CO)(C_6D_5)

Empirical formula	C31 H49 Ir O P2	
Formula weight	691.84	
Temperature	100(2) K	
Wavelength	0.71073 Å	
Crystal system	Triclinic	
Space group	P-1	
Unit cell dimensions	a = 9.1027(5) Å	α= 80.624(1)°.
	b = 10.6085(6) Å	β= 74.301(1)°.
	c = 16.5409(9) Å	γ = 81.318(1)°.
Volume	1507.53(14) $Å^3$	
Z	2	
Density (calculated)	1.524 Mg/m^3	
Absorption coefficient	4.556 mm^{-1}	
F(000)	700	
Crystal size	0.30 x 0.20 x 0.13 mm^3	
Theta range for data collection	1.96 to 31.00°.	
Index ranges	-13<=h<=13, -15<=k<=15, -23<=l<=23	
Reflections collected	18465	
Independent reflections	9445 [R(int) = 0.0190]	
Completeness to theta = 31.00°	98.2 %	
Absorption correction	Semi-empirical from equivalents	
Max. and min. transmission	0.588 and 0.341	
Refinement method	Full-matrix least-squares on F^2	
Data / restraints / parameters	9445 / 4 / 341	
Goodness-of-fit on F^2	1.007	
Final R indices [I>2sigma(I)]	R1 = 0.0279, wR2 = 0.0637	
R indices (all data)	R1 = 0.0304, wR2 = 0.0647	
Largest diff. peak and hole	1.820 and -1.732 e.$Å^{-3}$	

Table 9.10 Selective bond lengths [Å] and angles [°] of (^{tBu4}PCP)Ir(D)(CO)(C_6D_5)

Ir(1A)-C(31A)	1.908(3)	P(2)-C(8)	1.843(3)
Ir(1A)-C(1)	2.113(3)	P(2)-C(21)	1.889(3)
Ir(1A)-C(25)	2.151(3)	P(2)-C(17)	1.890(3)
Ir(1A)-P(1)	2.3347(7)	C(1)-C(2)	1.403(4)
Ir(1A)-P(2)	2.3391(7)	C(1)-C(6)	1.411(4)
Ir(1A)-D(1A)	1.601(10)	C(2)-C(3)	1.391(4)
Ir(1A)-D(1B)	1.1177(2)	C(2)-C(7)	1.522(4)
C(31A)-O(1A)	1.147(4)	C(3)-C(4)	1.388(4)
C(31A)-D(1B)	0.801(3)	C(4)-C(5)	1.388(4)
Ir(1B)-C(31B)	1.904(10)	C(5)-C(6)	1.398(4)
Ir(1B)-C(1)	2.171(3)	C(6)-C(8)	1.508(4)
Ir(1B)-C(25)	2.179(3)	C(9)-C(12)	1.533(5)
Ir(1B)-P(1)	2.280(2)	C(9)-C(10)	1.538(5)
Ir(1B)-P(2)	2.387(2)	C(9)-C(11)	1.540(4)
Ir(1B)-D(1A)	1.061(11)	C(13)-C(15)	1.528(4)
Ir(1B)-D(1B)	1.667(4)	C(13)-C(14)	1.540(5)
C(31B)-O(1B)	1.146(10)	C(13)-C(16)	1.543(5)
C(31B)-D(1A)	0.91(2)	C(17)-C(20)	1.540(4)
P(1)-C(7)	1.828(3)	C(17)-C(19)	1.543(4)
P(1)-C(9)	1.882(3)	C(17)-C(18)	1.545(4)
C(31A)-Ir(1A)-C(1)	91.44(11)	P(2)-Ir(1A)-D(1A)	78.2(13)
C(31A)-Ir(1A)-C(25)	94.32(12)	C(31A)-Ir(1A)-D(1B)	5.24(9)
C(1)-Ir(1A)-C(25)	174.17(11)	C(1)-Ir(1A)-D(1B)	96.52(8)
C(31A)-Ir(1A)-P(1)	94.65(9)	C(25)-Ir(1A)-D(1B)	89.25(8)
C(1)-Ir(1A)-P(1)	80.00(8)	P(1)-Ir(1A)-D(1B)	96.748(19)
C(25)-Ir(1A)-P(1)	98.55(7)	P(2)-Ir(1A)-D(1B)	99.08(2)
C(31A)-Ir(1A)-P(2)	99.67(9)	D(1A)-Ir(1A)-D(1B)	174.5(13)
C(1)-Ir(1A)-P(2)	81.91(8)	O(1A)-C(31A)-Ir(1A)	177.8(3)
C(25)-Ir(1A)-P(2)	98.04(7)	O(1A)-C(31A)-D(1B)	174.8(4)
P(1)-Ir(1A)-P(2)	157.15(3)	Ir(1A)-C(31A)-D(1B)	7.32(12)
C(31A)-Ir(1A)-D(1A)	177.9(13)	C(31B)-Ir(1B)-C(1)	103.0(14)
C(1)-Ir(1A)-D(1A)	87.8(13)	C(31B)-Ir(1B)-C(25)	100.6(14)
C(25)-Ir(1A)-D(1A)	86.4(13)	C(1)-Ir(1B)-C(25)	156.4(2)
P(1)-Ir(1A)-D(1A)	87.2(13)	C(31B)-Ir(1B)-P(1)	93.0(13)

CURRICULUM VITAE

Sabuj Kundu

EDUCATION:

2002 B.Sc. Chemistry, University of Calcutta, Calcutta, India.

2004 M.Sc. Chemistry, Indian Institute of Technology Bombay, Mumbai, India

2010 Ph.D. Chemistry, Rutgers, The State University of New Jersey, New Brunswick, NJ

PUBLICATIONS:

1. "Catalytic ring expansion, contraction, and metathesis-polymerization of cycloalkanes" Ahuja, Ritu; **Kundu, Sabuj**; Goldman, Alan S.; Brookhart, Maurice; Vicente, Brian C.; Scott, Susannah L. *Chemical Communications* **2008**, *2,* 253-255.

2. "Evaluation of Molybdenum and Tungsten Metathesis Catalysts for Homogeneous Tandem Alkane Metathesis" Bailey Brad C.; Schrock Richard R.; **Kundu, Sabuj**; Goldman, Alan S.; Huang, Zheng; Brookhart, Maurice. *Organometallics* **2009**, *28,* 355-360.

3. "Highly Active and Recyclable Heterogeneous Iridium Pincer Catalysts for Transfer Dehydrogenation of Alkanes"Huang, Zheng; Brookhart, Maurice; Goldman, Alan S.; **Kundu, Sabuj**; Vicente, Brian C.; Scott, Susannah L. *Adv. Synth. Catal.* **2009**, *351*, 188-206.

4. "Rational Design and Synthesis of Highly Active Pincer-Iridium Catalysts for Alkane Dehydrogenation" **Kundu, Sabuj**; Choliy,Yuriy; Gao, Zhuo; Ahuja, Ritu; Ray, Amlan; Warmuth, Ralf; Brookhart, Maurice; Krogh-Jespersen, Karsten; Goldman, Alan S. *Organometallics,* **2009**, *28*, 5432-5444.